TECHNISCHE UNIVERSITÄT MÜNCHEN
Lehrstuhl für Mikrobielle Ökologie

Effect of Nitrite on *Salmonella* Typhimurium and *E. coli* O157:H7 (EHEC) under Food-Related Conditions

Anna Mühlig

Vollständiger Abdruck der von der Fakultät Wissenschaftszentrum Weihenstephan für Ernährung, Landnutzung und Umwelt der Technischen Universität München zur Erlangung des akademischen Grades eines

Doktors der Naturwissenschaften

genehmigten Dissertation.

Vorsitzender: Univ.- Prof. Dr. W. Liebl

Prüfer der Dissertation:
1. Univ.- Prof. Dr. S. Scherer
2. apl. Prof. Dr. M. A. Ehrmann

Die Dissertation wurde am 25.10.2016 bei der Technischen Universität München eingereicht und durch die Fakultät Wissenschaftszentrum Weihenstephan für Ernährung, Landnutzung und Umwelt am 06.02.2017 angenommen.

Contents

Publications

Parts of this thesis have been published in peer-reviewed journals:

Mühlig, A., Kabisch, J., Pichner, R., Scherer, S., and Müller-Herbst, S. (2014). Contribution of the NO-detoxifying enzymes HmpA, NorV and NrfA to nitrosative stress protection of *Salmonella* Typhimurium in raw sausages. *Food Microbiology*. **42**: 26–33.

Chapter III1.1.1, III1.1.2 and IV1

Mühlig A. constructed the deletion mutants, designed, performed and analyzed the *in vitro* growth assays and qPCR experiment, and wrote the manuscript. Kabisch J. and Pichner R. were responsible for the design, performance and analysis of the challenge assays in raw sausages. Scherer S. and Müller-Herbst S. supervised the study and proofread the manuscript.

Mühlig, A., Behr, J., Scherer, S., and Müller-Herbst, S. (2014). Stress Response of *Salmonella enterica* serovar Typhimurium to Acidified Nitrite. *Applied and Environmental Microbiology*. **80**(20): 6373–6382.

Chapter III1.2.2.1, III1.2.2.2, III1.2.3, III1.2.4 and IV2.2

Mühlig A. designed, performed and analyzed the RNA-seq and qPCR experiments, constructed the mutant bacterial strains and analyzed their growth behavior, performed the intracellular pH measurements, and wrote the manuscript. Behr J. helped with the experimental design and measurements of the intracellular pH. Scherer S. and Müller-Herbst S. supervised the study and proofread the manuscript.

Other publications:

Müller-Herbst, S., Wüstner, S., **Mühlig, A.**, Eder, D., M Fuchs, T., Held, C., Ehrenreich, A., and Scherer, S. (2014). Identification of genes essential for anaerobic growth of *Listeria monocytogenes*. *Microbiology (Reading, England)*. **160**(Pt 4): 752–765.

Simon, S., Mittelstädt, S., Kwon, B. C., Stoffel, A., Landstorfer, R., Neuhaus, K., **Mühlig, A.**, Scherer, S., and Keim, D. A. (2015). VisExpress. Visual exploration of differential gene expression data. *Information Visualization*. doi: 10.1177/1473871615612883.

Fellner, L., Huptas, C., Simon, S., **Mühlig, A.**, Scherer, S., and Neuhaus, K. (2016). Draft Genome Sequences of Three European Laboratory Derivatives from Enterohemorrhagic *Escherichia coli* O157:H7 Strain EDL933, Including Two Plasmids. *Genome announcements*. **4**(2).

Summary

The curing agent sodium nitrite ($NaNO_2$) is traditionally used as a preservative in the production of raw sausages. Under the acidic conditions in the meat matrix, reactive nitrite-derivatives are formed, such as nitric oxide (NO). However, the mechanisms underlying the antimicrobial action of acidified nitrite on the Gram-negative foodborne pathogens *Salmonella* and enterohemorrhagic *Escherichia coli* (EHEC) are only poorly understood. What is more, the countermeasures employed by these bacteria to combat acidified nitrite stress are largely unexplored.

In this study, the effect of $NaNO_2$ on *Salmonella* (*S.*) Typhimurium 14028 and EHEC O157:H7 EDL933 under food-related conditions was investigated by transcriptional studies, growth assays and mutant analysis.

In vitro growth assays of *S.* Typhimurium single deletion mutants of the main NO-detoxifying enzymes flavohemoglobin (Δ*hmpA*), flavorubredoxin (Δ*norV*) and cytochrome *c* nitrite reductase (Δ*nrfA*) revealed a growth defect of Δ*hmpA* in the presence of acidified $NaNO_2$. A strong increase in *hmpA* transcript levels in the wild-type (WT) treated with 150 mg/l acidified $NaNO_2$ was observed by qPCR. However, challenge assays with short-ripened spreadable sausages produced with 0 or 150 mg/kg $NaNO_2$ performed by cooperation partners failed to reveal a phenotype for any of these mutants compared to the WT. Hence, none of the NO detoxification systems HmpA, NorV and NrfA is solely responsible for nitrosative stress tolerance of *S.* Typhimurium in raw sausages.

Global transcriptome analyses were performed to further investigate the effect of acidified nitrite on *S.* Typhimurium. The transcriptional responses to the NO donor sodium nitroprusside (SNP), to acidified $NaNO_2$ in LB broth (10 min shock and adaptational responses) and in media simulating conditions in raw sausages on ripening days 0 (RD0) and 3 (RD3) were assessed by RNA-sequencing (RNA-seq). Besides induction of a NO-specific response mediated via the NO-sensitive regulators NsrR and/or NorR, several other stress-associated genes were specifically up-regulated by 150 mg/l acidified $NaNO_2$ in LB broth (acid tolerance systems) and on RD0 (copper tolerance genes). Moreover, acidified $NaNO_2$ shock resulted in reduced transcript levels of genes involved in translation, transcription, replication and motility. Induction of stress tolerance and reduction of cell proliferation obviously promote survival under harsh acidified $NaNO_2$ stress. On the contrary, the residual $NaNO_2$ amount of 30 mg/l $NaNO_2$ on RD3 did not affect the transcriptome of *S.* Typhimurium. However, RNA-seq data revealed massive transcriptional changes on RD3 compared to RD0 indicative of enhanced stress and growth arrest on RD3. These data support the importance of additional hurdles apart from nitrite to create unfavourable growth conditions during the later stages of raw sausage ripening.

Strikingly, disruption of the *cadA* gene, which codes for lysine decarboxylase and which was strongly induced upon acidified nitrite shock, resulted in increased sensitivity to acidified $NaNO_2$. The induction of systems known to be involved in acid resistance indicates a nitrite-mediated increase of acid stress. Intracellular pH measurements using a pH-sensitive GFP variant showed that the cytoplasmic pH of

S. Typhimurium in LB pH 5.5 is decreased upon addition of $NaNO_2$. These data provide the first evidence that intracellular acidification is an additional antibacterial mode of action of acidified $NaNO_2$. The stress responses of EHEC to a 10 min shock and a 1 hour treatment with 150 mg/l $NaNO_2$ in LB pH 5.5 revealed both similarities and differences compared to the results from *S.* Typhimurium. The shock response was characterized by up-regulation of NsrR- and NorR-controlled genes similar to *S.* Typhimurium. Moreover, three YhcN family genes, which have previously been linked to biofilm growth and stress tolerance, displayed higher transcript levels. Prolonged acidified nitrite exposure resulted in additional up-regulation of multiple stress-related genes, including genes of the glutamate-dependent acid resistance system, supporting intracellular acidification as potential action mode of nitrite on Gram-negative bacteria. The RNA-seq data further indicate stringent control of high-energy processes such as translation and cell motility. Favoring survival over growth seems to be a common strategy of *S.* Typhimurium and EHEC to overcome harsh acidified $NaNO_2$ stress.

Although data provided herein and by other studies clearly indicate a positive impact of the addition of nitrite or nitrate on the microbiological safety of raw sausages, these chemical preservatives are considered critical by some consumers. Therefore, another part of this study dealt with the search for natural nitrate curing salt (KNO_3) substitutes. Different plant extracts were screened for antimicrobial activity on *S.* Typhimurium and EHEC. Celery extract reduced cell culture density of both bacteria *in vitro*; however, transcriptome data of *S.* Typhimurium cultivated in the presence of KNO_3 or celery extract were nearly identical. This congruence contradicts the idea of a growth-inhibitory phytochemical in the celery extract.

In conclusion, this study provides evidence that acidified nitrite acts via multiple modes of action to inhibit cell growth of *S.* Typhimurium and EHEC, which, in turn, seem to deploy common as well as individual strategies to cope with this stress.

Zusammenfassung

Nitritpökelsalz ($NaNO_2$) wird traditionell zur Konservierung bei der Rohwurstherstellung eingesetzt. Unter den sauren Bedingungen in der Fleischmatrix entstehen reaktive Nitrit-Derivate, unter anderem Stickstoffmonoxid (NO). Die Mechanismen, die der antimikrobiellen Wirkung von angesäuertem Nitrit auf die Gram-negativen Lebensmittelpathogene *Salmonella* und enterohämorrhagische *Escherichia coli* (EHEC) zugrunde liegen, sind allerdings kaum verstanden. Zusätzlich sind die Gegenmaßnahmen größtenteils unbekannt, welche diese Bakterien zur Bekämpfung von saurem $NaNO_2$-Stress ergreifen.

In dieser Arbeit wurde die Wirkung von $NaNO_2$ auf *Salmonella* (*S.*) Typhimurium 14028 und EHEC O157:H7 EDL933 unter lebensmittelrelevanten Aspekten mittels Transkriptionsstudien, Wachstumsversuchen und der Analyse von Mutanten untersucht.

In vitro Wachstumsversuche von *S.* Typhimurium Einzeldeletionsmutanten der wichtigsten NO-entgiftenden Systeme Flavohämoglobin (Δ*hmpA*), Flavorubredoxin (Δ*norV*) und der Cytochrom *c* Nitrit-Reduktase (Δ*nrfA*) zeigten einen Wachstumsdefekt von Δ*hmpA* in Gegenwart von saurem $NaNO_2$. Eine deutliche Transkriptionserhöhung von *hmpA* im Wildtyp (WT) wurde bei Behandlung mit 150 mg/l saurem $NaNO_2$ mittels qPCR beobachtet. Dagegen ergaben Challenge-Versuche von Kooperationspartnern mit kurzgereiften streichfähigen Rohwürsten, die entweder mit 0 oder 150 mg/kg $NaNO_2$ hergestellt wurden, für keine der Mutanten einen Phänotyp im Vergleich zum WT. Somit ist keines der NO-entgiftenden Systeme HmpA, NorV und NrfA alleinig für die nitrosative Stresstoleranz von *S.* Typhimurium in Rohwürsten verantwortlich.

Globale Transkriptomanalysen wurden durchgeführt um die Wirkung von saurem Nitrit auf *S.* Typhimurium näher zu untersuchen. Die transkriptionellen Antworten auf den NO-Donor Natrium-Nitroprussid (SNP), auf saures $NaNO_2$ in LB Medium (10 min Schock- und Anpassungsantwort) und in Medien, welche die Rohwurstbedingungen an den Reifetagen 0 (RT0) und 3 (RT3) simulieren, wurden mittels RNA-Sequenzierung (RNA-seq) ermittelt. Abgesehen von der Induktion einer durch die NO-sensitiven Regulatoren NsrR und/oder NorR vermittelten NO-spezifischen Antwort, wurden mehrere andere stressassoziierte Gene durch 150 mg/l saures $NaNO_2$ in LB Medium (Säuretoleranz Systeme) und an RT0 (Kupfertoleranzgene) spezifisch hochreguliert. Außerdem führte saurer $NaNO_2$ Schock zu verminderten Transkriptleveln von Genen, die an der Translation, Transkription, Replikation und Motilität beteiligt sind. Die Aktivierung von Stresstoleranz und eine verminderte Zellvermehrung fördern offensichtlich das Überleben unter starkem, saurem Nitritstress. Im Gegensatz dazu beeinflusste die Restmenge von 30 mg/l $NaNO_2$ an RT3 das Transkriptom von *S.* Typhimurium nicht. Die RNA-seq Daten zeigten jedoch massive transkriptionelle Veränderungen an RT3 im Vergleich zu RT0, welche auf erhöhten Stress und Wachstumsarrest an RT3 hindeuten. Diese Daten stützen die Bedeutung zusätzlicher Hürden außer Nitrit, um zu späteren Zeitpunkten der Rohwurstreifung ungünstige Wachstumsbedingungen zu schaffen.

Auffallend war, dass eine Unterbrechung des *cadA* Gens, das für die Lysin-Decarboxylase codiert und unter saurem Nitritschock stark induziert wurde, die Sensitivität gegenüber angesäuertem $NaNO_2$ erhöhte. Die Induktion von bekannten Säureresistenzsystemen deutet auf eine durch Nitrit bedingte Erhöhung des Säurestresses hin. Intrazelluläre pH-Messungen unter Verwendung einer pH-sensitiven GFP Variante ergaben, dass die Zugabe von $NaNO_2$ den zytoplasmatischen pH-Wert von *S.* Typhimurium in LB pH 5.5 herabsetzt. Diese Daten zeigen erstmals, dass die intrazelluläre Ansäuerung einen zusätzlichen antibakteriellen Wirkmechanismus von angesäuertem $NaNO_2$ darstellt.
Die Stressantworten von EHEC auf einen 10-minütige Schock und eine 1-stündige Behandlung mit 150 mg/l $NaNO_2$ in LB pH 5.5 zeigten sowohl Übereinstimmungen als auch Abweichungen im Vergleich zu den Ergebnissen aus *S.* Typhimurium. Die Schockantwort war gekennzeichnet durch die Hochregulation NsrR- und NorR-kontrollierter Gene ähnlich wie in *S.* Typhimurium. Darüber hinaus zeigten drei Gene der YhcN Familie, die bereits mit Biofilmwachstum und Toleranz gegenüber verschiedenen Stressoren assoziiert wurden, erhöhte Transkriptlevel. Länger andauernde Exposition gegenüber saurem Nitrit führte zu einer zusätzlichen Hochregulation vielfältiger stressassoziierter Gene, darunter auch welche des Glutamat-abhängigen Säureresistenz Systems. Dies stützt wiederum die intrazelluläre Ansäuerung als möglichen Wirkmechanismus von saurem Nitrit auf Gram-negative Bakterien. Die RNA-seq Daten deuten außerdem daraufhin, dass energieaufwendige Prozesse wie die Translation und die Zellmotilität stringent kontrolliert wurden. Dass das Überleben dem Wachstum vorgezogen wird, scheint eine gemeinsame Strategie von *S.* Typhimurium und EHEC zu sein, um extremen, sauren $NaNO_2$ Stress zu überstehen.
Obwohl die Daten dieser und anderer Studien stark darauf hindeuten, dass die Zugabe von Nitrit und Nitrat sich positiv auf die mikrobielle Sicherheit von Rohwurstprodukten auswirkt, stehen manche Verbraucher diesen chemischen Konservierungsstoffen kritisch gegenüber. Ein weiterer Teil dieser Arbeit beschäftigte sich deshalb mit der Suche nach einem natürlichen Ersatz für Nitratpökelsalz (KNO_3). Verschiedene Pflanzenextrakte wurden hinsichtlich ihrer antimikrobiellen Wirkung auf *S.* Typhimurium und EHEC untersucht. Ein Sellerieextrakt reduzierte die Zellkulturdichte beider Bakterien *in vitro*; die Transkriptomdaten von *S.* Typhimurium Kulturen, welche in Gegenwart von KNO_3 oder Sellerie gezogen wurden, waren jedoch annähernd gleich. Diese Übereinstimmung widerspricht der Idee eines wachstumsinhibierenden sekundären Pflanzenstoffes im Sellerieextrakt.
Schlussfolgernd liefert diese Arbeit Beweise dafür, dass angesäuertes Nitrit mittels mehrerer Wirkmechanismen das Wachstum von *S.* Typhimurium und EHEC hemmt. Diese scheinen ihrerseits sowohl gemeinsame als auch individuelle Strategien gegen diesen Stress anzuwenden.

I Introduction

1 The Gram-negative enteropathogens *Salmonella* and enterohemorrhagic *Escherichia coli* (EHEC) and their significance to the food industry

Non-typhoidal *Salmonella* gastroenteritis is a major health burden, with an estimated 93.8 million cases worldwide each year, of which the vast majority (estimated 80.3 million) is foodborne (Majowicz *et al.*, 2010). In the European Union, salmonellosis with a total of 88,715 confirmed human cases was the second most commonly reported zoonotic disease in 2014, following campylobacteriosis (EFSA, 2015). Although the incidence of infections with Shiga toxin-producing *Escherichia coli* (STEC) is lower (Majowicz *et al.*, 2014; EFSA, 2015), STEC cases may suffer from severe sequelae (Mead and Griffin, 1998; Tarr *et al.*, 2005; Gould *et al.*, 2009). Hence, these bacteria comprise important Gram-negative food-associated enteropathogens.

Salmonella is a genus of Gram-negative, rod-shaped, facultative anaerobic bacteria closely related to *E. coli* within the family Enterobacteriaceae. The genus is subdivided into two species, *S. bongori* and *S. enterica*, the latter of which comprises six subspecies with over 2500 serovars (Tindall *et al.*, 2005). While typhoidal *Salmonella* serovars such as *S.* Typhi and *S.* Parathypi cause enteric fever in humans, non-typhoidal *Salmonella* serovars such as *S.* Typhimurium and *S.* Enteritidis are commonly associated with self-limiting gastroenteritis (Coburn *et al.*, 2007). About 5% of patients with gastrointestinal illness caused by non-typhoidal *Salmonella*, especially young children and immunocompromised patients, develop bacteremia, a serious potentially life-threatening complication (Hohmann, 2001; Gordon, 2008). *S.* Typhimurium and *S.* Enteritidis naturally reside within the gastrointestinal tract of animals, commonly in those of chicken and farm animals such as pigs and cattle. Hence, infections are mostly acquired via consumption of contaminated food such as eggs and raw meat (EFSA, 2015).

The ability of *S.* Typhimurium to actively invade host cells and replicate intracellularly is crucial for its pathogenesis. Upon ingestion, *S.* Typhimurium reaches the stomach. An adaptive acid tolerance response (ATR) might enable some bacteria to survive the harsh acidic conditions there (Foster and Hall, 1991). After colonizing the intestine, salmonellae cross the intestinal barrier by entering through M cells of the Payer's patches and invading enterocytes via bacterial-mediated endocytosis (Haraga *et al.*, 2008). *S.* Typhimurium uses a trigger mechanism, causing actin rearrangement and membrane ruffles that engulf the bacteria (Finlay *et al.*, 1991). Modulation of host cell signaling and bacterial internalization induce a local inflammatory response, which eventually causes diarrhea (Haraga *et al.*, 2008). Once inside the cell, salmonellae survive and multiply in a modified phagosome, referred to as the *Salmonella* containing vacuole (SCV) (Haraga *et al.*, 2008). Across the intestinal epithelium, *Salmonella* are engulfed by phagocytic cells, and transported to the lymph nodes. Migration of infected macrophages, in which *Salmonella* again survive and replicate within SCVs, supports systemic dissemination of the bacteria via the bloodstream to tissues (Fabrega and Vila, 2013).

The ability for the intracellular lifestyle of *S.* Typhimurium principally depends on two type three secretion systems (T3SS) encoded within two *Salmonella* pathogenicity islands (SPI), SPI1 and SPI2. While effectors of SPI1 are responsible for the intestinal colonization, invasion of host cells and the onset of inflammation and diarrhea, the SPI2 T3SS mediates intracellular survival and replication as well as systemic dissemination (Fabrega and Vila, 2013). However, there is evidence that argues against this simplistic division and rather points to a cooperative function of these two T3SS in intracellular pathogenesis (Haraga *et al.*, 2008).

Since *Salmonella* effectively mount protective responses to numerous stressors, including acid and osmolarity, they can survive food conservation procedures (Humphrey, 2004; Shen and Fang, 2012).

EHEC is a diarrheagenic pathotype of the commensal gut bacterium *E. coli* that has evolved by the acquisition of several virulence factors via mobile genetic elements (Reid *et al.*, 2000). EHEC are a subtype of STEC characterized by the presence of one or two Shiga toxins (Stx), encoded on a lambda-like bacteriophage in the genome, the locus of enterocyte effacement (LEE) pathogenicity island (PAI) and the 93 kb virulence plasmid pO157 (Nataro and Kaper, 1998). The serotype O157:H7 was first associated with human illness in two outbreaks of hemorrhagic colitis after consumption of undercooked meat in 1982 (Riley *et al.*, 1983). Cattle are the main reservoir of EHEC (Ferens and Hovde, 2010). Human infections range from asymptomatic over abdominal cramps and non-bloody diarrhea to heamorrhagic colitis, that resolves in 95% of the cases. However, about 5% of patients develop the life-threatening hemolytic-uremic syndrome (HUS), which is fatal in 3-5% of the cases, or suffer from severe sequelae (Mead and Griffin, 1998). In this context, the serotype O157:H7 has been most often associated with HUS (Tarr *et al.*, 2005).

After ingestion of as little as 10-100 bacteria, EHEC survive the harsh aciditity of the stomach thanks to their intricate acid resistance system and reach the colon (Kaper *et al.*, 2004). After initial adherence, the bacteria express a LEE-encoded T3SS and inject effector proteins into the host cell cytosol similar to *Salmonella* (Kaper *et al.*, 2004). However, in marked contrast to *Salmonella*, EHEC remain extracellular and intimately attache to the cell by inducing cytoskeletal rearrangements that result in the destruction of microvilli and the formation of a pedestal like structure under the attachment site (Kaper *et al.*, 2004). These characteristic histopathological alterations are referred to as attaching and effacing lesions. The severity of disease depends on the expression of Stx, also known as verocytotoxin (VT). EHEC O157:H7 produce Shiga toxins Stx1 and Stx2, which share about 55% amino acid homology and of which Stx2 is epidemiologically most frequently linked to HUS (Kaper *et al.*, 2004; Ostroff *et al.*, 1989; Boerlin *et al.*, 1999). Stx is an AB_5 toxin. The five B-subunits mediate binding of the holotoxin to the cell surface glycolipid globotriaosylceramide (Gb_3), while the translocated A-subunit cleaves ribosomal RNA, resulting in a stop of protein synthesis and also in apoptosis of the affected cells (Bergan *et al.*, 2012). Besides local damage in the colon, Stx is systemically distributed via the blood-stream and preferentially targets Gb_3-rich endothelial cells of the kidney. HUS may then be the result of the damage

of renal endothelial cells combined with inflammatory processes leading to occlusion of the microvasculature (Kaper *et al.*, 2004).
Similar to *Salmonella*, EHEC are highly adaptable and can survive adverse conditions, including acid and heat, thereby posing a challenge to food manufacturing (Chung *et al.*, 2006).

Being natural residents of the gastrointestinal tract of farm animals and having a high prevalence in the farm environment (Blanco *et al.*, 2004; Baer *et al.*, 2013; Callaway *et al.*, 2008), one important transmission route of *Salmonella* and EHEC is ingestion of raw or inadequately cooked animal produce, including meat (EFSA, 2015). Pig and bovine meat are traditionally used in the production of raw fermented sausages in Germany (Federal Ministry of Food and Agriculture, 2010). Both bacteria are known to be present in the raw material (Meyer *et al.*, 2010; Delhalle *et al.*, 2009; Prendergast *et al.*, 2009; Schmid *et al.*, 2008; Beutin *et al.*, 2007) and can survive the maturation process of raw sausages (CDC, 1995; Glass *et al.*, 1992; Birzele *et al.*, 2005; Dourou *et al.*, 2009). Indeed, there are reported outbreaks of *E. coli* O157:H7 and *S.* Typhimurium that were traced back to raw sausage products (CDC, 1995; Williams *et al.*, 2000; MacDonald *et al.*, 2004; Hjertqvist *et al.*, 2006; Nygard *et al.*, 2007; Luzzi *et al.*, 2007). According to the legislation of the European Union, there is a zero tolerance policy for *Salmonella* and EHEC in ready-to-eat meat products (European Commission, 2005). Upon detection of these bacteria, the contaminated products are consequently withdrawn from the market, which is associated with considerable financial loss and reputational damage for the respective company. Hence, combating these two bacteria is crucial to the meat processing industry.

2 The function of the curing agent sodium nitrite ($NaNO_2$) in the production of raw sausages

In food preservation, the hurdle technology is a potent concept to prevent or control the outgrowth of undesired microorganisms (Leistner, 2000). Different preservation measures, so called hurdles, are sequentially or concurrently combined in the course of the manufacturing process, resulting in safe and stable foods while preserving their sensory and qualitative properties (Leistner, 2000). In raw sausage ripening, initially added preservatives (curing salts such as sodium nitrite ($NaNO_2$) or potassium nitrate (KNO_3)), a decrease in the redox potential (low Eh) as well as acidification (low pH) and drying (low water activity a_w) are important hurdles at different stages. Regarding nitrite (NO_2^-) added as $NaNO_2$, its presence is especially critical at the early stages of ripening (Leistner and Gorris, 1995).
The use of curing salts has a long tradition in the fermentation of raw meat products. Besides contributing to the microbiological safety of the product, nitrite is responsible for the formation of the characteristic and heat-stable red color, contributes to the curing flavor and acts as an effective antioxidant (Jira, 2004). If nitrate (NO_3^-) is used for curing, it is converted to nitrite during the ripening process by nitrate-reducing starter cultures, thereby serving as a nitrite reservoir.

Nitrite is converted to reactive nitrogen species (RNS) in a series of complex chemical reactions in the meat matrix (Figure 1), which are influenced by meat ingredients and additives such as salt or the cure accelerator sodium ascorbate (Skibsted, 2011). Under the slightly acidic conditions (pH 5.5) in the meat due to the presence of lactic acid, nitrite is protonated to nitrous acid (HNO_2), which is in equilibrium with its anhydride, dinitrogen trioxide (N_2O_3) (Skibsted, 2011). N_2O_3, a potent nitrosating agent, primarily targets thiol groups and secondary amines, resulting in the formation of *S*-nitrosothiols and *N*-nitrosamines, respectively (Ridnour *et al.*, 2004). N_2O_3 may further disproportionate into nitric oxide (NO) and nitrogen dioxide (NO_2) (Skibsted, 2011). NO_2 reacts with water to reform HNO_2 and additionally nitric acid (HNO_3), which dissociates to form nitrate (Honikel, 2008). The reaction of nitrite /N_2O_3 with ascorbic acid/ascorbate further fosters the formation of NO and abrogates the reaction of N_2O_3 with secondary amines, thereby reducing the formation of potentially toxic *N*-nitrosamines in the product (Skibsted, 2011).

NO is a key reactant, since it can participate both in oxidative and reductive chemistry (Fukuto *et al.*, 2000). Being a free radical gas it rapidly reacts with other radical species or with metals (Ridnour *et al.*, 2004). By reacting with lipid-derived radicals, e.g. peroxyl radicals ($LOO^{\cdot}$), formed in the meat, NO is capable of terminating lipid peroxidation (Skibsted, 2011). The antioxidant property of NO contributes to product stability and prolongs shelf-life (Jira, 2004). On the other hand, in the presence of superoxide radical (O_2^{-}) in the meat batter, the highly prooxidative peroxynitrite ($ONOO^{-}$) can be formed (Cammack *et al.*, 1999), which may mediate oxidative damage to macromolecules, including DNA strand-breaks, oxidation or nitration of functional amino acid groups in proteins (e.g. tyrosine nitration) and lipid peroxidation (Miranda *et al.*, 2000). Concerning its reactivity with metals, NO forms nitrosyl complexes most notably with metalloproteins containing iron (Miranda *et al.*, 2000). Whereas low NO concentrations are sufficient to react with heme, higher concentrations of NO may allow modification of iron-sulfur (Fe-S) clusters (Miranda *et al.*, 2000). Nitrosylation of the heme in myoglobin results in the formation of nitrosylmyoglobin. This complex is attributable for the characteristic red color of cured meat and was first identified by Haldane in 1901. Potential important reactants in the complex series of reactions resulting in the formation of the red meat pigment also include the primarily added nitrite and probably nitroxyl (HNO) (Skibsted, 2011). Although only residual amounts of nitrite *per se* are detectable following the first days of ripening, nitrosylated proteins might serve as a long-term reservoir of NO and nitrosating agents (Skibsted, 2011).

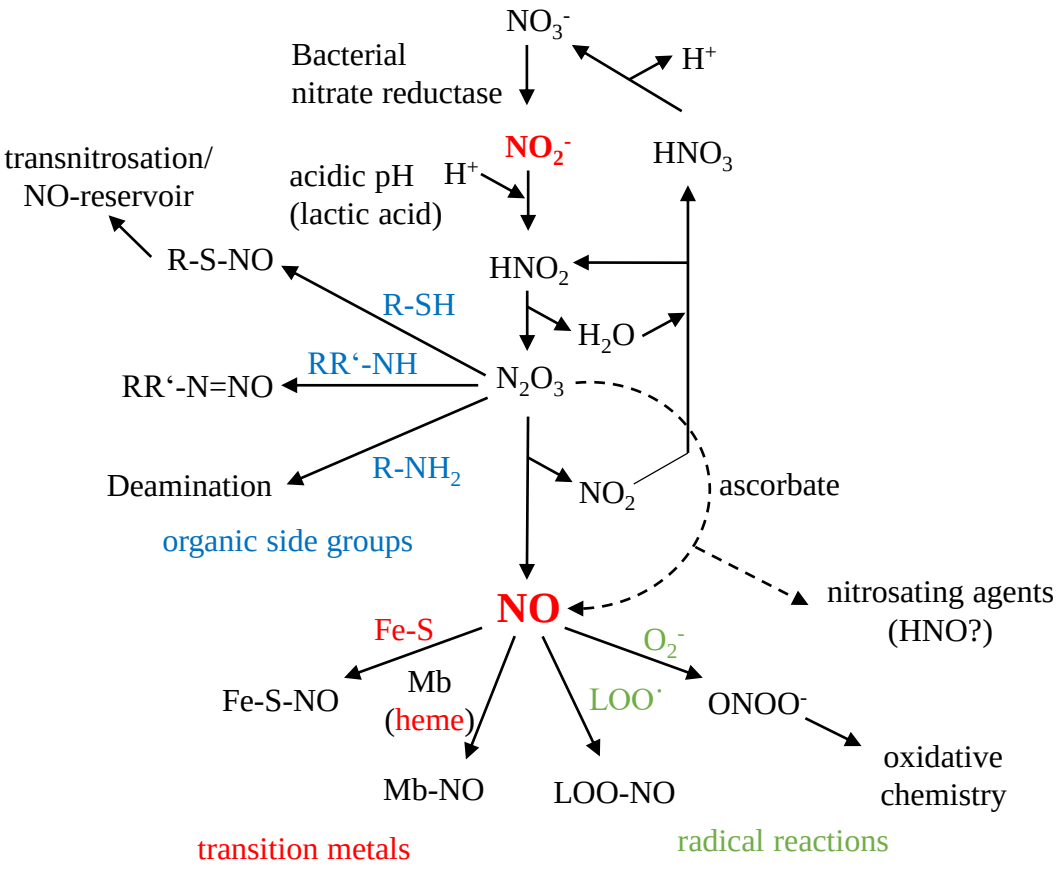

Figure 1: Simplified representation of important chemical reactions of nitrite in meat.
Reactions shown are according to Honikel (2008), Skibsted (2011) and Fukuto *et al.* (2000), and explained in the text. R-SH: reduced thiol group, R-S-NO: nitrosothiol, RR'-NH: secondary amine group, RR'-N=NO, nitrosamine; $R-NH_2$: amino group, Fe-S: iron-sulfur cluster, Fe-S-NO: iron-sulfur-nitrosyl complex, Mb: myoglobin, Mb-NO: nitrosylmyoglobin, LOO·: lipid peroxyl radical, LOO-NO: non-radical addition product, O_2^-: superoxide, $ONOO^-$: peroxynitrite, HNO: nitroxyl. The dashed line indicates that the reaction includes several intermediates, which are not depicted.

3 Bacterial targets of nitrite and RNS

The inhibitory effect of nitrite on the growth and toxin production of *Clostridium botulinum* is well documented (reviewed in Cammack *et al.*, 1999). Challenge assays were previously performed by cooperation partners from the Max Rubner Institute (MRI) in Kulmbach to investigate the impact of $NaNO_2$ on *Salmonella* and EHEC in short-ripened spreadable type sausages (Rohtraud Pichner and Jan Kabisch, personal communication). For each genus, pools of strains and serovars associated with a high danger potential in sausage manufacturing were used. This study revealed, that *Salmonella* and EHEC can survive the ripening process in short-ripened type sausages (Kabisch, 2014). Strikingly, addition of nitrite to the sausages had a different impact on growth and survival of these pathogens.

Whereas addition of 50 - 200 mg/l $NaNO_2$ to a tea sausage spread inhibited multiplication of *Salmonella* spp. in the first few days of ripening compared to a sausage produced without $NaNO_2$, survival of EHEC was not affected by $NaNO_2$. However, EHEC were incapable of growing in the product but still survived till the end of the maturation period. These findings indicate that *Salmonella* spp. and EHEC not only are differently prone to the prevalent conditions in the first few days of ripening, as shown by their distinct behavior in the sausages without $NaNO_2$, but also seem to respond differently to nitrite-mediated stress. To unravel the differential impact of nitrite-derived stress on bacterial pathogens, a deeper understanding of the molecular action on these organisms as well as of the protective countermeasures they mount is required.

NO and a myriad of RNS are produced from nitrite in the meat matrix (Figure 1), which not only modify meat compounds, but may also interact with macromolecules of the bacterial cells (Cammack *et al.*, 1999). Due to its small stokes radius and lipophilic character, NO can easily pass across biological membranes and, thereby, also enter bacterial cells (Denicola *et al.*, 1996). Thus, DNA and proteins were identified as major microbial targets subjected to modification by RNS (Fang, 1997, 2004). Interference with crucial cellular processes contributes directly to NO-mediated bacteriostasis.

DNA can be directly modified by NO congeners. HNO_2 and $ONOO^-$ induce deamination of nucleobases and oxidative damage of DNA (Wink *et al.*, 1991; Burney *et al.*, 1999). HNO_2 and its anhydride N_2O_3 deaminate the DNA bases guanine, adenine and cytosine generating the base analogs xanthine, hypoxanthine and uracil, respectively. Due to their different pairing specificities, transition mutations during DNA replication may occur. $ONOO^-$ primarily confers oxidative DNA damage, including abasic sites and single strand-breaks (Fang, 1997). Impairment of DNA integrity as one mode of the antimicrobial action of NO congeners is further supported by the increased sensitivity of *E. coli* and *Salmonella* strains missing different DNA repair systems (Schouten and Weiss, 1999; Spek *et al.*, 2001; Richardson *et al.*, 2009).

Besides targeting DNA directly, NO and congeners were found to modify proteins involved in DNA synthesis. The tyrosyl radical of ribonucleotide reductase, whose activity in providing deoxyribonucleotides is rate-limiting for DNA synthesis, was shown to be quenched by RNS (Lepoivre *et al.*, 1991; Lepoivre *et al.*, 1994). Moreover, zinc mobilization from DNA-binding zinc metalloproteins under nitrosative stress has been connected to arrest of DNA replication in *S.* Typhimurium (Schapiro *et al.*, 2003).

Moreover, the bacteriostatic action of NO and RNS might result from metabolic constraints imposed by modification of proteins in central cellular functions. Fe-S proteins constitute one crucial group highly susceptible to modification by NO. NO-mediated formation of protein-bound dinitrosyl-iron complexes (DNICs) has been observed in *E. coli* (Ren *et al.*, 2008; Landry *et al.*, 2011). The solvent-exposed [4Fe-4S] clusters of dihydroxyacid dehydratase IlvD and aconitase were found to be highly sensitive to NO (Duan *et al.*, 2009), interfering with branched-chain amino acid synthesis and the tricarboxylic acid (TCA) cycle in the central metabolism of *E. coli*, respectively (Ren *et al.*, 2008; Hyduke *et al.*, 2007;

Gardner *et al.*, 1997). Heme proteins constitute a second group of proteins found to be targeted by NO in bacteria. Thus, bacterial respiration was found to be transiently arrested by interaction of NO with terminal oxidases (Yu *et al.*, 1997; Stevanin *et al.*, 2000; Stevanin *et al.*, 2002; Borisov *et al.*, 2004). In *Salmonella*, lipoamide dehydrogenase (LpdA), which contains a redox-active cysteine residue and is essential for the catalytic function of the pyruvate and alpha-ketoglutarate dehydrogenase complexes in the TCA cycle, has been identified as one key metabolic target of NO, resulting in massive metabolic perturbations including a transient auxotrophy for methionine and lysine (Richardson *et al.*, 2011). Moreover, there is evidence that Fe-S enzymes involved in branched-chain amino acid synthesis are inactivated by NO in *S.* Typhimurium (Park *et al.*, 2011; Park *et al.*, 2015).

Another antimicrobial action of NO might be interference with adaptive stress responses, which are necessary for the pathogens' survival in adverse environments. For example, NO was found to interfere with the PhoPQ signaling cascade necessary to mount the ATR in *Salmonella* (Bourret *et al.*, 2008), which is a prerequisite to pass the acidic stomach or survive in acidic foodstuff.

4 Bacterial tolerance to NO and RNS

The different susceptibility of bacteria to nitrite and derived RNS might be ascribed to their different equipment with metabolic pathways to use nitrite and detoxify toxic derivatives such as NO.

4.1 Sources of exogenous and endogenous NO

Salmonella and *E. coli* naturally encounter exogenously or endogenously produced NO (Figure 2A).

As enteric bacteria, they are subjected to exogenous NO in their natural habitat, the gastrointestinal tract of mammalian hosts. NO is a gaseous mediator of versatile physiological functions in mammalian cells, such as vasodilation, hypoxic signaling and neurotransmission (Moncada *et al.*, 1991). NO is generated either non-enzymatically from salivary nitrite in the acidic and reducing (vitamin C/ascorbic acid) milieu of the stomach (Lundberg *et al.*, 1994), or is produced enzymatically by the host nitric oxide synthase (NOS) from L-arginine (Moncada and Higgs, 1993). The production of high levels of NO by the inducible NOS isoform (iNOS) in phagocytes upon infection provides a crucial antimicrobial defense mechanism of the host innate immunity (Chakravortty and Hensel, 2003).

Endogenous NO, on the other hand, emerges as a by-product of anaerobic nitrate and nitrite metabolism in *S.* Typhimurium and *E. coli* (Gilberthorpe and Poole, 2008; Corker and Poole, 2003; Vine *et al.*, 2011). Upon shortening of their preferred electron acceptor oxygen (O_2), these facultative anaerobes can switch to anaerobic respiration using alternative terminal electron acceptors including nitrate and nitrite (Unden and Bongaerts, 1997). Nitrate and nitrite are transported across the cytoplasmic membrane via the membrane transporters NarK, NarU and NirC (Jia and Cole, 2005; Jia *et al.*, 2009).

Nitrate is reduced to nitrite by one of three nitrate reductases: the membrane-bound nitrate reductases A and Z (encoded by the *narGHJI* and *narZYWV* operons, respectively), with their catalytic subunits NarG and NarZ oriented towards the cytoplasm, or the periplasmic nitrate reductase Nap (Cole, 1996). The final step in dissimilatory nitrate reduction in enteric bacteria, the reduction of nitrite to NH_4^+, is likewise catalyzed by one of two nitrite reductase enzymes: either by the periplasmic cytochrome *c* nitrite reductase Nrf or the cytoplasmic NADH-dependent Nir nitrite reductase (Cole, 1996). Transcriptional activation of the operons encoding NarGHI, Nap, Nrf and Nir is mediated by the FNR (fumarate nitrate reduction) regulatory protein during anaerobic growth, and further modulated by the presence of nitrate/nitrite via the two component systems NarX/L and NarP/Q (Rabin and Stewart, 1993; Unden and Bongaerts, 1997). While the periplasmic pathway comprising of Nap and Nrf is efficient at low external nitrate concentrations, the cytoplasmic pathway with the energy-conserving NarGHI and NirBD is preferentially induced at high nitrate levels (Cole, 1996; Wang *et al.*, 1999; Wang and Gunsalus, 2000). The need to control levels of endogenously produced NO is underlined by the fact, that *S*-nitrosylation of proteins (Seth *et al.*, 2012) and DNA mutagenesis (Weiss, 2006) were reported to occur during anaerobic growth on nitrate.

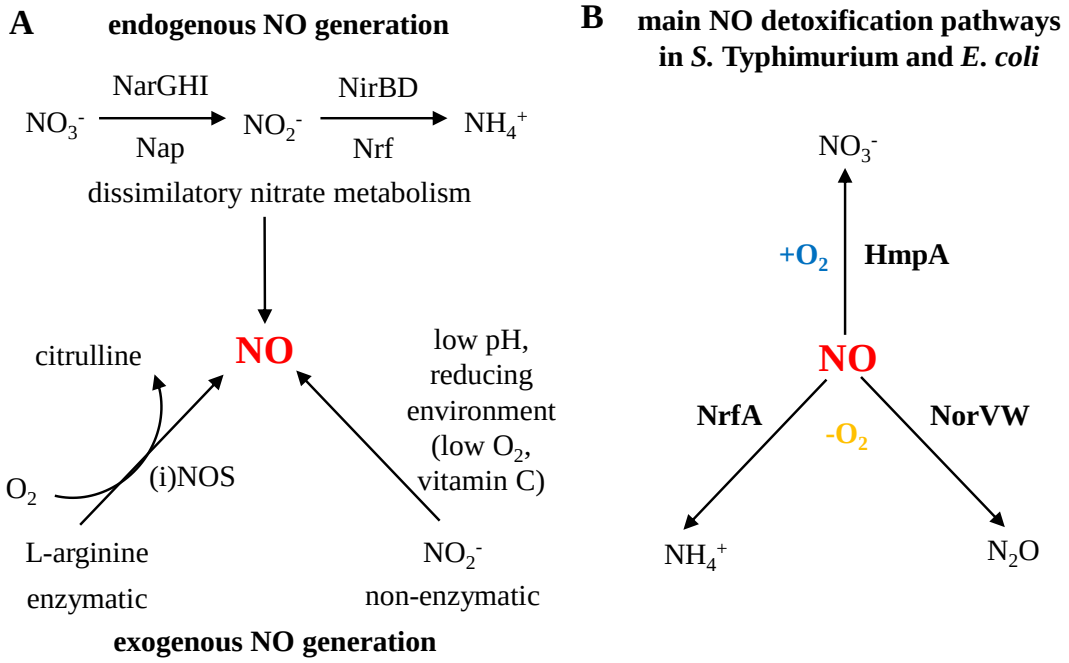

Figure 2: Overview of the exogenous and endogenous pathways for generation of NO (A) and the main NO detoxification pathways in *S.* Typhimurium and *E. coli* (B).

4.2 Bacterial tolerance systems against NO and reactive nitrite derivatives

As a consequence of being exposed to NO and concomitant RNS, *Salmonella* and *E. coli* have developed the ability to protect themselves against the cytotoxicity of these species by means of scavenging, repair of damaged DNA and proteins and, most important, detoxification.

4.2.1 Scavenging and repair of RNS-damaged DNA and proteins

The low-molecular-weight thiols homocysteine (Groote *et al.*, 1996) and glutathione (GSH) (Song *et al.*, 2013) present a first line of defense against the bacteriostatic activity of RNS by scavenging these reactive species and safeguarding enzymes containing redox active cysteines from *S*-nitrosylation.
More recently, it was reported that the export of reduced thiols by the glutathione/cysteine exporter CydDC provides protection against nitrosative stress in *E. coli* (Holyoake *et al.*, 2016).
The cytochrome *bd* terminal quinol oxidase of the respiratory chain was found to provide NO resistance in *E. coli* due to its high NO dissociation rate (Mason *et al.*, 2009). In addition, a role of cytochrome *bd* in the decomposition of $ONOO^-$ was reported recently (Borisov *et al.*, 2015). Scavenging of NO and RNS reduces but does not entirely prevent the insult imposed on the cell by these cytotoxic species.
However, the bacteria are capable of repairing damaged DNA and proteins.
The higher sensitivity to nitrosative DNA damage of mutants lacking components of the DNA base excision repair (BER) or the recombinational repair system indicates that these systems are important in maintaining DNA integrity under conditions of nitrosative stress (Schouten and Weiss, 1999; Spek *et al.*, 2001; Richardson *et al.*, 2009).
Regarding the repair of damaged Fe-S clusters, an important role has been ascribed to the di-iron protein YtfE, recently renamed RIC (repair of iron centers). Being one of the most strongly induced genes under nitrosative stress conditions, YtfE was shown to restore the activity of damaged Fe-S containing proteins (Justino *et al.*, 2007) and suggested to be important for the delivery of iron to Fe-S clusters, which was finally shown by Nobre *et al.* (2014). The concerted action of iron-donating YtfE and the sulfur-donating cysteine desulfurases IscS/SufS enables the reassembly of Fe-S clusters.
Moreover, the function of several genes, whose transcription is consistently up-regulated in response to sources of nitrosative stress, such as *nrdH* (glutaredoxin-like protein) or *ygbA* (uncharacterized protein), remains to be characterized.

4.2.2 Enzymatic NO detoxification

The most effective mean to reduce nitrosative stress is to enzymatically detoxify NO. Although evidence suggests that there are yet unresolved pathways involved in NO reduction (Vine and Cole, 2011b; Arkenberg *et al.*, 2011), so far, three systems demonstrably mediate NO detoxification under different conditions in *E. coli* and *Salmonella*: the flavohemoglobin HmpA, the flavorubredoxin NorV and the periplasmic cytochrome *c* nitrite reductase NrfA (Figure 2).

4.2.2.1 Flavohemoglobin HmpA

The flavohemoglobin HmpA (also Hmp) from *E. coli* was the first of the flavohemoglobin family discovered in 1991 (Vasudevan *et al.*, 1991). Flavohemoglobins are cytoplasmic monomeric proteins made of two domains: a C-terminal NAD- and FAD-binding domain, and an N-terminal heme *b* containing globin domain. The C-terminal reductase domain transfers electrons from NAD(P)H via FAD to heme-bound ligands (Bonamore and Boffi, 2008). In both *E. coli* and *S.* Typhimurium, the main regulator of *hmpA* transcription in response to nitrosative stress is the highly conserved NO-sensitive repressor NsrR (nitric oxide sensitive repressor), although some other transcription factors have been implicated in modulating *hmpA* transcription in *E. coli* (Forrester and Foster, 2012a).

Aerobically, HmpA catalyzes the oxidation of NO to nitrate by acting via a NO dioxygenase (Gardner *et al.*, 1998) or a denitrosylase (Hausladen *et al.*, 2001) mechanism, which is still under debate (Forrester and Foster, 2012a; Hausladen and Stamler, 2012; Forrester and Foster, 2012b). Under anoxic conditions *in vitro*, HmpA is able to reduce NO to N_2O (Kim *et al.*, 1999). The NO dioxygenase activity has been well characterized, and HmpA has been shown to protect aerobically grown *E. coli* (Gardner *et al.*, 1998; Hausladen *et al.*, 1998) and *S.* Typhimurium (Crawford and Goldberg, 1998) against the growth inhibitory effects of NO or NO releasers including acidified nitrite. In contrast, the physiological significance of the O_2-independent NO reductase activity remains to be fully elucidated. *HmpA* transcription is induced anaerobically by different sources of NO, including acidified nitrite (Mukhopadhyay *et al.*, 2004) and endogenously produced NO (Bodenmiller and Spiro, 2006) in *E. coli*, and an anaerobically grown *Salmonella hmpA* mutant was sensitive to the NO releaser GSNO (Crawford and Goldberg, 1998). However, it has been argued that the NO turnover number of HmpA is substantially less under anaerobic than under aerobic conditions (Gardner and Gardner, 2002). Therefore, it is assumed that NO detoxification under anaerobic conditions is mainly attributed to NorV and NrfA.

In the context of pathogenesis, HmpA has been shown to contribute to *Salmonella* virulence (Bang *et al.*, 2006) and to its protection against nitrosative stress *in vivo* (Gilberthorpe *et al.*, 2007; Karlinsey *et al.*, 2012; McCollister *et al.*, 2007; Stevanin *et al.*, 2002). Concerning pathogenic *E. coli*, it was found to be important for resistance of uropathogenic *E. coli* (UPEC) to RNS (Svensson *et al.*, 2010), but did not contribute to protect EHEC from NO-related killing in macrophages (Shimizu *et al.*, 2012).

4.2.2.2 Flavorubredoxin NorV

The enterobacterial *norV* gene encodes the O_2-sensitive NO reductase flavorubredoxin. This protein is built of two core domains common to A-type flavoproteins, namely a metallo-ß-lactamase-like domain at the N-terminal region, harboring a non-heme di-iron site, and a flavodoxin-like domain, containing one FMN moiety (Gomes *et al.*, 2002). In addition, flavorubredoxin possesses a C-terminal module containing a rubredoxin-like center (Gomes *et al.*, 2002). Downstream adjacent to the *norV* gene is a gene, *norW*, encoding a NADH:rubredoxin oxidoreductase (Gardner *et al*., 2002). Both genes possibly form a dicistronic transcription unit. The gene coding for the NO-responsive transcriptional regulator, NorR (Hutchings *et al.*, 2002), is oppositely transcribed from the *norVW* operon. *NorV* transcription is up-regulated upon exposure to a variety of NO sources including acidified nitrite (Mukhopadhyay *et al.*, 2004; Justino *et al.*, 2005) and depends on its regulator NorR (Hutchings *et al.*, 2002; Mukhopadhyay *et al.*, 2004).

NorV catalyzes the reduction of NO to N_2O under anoxic and microoxic conditions (Gardner *et al.*, 2002; Gomes *et al.*, 2002). Electrons for reduction of NO are supplied via the electron transfer chain rubredoxin – FMN – diferrous center, to which presumably two NO molecules bind. These are univalently reduced to form nitroxyl anions, which combine to form N_2O and water (Gomes *et al.*, 2000; Gomes *et al.*, 2002). For turnover, the NADH-dependent oxidoreductase NorW would supply two electrons via the rubredoxin domain of NorV (Gomes *et al.*, 2000).

An *E. coli norV* deletion mutant showed impaired anaerobic growth in the presence of NO under growth conditions which require the function of NO-sensitive enzymes such as those involved in gluconate metabolism (6-phosphogluconate dehydratase) or branched-chain amino acid biosynthesis (α,β-dihydroxyacid dehydratase) (Gardner *et al.*, 2002). Results obtained with *S.* Typhimurium deletion mutants of NO-detoxifying enzymes revealed a combined protective effect of NorV and NrfA against NO under anaerobic conditions *in vitro* (Mills *et al.*, 2005; Mills *et al.*, 2008), and *norV* is up-regulated in macrophage-internalized *Salmonella* at a time corresponding to the NO-burst (Eriksson *et al.*, 2003). Interestingly, the *norV* copies in EDL933 and Sakai, two EHEC strains, have a 204 bp deletion resulting in loss of 68 amino acids spanning the entire flavodoxin domain (Hayashi *et al.*, 2001; Perna *et al.*, 2001). This truncated NorV, designated NorVs, loses its NO reductase activity and is incapable to protect cells from NO-mediated growth inhibition under anaerobic conditions (Shimizu *et al.*, 2012). Kulasekara *et al.* (2009) found that the presence of an intact *norV* gene in strain TW14359 correlated with increased virulence and greater propensity for development of HUS (Kulasekara *et al.*, 2009). What is more, NorV-type EHEC strains showed a higher level of Stx2 production and better survival in macrophages (Shimizu *et al.*, 2012). The rationale for loss of this virulence determinant in EHEC strains EDL933 and Sakai is unclear.

4.2.2.3 Periplasmic cytochrome *c* nitrite reductase NrfA

The periplasmic cytochrome *c* nitrite reductase NrfA is thought to catalyze the anaerobic five-electron reduction of NO besides the six-electron reduction of nitrite to ammonium (NH_4^+) and, thus, to participate in NO detoxification (Poock *et al.*, 2002; van Wonderen *et al.*, 2008). NrfA constitutes the catalytic subunit of the Nrf nitrite reductase complex, which has a well-established role in contributing to the membrane potential by coupling quinol oxidation to nitrite reduction during anoxic or microoxic growth in the presence of nitrate or nitrite (Simon, 2002).

The *nrf* operon (*nrfABCDEFG*) is activated by FNR under anaerobiosis and is additionally induced under low-nitrate growth conditions by NarL and NarP while it is repressed at high nitrate concentrations by NarL (Wang and Gunsalus, 2000). Consistent with a role in NO detoxification, NsrR in *E. coli* K-12 has been shown to be a weak repressor of the complex *nrfA* promotor (Filenko *et al.*, 2007; Browning *et al.*, 2010). In contrast to *E. coli*, the *Salmonella nrfA* promoter seems not to be subject to NsrR-dependent regulation (Browning *et al.*, 2010).

E. coli mutants lacking *nrfA* were shown to be more sensitive to NO under anaerobic growth conditions (Poock *et al.*, 2002). Since the K_m for NO removal of NrfA is much higher than that of flavohemoglobin or flavorubredoxin, is has been proposed that NrfA detoxifies exogenously produced NO encountered in the periplasm, thereby maintaining low NO levels that diffuse into the cytoplasm (van Wonderen *et al.*, 2008). In *S.* Typhimurium, NrfA has been shown to protect bacteria in anoxic environments acting in concert with NorV, at least under growth conditions under which NrfA is active (Mills *et al.*, 2005; Mills *et al.*, 2008).

4.3 Regulators of the bacterial response to NO

Adaptive bacterial responses to NO and nitrosative stress are regulated either by dedicated or by secondary NO sensors. Dedicated NO sensors, such as NsrR and NorR, mediate a physiological response to NO. On the other hand, secondary NO sensors, including FNR, Fur (ferric uptake regulator) and SoxR, principally sense another signal, but their activity can be modulated by NO (Spiro, 2007).

4.3.1 Primary NO sensors NsrR and NorR

NsrR is a dedicated NO-sensitive transcriptional repressor mediating the nitrosative stress response in *E. coli* (Bodenmiller and Spiro, 2006; Filenko *et al.*, 2007) and *S.* Typhimurium (Gilberthorpe *et al.*, 2007; Karlinsey *et al.*, 2012). It belongs to the Rrf2 family of transcription factors and directly senses NO via a Fe-S cluster (Tucker *et al.*, 2010). After controversies regarding the nature of the cluster (Tucker *et al.*, 2010), recent studies indicate that NsrR accommodates a [4Fe-4S] cluster (Crack *et al.*, 2015). The presence of an iron-containing cofactor provides a reasonable explanation for the observed derepression of NsrR-regulated genes under iron deprivation observed by Bodenmiller and Spiro (2006).

In the absence of NO, NsrR binding to target genes prevents transcription by RNA polymerase. Nitrosylation of the Fe-S cluster by NO abrogates the DNA binding activity of NsrR, resulting in derepression of target gene transcription (Tucker *et al.*, 2008a). The responsiveness of NsrR regulation to very low NO concentrations compared to other NO-sensitive regulators demonstrated in *S.* Typhimurium, supports its role as primary regulator of the nitrosative stress response (Karlinsey *et al.*, 2012). Computational analysis as well as transcriptomic and ChIP-chip data uncovered potential NsrR target genes in *E. coli* (Rodionov *et al.*, 2005; Bodenmiller and Spiro, 2006; Filenko *et al.*, 2007; Partridge *et al.*, 2009). Unexpectedly, they were not only implicated in nitrosative stress protection such as *hmpA* or *ytfE*, but also in diverse cellular functions like motility and more general stress responses. In *S.* Typhimurium, the NsrR regulon comprises *hmpA*, *ytfE*, *hcp-hcr*, *ygbA* and *yeaR-yoaG*, which is in accordance with *E. coli*, and additionally STM1808 (STM14_2185), a putative zinc metalloprotein (Gilberthorpe *et al.*, 2007; Karlinsey *et al.*, 2012). Data supported a contributive role for YgbA, STM1808, YtfE and Hcp-Hcr in nitrosative stress protection *in vitro* or/and *in vivo* (Karlinsey *et al.*, 2012). Interestingly, there is evidence linking NsrR to the regulation of virulence-associated genes SPI1 and SPI4 in *S.* Typhimurium (Karlinsey *et al.*, 2012) and genes of the LEE PAI in EHEC (Branchu *et al.*, 2014). Hence, bacteria might exploit NO as a signal to coordinate virulence gene expression.

The NorR protein is the second dedicated NO sensor in *E. coli* and *S.* Typhimurium (Spiro, 2007). NorR is a σ^{54}-dependent bacterial enhancer binding protein consisting of a C-terminal DNA binding domain, that binds to conserved enhancer sites in the promoter region, a central AAA domain responsible for ATPase activity and interaction with σ^{54}-RNA polymerase, and an N-terminal regulatory GAF domain. The latter contains a mononuclear non-heme iron centre that reversibly binds NO. Formation of the mononitrosyl complex releases intra-molecular repression on the ATPase domain, resulting in ATP-driven σ^{54}-dependent transcription (D'Autréaux *et al.*, 2005; Tucker *et al.*, 2008b). In *E. coli* and *S.* Typhimurium, the only known target described so far to be activated by NorR in response to NO comprises the divergently transcribed *norVW* operon, which encodes the NO-detoxifying flavorubredoxin and its associated reductase (Pullan *et al.*, 2007).

4.3.2 Secondary NO-sensing regulators

The FNR protein, the regulator of the aerobic-anaerobic transcription switch, and the Fur protein, the global regulator controlling bacterial iron homeostasis, are examples for secondary NO sensors (Spiro, 2007). FNR primarily senses changes in O_2 availability and, in the absence of O_2, activates genes involved in anaerobic metabolism, such as those required for anaerobic respiration or fermentation (Spiro and Guest, 1990). Fur senses the iron status of the cell and acts as a repressor of genes involved in iron acquisition and utilization under iron-replete conditions (Escolar *et al.*, 1999).

Nitrosylation of the [4Fe-4S] cluster of FNR (Cruz-Ramos *et al.*, 2002) and of Fe^{2+} in Fe-Fur (D'Autreaux *et al.*, 2002) inhibits the DNA binding activity of these proteins.

Indeed, differential regulation of FNR- and Fur-regulated genes in response to NO, GSNO or acidified nitrite was observed in some transcriptomic studies (Bower *et al.*, 2009; Justino *et al.*, 2005; Mukhopadhyay *et al.*, 2004; Pullan *et al.*, 2007).

5 Controversy regarding the use of nitrite as curing additive and the use of plant extracts in "natural" curing

Despite the benefits conferred by added $NaNO_2$ to cured meat, its application has been controversial (Sindelar and Milkowski, 2012). The two major health concerns with inorganic nitrite and nitrate intake are the risk for development of methemoglobinemia, and their potential carcinogenic effects (Mensinga *et al.*, 2003) owing to the formation of cancerogenic *N*-nitrosamines in protein-rich products or in the human gut (Abnet, 2007). Although some epidemiological studies have suggested a link between dietary nitrite and cancer (e.g. Liu *et al.*, 2009), others failed to show a correlation (e.g. van Loon *et al.*, 1998). Due to these concerns, the maximum legally permitted amount of ingoing $NaNO_2$ is 150 mg/kg meat batter in the EU (directive 2006/52/EC, European Parliament, 2006). The finding that nitrate and nitrite are endogenously produced in diverse tissues and organs like the vascular endothelium, neurons, or the stomach (Moncada and Higgs, 1993; Benjamin *et al.*, 1994; Lundberg *et al.*, 1994) and provide a physiological store for NO homeostasis in humans (Lundberg *et al.*, 2008) shed new light onto the debate (Bryan *et al.*, 2012). Dietary intake of nitrite and nitrate is even considered to be beneficial to health (Hord *et al.*, 2009).

Nevertheless, owing to the controversial public discussion about the adverse effects of nitrite as food preservative, consumers seek for ecologically produced "naturally" cured meat, in which curing salts are substituted with natural ingredients, e.g. plant extracts (Sebranek and Bacus, 2007a; Sebranek *et al.*, 2012). Due to their high nitrate content, plant extracts constitute a nitrite reservoir via transformation of nitrate by microbiological or chemical processes. Additionally, plant extracts contain potential antimicrobial phytochemicals, such as polyphenols, terpenoids and alkaloids (Cowan, 1999). A large-scale study investigated the inhibitory action of 52 different essential oils and plant extracts on a diverse range of bacteria *in vitro*, supporting the potential use as therapeutics and food preservatives (Hammer *et al.*, 1999). The mechanisms of action of these natural antimicrobials are not fully understood. However, membrane disruption with concomitant leakage of intracellular contents and perturbance of associated functions such as inhibition of respiration or dissipation of proton motive force appears to be a common feature (Cowan, 1999; Negi, 2012). Moreover, some of them like phenolics and flavonoids target enzyme function (Cowan, 1999). However, scientifically founded and statistically affirmed data need to be collected concerning the impact of a reduction of $NaNO_2$ or the use of plant extracts on the microbiological safety and quality of meat products (Sebranek and Bacus, 2007b).

6 Aim of this thesis

Little is known about the molecular basis of the inhibitory action of the curing agent sodium nitrite on the Gram-negative pathogens *S.* Typhimurium and EHEC in raw meat products under practice-relevant conditions (e.g. pH, temperature, etc.). Likewise, there is scarce information on how these bacteria might respond to and protect themselves against this nitrite-imposed stress. Knowledge about the impact of nitrite on these bacteria, however, is a prerequisite in the effort to reduce the ingoing nitrite concentration without jeopardizing the microbiological safety of these products. Moreover, a deeper understanding of the inhibitory action of $NaNO_2$ and the protective counter-measures employed by the bacteria is necessary in order to find suitable antimicrobial plant extracts as nitrite salt substitutes.

The aim of this work is to characterize the action of the curing agent $NaNO_2$ on *S.* Typhimurium and EHEC under conditions related to raw sausage ripening, and to identify systems involved in coping with the imposed nitrosative stress.

For this purpose, global transcriptional studies via RNA-seq of *S.* Typhimurium under *in vitro* conditions considering parameters relevant for raw sausage production, including acidified nitrite and prevalent conditions on ripening days 0 (RD0) and 3 (RD3), were performed to assess the adaptive responses. RNA-seq data were validated by qPCR on a subset of selected differentially regulated genes, and contribution of the respective gene products to the nitrite stress response were investigated by *in vitro* growth experiments of constructed deletion mutants compared to the wild-type (WT). Moreover, a putative involvement of the NO-detoxifying systems HmpA, NorV and NrfA in survival of nitrite-related stress in raw sausages was assessed by construction and analysis of the respective deletion mutants. As a second approach to identify further gene products putatively involved in resistance to nitrite stress, but with unaltered transcription in response to nitrite, a *S.* Typhimurium insertion-duplication mutant library was screened for mutants displaying a NO- or acidified nitrite-sensitive phenotype under selected practice-oriented parameters.

To get a hint to the molecular causes for the differential impact of nitrite on *Salmonella* vs EHEC observed in previous challenge experiments, the transcriptome of *E. coli* O157:H7 in response to acidified nitrite was assessed by RNA-seq. Deletion mutants in HmpA and NrfA were constructed to assess their nitrite sensitivity compared to the WT.

Furthermore, different plant extracts were screened concerning their aptitude to be employed as nitrite substitutes. First, plant extracts with antimicrobial activity against *S.* Typhimurium and EHEC were identified by *in vitro* screening under practice relevant conditions. As plant extracts, in addition to serving as a source of nitrate, might exert antimicrobial activity via phytochemicals, the transcriptional response of *S.* Typhimurium to nitrate and the respective plant extracts was assessed and compared.

II Materials and Methods

1 Materials

1.1 Bacterial strains

Table 1: Strains used in this thesis

Strain	Genotype/Description	Reference or source
S. Typhimurium strains		
WT	*Salmonella enterica subsp. enterica* serovar Typhimurium ATCC 14028 wild-type strain	DSM 19587 (Jarvik *et al.*, 2009)
WT pKD46	WT strain carrying pKD46, expressing the lambda Red recombinase system used for mutant construction	this study
Δ*hmpA*	in-frame *hmpA* (STM14_3135) deletion mutant	this study
Δ*norV*	in-frame *norV* (STM14_3431) deletion mutant	this study
Δ*nrfA*	in-frame *nrfA* (STM14_5143) deletion mutant	this study
Δ*hmpA* Δ*norV*	in-frame *hmpA* and *norV* double deletion mutant	this study
Δ*hmpA* Δ*nrfA*	in-frame *hmpA* and *nrfA* double deletion mutant	this study
Δ*norV* Δ*nrfA*	in-frame *norV* and *nrfA* double deletion mutant	this study
Δ*hmpA* Δ*norV* Δ*nrfA*	in-frame *hmpA*, *norV* and *nrfA* triple deletion mutant	this study
Δ*cadA*	in-frame *cadA* (STM14_3138) deletion mutant	this study
Δ*hdeB*	in-frame *hdeB* (STM14_1885) deletion mutant	this study
Δ*pta*	in-frame *pta* (STM14_2883) deletion mutant	(Schürch, 2012)
Δ*cobS*	in-frame *cobS* (STM14_2505) deletion mutant	this study
Δ*pphA*	in-frame *pphA* (STM14_2241) deletion mutant	this study
Δ*ppk*	in-frame *ppk* (STM14_3066) deletion mutant	this study
Δ*treA*	in-frame *treA* (STM14_2172) deletion mutant	(Schürch, 2012)
Δ*cbiE*	in-frame *cbiE* (STM14_2519) deletion mutant	(Schürch, 2012)
WT pBR322	WT carrying plasmid pBR322	this study
Δ*cadA* pBR322	Δ*cadA* carrying plasmid pBR322	this study
Δ*cadA*-comp	Δ*cadA* carrying complementation plasmid pBR322-*cadA*	this study
WT pBAD/HisA(Tet^R)	WT carrying plasmid pBAD/HisA(Tet^R)	this study
Δ*pta* pBAD/HisA(Tet^R)	Δ*pta* carrying plasmid pBAD/HisA(Tet^R)	this study
Δ*pta*-comp	Δ*pta* carrying complementation plasmid pBAD-*pta*	this study
WT pEGFP	WT carrying pEGFP for intracellular pH measurements	this study
E. coli O157:H7 (EHEC) strains		
WT	*Escherichia coli* O157:H7 EDL933 wild-type strain	CIP 106327 (Perna *et al.*, 2001)
WT pKM208	WT strain carrying pKM208, expressing the lambda Red recombinase system used for mutant construction	provided by Dr. Klaus Neuhaus
Δ*hmpA*	in-frame *hmpA* (Z3828) deletion mutant	this study
Δ*nrfA*	in-frame *nrfA* (Z5669) deletion mutant	this study
E. coli strains		
DH5α	*deoR endA1 gyrA96 hsdR17*(*rk- mk+*) *recA1 relA1 supE44 λthi-1* Δ(*lacZYA-argFV169*)	strain collection Weihenstephan, (Hanahan, 1983)

1.2 Plasmids

Table 2: Plasmids used in this thesis

Plasmid	Description	Reference or source
pKD4	*pir*-dependent, FRT sites, Kan^R	(Datsenko and Wanner, 2000)
pKD46	Arabinose-inducible lambda Red recombinase expression plasmid for gene deletions in *Salmonella*, Amp^R	(Datsenko and Wanner, 2000)
pKM208	IPTG-inducible lambda Red recombinase expression plasmid for gene deletions in EHEC, Amp^R	(Murphy and Campellone, 2003)
pCP20	Flp recombinase expression plasmid, Amp^R, Cm^R	(Datsenko and Wanner, 2000)
pBR322	pMB1 replicon cloning vector, Amp^R, Tet^R	(Bolivar *et al.*, 1977)
pBR322-*cadA*	Complementation plasmid containing the *cadA* coding sequence under control of its native promoter P_{cadBA}, Amp^R	this study
pEGFP	EGFP expression vector, Amp^R	Clontech, Germany; donated by Prof. Matthias Ehrmann
pBAD/HisA(Tet^R)	Expression vector with N-terminal polyhistidine tag, pBR322 origin, *ara*BAD promoter, *araC*, Tet^R	(Starke *et al.*, 2013)
pBAD-*pta*	Complementation plasmid containing the *pta* coding sequence under control of the *ara*BAD promoter, Tet^R	this study
pIDM1	Temperature-sensitive vector, *repA*, Tet^R	(Fuchs *et al.*, 2006)

1.3 Oligonucleotides

Lyophilized oligonucleotides were purchased from Invitrogen (Darmstadt, Germany) or Eurofins MWG Operon (Ebersberg, Germany) and dissolved in dH_2O to a stock concentration of 100 pmol/µl. Primers for quantitative real-time reverse transcription PCR (qPCR) were dissolved in diethylpyrocarbonate (DEPC)-treated (0.1% (v/v)) dH_2O.

Table 3: Oligonucleotides used for mutagenesis

Construction of deletion mutants		
S. Typhimurium		
Target gene	Primer name	Sequence 5' - 3'[a]
hcp (STM14_1052)	del_hcp_F	GTATATTAAATATAACTTTAAAAGGTGTGACCATGTTT TGTGTGCAATGTgtgtaggctggagctgcttc
	del_hcp_R	CATCATTGACCTCCTTACGCGCTCAGCAATTGCTTCAT GTCTTCTTCAACcatatgaatatcctcctta
	Test_hcp_F	TATCCTCAGCCTGCTGGT
	Test_hcp_R	CGTTTCCGCTGAATTGCG
hdeB (STM14_1885)	del_hdeB_F	AGGTTATTTATATAATTATTGGAGCAACAACAATGAA TAAATTCTCCCTTgtgtaggctggagctgcttc
	del_hdeB_R	ATATCAGTTTACTCTTATTTTGAGAGTTCTTTCTTGATT TCGTCTTTTATcatatgaatatcctcctta
	Test_hdeB_F	GTCTATCTGAGATCCTG
	Test_hdeB_R	TAGGTCTCCATATAGTGA
treA (STM14_2172)	del_treA_F	TGGCTTTGGCTCACCGCTAAGGAGATAACTTGATGAT ACCCCCAGAGATTgtgtaggctggagctgcttc
	del_treA_R	ACTATAAACACGCGTTACTGCGTCGCTGCAGACGGCG TTTTTGTCGGCGTcatatgaatatcctcctta
	Test_treA_F	TCTATCCAGGTTAAGGCG
	Test_treA_R	TTGGCGGCAGTATCAGCG

pphA (STM14_2241)	del_pphA_F	CACACGCTATCTTTTTATATCTGTCCTGGATAATGAAC GACAGGAAAAACgtgtaggctggagctgcttc
	del_pphA_R	GGTCGCTGATACCGCTATTGTATCCGCGCTAACGTCAA TTGCCCGCCAAAcatatgaatatcctcctta
	Test_pphA_F	ATTGAAGGTGAACAGGCG
	Test_pphA_R	GAGGATATTGTCGTGGAC
cobS (STM14_2505)	del_cobS_F	CTGGTAGTCTCAGGTATTGGAGTCAAAATTAAATGAG TAAGCTGTTTTGGgtgtaggctggagctgcttc
	del_cobS_R	CCGTAATAATCGGCTCATAACAGAGCCAGCAGAAAGA TCAATTCACCAAGcatatgaatatcctcctta
	Test_cobS_F	AATTGCAGCCTGCCAGCG
	Test_cobS_R	TACCGTTAAGACCCGGCA
	Test_cobS_F2	CGAACAGTGGGATTACG
	Test_cobS_R2	ACGGCTAAGGTTTCCAGT
cbiE (STM14_2519)	del_cbiE_F	CGTCCCGTCGACGAGATTGCTAAGGAGCTGCAATGCT AACGGTCGTGGGAgtgtaggctggagctgcttc
	del_cbiE_R	CGCGCAGAAAAAGCTCATCTTTCATCAAGGATCACCA CTGCATTCATTTCcatatgaatatcctcctta
	Test_cbiE_F	TGCGATACCACCGAAGCG
	Test_cbiE_R	TCGATAGCCGTCACCTGC
pta (STM14_2883)	del_pta_F	CCCCAAAAGACGGTAACGAAAGAGGATAAACCGTGT CCCGTATTATTATGgtgtaggctggagctgcttc
	del_pta_R	ATTAGCTTTTACTGTTACTGCTGCTGCTGAGAAGCCTG GATCGCCGTCAGcatatgaatatcctcctta
	Test_pta_F	CACGAACGTAACCTGGCG
	Test_pta_R	TATTCATTGATGCAGCGC
ppk (STM14_3066)	del_ppk_F	TGTCCCGTGAATAAAACGGAGTATAGGTAGTAATGGG TCAGGAAAAGCTAgtgtaggctggagctgcttc
	del_ppk_R	AAATTGGCATAGCGTTAGTCTGGTTGCTCGAGTGATTT GATGTAGTCATAcatatgaatatcctcctta
	Test_ppk_F	TATGTCATCGGACAGGAC
	Test_ppk_R	TTGTTATCTGCGCCCAGC
hmpA (STM14_3135)	del_hmpA_F	CATCATTAGATTTTCACATAAAGGAAGCACGTATGCTT GACGCACAAACCgtgtaggctggagctgcttc
	del_hmpA_R	AGGATTTGTTGCAATTACAGCACTTTATGCGGGCCGA AGCATTCGTAATGcatatgaatatcctcctta
	Test_hmpA_F	TATGCGTCAGATAAGGGT
	Test_hmpA_R	AACGAGCTAAGTCAAACG
cadA (STM14_3138)	del_cadA_F	CGGGAGGGGCCCACTTTACCAGGAACAAGACTATGAA CGTTATTGCTATCgtgtaggctggagctgcttc
	del_cadA_R	CTTCCCTTTGGTACTTATTTCGTATTTTCTTTCAGCACC TTAACGGTGTAcatatgaatatcctcctta
	Test_cadA_F	CTTCGAACTCTCCGGCAC
	Test_cadA_R	GTAAGGCACGCATGCCGT
norV (STM14_3431)	del_norV_F	TTTTTGTAAACGTTGAATGAATTGAGGTGGTTATGTCT ATTCTGGTTAAAgtgtaggctggagctgcttc
	del_norV_R	GATGATCCCCCGACTCATTTTGCCTCCGTCGCCAGTAC GTCGAACACGTCcatatgaatatcctcctta
	Test_norV_F	CTCATGGTTACCTCATTG
	Test_norV_R	TAACTGGCGGGTGAGAT
nrfA (STM14_5143)	del_nrfA_F	AAAGATAATGGCGCAATCTGGATGAGACCTCTATGGC AAGGAAAACACTAgtgtaggctggagctgcttc
	del_nrfA_R	TGTCACATGTGAGGTTATTGGCTTAACAGACCGTTTTT ACGCGCCTGATCcatatgaatatcctcctta
	Test_nrfA_F	TGTCCAGGTTACTAACTC
	Test_nrfA_R	TAATTCCACTCAGGCTC

EHEC		
hmpA (Z3828)	del_Z3828_F	CATCAATTAAGATGCAAAAAAAGGAAGACCATATGCT TGACGCTCAAACCgtgtaggctggagctgcttc
	del_Z3828_R	CCGGCAACATCAAATCACAGCACCTTATGCGGGCCAA AGCATTCGTAATGcatatgaatatcctcctta
	Test_Z3828_F	TACGCAAGGCTTTGGAGA
	Test_Z3828_R	CGACATTGTCGATACCTG
nrfA (Z5669)	del_Z5669_F	TGCAACAATGGCGCAATTCGGATGAAGCCCCTATGAC AAGGATAAAAATAgtgtaggctggagctgcttc
	del_Z5669_R	GAGGCGGAACGGGGTTATTGGCTTAACAGACCGTTTT TACGTGCCTGCTCcatatgaatatcctcctta
	Test_Z5669_F	GAAGATACTGACTAACTC
	Test_Z5669_R	CTGCTGGGTAACTTCGTA
Construction of *S.* Typhimurium complementation mutants		
pta (STM14_2883)	C_pta_F2 (*Sac*I)	GGATTAGAGCTCGTGTCCCGTATTATTATGCTG
	C_pta_R (*EcoR*I)	AGCTGGGAATTCTTACTGCTGCTGCTGAGA
cadA (STM14_3138)	C_cadA_A (*Hind*III)[b]	AATAAGCTTATTTAACGCTGAACCATGAC
	C_cadA_B *(Xba*I)	ttctctagaaagtataggaacttcgaagcagctccagcctacacGTTCATTTCTC CTGAGCTGT
	C_cadA_C (*Xba*I)	ctttctagaggaataggaacttcggaataggaactaaggaggatattcatatgCCGCTA ACTCCTTTTTCTCA
	C_cadA_D (*Bam*HI)[b]	AATGGATCCCGCCACGATGTAAAAAATCG
Plasmid- or antibiotic cassette-specific primers		
pBAD/HisA (Tet^R)	pBADforward	ATGCCATAGCATTTTTATCC
	pBADreverse	TGATTTAATCTGTATCAGGC
pBR322	seq_pBR322_F	TGCCACCTGACGTCTAAG
	seq_pBR322_R	AGTCATGCCCCGCGC
pKD4 Kan cassette	kanR3	GCGCTGCGAATCGGG
	kanR2	CCGGCTACCTGCCC
pIDM1	IDM1A	CCAGTCACGACGTTGTAA
	IDM2A	AGGCTTTACACTTTATGC

[a] Priming sites for, or sequence parts corresponding to, pKD4 are in lowercase letters. Restriction enzyme sites are underlined.
[b] Primer binding sequence to the *S.* Typhimurium 14028 genome is taken from Viala *et al.* (2011).

Table 4: Oligonucleotides used for qPCR

S. Typhimurium				
14028 identifier	Gene name	Primer name	Sequence 5' - 3'	Amplicon size (bp)
16S rDNA		STM_16S_qRT_F	GTCTGTCAAGTCGGATGTG	122
		STM_16S_qRT_R	AGATCTCTACGCATTTCACC	
STM14_0175	*ampD*	ST14_0176_qRT_F	ATTATTCACCGGAACGATAG	114
		ST14_0176_qRT_R	ACATACTGGACGATTTCACC	
STM14_0228	*fhuA*	ST14_0228_qRT_F	GCCTCTATGTTCAGGATCAG	145
		ST14_0228_qRT_R	AACTGGTGGTCATTACGTTC	
STM14_0725	*citC*	ST14_0725_qRT_F	TTGGCTGTATTGTGATGAAC	144
		ST14_0725_qRT_R	GATCGAGTCGGTCTTCATAG	
STM14_0818	*speF*	ST14_0818_qRT_F	ACAATTTATTCCGATGATGG	132
		ST14_0818_qRT_R	TTATGGATCTGCGAGGTCT	

STM14_0854	*sdhB*	ST14_0854AqRT_F	TGATGGTTTGAATATGAACG	147
		ST14_0854AqRT_R	TAGAATTGCCCCATGTCTAC	
STM14_985	*pflE*	ST14_985_qRT_F	GTACTGCGCGATAAACCTT	151
		ST14_985_qRT_R	CATGCAGACAGGTCTCAAC	
STM14_1052	*hcp*	ST14_1052_qRT_F	CGTAAATTCAAGCATCTGGT	142
		ST14_1052_qRT_R	AGATACGGTCGTCATAGCTG	
STM14_1089	*dmsA*	ST14_1089_qRT_F	GTTGGGATTAACGGAGGTA	110
		ST14_1089_qRT_R	ATAAACATGGAGATGCTGGT	
STM14_1402	*potB*	ST14_1402_qRT_F	CGTGATTGATACACCGATT	127
		ST14_1402_qRT_R	TAGTGGTTTGTCGAGCTTCT	
STM14_1410	*purB*	ST14_1410_qRT_F	ATCAGTTCAGCGAAGAGTTC	128
		ST14_1410_qRT_R	GATCAGGATGGTGTTAAAGC	
STM14_1677	*ttrA*	ST14_1677_qRT_F	GTTAAGTATTGCCCGTAGCA	141
		ST14_1677_qRT_R	GAGGTCAACAGTTCGGTAAG	
STM14_1678	*ttrC*	ST14_1678BqRT_F	TATGCACACTGCTGTTCTGT	132
		ST14_1678BqRT_R	CGGTTTGTACCTGAATCAAC	
STM14_1885	*hdeB*	ST14_1885_qRT_F	TTACGCCTAAAGGTATGAGC	145
		ST14_1885_qRT_R	ACTGCTGTCGTCTCAGTTTC	
STM14_2132	*narG*	ST14_2132_qRT_F	ATATGTTGGTGTTCTGTGGTT	150
		ST14_2132_qRT_R	AGGTGCTATTCATGTGACG	
STM14_2134	*narK*	ST14_2134_qRT_F	TAAGGCCTCGCTAAAAGAG	135
		ST14_2134_qRT_R	AATTGCGTTTTAGACAGCAT	
STM14_2390	*fliF*	ST14_2390_qRT_F	TGCTAATGATGTGGAAAGC	116
		ST14_2390_qRT_R	CTTTATTGGCAAAATCCAAC	
STM14_2555	*phsA*	ST14_2555_qRT_F	GTTAACCCAGAAGCCTTACC	145
		ST14_2555_qRT_R	GCTCTCGCTCAAATAGACAT	
STM14_3127	*asrB*	ST14_3127_qRT_F	CATAAGCCCTTACTGGTTGT	117
		ST14_3127_qRT_R	ATAGCCGAGAATCATATCCA	
STM14_3135	*hmpA*	ST14_3135_qRT_F	CCGAGATTTATCACGAGAAC	119
		ST14_3135_qRT_R	GACTGGTTCAAACTCAAAGC	
STM14_3138	*cadA*	ST14_3138_qRT_F	TCATTTATGAAACCCAGTCC	123
		ST14_3138_qRT_R	TGGTGGTATGCATCATGTAG	
STM14_3266	*yfiA*	ST14_3266_qRT_F	ATTAATACACCGAACGGACA	113
		ST14_3266_qRT_R	TTGTGCTGCACTTTATTGAG	
STM14_3431	*norV*	ST14_3431AqRT_F	GCTACTACGCCAATATCCTG	160
		ST14_3431AqRT_R	GCCCATTTCAGATACAGTTC	
STM14_3445	*hycC*	ST14_3445_qRT_F	TATCCTCACGCTATCTCTGC	125
		ST14_3445_qRT_R	GCTGAATGTTATGCTCCATC	
STM14_3456	*ygbA*	ST14_3456_qRT_F	CAAAAACGTCTTGATAAATGC	111
		ST14_3456_qRT_R	ACGCATAATCTGCTTCATCT	
STM14_3956	*yhbU*	ST14_3956A_qRT_F	CGCTGCTATCTTTCTTCCTA	138
		ST14_3956A_qRT_R	GTAACGGTCAATCAGGACAT	
STM14_4037	*rplM*	ST14_4037_qRT_F	AATACACTCCGCACGTAGAT	140
		ST14_4037_qRT_R	AAAGGTCGCTTGTTTGATAC	
STM14_4083	*fis*	ST14_4083_qRT_F	CGTTAACTCTCAGGATCAGG	137
		ST14_4083_qRT_R	GCTGTTCTACTTCAGCCAGT	

STM14_4129	*rpsH*	ST14_4129_qRT_F	CCAGGGTAAAGCTGTTGTAG	148
		ST14_4129_qRT_R	TGCACGATCAGTCATAACAC	
STM14_4183	*nirB*	ST14_4183_qRT_F	CGCGTAGTTACGTTTACCTC	145
		ST14_4183_qRT_R	ATGGCGTTCAGTACCAGTT	
STM14_4222	*feoB*	ST14_4222_qRT_F	ATTCAATGGATTGGCTACAC	132
		ST14_4222_qRT_R	GGAGAGGAACAGGTACATCA	
STM14_4453	*lldD*	ST14_4453_qRT_F	GTGATGCACCCTAAATGG	136
		ST14_4453_qRT_R	ACGGATCGAAGTTATTTGC	
STM14_4495	*pyrE*	ST14_4495_qRT_F	GTACTGCTTTAACCGCAAAG	145
		ST14_4495_qRT_R	CGCCTGAATAATCTCCATT	
STM14_4568	*uhpT*	ST14_4568_qRT_F	TCTGGGTAAAGCTGAAGAAC	146
		ST14_4568_qRT_R	AGATATTGGAGAAACACAGCA	
STM14_4635	*rnpA*	ST14_4635_qRT_F	TCCCCGTATCGGTCTTAC	124
		ST14_4635_qRT_R	GAAATCCATTGCAGGAAGT	
STM14_5127	*soxS*	ST14_5127_qRT_F	GATGAACATATCGACCAACC	118
		ST14_5127_qRT_R	TATACTCGCCTAATGTTTGATG	
STM14_5143	*nrfA*	ST14_5143_qRT_F	CGGAATATGAAACCTGGAG	117
		ST14_5143_qRT_R	CGATTTTATGGTCGGTGTAG	
STM14_5155	*fdhF*	ST14_5155_qRT_F	AGATTGTCGAAGGCTATACG	145
		ST14_5155_qRT_R	CCCTGATAGAACTGGGTGA	
STM14_5169	*adi*	ST14_5169_qRT_F	CACGCACAAACTACTGAATG	128
		ST14_5169_qRT_R	CATATAACGGAGAGGTGGTG	
STM14_5179	-	ST14_5179_qRT_F	CTGTCGTTATTGTGAAATGC	131
		ST14_5179_qRT_R	AAGAATCCACACAAATAGGG	
STM14_5202	*aspA*	ST14_5202_qRT_F	ATTTTGGACATCTTCACTGC	129
		ST14_5202_qRT_R	AAAACTGGCTGAAGTCACTG	
STM14_5283	*ytfE*	ST14_5283_qRT_F	ACCATATCGTTGTTCGCTAT	132
		ST14_5283_qRT_R	CGGTGAGATATTTTGTCAGG	
STM14_5343	*nrdD*	ST14_5343_qRT_F	CGAAACTGGTCTTCGCTAT	133
		ST14_5343_qRT_R	ACCACCTGATCGTAGTTGAG	
STM14_5361	-	ST14_5361AqRT_F	TGTTGATCGGTATGTCTGAA	136
		ST14_5361AqRT_R	GTGTCAAGGTGCATACAGG	

EHEC

EDL933 identifier	Gene name	Primer name	Sequence 5' - 3'	Amplicon size (bp)
16S rDNA		16S_qRT_F	GTGGTTTAATTCGATGCAA	128
		16S_qRT_R	ACAACACGAGCTGACGAC	
Z1062	*bssR*	Z1062_qRT_F	AAAGGATACATGTCCGTCAG	130
		Z1062_qRT_R	GATGAAGAGCACTCCACTCT	
Z1294	*pyrD*	Z1294_qRT_F	ATCGCCATCAATATTTCATC	132
		Z1294_qRT_R	CACATATTTATGGTGCATCG	
Z1304	*fabA*	Z1304_qRT_F	AAGGGTATGTTGAAGCAGAA	132
		Z1304_qRT_R	CGAGGTAGAACCCTACCAG	
Z2015	*tdk*	Z2015_qRT_F	GTCAGTTCGCGTATAGGTTT	137
		Z2015_qRT_R	CTGGTTAAAAACTGGCATTC	
Z2329	*ldhA*	Z2329_qRT_F	TCTGAAAGGTTTTGGTATGC	126
		Z2329_qRT_R	TGCAGAGAGATAACGTCTGAT	

Z3028	*fliF*	Z3028_qRT_F	TGTTAACCCAGTCCAATACC	136
		Z3028_qRT_R	GCGTGAATATTACCGTTACC	
Z3658	-	Z3658_qRT_F	AACTCATTCTTGGTGTTTCG	134
		Z3658_qRT_R	GGCAACAAACAACAGTAACC	
Z3828	*hmpA*	Z3828_qRT_F	TACTCTTTGACTCGCAAACC	124
		Z3828_qRT_R	CGACCAGTTTCACGACAT	
Z3902	*rimM*	Z3902_qRT_F	GACATGATCATCAAGCTGAA	133
		Z3902_qRT_R	CCATCAGGTCTTTCCAGTAG	
Z4018	*norVs*	Z4018_qRT_F	AACGATGAAGTGGATCAGAC	119
		Z4018_qRT_R	AAGTTAAAGCCCAGGATCTC	
Z4537	*secG*	Z4537_qRT_F	GGTTCAAGTGGTTCTGGTAA	118
		Z4537_qRT_R	CGCTACCTTTATTGGTCTTG	
Z4597	*yhcN*	Z4597_qRT_F	GCTGCATTAAGCGTACTTTC	113
		Z4597_qRT_R	ACACCACTTACGGATACGG	
Z4929	*yhiX*	Z4929_qRT_F	TCGTTCATCACTGTAGCAGA	160
	(*gadX*)	Z4929_qRT_R	AGAAGCAGCGGTATAAAGTG	
Z4981	*cspA*	Z4981_qRT_F	ACTCCTGACGATGGCTCTA	101
		Z4981_qRT_R	ATGGTGAAGGACACTTTCTG	
Z5049	*waaL*	Z5049_qRT_F	CTTTCCGTGTTAGTCATTGG	110
		Z5049_qRT_R	TGTGTGAAAATAACCGACAA	
Z5236	*atpB*	Z5236_qRT_F	GATGGATTTACTGCCTATCG	109
		Z5236_qRT_R	CATAGACAGCGTTACGTTCA	
Z5669	*nrfA*	Z5669_qRT_F	TTACGACAAAATTGCCTTCT	123
		Z5669_qRT_R	CAGGTCACGTTGTTTTTACC	
Z5820	*ytfE*	Z5820_qRT_F	GATTGAGAAAGACTGGCGTA	116
		Z5820_qRT_R	CTTTAGTCGCTTGCAGAATC	

1.4 Media and media additives

Media ingredients were dissolved in dH_2O. Liquid media were stored at room temperature (RT), while agar plates were stored at 4°C. Additives were added to sterilized agar after cooling to 50-60°C. Liquid media were supplemented with additives directly before inoculation.

LB broth (Lennox formulation)

10 g/l Tryptone (Oxoid, Wesel, Germany)

5 g/l Yeast extract (Oxoid)

5 g/l NaCl (Roth, Karlsruhe, Germany)

autoclaved for 17-20 min at 121°C

LB agar plates

For LB agar plates, 1.5% (w/v) bacteriological agar (Oxoid) was added to the medium.

LB pH 7 / LB pH 5.5

To prepare LB media at different pH values, the pH was adjusted to 7.0 or 5.5 with lactic acid (LA; 90%, Merck, Darmstadt, Germany) prior to autoclaving (17 min, 121°C).

SOC medium (Super Optimal Broth with Catabolite Repression)

20 g/l Tryptone
5 g/l Yeast extract
0.6 g/l NaCl
0.2 g/l KCl (Roth)
2.5 g/l $MgSO_4 \cdot 7H_2O$ (Merck)
2.1 g/l $MgCl_2 \cdot 6H_2O$ (Roth)
3.9 g/l Glucose (Fluka, Neu-Ulm, Germany)
autoclaved for 17 min at 121°C

Green indicator plates (Chan *et al.*, 1972)

Base agar:
8 g/l Tryptone
1 g/l Yeast extract
5 g/l NaCl
15 g/l Agar
autoclaved for 17-20 min at 121°C

Additives:

21 ml/l Glucose (40% w/v)	autoclaved separately, stored at 4°C
25 ml/l Alizarin yellow G (2.5% w/v) (Sigma-Aldrich, Taufkirchen, Germany)	autoclaved separately, stored at RT; stock gently heated in a microwave prior to addition to the base agar
3.3 ml/l Aniline blue (2% w/v) (Riedel-de Haën, Seelze, Germany)	filter-sterilized (Millex-GP, 0.22 µm, Merck Millipore), stored at RT

Meat extract broths

<u>Meat extract broth</u>

100 g/l Meat extract (Merck)

pH 5.8 adjusted with LA

<u>Meat extract base broth to simulate ripening day 0 (MEB0)</u>

100 g/l Meat extract
33.9 g/l NaCl
pH 5.8 adjusted with LA

Meat extract base broth to simulate ripening day 3 (MEB3)

100 g/l Meat extract

43 g/l NaCl

pH 5.2 adjusted with LA

Meat extract broths were autoclaved for 15 min at 121°C.

Media additives

Media additives were filter-sterilized (0.22 µm) except for glucose, which was autoclaved (17-20 min, 121°C). Stock solutions of antibiotics, IPTG and L-arabinose were stored at -25°C. All other additives were stored at 4°C.

Table 5: Media additives

Additive	Supplier	Solvent	Stock solution	Final concentration
Tetracycline hydrochloride	Sigma-Aldrich	70% (v/v) EtOH	17.5 mg/ml	17.5 µg/ml
Chloramphenicol	USB	100% (v/v) EtOH	25 mg/ml	25 µg/ml
Kanamycin sulphate	Roth	dH_2O	50 mg/ml	50 µg/ml
Ampicillin sodium salt	Roth	dH_2O	100 mg/ml	150 µg/ml
Sodium nitroprusside (SNP) dihydrate	Merck	dH_2O	10 mM	diverse
$NaNO_2$	Sigma-Aldrich	dH_2O	50 mg/ml	diverse, 150 mg/l
$NaNO_3$	Roth	dH_2O	50 mg/ml	150 mg/l
KNO_3	Roth	dH_2O	50 mg/ml	70 mg/l
Sodium L(+)-ascorbate	AppliChem, Darmstadt, Germany	dH_2O	500 mg/ml	500 mg/l
IPTG	AppliChem	dH_2O	1 M	1 mM
L(+)-arabinose	Roth	dH_2O	1 M 20% (w/v)	1 mM (pKM208) 0.002% (w/v) (pBAD/HisA(Tet^R))
D-(+)-glucose monohydrate	Fluka	dH_2O	40% (w/v)	0.2% (w/v)

2 Methods

2.1 Microbiological methods

2.1.1 Storage and cultivation of bacteria

Bacterial strains were stored frozen at -80°C in medium containing 20% (v/v) glycerol. Streak plates on LB agar containing appropriate antibiotics if needed were created from the glycerol stocks and incubated overnight at 37°C or 30°C (temperature-sensitive vectors). Single colonies were used to start shaken (160 rpm) 5 ml (for Bioscreen experiments) or 50 ml (for growth curves in flasks or preparation of cell pellets) overnight cultures in LB, if not stated otherwise. 500 ml baffled flasks were used for culture volumes greater than or equal to 150 ml, while cultures less than or equal to 100 ml were grown in 200 ml non-baffled flasks (*S.* Typhimurium) or 250 ml Schott bottles (EHEC). Growth curves were recorded

by measuring the optical density at 600 nm (OD_{600}) every hour (*S.* Typhimurium: Ultrospec 2000 UV/Visible Spectrophotometer, Pharmacia Biotech, Freiburg, Germany; EHEC: GeneQuant pro Spectrophotometer, Amersham Pharmacia Biotech). Starting from an $OD_{600} = 1$, a tenfold dilution of the cultures in the respective growth medium was measured.

2.1.2 Growth analysis using Bioscreen C

In vitro growth of *S.* Typhimurium and EHEC strains was monitored in a micro-volume of 200 µl using a Bioscreen C growth curve reader (*Oy Growth Curves* Ab *Ltd.*, Helsinki, Finland).

Growth analysis of WT, deletion and complementation strains

Shaken (160 rpm) overnight cultures in LB broth at 24°C or 37°C (depending on the incubation temperature of the growth assay) were diluted 1:200 in LB broth pH 5.5 with 0, 50, 100 or 150 mg/l $NaNO_2$ or in LB pH 7 with 0, 40, 80 or 150 µM SNP in the micro-wells of a honeycomb plate. If needed, the medium was supplemented with appropriate antibiotics and 0.002% (w/v) arabinose to induce expression from the P_{BAD} promoter. Aerobic cultures were incubated at 24°C or 37°C as indicated with continuous medium shaking (shaking step 60). The OD_{600} of each well was automatically recorded every 30 min over a period of 48 h (*S.* Typhimurium) or 47 h (EHEC). For micro-aerobic growth curves, cultures were overlaid with 200 µl sterile liquid paraffin (Roth). The shaking speed was set to low (shaking step 20) and culture growth was monitored for 72 h.

Recording of the growth curves and microbiological calculations for each experiment were performed using the Software Research Express v. 1.05 (Transgalactic Ltd, Helsinki, Finland). A fixed first OD_{600} value of 0.000 was set for all growth curves and subsequent OD_{600} values were recalculated accordingly. The time needed to reach an $OD_{600} = 0.2$ or 0.6 and the area under the growth curve (AUC) by 48 h (*S.* Typhimurium) or 47 h (EHEC) were used as parameters to display growth differences caused by $NaNO_2$. For cultures that did not reach the OD_{600} of interest within the time frame of the experiment, the time to OD_{600} was defined as the last time point measured (e.g. 48 h). The ratio AUC_{+SNP}/AUC_{-SNP} by 20 h was calculated to display the effect of SNP on growth (the lower the ratio, the greater the effect of SNP). Mean values and SD (standard deviation) were calculated from three independent experiments each including duplicates.

Screening of plant extracts for growth inhibitory effects on *S.* Typhimurium and EHEC *in vitro*

Different plant extracts were screened for an inhibitory action on the growth of *S.* Typhimurium and EHEC under RD0 (ripening day 0) simulating conditions (MEB0, 0.2% (w/v) glucose, 500 mg/l sodium ascorbate). For comparison, the effects of $NaNO_2$ and $NaNO_3$ were also investigated. The different plant extracts were employed at the maximum concentrations recommended by the suppliers and are listed in Table 6. Powders were dissolved in MEB0, whereas liquid extracts were added to MEB0 to the desired concentration. Filter-sterilization (0.22 µM) of the media containing celery powder and liquid extracts from balm mint and nettle leaves did not influence growth assay results compared to non filter-sterilized

media, indicating that extracts were free of bacterial contaminants (data not shown). Hence, it was decided to refrain from filter-sterilization and uninoculated wells containing non filter-sterilized plant extract media only served as controls for absence of contamination instead. Shaken overnight cultures of *S.* Typhimurium and EHEC grown in meat extract broth were diluted 1:100 in RD0 simulating medium without and with plant extracts, 150 mg/l $NaNO_2$, or 150 mg/l $NaNO_3$ in the microwells. Growth at 24°C with continuous medium shaking (shaking step 60) was automatically recorded every 30 min over a period of 48 h. A fixed first OD_{600} value of 0.000 was set for all growth curves and subsequent OD_{600} values were recalculated accordingly using the Software Research Express v. 1.05. Two independent experiments were performed, except for the celery extract which was tested seven times.

Table 6: Texture and concentration of plant extracts screened for *in vitro* antimicrobial activity

plant extract	texture	concentration tested
*celery	powder	10 g/l
chili infusion	liquid	100 ml/l
balm mint	powder	3 g/l
	liquid	3 g/l
elderflower	powder	3 g/l
nettle leaves	powder	3 g/l
	liquid	3 g/l
mustard seed	powder	3 g/l

* Since celery extract already contains 3.8 g/kg glucose, the amount of glucose added to the medium was reduced to yield a final concentration of 0.2% (w/v) glucose.

2.1.3 Screening of a *S.* Typhimurium insertion mutant library

Part of a *S.* Typhimurium insertion mutant library (Knuth *et al.*, 2004; Klumpp and Fuchs, 2007) was screened for mutants displaying increased sensitivity to the NO donor SNP under neutral conditions (LB pH 7) or mildly acidified $NaNO_2$ (LB pH 5.5). The mutant library, which was kindly provided by Prof. Dr. Thilo Fuchs, was constructed by insertion-duplication mutagenesis using the temperature-sensitive vector pIDM1 with randomly generated chromosomal fragments of *S.* Typhimurium 14028 (Knuth *et al.*, 2004). Homologous recombination between a cloned fragment and its corresponding chromosomal site yields an insertion mutant strain, which is stable at non-permissive temperature (37°C). 96-well microtiter plates containing a single insertion mutant per well stored in medium containing 20% (v/v) glycerol were thawed at RT. 2 µl of the cell suspensions were used to inoculate overnight cultures in 200 µl LB pH 7 + 17.5 µg/ml tetracycline grown in 96-well plates with shaking (500 rpm) at 37°C. Cultures per well were then diluted 1:100 either in 200 µl LB pH 7 with 0 or 40 µM SNP or in 200 µl LB pH 5.5 with 0 or 150 mg/l $NaNO_2$ in honeycomb plates. Since insertion in *cadA*, which resulted in a severe delay in growth in the presence of acidified $NaNO_2$, was demonstrably stable over 24 h at the non-permissive temperature (37°C) even in the absence of selective pressure (data not shown),

tetracycline was omitted in later screening experiments. Honeycomb plates were incubated in a Bioscreen C growth curve reader at 37°C for 20 h with continuous medium shaking (shaking step 60). Insertion mutants displaying increased sensitivity towards NO and acidified $NaNO_2$ were identified by mathematical calculations and visual inspection of the growth curves. A fixed first OD_{600} value 0.000 was set for all the mutants and subsequent OD_{600} values were adjusted automatically.

To calculate the inhibitory effect on growth by SNP, the area under the growth curve (AUC) by the end of the experiment was automatically calculated by the Research Express Software. From the AUC, the following ratio was calculated:

$$R = \frac{AUC_{+SNP}}{AUC_{-SNP}}$$

The smaller the ratio, the greater is the sensitivity towards SNP. The mean ratio (M_R) and standard deviation (SD) of the insertion mutants within one experimental setup were calculated, excluding those two mutants with the greatest and lowest R as outliers. Insertion mutants were judged to be NO-sensitive if they fulfilled the following criterion:

$$R < M_R - 2\times SD$$

Sensitivity towards acidified $NaNO_2$ is characterized by an increased lag phase. Hence, the difference in time Δt between the $NaNO_2$ treated and the control culture to reach an OD_{600} of 0.2, 0.5 and 0.8 was computed. The time needed to reach each OD was calculated by the Research Express Software. The greater Δt, the higher is the sensitivity towards acidified $NaNO_2$. To truncate outliers, those mutants with Δt among the upper or lower 5% Δt of all insertion mutants at all three time points were omitted from the mean (M) and SD calculations. Mutants were defined as acidified $NaNO_2$ sensitive and selected for further analysis if they met the following criterion:

$$\Delta t(\text{OD } 0.2) > M_{\Delta t(\text{OD } 0.2)} + 2\times SD_{\Delta t(\text{OD } 0.2)} \cap \Delta t(\text{OD } 0.5) > M_{\Delta t(\text{OD } 0.5)} + 2\times SD_{\Delta t(\text{OD } 0.5)}$$

$$\cap \Delta t(\text{OD } 0.8) > M_{\Delta t(\text{OD } 0.8)} + 2\times SD_{\Delta t(\text{OD } 0.8)}$$

NO and acidified $NaNO_2$ sensitive mutants were re-tested in the Bioscreen, along with insertion mutants displaying average sensitivity. Calculations described above were performed on the control mutants, and sensitivity of the conspicuous mutants was confirmed if they fulfilled the same criteria as defined above.

To identify the site of insertion-duplication mutagenesis, the mutagenesis vector pIDM1-x (x = cloned chromosomal fragment for recombination) was retrieved by growth under permissive temperature (30°C). The recombinant fragment was amplified using primers IDM1A and IDM2A, purified and sequenced by GATC (Konstanz, Germany) using IDM1A as sequencing primer.

2.2 Molecular biological methods

2.2.1 DNA isolation

Isolation of genomic DNA

1.5 ml from an overnight culture was harvested (3 min, 13200 rpm) and resuspended in 0.4 ml lysis buffer (100 mM Tris pH 8.0 (Roth), 5 mM EDTA (Roth), 200 mM NaCl). 100 µl Lysozyme (10 mg/ml in lysis buffer, prepared from a 120 mg/ml stock solution, Sigma-Aldrich) was added, and the sample was incubated on ice for 15 min. To degrade proteins in the sample, 10 µl 10% (w/v) SDS (Roth) and 2.5 µl Proteinase K solution (20 mg/ml, AppliChem) were added and the Eppendorf tube was incubated overnight at 55°C. DNA was precipitated by addition of 500 µl isopropanol (Roth) and successively washed in 100% (v/v) and 70% (v/v) EtOH (J.T. Baker). Finally, the pellet was air-dried at 37°C to remove residual EtOH, dissolved in 75 µl TE-buffer pH 7.5 and 75 µl dH_2O with 1 µl RNase A (10 mg/ml, Sigma-Aldrich) at RT and finally stored at -20°C.

Isolation of plasmid DNA

Plasmid DNA was isolated in medium-scale using Pure Link™ Hi Pure Plasmid Midiprep Kit (Invitrogen) or in small-scale using GenElute™ Plasmid Miniprep Kit (Sigma-Aldrich) following the manufacturer's instructions. For medium-scale extraction, 50 ml (high-copy plasmid) or 100 ml (low-copy plasmid) of an overnight culture of the plasmid-bearing bacteria in selective LB broth were collected (10 min, 4186 × *g*, RT). Concerning small-scale isolation, 5-10 ml overnight cultures were used as starting material.

2.2.2 General cloning techniques

2.2.2.1 Polymerase chain reaction (PCR)

For screening purposes, a self-purified *Taq* polymerase that lacks proofreading activity was employed. For control PCR to validate the absence of DNA in samples in which even minute amounts of contaminating DNA could falsify the results, such as RNA samples used for qPCR, the commercial ThermoPrime *Taq* DNA Polymerase (Thermo Scientific) was used. For cloning purposes requiring high fidelity, *Pfu* DNA polymerase (Fermentas, St. Leon-Rot, Germany/Thermo Scientific) or Phusion High-Fidelity DNA Polymerase (NEB, Frankfurt, Germany) (fragments > 2.1 kb) which exhibit 3' to 5' exonuclease (proofreading) activity were applied. PCR reaction set-ups and thermocycling conditions (Primus 96 advanced, Primus 25 advanced (Peqlab, Erlangen, Germany); MJ Mini™ Personal Thermal Cycler (Bio-Rad, Muenchen, Germany)) are summarized in Table 7 and Table 8, respectively.

Table 7: PCR reaction setup

***Taq* polymerase**		***Pfu* polymerase**		**Phusion polymerase**	
component	50 µl	component	50 µl	component	50 µl
forward primer (10 µM)	2 µl	forward primer (10 µM)	2 µl	forward primer (10 µM)	2.5 µl
reverse primer (10 µM)	2 µl	reverse primer (10 µM)	2 µl	reverse primer (10 µM)	2.5 µl
dNTPs (20 mM)	1 µl	dNTPs (20 mM)	0.5 µl	dNTPs (20 mM)	0.5 µl
10x *Taq* buffer with $(NH_4)_2SO_4$	5 µl	10x *Pfu* buffer with $MgSO_4$	5 µl	5x Phusion HF buffer	10 µl
$MgCl_2$ (25 mM)	5 µl				
Taq Polymerase	0.2 µl	*Pfu* polymerase (2.5 U/µl)	0.5 µl	Phusion Polymerase (2 U/µl)	0.5 µl
DNA template	varied	DNA template	varied	DNA template	varied
dH_2O	ad 50 µl	dH_2O	ad 50 µl	dH_2O	ad 50 µl

Table 8: Thermocycling conditions

	***Pfu*/*Taq* polymerase**		**Phusion polymerase**	
step	temperature	time	temperature	time
initial denaturation	95°C	3 min	98°C	30 sec
PCR cycling (30x)				
denaturation	95°C	30 sec	98°C	10 sec
annealing	50°C - 52°C	30 sec	T_m of lower T_m primer (<20 nt)	10 sec
elongation	72°C	2 min/kb (*Pfu*), 1 min/kb (*Taq*)	72°C	30 sec/kb
final elongation	72°C	5 min	72°C	5 min
hold	15°C	forever	15°C	forever

For colony PCR, reaction volumes were downscaled to 25 µl. Single colonies were transferred to the reaction tube with sterile pipette tips and initial denaturation was extended (10 min) in order to lyse bacteria and release DNA. Alternatively, colony material was resuspended in 50 - 100 µl dH_2O and an aliquot (1.0 - 2.5 µl) of this suspension was applied in the reaction. Concerning amplification of fragments for DNA sequencing, an overnight culture or 10^{-1} dilution was heated for 10 min at 100°C. 10 µl of the lysate, cleared of cell debris by centrifugation (3 min, 13200 rpm, RT), was used in the reaction.

2.2.2.2 Agarose gel electrophoresis

50x TAE buffer

2 M	Tris base
5.71% (v/v)	96% Acetic acid (Roth)
50 mM	Na_2EDTA (pH 8)
pH 8.3	

Length of DNA fragments was analyzed by agarose gel electrophoresis. 1% (w/v) or 2% (w/v) LE agarose (Biozym, Hamburg, Germany; Bioline, Luckenwalde, Germany) dissolved in 1x TAE buffer was used for gel casting, and 1 kb DNA Ladder (Fermentas) or 100 bp DNA Ladder (Fermentas) served as size standards. DNA samples (3 - 5 µl) were mixed with 2 µl 6x DNA Loading Dye (Fermentas) and

loaded into the slots. Electrophoresis was performed in 1x TAE buffer in a horizontal electrophoresis chamber (Peqlab) at 80 - 120 V for 30 - 60 min. Finally, DNA was stained with ethidium bromide (0.5 µg/ml dH_2O, Roth) or GelRed (3x staining solution in dH_2O containing 0.1 M NaCl, Biotium, Hayward, CA, USA) for at least 15 min and visualized under UV light (ImageMaster VDS, Pharmacia Biotech; UVsolo TS Imaging System, Biometra).

2.2.2.3 Purification of DNA fragments

DNA fragments from PCR or enzymatic reactions were purified from primers, nucleotides, enzymes and salts using E.Z.N.A Cycle Pure Kit (Omega Bio-Tek, VWR, Darmstadt, Germany) according to manufacturer's instructions. DNA extraction from agarose gels was performed via E.Z.N.A Gel Extraction Kit (Omega Bio-Tek).

2.2.2.4 Restriction enzyme digestion of DNA

DNA was digested using site-specific restriction endonucleases. All restriction enzymes and recommended buffers were obtained from Fermentas. In general, 2 µg vector DNA or all available purified PCR product were digested at optimum temperature for at least 2 h.

Digestion mix	100 µl
DNA (dissolved in dH_2O)	86 µl
10x restriction buffer	10 µl
restriction enzyme (10 U\µl)	4 µl

2.2.2.5 Dephosphorylation of plasmid DNA

To prevent re-circularization, linearized plasmid DNA was dephosphorylated by Shrimp Alkaline Phosphatase (SAP) (Fermentas) for 1 h at 37°C. Following incubation, plasmid DNA was re-purified.

Dephosphorylation mix	100 µl
plasmid DNA (dissolved in dH_2O)	88 µl
10x SAP buffer	10 µl
SAP (1 U/µl)	2 µl

2.2.2.6 Ligation of DNA

Ligation of double-stranded DNA molecules with compatible ends was catalyzed by ATP-dependent T4 DNA Ligase (Fermentas). DNA fragments were mixed in equimolar amounts (2 µl) whereas linearized vector and insert were mixed in different ratios (1:3 to 1:7) dependent on their concentration.

Ligation mix	10 µl
DNA fragment 1 / insert	variable
DNA fragment 2 / vector	variable
10x T4 DNA Ligase buffer	1 µl
T4 DNA Ligase (5 U/µl)	1 µl
dH_2O	ad 10 µl

The ligation mix was incubated overnight at 15°C.

2.2.3 Transformation

2.2.3.1 Preparation of $CaCl_2$ competent *E. coli* cells

1 ml of a shaken overnight culture of *E. coli* DH5α at 37°C was transferred into 100 ml fresh LB medium. Cells were grown at 37°C with shaking (150 rpm) to logarithmic growth phase (OD_{600} = 0.3 - 0.6). Then, they were harvested in 50 ml Falcon tubes (10 min, 1860 × *g*, 4°C), supernatant was removed and bacteria were carefully resuspended in 10 ml cold 0.1 M $CaCl_2$. After resting on ice for 30 min, cells were collected (10 min, 1860 × *g*, 4°C), supernatant was discarded and the bacterial pellet was resuspended in 10 ml chilled 0.1 M $CaCl_2$ containing 20% (v/v) glycerol. Aliquots of 100 - 300 µl were dispensed, shock frozen in liquid nitrogen and stored at -80°C.

2.2.3.2 Heat shock transformation of $CaCl_2$ competent *E. coli* cells

100 µl $CaCl_2$ competent *E. coli* DH5α cells were thawed on ice and added to 10 µl ligation mix. After 30 min incubation on ice, cells were heat shocked in a heating block at 42°C for 90 sec, then immediately placed on ice for 2 min. 1 ml SOC medium was added and cells were shaken at 37°C for at least 1 h to allow expression of antibiotic resistance genes encoded on the plasmid. 100 µl were then plated on LB agar plates containing suitable antibiotics. The remaining cells were collected (3 min, 6000 rpm), supernatant discarded, cells resuspended in the rest of the medium and plated on agar plates likewise. The plates were incubated for 1 day at 37°C until colonies reached a sufficient size to be picked. Colonies were screened by Colony-PCR to prove presence of insert-containing vectors.

2.2.3.3 Preparation of electrocompetent *S.* Typhimurium and EHEC cells

A shaken overnight culture of *S.* Typhimurium or EHEC strains at the appropriate temperature (see Table 9) was diluted 1:100 into fresh LB medium. Cells were grown with shaking (160 rpm) to logarithmic growth phase (OD_{600} = 0.4 - 0.6). After chilling on ice for 15 min, cells were harvested in 50 ml Falcon tubes (10 min, 5000 × *g*, 4°C), supernatant was removed and bacteria were carefully resuspended in one culture volume cold 5% (v/v) glycerol. Washing with 5% (v/v) glycerol was repeated twice with 2/5 and 1/50 of the starting culture volume. After the final centrifugation step, cells were resuspended in 1/250 culture volume 10% (v/v) glycerol. Alternatively, centrifugation was performed in Eppendorf tubes by washing thrice in 1/25 culture volume 5% (v/v) glycerol, microfugation (1 min,

5000 × *g*, 4°C) and final resuspension in 180 µl 10% (v/v) glycerol. Aliquots were dispensed, shock frozen in liquid nitrogen and stored at -80°C.

Electrocompetent *S.* Typhimurium pKD46 cells were prepared likewise except that 1 mM L-arabinose was added to both the overnight and the sub-culture to induce lambda Red recombinase expression. Incubation was performed at 30°C and cells were collected at OD_{600} = 0.5 - 0.6.

Electrocompetent *E. coli* O157:H7 pKM208 cells were prepared following the protocol described by Savage *et al.* (2006). Shaken cultures were grown at 30°C to an OD_{600} = 0.3. 1 mM IPTG was added to induce expression of the lambda Red recombinase system and the culture was further grown to OD_{600} = 0.5 - 0.6. Then, the culture was incubated in a water bath at 42° for 15 min with gently shaking every 5 min and subsequently chilled on ice for 10 min. Collecting and washing of the cells was performed as described above but using 20% (v/v) glycerol.

Table 9: Incubation temperatures for preparation of electrocompetent *S.* Typhimurium and EHEC cells

Strain characteristics	Incubation temperature
WT strains	37°C
strains with chromosomally integrated kanamycin cassette	37°C
deletion strains	37°C
strains with temperature-sensitive plasmids (pKM208, pKD46)	30°C

2.2.3.4 Electroporation of *S.* Typhimurium and EHEC

40 µl (*S.* Typhimurium) or 50 µl (EHEC) aliquots of electro-competent cells were thawed on ice and mixed with 1 - 7 µl linear or 0.1 - 2.0 µg plasmid DNA. The mix was transferred to a chilled electroporation cuvette (2 mm) (Peqlab) and pulsed in a Bio-Rad Gene Pulser (2.5 kV, 200 Ω and 25 µF, *S.* Typhimurium) or MicroPulser (preset program Ec2, EHEC). 1 ml SOC medium was immediately added to the cuvette and cells were generally shaken for 1 h at 37°C or, in the case of electroporation with pCP20, for 1.0 - 1.5 h at 30°C to allow expression of antibiotic resistance genes. Appropriate dilutions or cells sedimented (3 min, 6000 rpm, RT) and resuspended in SOC medium were then plated on selective LB agar plates. The plates were incubated for one day at 37°C or 30°C.

2.2.4 Transduction

Selectable genetic markers were moved between *S.* Typhimurium strains using the general transducing phage P22.

Preparation of phage lysate

Overnight cultures of donor *S.* Typhimurium cells, grown with shaking in LB containing appropriate antibiotic at 37°C, were used to inoculate 10 ml fresh LB medium (containing appropriate antibiotic) in a ratio 1:100. The sub-culture was grown with shaking (160 rpm) at 37°C. At OD_{600} = 0.15 - 0.20, 5 ml of the culture were transferred to a 15 ml Falcon tube and 5 µl of a P22 phage stock raised on WT cells was added to the donor cells. The culture was incubated standing at 37°C for further 6 h to allow phage

absorption, replication and subsequent lysis of donor cells. After incubation, remaining cells were lysed by addition of a few droplets chloroform (50 µl, 4°C) and vigorous shaking. The lysate was then incubated at 4°C for 2 h and cell debris was collected by centrifugation (10 min, 5700 × *g*, 4°C). The supernatant was filter-sterilized through a syringe-filter (0.22 µm) into a 15 ml Falcon tube and the filtrate was stored at 4°C.

Transduction

Recipient cells were prepared from a shaken (160 rpm) overnight culture in LB (containing appropriate antibiotics) at 37°C. 200 µl of the overnight culture was mixed with 10 µl of P22 phage lysate containing the selectable marker for transduction. The mixture was incubated for 60 min at 37°C to allow the cells to express the transduced antibiotic resistance gene. Then, the total mixture was plated on LB agar plates containing suitable antibiotics and incubated at 37°C overnight. As negative controls, 100 µl recipient cells only and 50 µl P22 lysate containing the transducible marker were spread onto selective LB agar plates and incubated likewise. Absence of bacterial growth on these control plates verified that recipient cells were Kan^S before transduction and that the lysate was free of bacterial cells, respectively. Transductants were picked immediately after overnight growth to prevent the formation of lysogens. To purify the phage-free transductants, colonies were streaked onto selective green indicator plates. Purified P22-free colonies appear white on these plates whereas pseudo-lysogenic colonies appear dark green. Single white colonies were picked once more onto selective green indicator plates and subsequently transferred to LB plates containing appropriate antibiotics. To test for lysogen formation, colonies were cross-streaked with P22 lysate (prepared on WT cells) on green indicator plates. Phage-free transductants display cell lysis, as indicated by dark green colonies on the plates.

2.2.5 DNA sequence analysis

DNA sequences were obtained from GATC Biotech AG in Konstanz. Recommended concentrations of purified PCR product or plasmid DNA were used as template for sequencing. DNA sequences were blasted (http://blast.ncbi.nlm.nih.gov/Blast.cgi, nucleotide blast) against the genome sequences of *S.* Typhimurium 14028 (taxid ID: 588858) or *E. coli* O157:H7 EDL933 (taxid ID: 155864).

2.2.6 Mutagenesis strategies

2.2.6.1 Construction of deletion mutants

S. Typhimurium

In-frame deletion mutants were constructed in the genetic background of *S.* Typhimurium 14028 WT using the lambda Red recombinase method (Datsenko and Wanner, 2000). Briefly, PCR products comprising the kanamycin resistance cassette of plasmid pKD4, including the flanking FRT sites, were generated using 70- and 69-bp oligonucleotide primer pairs del_x_F and del_x_R (x = gene to be deleted; Table 3) that included 20-nt and 19-nt priming sequences for pKD4 as template (20 ng),

respectively. Homologous 50-bp primer extensions overlapped 18 nt with the 5' end and 36 nt with the 3' end of the target gene. Purified PCR products were electroporated in Red recombinase producing *S.* Typhimurium cells harboring plasmid pKD46. Allelic replacement of the target gene by the kanamycin resistance cassette was verified by PCR on single Kan^R colonies using combinations of chromosomal test-primers flanking the site of substitution and kanamycin-cassette specific primers (test_x_F and kanR3, test_x_R and kanR2). After curing of pKD46 by growth at non-permissive temperature (37°C), the mutant alleles were transduced by phage P22 into a *S.* Typhimurium 14028 WT background. Positive transductants were selected on kanamycin-containing LB agar plates and purified on green indicator plates. Phage-free transductants were identified by cross-streaking against P22 on green indicator plates. Non-polar deletions were obtained by removal of the kanamycin resistance marker via Flp recombinase after introducing plasmid pCP20 (200 ng). Cm^R colonies were then passaged on non-selective LB agar at non-permissive temperature (37°C) to remove pCP20. Gene deletions in Kan^S Cm^S colonies were verified by PCR analysis and DNA sequencing using test_x_F primer or both test-Primers. Mutants containing several knockouts were constructed by P22-mediated transduction using previously prepared phage lysates for construction of single deletion mutants.

EHEC

In-frame deletion mutants in EHEC were constructed by lambda Red recombination as outlined for *S.* Typhimurium but considering the protocol by Savage *et al.* (2006), which has been modified for gene replacement in EHEC. Instead of pKD46, the plasmid pKM208 was used, which encodes the phage lambda Red recombinase genes under control of the IPTG-inducible P_{tac} promoter. Moreover, the vector carries the *lacI* repressor gene for tight regulation of *red* and *gam* expression prior to induction. The phage transduction step described for *S.* Typhimurium was omitted. To induce excision of the kanamycin-cassette, pCP20 carrying Cm^R strains obtained by non-selective overnight growth at 30°C, were colony-purified on LB agar and incubated at 42°C. Then they were tested for loss of all antibiotic resistances (Cm^R, Kan^R) on selective agar plates.

2.2.6.2 Construction of complementation mutants

In trans arabinose-inducible complementation of Δ*pta* using pBAD/HisA(Tet^R)

Arabinose-inducible *in trans* complementation of gene deletions was achieved by introducing the coding sequence (CDS) of the respective gene into the low-copy vector pBAD/HisA(Tet^R). A fragment comprising the *pta* CDS was amplified using primers C_*pta*_F2 and C_*pta*_R (Table 3) and cloned into the *Sac*I and *Eco*RI restriction sites of pBAD/HisA(Tet^R). The resulting complementation plasmid pBAD-*pta* was introduced in competent *E. coli* DH5α cells by heat shock transformation and transformants were selected on tetracycline-containing LB agar plates at 37°C. Tet^R transformants containing the complementation plasmid were identified by colony-PCR using the primers pBADforward and pBADreverse and integrity of the insert was checked by sequencing. Finally, pBAD-

pta was purified from *E. coli* and introduced into the *S.* Typhimurium Δ*pta* strain by electroporation, yielding the complemented strain Δ*pta* comp-*pta*. As controls, plasmid pBAD/HisA(Tet^R) was transformed into Δ*pta* as well as the WT, resulting in strains Δ*pta* pBAD/HisA(Tet^R) and WT pBAD/HisA(Tet^R), respectively.

In trans complementation of Δ*cadA* using pBR322 and the gene specific promoter

For complementation of Δ*cadA*, a PCR product corresponding to the coding sequence of *cadA* under control of its own promoter was introduced at the *Hind*III and *Bam*HI cloning sites of pBR322. Since *cadA* is the second gene of the *cadBA* operon, it was fused to its promoter via an artificially generated 84 bp "scar" sequence of pKD4 that usually remains after FLP-mediated excision of the antibiotic cassette (Datsenko and Wanner, 2000), which is based on a previously described complementation of Δ*cadA* (Viala *et al.*, 2011). This was done by 3' overhangs on primers C_cadA_B and C_cadA_C corresponding to the scar sequence. Briefly, the *cadBA* promoter region and the *cadA* coding sequence including 82 bp upstream and 100 bp downstream of *cadA*, were amplified using primer combinations C_cadA_A/C_cadA_B and C_cadA_C/C_cadA_D (Table 3), respectively. The PCR products were ligated via a natural *Xba*I restriction site in the "scar" sequence, and the corresponding fragment was amplified using primers C_cadA_A and C_cadA_D. The product was cloned into vector pBR322, resulting in the complementation vector pBR322-*cadA*, which was introduced into competent *E. coli* DH5α cells by heat shock transformation. Amp^R transformants containing the complementation plasmid were identified by colony-PCR using the primers seq_pBR322_F and seq_pBR322_R. Finally, for construction of the complementation mutant Δ*cadA*-comp, pBR322-*cadA* was introduced into *S.* Typhimurium Δ*cadA* by electroporation. As controls, plasmid pBR322 was transformed into Δ*cadA* as well as the WT, resulting in strains Δ*cadA* pBR322 and WT pBR322, respectively.

2.2.7 RNA methods

2.2.7.1 Preparation of cell pellets

All cell pellets were prepared from shaken (160 rpm) or standing cultures grown at 24°C. Growth was monitored by measuring the OD_{600}. Upon reaching the desired OD_{600} or after a defined incubation period, cells were collected by centrifugation (8 min, 4186 × *g*, RT). Following decanting of the supernatant and complete removal of residual medium, cell pellets were snap-frozen in liquid nitrogen and stored at -80°C until further processing.

NO donor SNP

A shaken overnight culture in LB broth was diluted 1:100 in 150 ml LB broth pH 7. The 150 ml culture was grown at 24°C with shaking to an OD_{600} = 0.80 - 0.85, then it was split into two 50 ml cultures. 40 µM SNP was added to one of these cultures, while the other was left untreated to serve as a reference. Both cultures were further grown with shaking and collected at OD_{600} = 1.50 ± 0.05.

Acidified $NaNO_2$

A shaken overnight culture in LB broth was diluted 1:100 in fresh LB broth pH 5.5 and grown with shaking. To analyze the shock response to acidified nitrite, a 150 ml culture at OD_{600} = 0.80 - 0.85 was split into two 50 ml cultures, and 150 mg/l $NaNO_2$ was added to one of these cultures while the other was left untreated to serve as a control. After further incubation for 10 min at 24°C with shaking, cells from both cultures were harvested. To analyze the adaptive response to acidified nitrite, a 50 ml reference culture and a 50 ml culture, to which 150 mg/l $NaNO_2$ was added at OD_{600} = 0.80 - 0.85, were grown until both (*S.* Typhimurium) or the reference culture (EHEC) reached an OD_{600} = 1.50 ± 0.05.

Raw-sausage simulating conditions

The impact of the traditional curing agents $NaNO_2$ and KNO_3 as well as celery extract on the transcriptome of *S.* Typhimurium was analyzed under conditions mimicking those in raw sausages on ripening days 0 and 3. For this purpose, meat extract broth at different pH values and NaCl concentrations (MEB0, MEB3, II1.4) and with typical additives such as glucose and sodium ascorbate was employed (Table 10).

The previous day, MEB0, MEB0 with dissolved celery extract powder and MEB3 were filter-sterilized (0.22 µm) and 14.8 ml aliquots prepared in 15 ml Falcon tubes. To reduce the amount of dissolved O_2 in the media, they were incubated at RT in an anaerobic jar using Anaerocult A (Merck) for 24 h as instructed by the supplier. Anaerotest strips verified the creation of an anaerobic atmosphere by turning from blue into white. A pre-culture of *S.* Typhimurium 14028 WT was grown in 5 ml meat extract broth with shaking for about 8.0 - 8.5 h and used to inoculate a 70 ml overnight culture (at OD_{600} = 0.01) in fresh meat extract broth. The culture was grown with shaking for 16 h. 10 ml aliquots of the culture were then collected (8 min, 4186 × *g*, RT), the supernatant was discarded and the cell pellets were dissolved in either 1 ml MEB0 or MEB3. After addition of supplements according to Table 10 and 1.1 ml of cells resuspended in the respective medium to the anaerobically pre-incubated media, Falcon tubes were tightly closed and carefully mixed for three times. Cells were collected after standing incubation for 1 h.

Table 10: Raw sausage-like conditions for RNA-seq

Ingredients	Sample names					
	RD0 Ctrl	RD0 $NaNO_2$	RD0 celery	RD0 KNO_3	RD3 Ctrl	RD3 $NaNO_2$
Broth	MEB0	MEB0	MEB0	MEB0	MEB3	MEB3
Celery extract	-	-	[a]10 g/l	-	-	-
Glucose	0.200% (w/v)	0.200% (w/v)	[b]0.196% (w/v)	0.200% (w/v)	-	-
KNO_3	-	-	-	70 mg/l	-	-
$NaNO_2$	-	150 mg/l	-	-	-	30 mg/l
Sodium ascorbate	500 mg/l	500 mg/l	500 mg/l	500 mg/l	-	-

[a] Corresponds to about 70 mg/l KNO_3.

[b] Final concentration added was 0.200% (w/v), since celery extract contains some glucose.

2.2.7.2 RNA extraction

Total RNA was extracted using TRI Reagent (Sigma-Aldrich) and the RNeasy Mini Kit (Qiagen, Hilden, Germany). Briefly, the cells were resuspended in 1 - 3 ml TRI Reagent, subdivided into 1 ml aliquots if needed, and incubated at RT for 5 min. Cells were mechanically disrupted three times for 45 sec at 6.5 m/sec using 0.1 mm silica beads (Roth) in a Ribolyzer FastPrep®-24 (MP Biomedicals, Eschwege, Germany) with cooling on ice for 5 min in between. After addition of 200 µl chloroform and mixing, samples were incubated for 5 min at RT before the organic and aqueous phases were separated by centrifugation (15 min, 12000 × *g*, 4°C). The aqueous phase was transferred to a new tube and total RNA was precipitated by addition of 0.5 ml isopropyl alcohol (10 min, RT followed by 10 min, 12000 × *g*, 4°C). The RNA pellet was washed twice with 1 ml 70% EtOH (5 min, 7500 × *g*, 4°C), air-dried at RT for 10 - 20 min and dissolved in DEPC-treated (0.1% (v/v)) dH_2O. Individually processed aliquots from the same sample were pooled then. DNA was removed by digestion with RQ1 RNase-free DNase (Promega, Mannheim, Germany) for 45 min at 37°C in a total reaction volume of 100 µl. DNase was removed by chloroform extraction (100 µl, 15 min, 15000 × *g*, 4°C). The RNA was further purified using RNeasy Mini Kit (Qiagen) following the RNA clean-up protocol with an additional on-column DNase I digestion according to the manufacturer's instruction. RNA was finally eluted in 30 µl RNase-free dH_2O. Absence of genomic DNA in the RNA extracts was checked by control PCR performed in a 25 µl reaction volume using 0.5 µl RNA sample as template and chromosomally binding primers. Genomic DNA served as a positive control. RNA concentration and purity from DNA and organic contaminants was determined using a NanoDrop ND-1000 Spectrophotometer (Thermo Scientific, Wilmington, DE, USA), and RNA integrity was checked electrophoretically on a 2% (w/v) agarose gel.

2.2.7.3 Quantitative real-time reverse transcription PCR (qPCR)

qPCR was performed to validate RNA-seq data and to analyze transcription of selected genes.

Amplicon and primer design

Primers for qPCR (Table 4) were designed using the free software Primer3 (v. 0.4.0) (http://frodo.wi.mit.edu/primer3). Forward and reverse primers (18 - 23 bp, optimum 20 bp) were chosen that amplified a 100 - 170 bp (preferred size 120 - 150 bp) centrally located fragment of the target gene sequence obtained from the NCBI Genbank (*S.* Typhimurium 14028s: http://www.ncbi.nlm.nih.gov/nuccore/CP001363.1, *E. coli* O157:H7 EDL933: http://www.ncbi.nlm.nih.gov/nuccore/56384585;) and had an annealing temperature of 54 - 56°C. Additionally, primers that contained 2 to 3 GC at the 3' end and had low self- and pair-complementarity were preferred. Specific binding of the oligonucleotides to the target region was checked by aligning the primers to the target genome (*S.* Typhimurium 14028 taxid ID 588858, *E. coli* O157:H7 EDL933 taxid ID 155864) using Primer-Blast (http://www.ncbi.nlm.nih.gov/tools/primer-blast/).

Primer efficiency (E) was determined by recording a standard curve from a linear 4 - 5 point dilution series of the respective, purified PCR product, where log template amount is plotted against the corresponding C_T value. Each dilution was assayed in duplicate. From the value of the slope (S), primer efficiency (E) was calculated according to the following equation (Bustin, 2000):

$$E = 10^{(-1/S)}$$

Primer efficiencies between 1.8 and 2.1 were within the acceptable range.

cDNA synthesis

One µg total RNA was subjected to first strand cDNA synthesis using the qScript cDNA SuperMix Kit (Quanta Biosciences, Gaithersburg, MD) in a total reaction volume of 20 µl following the manufacturer's protocol. Reverse transcription was performed in a thermocycler as follows: 5 min at 25°C, 30 min at 42°C, 5 min at 85°C, hold at 8°C. Finally, cDNA was diluted 5-fold with DEPC-dH_2O and stored at -20°C.

qPCR assays

Gene-specific primers (Eurofins MWG Operon) are listed in Table 4. qPCR assays were prepared as follows: 10 µl PerfeCTa SYBR Green FastMix (Quanta Biosciences), 1 µl of each primer (10 pmol/µl, forward and reverse), 3 µl DEPC-treated dH_2O, 5 µl cDNA template (diluted 5-fold, corresponding to 50 ng total RNA). When 16S rRNA was used as reference gene, cDNA further diluted 1000-fold (corresponding to 50 pg total RNA) was employed in combination with the 16S primers. The qPCR reactions were performed either in single tubes in a SmartCycler (Cepheid, Germany) or in 96-well plates (ThermoFast 96 semi skirted plates, Thermo Scientific) in an iCycler (Bio-Rad), with cycling once at 95°C for 10 min, followed by 40 cycles of 95°C for 20 sec, 53°C for 30 sec and 72°C for 30 sec. Additionally, melt curves were recorded (SmartCycler: 53°C to 97°C at 0.2°C/sec; iCycler: 50°C to 93°C at 0.5°C/10 sec) to check specificity of the amplification reactions. Each cDNA sample was run in technical duplicate and, for each primer pair, a no template control was included. For each growth condition, cDNAs synthesized from total RNA extracted from three to four independent cultures were analyzed.

Data analysis

Relative quantification of transcripts from a sample culture compared to those from the respective control culture was evaluated using the comparative C_t (threshold cycle) method implemented in the software REST (Relative Expression Software Tool) (Pfaffl *et al.*, 2002). In this method, expression of a target gene is normalized by a non-regulated reference (ref) gene. Relative gene expression (R) is calculated based on the PCR efficiencies (E_{target}, E_{ref}) and the mean threshold cycle deviation (ΔC_t) between the sample and control group. *ampD* (encoding a cytosolic *N*-acetyl-anhydromuramyl-L-

alanine amidase) or 16S rRNA, transcript levels of which are invariant across a wide range of growth conditions (Rowley *et al.*, 2012; Livak and Schmittgen, 2001), were used as non-regulated endogenous normalization controls.

$$R = \frac{E_{target}^{\Delta Ct_{target}(\text{MEAN control} - \text{MEAN sample})}}{E_{ref}^{\Delta Ct_{ref}(\text{MEAN control} - \text{MEAN sample})}}$$

The relative gene expression R was $\log_2$ transformed, and, if not stated otherwise, the mean and SD of the $\log_2$ fold-change (FC) from the independent experiments were calculated.
To compare relative transcription levels of different conditions, they were converted to % mRNA expression.

$$\text{mRNA expression (\%)} = R \times 100$$

mRNA expression level of the control culture was set 100%. Data shown represent the geometric mean and SE (standard error) of three independent experiments.

2.2.7.4 RNA-sequencing (RNA-seq)

Sample preparation

For RNA-seq, RNA was isolated following the TRI Reagent extraction protocol described above. In this case, RNA was dissolved in RNase-free dH_2O (Qiagen). 90 µg of TRI Reagent-extracted RNA (exception: SNP control sample, 45 µg; 40 µM SNP-treated sample, 34 µg) was subjected to the column-based purification steps of the RNeasy Mini Kit without prior DNase digestion. Also, the on-column DNase treatment and, consequently, the control PCR were omitted.
16S and 23S ribosomal RNA (rRNA) were removed from 5 µg total RNA (exception: SNP-treated and control sample, 5.3 µg) using the MICROBExpress Kit (Ambion, Life Technologies, Darmstadt, Germany) following the manufacturer's instructions with the following modifications: Concerning *S.* Typhimurium, two additional oligonucleotides targeting fragments of the *S.* Typhimurium 23S rRNA (5'-xCCTCGGGGTACTTAGATGTTTCA-3', 5'-xGTCGGTTCGGTCCTCCAGTTAGT-3'; x = sequence needed for hybridization to Oligo MagBeads) were added (2 µl of a 10 µM mix, corresponding to 20 pmol of each probe) in addition to the capture oligonucleotide mix supplied with the kit. In general, annealing of the oligonucleotides was performed for 30 min (exception: SNP-treated and control sample, 20 min).
The mRNA enriched sample was then treated with the TURBO DNA-free Kit (Ambion) to remove residual DNA. In a 50 µl reaction, rRNA-depleted RNA was mixed with 5 µl 10x Turbo DNase buffer and 1 µl Turbo DNase and incubated at 37°C for 30 min in a thermoblock. 5 µl of DNase inactivation reagent was then added and the sample was incubated for 5 min at RT, flicking the tube occasionally. The inactivation solution was then sedimented by spinning (1.5 min, 13000 rpm, RT) and the supernatant containing the RNA was moved to a new tube. RNA was then concentrated by ethanol precipitation.

The RNA was mixed with 3 volumes 100% EtOH and 1/10 volume 3 M sodium acetate and precipitated for 1 h at -20°C. Following centrifugation (15 min, 12500 × *g*, 4°C), the RNA pellet was washed twice with 750 µl 70% EtOH (5 min, 12500 × *g*, 4°C). The pellet was then dried for 5 min at RT and rehydrated for 15 min in 15 µl Nuclease-free dH_2O.

The sequencing library was constructed with the SOLiD Total RNA-Seq Kit and the SOLiD Transcriptome Multiplexing Kit (Applied Biosystems, Foster City, USA) as previously described (Landstorfer *et al.*, 2014). Briefly, RNA (500 ng) was fragmented with RNase III for 9 min and cleaned up with the miRNeasy Mini Kit (Qiagen) following the "Purification of Total RNA from Animal Tissues" Protocol, but omitting the homogenization step. Quantitation and quality control after each RNA treatment step was performed using the NanoDrop and a RNA 6000 Pico Chip in a 2100 Bioanalyzer (Agilent Technologies, Santa Clara, CA, USA), respectively. 100 ng fragmented RNA was dried in a SpeedVac at 30°C for 10 - 15 min and resuspended in 3 µl Nuclease-free dH_2O. SOLiD adaptors were hybridized and ligated to the fragmented RNA, and the ligated fragments were reverse transcribed. The resulting cDNA was purified and size-selected by two rounds of bead capture using the Agencourt AMPure XP Reagent (Beckman Coulter, Krefeld, Germany) and amplified by 15 PCR cycles according to the SOLiD manual. For each library, a different barcoded SOLiD 3' PCR Primer from the SOLiD Transcriptome Multiplexing Kit was used. The resulting amplified cDNA library was purified using the PureLink PCR Micro Kit (Invitrogen). The size distribution and yield of the purified libraries was assessed on the 2100 Bioanalyzer with a DNA 1000 or High Sensitivity DNA Chip (Agilent Technologies) and using a Qubit 2.0 Fluorometer and the dsDNA HS Assay Kit (Life Technologies). SOLiD system templated bead preparation and sequencing on the SOLiD 5500xl system was conducted by CeGaT GmbH (Tübingen, Germany). Six differently barcoded libraries were pooled and sequenced on one, three or six lanes of one SOLiD slide (Table 11). For each library sequenced on multiple lanes, the SOLiD output files (.csfasta, .qual) from the different lanes were merged into single files for further analysis.

Table 11: Assignment of the RNA-seq samples to the number of lanes they were sequenced on

Number of lanes sequenced on	Samples
1	*S.* Typhimurium response to SNP
3	EHEC 10 min shock and 1 h response to acidified $NaNO_2$
	S. Typhimurium 10 min shock response to acidified $NaNO_2$
6	*S.* Typhimurium adaptation response to acidified $NaNO_2$
	S. Typhimurium under raw-sausage simulating conditions

Data analysis

Data processing steps to convert SOLiD output files to sorted, indexed BAM files containing reads mapping to the reference genome of *S.* Typhimurium 14028 (NCBI RefSeq NC_016856.1 (chromosome) and NC_016855.1 (plasmid)) or *E. coli* O157:H7 EDL933 (NCBI RefSeq NC_002655 (chromosome) and NC_007414 (plasmid pO157)) were performed as previously described (Landstorfer

et al., 2014). Briefly, SOLiD output files were converted to FASTQ with Galaxy (Blankenberg *et al.*, 2010; Goecks *et al.*, 2010). The reads were mapped to the reference genome of *S.* Typhimurium 14028 or *E. coli* O157:H7 EDL933 using Bowtie (Langmead *et al.*, 2009) with default settings (seed length: 28, maximum number of mismatches permitted in the seed: 2, maximum permitted total of quality values at mismatched read positions: 70). Output SAM files were filtered for mapped reads only using SAMTools (Li *et al.*, 2009), and further converted to BAM files, which were then indexed using Picard Tools. The number of reads overlapping a gene on the same strand (counts) were calculated in Artemis (version 15.0.0) (Rutherford *et al.*, 2000; Carver *et al.*, 2012) based on the GenBank file of the reference genome (downloaded on 01/14/2014 (*S.* Typhimurium) and 02/27/2014 (EHEC)). Counts of all protein-coding genes of *S.* Typhimurium 14028 or *E. coli* O157:H7 EDL933 according to RefSeq .ptt files downloaded from the FTP NCBI database (ftp://ftp.ncbi.nlm.nih.gov/genomes/Bacteria/; 01/14/2014 (*S.* Typhimurium) and 03/06/2014 (EHEC)) were subjected to differential gene expression analysis using the Bioconductor (Gentleman *et al.*, 2004) package edgeR (Robinson *et al.*, 2010). Pairwise comparisons were made to identify differentially expressed genes between conditions. Genes with less than 10 counts per million (cpm) in both conditions were filtered, and library sizes were recomputed before TMM (trimmed mean of M-values) normalization (Robinson and Oshlack, 2010) was applied to account for compositional differences between the libraries. To analyze distances between several libraries, filtering and normalization was performed on all libraries as described, and a multidimensional scaling (MDS) plot was created using the plotMDS function. The leading log FC for each pair of samples is defined as the root-mean-square average of the largest $\log_2$ FC of a set of 500 genes for the respective pairwise comparisons. Differential expression analysis was performed using the exact test function. A common dispersion 0.1 was used, as suggested for genetically identical model organisms in the edgeR user's guide (revised version from 4 May 2012). The false discovery rate (FDR) was controlled using the Benjamini-Hochberg (BH) method (Benjamini and Hochberg, 1995) in edgeR. Genes with a BH-corrected p-value < 0.05 were regarded as differentially expressed and assigned to COGs (clusters of orthologous genes) according to the .ptt files of *S.* Typhimurium strain LT2 (NC_003197 (genome), NC_003277 (plasmid); downloaded on 01/14/2014) or *E. coli* O157:H7 EDL933. The assignment of *S.* Typhimurium 14028 genes to *S.* Typhimurium LT2 genes was performed using a table of all *S.* Typhimurium 14028 genes with the best hit in LT2 from Duan *et al.* (2009) and KEGG (Kyoto Encyclopedia of Genes and Genomes; http://www.genome.jp/kegg/).

To compare qPCR results with RNA-seq data, mRNA expression (%) for the RNA-seq data was calculated based on the cpm-values of the sample conditions relative to the control condition.

$$\text{RNA-seq mRNA expression (\%)} = \frac{\text{cpm}_{\text{sample}}}{\text{cpm}_{\text{control}}} \times 100$$

2.2.8 Intracellular pH measurement of *S.* Typhimurium

A pH-sensitive GFP variant (EGFP) was used as intracellular pH indicator (Kneen *et al.*, 1998) to monitor changes in the intracellular pH of *S.* Typhimurium exposed to acidified $NaNO_2$. A shaken overnight culture of WT pEGFP grown for 17 h in LB supplemented with 150 µg/ml ampicillin at 24°C was collected (8 min, 4186 × *g*, RT) and washed first with 1 and then with 0.5 volumes PBS, pH 7.4. An OD_{600} of approximately 10 was then adjusted in PBS, pH 7.4 and the cell suspension was stored on ice. The suspension was diluted in sample buffer to an OD_{600} of 1.0 and incubated for 5 min at RT before fluorescence was measured in a Perkin Elmer LS-50B luminescence spectrophotometer (Waltham, MA, USA). Emission spectra resulted from averaging five subsequent scans recorded from 500 to 580 nm with excitation at 490 nm, slit 3.5 to 4.0 nm and scan speed 1000 nm/min. To analyze the impact of $NaNO_2$ addition on the intracellular pH dependent on the pH of the growth medium, WT pEGFP assayed in LB pH 5.5 or neutral LB was measured before and immediately after addition of 150 mg/l $NaNO_2$. To verify that a decrease in fluorescence intensity was due to $NaNO_2$ rather than to mere photobleaching of EGFP due to repeated measurement of the same sample, a second sample was measured, to which dH_2O was added instead of $NaNO_2$. The experiment was performed three times independently.

III Results

1 *Salmonella* Typhimurium

Salmonella naturally reside in the intestinal tract of animals including pigs and cattle and may therefore be present in the raw meat of these animals (Callaway *et al.*, 2008; EFSA, 2015). To prevent outgrowth of undesired bacteria, nitrite curing salt is traditionally added as a preservative to raw meat products. However, the inhibitory effect of nitrite varies depending on the bacterial species, as revealed by challenge assays of *Salmonella* and EHEC in raw sausages performed by cooperation partners from the MRI in Kulmbach (Kabisch, 2014). Little experimental data exist to clarify the distinct ability of these organisms to cope with nitrite stress in the context of raw sausage curing. Hence, in this study, the effect of acidified $NaNO_2$-derived stress on *S.* Typhimurium and the means by which this organism might counteract this stress were analyzed with a special focus on the conditions of raw sausage ripening.

1.1 Contribution of the NO-detoxifying enzymes HmpA, NorV and NrfA to nitrosative stress protection under food-related conditions

NO is one key reactant that is formed from nitrite under the acidic conditions in the meat (Jira, 2004; Honikel, 2008) and might be one important mediator of the antibacterial action of nitrite in this food matrix. It is well established that the flavohemoglobin HmpA, the flavorubredoxin NorV and the periplasmic cytochrome *c* nitrite reductase NrfA participate in NO detoxification under different environmental conditions *in vitro* (Crawford and Goldberg, 1998; Mills *et al.*, 2005; Mills *et al.*, 2008) and that HmpA is important for survival of *S.* Typhimurium in macrophages (Stevanin *et al.*, 2002; Gilberthorpe *et al.*, 2007) and virulence in mice (Bang *et al.*, 2006). However, it is unknown if these enzymes might also be crucial for resistance against acidified nitrite-derived stress in raw sausages during the first few days of ripening. The role of HmpA, NorV and NrfA in this context was investigated in this study.

1.1.1 Transcriptional analysis of *hmpA*, *norV* and *nrfA* in response to acidified $NaNO_2$

$NaNO_2$-dependent transcription of the genes *hmpA*, *norV* and *nrfA* in the *S.* Typhimurium WT was analyzed by qPCR (Figure 3) in three independent cultures. A strong induction of *hmpA* transcription (log_2 FC 6.6, 4.2 and 2.9) was observed in cells treated with 150 mg/l $NaNO_2$. To the contrary, transcript levels of *norV* (log_2 FC -0.3, -0.9 and -1.4) and even more of *nrfA* (log_2 FC -2.3, -4.5 and -0.5) were reduced in nitrite-stressed cultures compared to the control cultures. The increased transcription of *hmpA* might indicate a high demand of HmpA to protect *S.* Typhimurium from acidified nitrite stress under the conditions employed.

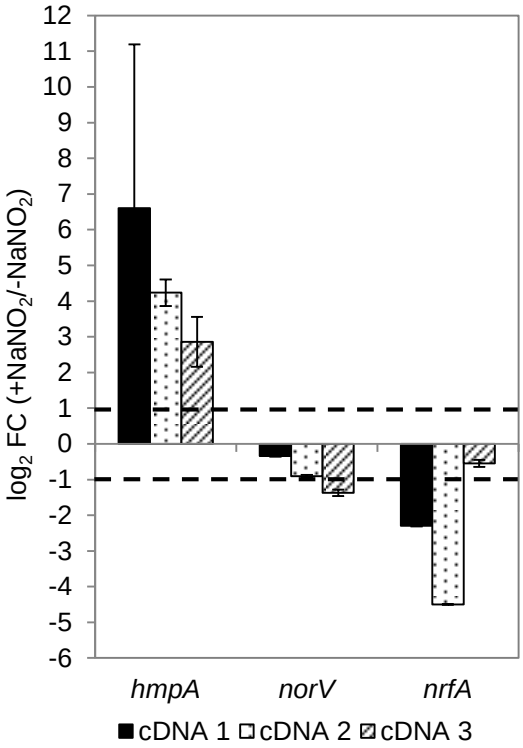

Figure 3: Increased transcription of the *hmpA* gene in the presence of acidified $NaNO_2$.
Transcription of the genes *hmpA*, *norV* and *nrfA* was analyzed by qPCR in *S.* Typhimurium 14028 WT cultures inoculated in LB pH 5.5 at 24°C with shaking. The relative transcription level of the respective genes in cultures treated with 150 mg/l $NaNO_2$ (+$NaNO_2$) compared to untreated (-$NaNO_2$) cultures was determined. cDNAs were synthesized from RNA isolated from three independent experiments. Depicted is the $\log_2$ FC ± SE of $NaNO_2$ treated vs. control cultures for each cDNA, calculated from duplicates by the comparative C_t-method with the *ampD* gene used as non-regulated reference. Log_2 FC with an absolute value of at least 1 (bold dashed lines) were considered as indicating a $NaNO_2$-dependent transcription.

1.1.2 Characterization of single deletion mutants in *hmpA*, *norV* and *nrfA* under food-related conditions

Although transcription of *norV* and *nrfA* is unaltered in the presence of acidified $NaNO_2$, it cannot be excluded that the respective enzymes still play a role in protection against acidified $NaNO_2$ stress in raw sausages. To pursue the question of the relative contribution of the NO-detoxifying systems, *hmpA*, *norV* and *nrfA* single knockout mutants were constructed and phenotypically characterized by growth assays (Figure 4). To consider conditions relevant for raw sausage ripening, nitrosative stress was exerted by $NaNO_2$ at concentrations encountered during raw sausage ripening (50, 100, 150 mg/l $NaNO_2$) in LB medium acidified to a pH value of 5.5 with lactic acid, which is normally produced by the starter cultures during fermentation. All growth analyses were performed at 24°C, a relevant ripening temperature, both under high and low O_2 supply.

Growth of the *S.* Typhimurium WT as well as of the Δ*norV* and Δ*nrfA* mutants is equally delayed with increasing concentrations of $NaNO_2$. To the contrary, Δ*hmpA* displayed similar aerobic growth in the absence of $NaNO_2$, but grew more slowly than the other strains, notably after addition of 100 or 150 mg/l $NaNO_2$. In the presence of 100 mg/l $NaNO_2$, the WT and the Δ*norV* and Δ*nrfA* mutants needed approximately 9 h to reach an $OD_{600} = 0.2$, whereas the Δ*hmpA* mutant needed 12 h.

This growth disadvantage of the Δ*hmpA* mutant was even more pronounced when grown with 150 mg/l $NaNO_2$. Under these conditions it took the WT and the Δ*norV* and Δ*nrfA* mutants 11 h to reach an OD_{600} = 0.2, the Δ*hmpA* mutant needed 31 h (Figure 4A). However, at some later time point, Δ*hmpA* resumed growth similar to that of the parent strain and finally diverged to the same maximum OD_{600}. Regarding growth kinetics over the whole time frame of the experiment, i.e. 48 h, the area under the growth curve of Δ*hmpA* in the presence of 100 and 150 mg/l $NaNO_2$ was strongly reduced compared to that of the other strains, further illustrating its growth defect (Figure 4B). When O_2 supply was reduced by overlaying cultures with mineral oil, similar results were obtained, with an even more pronounced nitrite-sensitivity of Δ*hmpA* at 100 mg/l $NaNO_2$ (Figure 4C, D). These data point to a possible contribution of HmpA in counteracting acidified $NaNO_2$ stress in raw sausages.

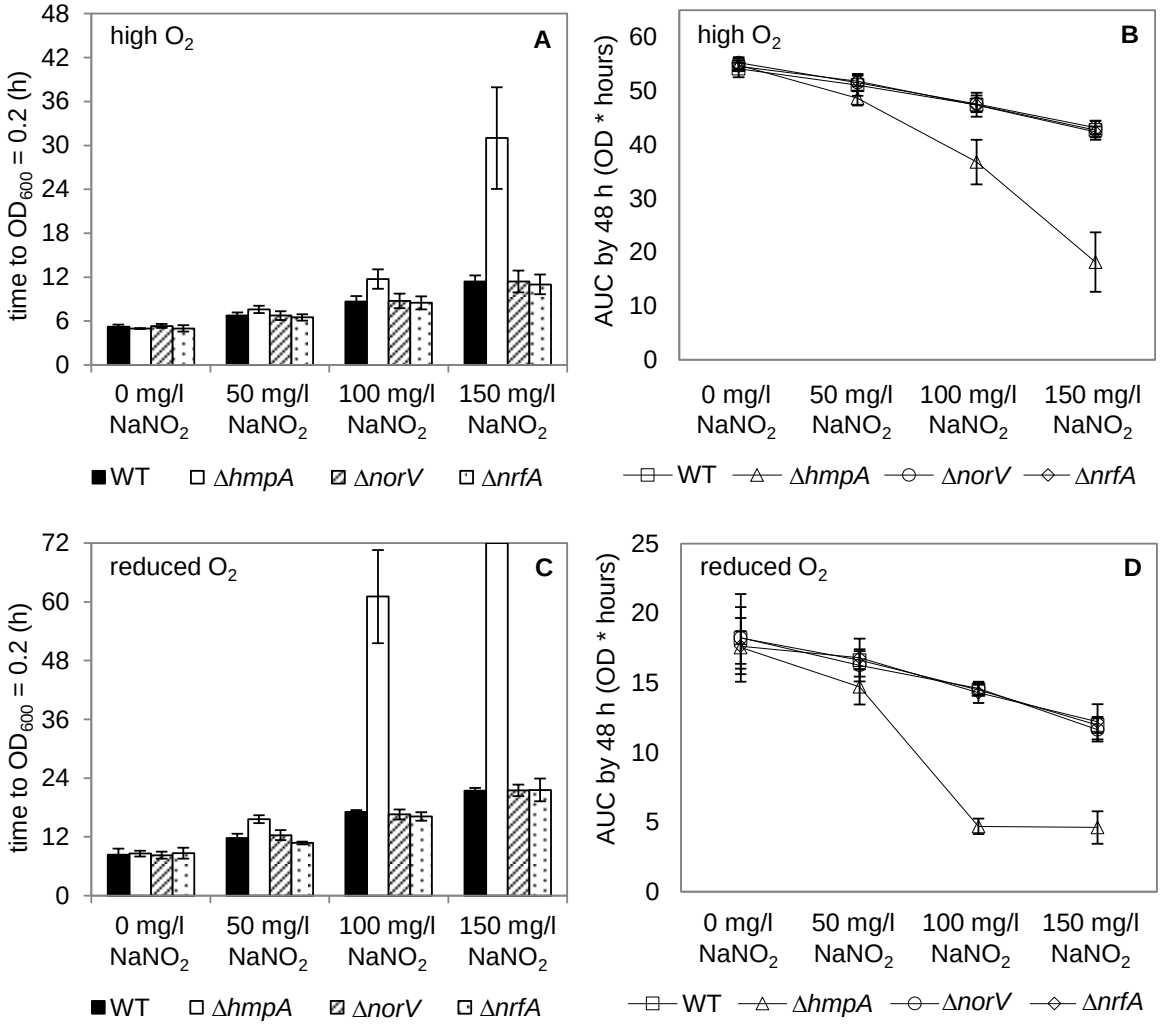

Figure 4: Impact of $NaNO_2$ on growth of *S.* Typhimurium 14028 WT and deletion mutants Δ*hmpA*, Δ*norV* and Δ*nrfA* under acidic conditions.
S. Typhimurium 14028 WT and deletion mutants were grown in LA acidified LB pH 5.5 in the presence of 0, 50, 100 or 150 mg/l $NaNO_2$ with agitation at 24°C under aerobic (A, B) or micro-aerobic conditions (C, D) in a Bioscreen C. Depicted are mean values ± SD from three independent experiments including duplicates. A, C: Time to reach OD_{600} = 0.2 (h) in dependence of the $NaNO_2$ concentration for cultures of *S.* Typhimurium WT (black), Δ*hmpA* (white), Δ*norV* (striped) and Δ*nrfA* (dotted). B, D: Area under the growth curve (AUC) after 48 h in dependence of the $NaNO_2$ concentration for cultures of *S.* Typhimurium WT (square), Δ*hmpA* (triangle), Δ*norV* (circle) and Δ*nrfA* (diamond).

To further elucidate the role of HmpA, NorV and NrfA in protecting *S.* Typhimurium 14028 from nitrosative stress in raw sausage products under natural conditions, growth kinetics of the deletion mutants Δ*hmpA*, Δ*norV* and Δ*nrfA* in short-ripened spreadable sausages were analyzed compared to the WT by cooperation partners from the MRI in Kulmbach (Figure 5). In these challenge assays, short-ripened spreadable sausages produced with 0 or 150 mg/kg $NaNO_2$ were artificially inoculated with 10^4 cfu *S.* Typhimurium WT or deletion mutant per gram meat.

To ensure that growth differences in the sausages with 0 and 150 mg/kg $NaNO_2$ are solely attributable to the action of the added $NaNO_2$, the pH-value and the water activity were measured in both types of sausages. These two additional hurdles in raw sausage ripening might vary between batches of sausages produced with or without $NaNO_2$ and thereby indirectly affect the growth kinetics of *S.* Typhimurium. An indirect growth-inhibitory effect of $NaNO_2$ via these two physico-chemical parameters could be ruled out, since they were similar in sausages produced without or with 150 mg/kg $NaNO_2$. The pH-value dropped from 5.8 (sausages without $NaNO_2$) or 5.7 (sausages with $NaNO_2$) on production day to 5.2 by ripening day 3 and 5.1 by day 13, and slightly rose to 5.2 by day 28 in both types of sausages (Figure 5B). The water activity (a_w) was reduced by 0.02 from 0.95 - 0.96 to 0.93 - 0.94 by day 28 (Figure 5C). In sausages cured with $NaNO_2$, the $NaNO_2$ content rapidly decreased from a mean of 140 mg/kg to 65 mg/kg by day 1 and 10 mg/kg by day 3. It remained constant at 7 mg/kg on average until the end of ripening (Figure 5D). Total plate count and lactic acid bacteria profiles were also not affected by addition of $NaNO_2$. Their initial number of approximately 10^7 cfu/g increased by two log units in the first three days of ripening and reached a maximum near 10^9 cfu/g (data not shown).

With regard to the *S.* Typhimurium WT and deletion mutants, their numbers were reduced by 1.0 - 1.7 log units to around 10^3 in sausages cured with $NaNO_2$ compared to those produced without $NaNO_2$ (Figure 5A). In the latter ones, after a slight increase till day 6, numbers did not decline below the inoculation level by the end of the ripening period. However, no difference was observed between the growth kinetics of mutants Δ*hmpA*, Δ*norV* and Δ*nrfA* compared to the WT, irrespective of whether nitrite was added or not. Contrary to the observed nitrite-sensitive phenotype of Δ*hmpA* in the *in vitro* growth assays, the mutant was no more sensitive in sausages produced with $NaNO_2$ compared with the other strains.

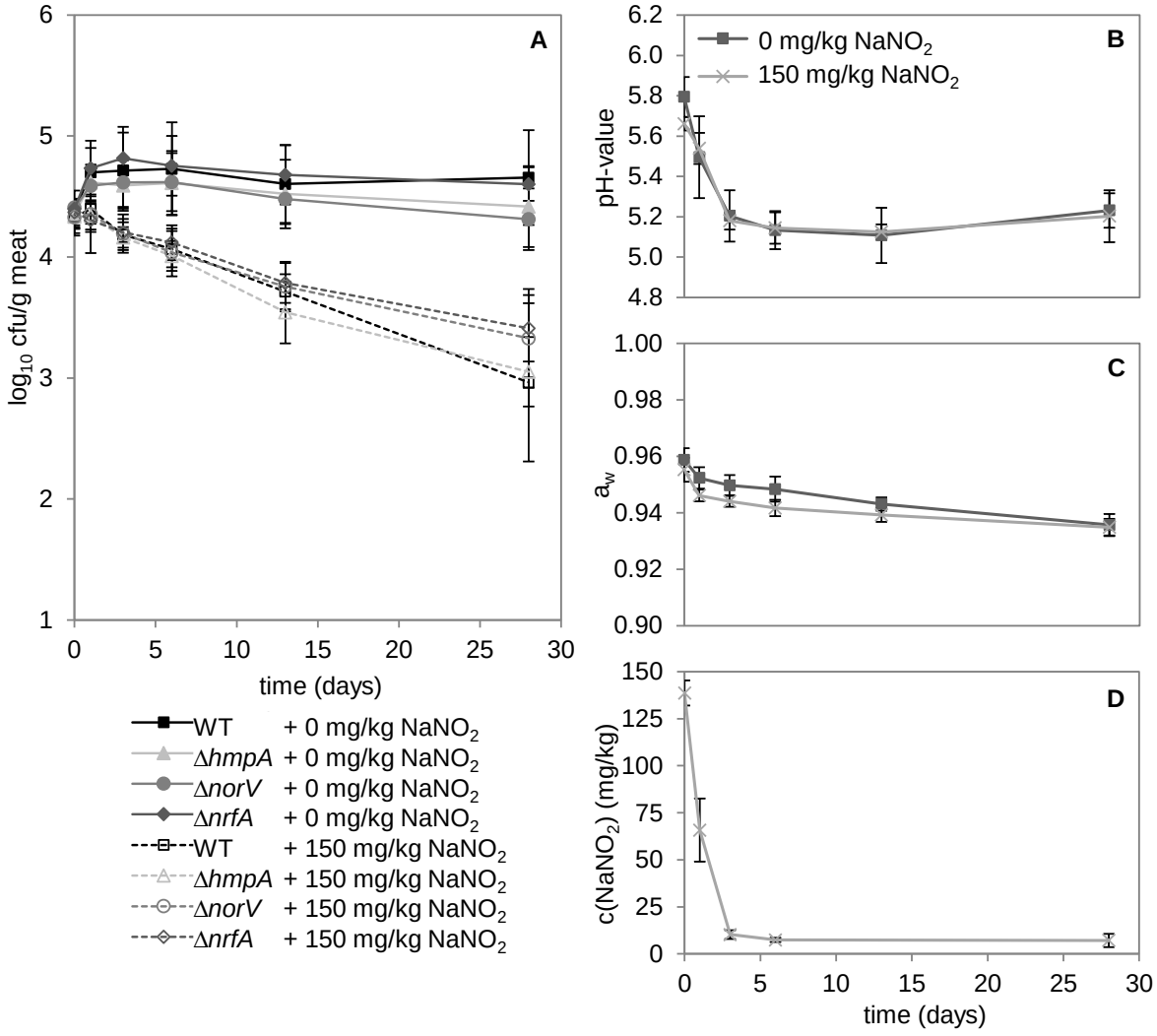

Figure 5: Impact of $NaNO_2$ on survival of *S.* Typhimurium 14028 WT and deletion mutants in NO-detoxifying systems in short-ripened spreadable sausages and course of physico-chemical parameters during ripening.

(A) Numbers of *S.* Typhimurium 14028 WT (square), Δ*hmpA* (triangle), Δ*norV* (circle) and Δ*nrfA* (diamond) were determined in short-ripened spreadable sausages produced without $NaNO_2$ (solid lines) or cured with 150 mg/kg $NaNO_2$ (dotted lines). Cfu/g meat matrix was determined via cell count on XLD and DHL agar plates. In control short-ripened spreadable sausages, which were not inoculated with *Salmonella* and either prepared with 0 (dark grey, square) or with 150 mg/kg $NaNO_2$ (light grey, cross), the pH-value (B), the a_w-value (C) and the nitrite concentration (D) were determined. Three different sausages per batch were sampled in duplicate on days 0, 1, 3, 6, 13 and 28. Values represent the mean ± SD from three biologically independent experiments. Data were kindly provided by Rohtraud Pichner (MRI Kulmbach).

1.1.3 Growth analysis of *hmpA*, *norV* and *nrfA* double mutants and the triple mutant in the presence of acidified $NaNO_2$

One possible explanation for the lack of a discernible nitrite-sensitive phenotype of any of the single deletion mutants might be some functional redundancy of HmpA, NorV and NrfA in detoxification of NO arising from acidified nitrite during sausage fermentation.

However, an additive contribution of these systems would be expected only under conditions of reduced O_2 tensions (Gardner *et al.*, 2003; Mills *et al.*, 2008), which might also prevail in raw sausages. To test this hypothesis, mutants lacking two (Δ*hmpA* Δ*norV*, Δ*hmpA* Δ*nrfA*, Δ*norV* Δ*nrfA*) or all three of these enzymes (Δ*hmpA* Δ*norV* Δ*nrfA*) were constructed. Growth of the deletion mutants compared to the WT was analyzed in LB pH 5.5 without $NaNO_2$ or in the presence of 50 mg/l $NaNO_2$ at 24°C in a Bioscreen C. This lower $NaNO_2$ concentration was used, since higher concentrations of $NaNO_2$ already strongly delayed or even impaired growth of the single mutant Δ*hmpA* (see Figure 4). Cultures were overlaid with mineral oil to reduce O_2 supply.

Growth of all strains was comparable without $NaNO_2$, taking about 8 h to reach OD_{600} = 0.2, but was distinctly affected by 50 mg/l $NaNO_2$ (Figure 6). While growth of the WT and Δ*norV* Δ*nrfA* was similarly delayed by this concentration of $NaNO_2$ (13 h and 12.5 h), Δ*hmpA* Δ*nrfA* needed about twice as long (27 h) to grow to the same optical density. By contrast, Δ*hmpA* Δ*norV* and the triple mutant did not grow at all to OD_{600} = 0.2 within the time frame of the experiment (72 h). These results indicate that both HmpA and NorV, with HmpA being more effective, are important to withstand acidified $NaNO_2$ stress under the conditions tested. If this combined action might hold true also for short-ripened spreadable sausages still needs to be investigated.

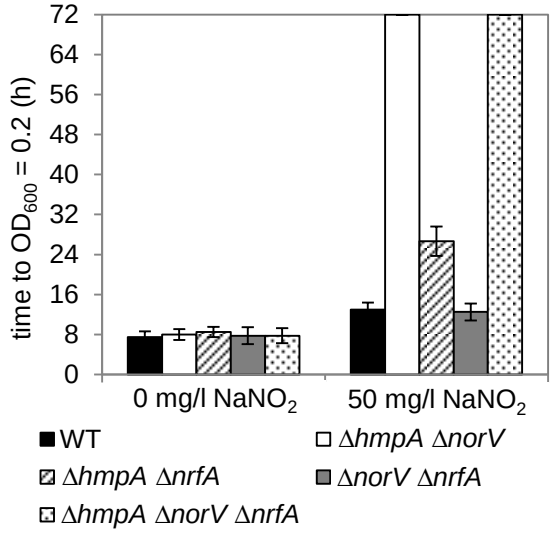

Figure 6: Impact of $NaNO_2$ under acidic conditions on growth of *S.* Typhimurium 14028 WT and mutants lacking two or all three NO-detoxifying enzymes HmpA, NorV and NrfA.

S. Typhimurium 14028 WT and deletion mutants were grown in LA acidified LB pH 5.5 in the presence of 0 or 50 mg/l $NaNO_2$ with agitation at 24°C under micro-aerobic conditions in a Bioscreen C. Depicted are mean values ± SD from three independent experiments including duplicates. The time the WT (black), Δ*hmpA* Δ*norV* (white), Δ*hmpA* Δ*nrfA* (striped), Δ*norV* Δ*nrfA* (grey) and Δ*hmpA* Δ*norV* Δ*nrfA* (dotted) strains needed to reach an OD_{600} = 0.2 (h) in dependence of the $NaNO_2$ concentration was analyzed. Columns represent mean values ± SD from three independent experiments.

1.2 Analysis of the NO and acidified $NaNO_2$ stress response of *S.* Typhimurium and identification of novel systems that contribute to nitrosative stress resistance in *S.* Typhimurium

One possible explanation for the lack of a discernible phenotype of single deletion mutants in raw sausages is, that they compensate loss of one another under these conditions, which is supported by the *in vitro* growth assays of double mutants, but awaits proof *in situ*. On the other hand, other reactive derivatives apart from NO might arise from acidified $NaNO_2$ that convey the growth inhibitory action. To better understand how NO- and acidified $NaNO_2$-derived stress affect *S.* Typhimurium on the molecular level, global transcriptional studies were performed considering parameters relevant for raw sausage production. In addition, a *S.* Typhimurium insertion mutant library was screened to identify novel systems that might contribute to the protection of *S.* Typimurium against NO and acidified $NaNO_2$ stress.

1.2.1 Analysis of the transcriptional response of *S.* Typhimurium to the NO donor SNP

NO is the most important reactive intermediate that arises from nitrite upon acidification in the raw meat (Jira, 2004; Honikel, 2008). Hence, the transcriptional response of *S.* Typhimurium 14028 WT to the NO donor SNP under neutral conditions was analyzed compared to a reference culture without SNP. In general, addition of 40 µM SNP at OD_{600} = 0.80 - 0.85 slightly delayed growth of *S.* Typhimurium WT cultures, so it took the SNP-treated culture 10 - 20 min longer to reach the harvest OD_{600} = 1.50 ± 0.05 compared to the reference culture (data not shown). The transcriptomes of both cultures were assessed by RNA-seq and compared to find differentially transcribed genes. In total, 5416 genes are annotated as protein-coding on the *S.* Typhimurium chromosome and virulence plasmid. Of these, 3339 (61.7%) genes passed the cpm 10 filter and were therefore assumed as being transcribed. Differential gene expression analysis revealed that transcription of only seven genes was altered in SNP-treated compared to control cultures under a BH-adjusted p-value cutoff < 0.05. Transcript abundance of five genes was higher and that of two genes was lower in cultures grown with SNP (Table 12). The up-regulated genes comprised exclusively genes that were described to be under control of the NO-responsive repressor NsrR in *S.* Typhimurium (Karlinsey *et al.*, 2012), namely *hmpA*, *hcp-hcr*, *ygbA* and STM14_2185 (corresponding to STM1808 in strain LT2). Upon exposure to NO, the Fe-S cluster of NsrR is nitrosylated, which results in the loss of DNA binding activity and hence relieves repression of target gene transcription (Tucker *et al.*, 2008a). The role of HmpA in NO detoxification has been described in the introduction (see I4.2.2.1). The exact function of STM14_2185, YgbA and Hcp has not been defined yet, however, analysis of strains lacking the functional proteins indicated that they may be important to resist nitrosative stress under certain growth conditions (Karlinsey *et al.*, 2012). The functional relevance of the genes with decreased transcript levels in response to SNP, *yhbU* and *yecH*, is unknown.

To identify more genes that might be less markedly affected by SNP, the p-value was relaxed to < 0.15. Eleven additional genes were found to be transcriptionally down-regulated upon SNP exposure (Table 12). Among these were three genes associated with anaerobic terminal reductases for nitrite (*nrfA*), tetrathionate (*ttrC*) and putatively for DMSO (STM14_5179).

Table 12: Differentially transcribed genes in response to 40 µM SNP in *S.* Typhimurium 14028
Log_2 FC with a BH-adjusted p-value < 0.05 are shown in bold.

14028 identifier	Gene name	Product	log_2 FC	p-value (BH-adjusted)
STM14_3135	*hmpA*	nitric oxide dioxygenase	**4.93**	**7.32E-07**
STM14_1052	*hcp*	hydroxylamine reductase	**4.78**	**1.12E-06**
STM14_3456	*ygbA*	hypothetical protein	**4.42**	**1.49E-05**
STM14_2185	-	putative cytoplasmic protein	**4.58**	**2.86E-05**
STM14_1051	*hcr*	HCP oxidoreductase	**3.69**	**5.83E-04**
STM14_3956	*yhbU*	putative protease	**-3.85**	**1.91E-03**
STM14_2354	*yecH*	putative cytoplasmic protein	**-3.06**	**0.04**
STM14_1515	-	putative ABC transporter periplasmic binding protein	-2.64	0.06
STM14_1516	-	putative ABC transporter protein	-2.66	0.06
STM14_2655	*stcA*	putative fimbrial-like protein	-2.64	0.06
STM14_3957	*yhbV*	putative protease	-2.80	0.06
STM14_1678	*ttrC*	tetrathionate reductase complex subunit C	-2.75	0.08
STM14_4819	-	hypothetical protein	-2.79	0.11
STM14_5143	*nrfA*	cytochrome *c* nitrite reductase	-2.39	0.14
STM14_1519	-	ABC transporter ATP-binding protein	-2.43	0.14
STM14_3785	-	putative cytoplasmic protein	-2.49	0.14
STM14_5179	-	putative anaerobic dimethylsulfoxide reductase subunit B	-2.56	0.14
STM14_5485	*yjjI*	hypothetical protein	-2.38	0.14

To validate the results of the RNA-seq data, the SNP-dependent transcription of the genes *hmpA*, *hcp*, *ygbA*, *yhbU*, *ttrC*, *nrfA* and STM14_5179 was analyzed via qPCR (Figure 7) (Schürch, 2012). Three independent RNA sets obtained from different reference and SNP-treated cultures were assayed. Consistent with the RNA-seq data, transcript levels of *hmpA*, *hcp* and *ygbA* (log_2 FC 4.1 ± 0.3; 4.2 ± 1.7; 3.3 ± 1.0) were higher in the presence of SNP, while those of *yhbU*, *ttrC*, *nrfA* and STM14_5179 (log_2 FC -3.7 ± 1.4; -3.6 ± 1.6; -2.8 ± 1.4; -3.3 ± 1.0) were lower.

In conclusion, RNA-seq and qPCR data revealed an NO-mediated transcriptional increase of NsrR-regulated genes and a decrease of three genes associated with anaerobic respiration.

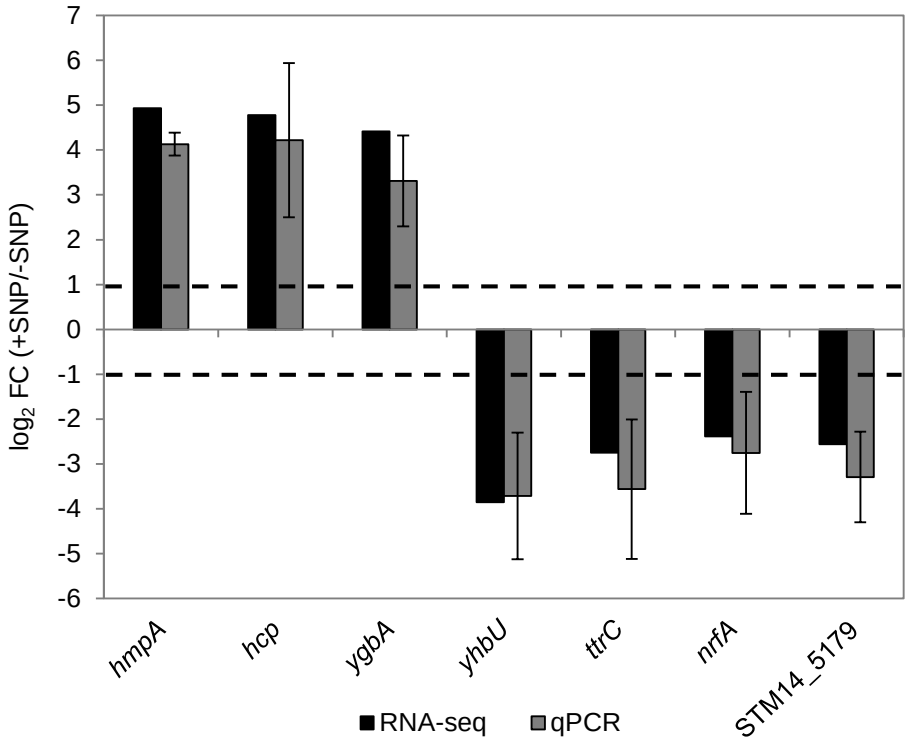

Figure 7: Validation of the NO stress RNA-seq data via qPCR
The log_2 FC of the genes *hmpA*, *hcp*, *ygbA*, *yhbU*, *ttrC*, *nrfA* and STM14_5179 in *S.* Tyhimurium cultures treated with 40 µM SNP compared to the respective control cultures were determined by RNA-seq (black columns) and qPCR (grey columns). qPCR columns represent the mean ± SD from three independent experiments. *ampD* was used as a reference gene for qPCR data normalization. Genes displaying log_2 FC with an absolute value of at least 1 (bold dashed lines) were considered to be differentially regulated by SNP. qPCR data were obtained from Schürch (2012).

1.2.2 Shock and adaptation response of *S.* Typhimurium to acidified $NaNO_2$

1.2.2.1 Transcriptome of *S.* Typhimurium under acidified $NaNO_2$ stress

A variety of reactive nitrogen intermediates apart from NO might arise from nitrite upon acidification by lactic acid in the meat (Honikel, 2008; Skibsted, 2011). These reactants could target the bacterial cell and might not be removed via the NO-detoxifying systems HmpA, NorV and NrfA, which would provide an explanation why growth of single mutants is not affected in $NaNO_2$-cured sausages compared to the WT. To analyze the response of *S.* Typhimurium to $NaNO_2$ acidified by lactic acid, transcriptional profiling was performed via RNA-seq of *S.* Typhimurium WT in LB pH 5.5 treated with 150 mg/l $NaNO_2$ under two different experimental set-ups to investigate both its shock response (Figure 8A) and adaptational response (Figure 8B).

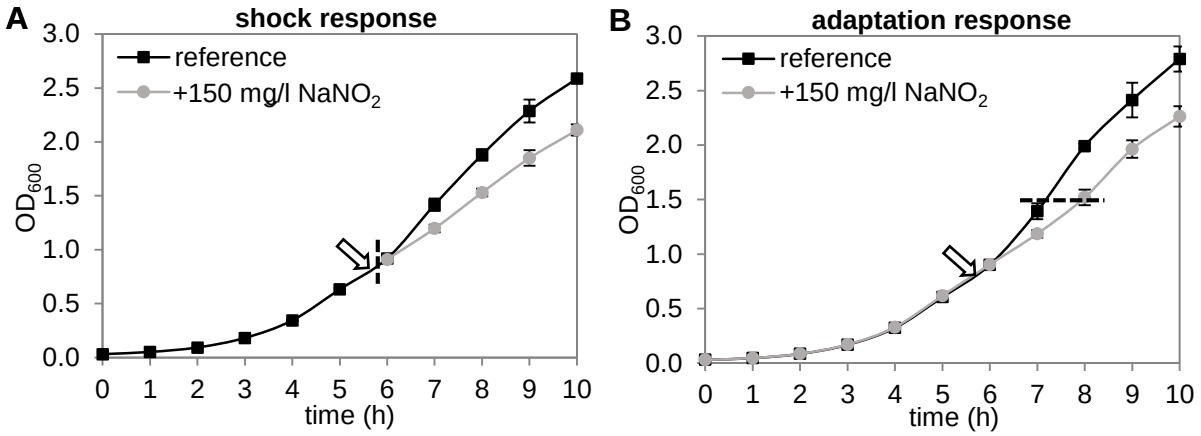

Figure 8: Growth curves of *S.* Typhimurium 14028 WT illustrating the experimental set-ups for the analysis of the transcriptional response to acidified $NaNO_2$ shock (A) and adaptation (B).
Growth of shaken flask cultures of the reference culture without $NaNO_2$ (black square) and the culture to which 150 mg/l $NaNO_2$ was added (grey circle) at 24°C was recorded. Data represent mean values ± SD from three independent experiments. The arrow indicates the time-point (OD_{600} = 0.80 - 0.85), at which 150 mg/l $NaNO_2$ was added. The time points of harvesting the cultures for RNA extraction (A: 10 min after addition of $NaNO_2$, B: OD_{600} = 1.50 ± 0.05) are indicated by the dashed line.

Differentially expressed genes were assessed by comparison with untreated reference cultures in the same growth medium. The up- and down-regulated genes were grouped according to their COGs class and are listed in appendix Table A 1 (shock-response, up-regulated genes), Table A 2 (shock-response, down-regulated genes), Table A 3 (adaptive response, up-regulated genes) and Table A 4 (adaptive response, down-regulated genes).

Filtering of genes with less than 10 cpm resulted in 3095 (57.1%; shock response) and 3080 (56.9%; adaptive response) genes out of the 5416 genes annotated as protein-coding on the *S.* Typhimurium genome that were then subjected to differential gene expression analysis.

After a 10 min shock with acidified $NaNO_2$, 102 genes (3.3%) were found up-regulated while 199 genes (6.4%) were down-regulated in *S.* Typhimurium WT. The adaptive response was characterized by increased transcription of 55 genes (1.8%) and a decrease in transcription of 53 genes (1.7%). These genes were functionally classified according to COGs (Figure 9).

More than one third of the genes up-regulated upon a 10-min acidified $NaNO_2$ shock are either poorly characterized (11%) or not assigned to any functional category (27%). Not surprisingly, genes under control of the dedicated NO sensors NorR (*norVW*) (Tucker *et al.*, 2004) and NsrR (STM14_2185, *hmpA, ytfE, ygbA, hcp, yeaR-yoaG*) (Karlinsey *et al.*, 2012) were induced in the presence of acidified $NaNO_2$, with most of them showing the highest FC values. These genes are distributed among diverse COGs. Besides these specific nitrosative stress response regulons, several other genes with a described role in protection against diverse stresses were also found to be up-regulated. Among these, two amino acid decarboxylases and associated amino acid/polyamine antiporters for lysine (*cadA, cadB*) and arginine (*adi, yjdE*) exhibited the greatest transcriptional changes. Both have an established role in acid resistance (Viala *et al.*, 2011; Alvarez-Ordóñez *et al.*, 2010).

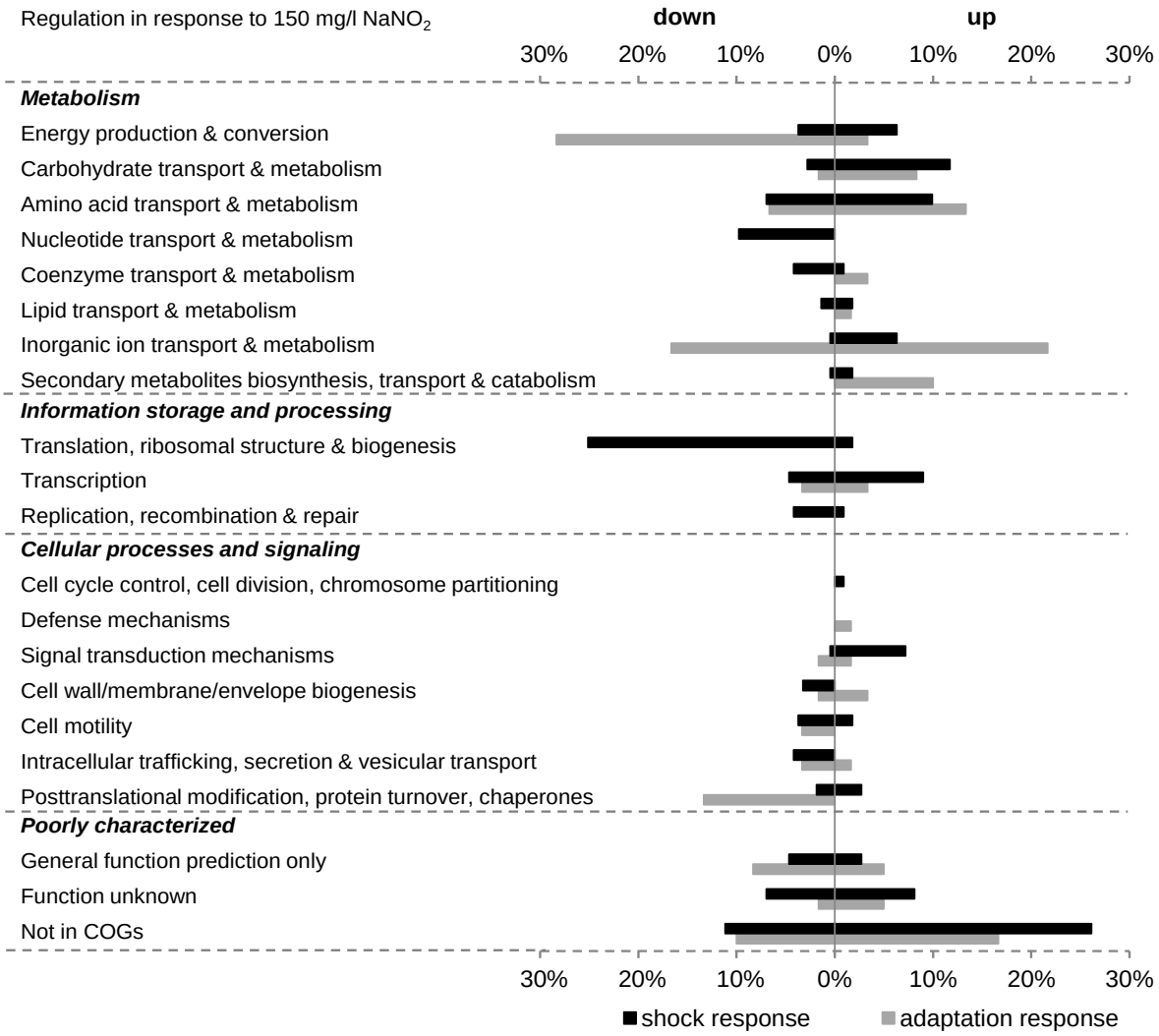

Figure 9: Overview of the differentially regulated genes in the acidified $NaNO_2$ shock and adaptation response of *S.* Typhimurium WT according to their functional category.
Genes significantly up- or down-regulated under acidified $NaNO_2$ shock (black bars) or adaptation (grey bars) in *S.* Typhimurium WT were grouped according to the NCBI COGs. Bars represent the percentage of genes with increased or decreased transcription of a given category relative to the total number of up- or down-regulated genes among all COG categories (corresponding to 100%) under the respective condition. Since one gene can be classified into more than one COG class, the total number of COG assignments is greater than the number of differentially expressed genes and relative percentages refer to the former.

Further examples which are less strongly induced are *ogt* and *dps*, which are involved in DNA repair and protection, respectively (Yamada *et al.*, 1995; Calhoun and Kwon, 2011). Two genes, *yfiA* and *yhbH*, whose proteins mediate inactivation of ribosomes in stationary phase (Polikanov *et al.*, 2012), also showed elevated transcript levels.

Most of the down-regulated genes belong to the functional category of information storage and processing that comprises transcription, translation and replication which are essential processes for cell proliferation. The largest part of them is involved in translation, ribosomal structure and biogenesis. Thus, genes encoding 30S (e.g. *rpsU*, *rpsH*) and 50S ribosomal subunits (e.g. *rplU*, *rplM*), translation initiation (*infA*) and termination (*prfC*) factors, tRNA (e.g. *queA*, *pheS*, *argS*, *trmU*, *trmD*, *yhdG*) and rRNA (e.g. *yciL*, *yfcB*, *rimM*, *rsmC*) modifying enzymes and ribonucleases (*rph*, *rnpA*) showed

decreased transcript levels. Furthermore, genes coding for ATP-dependent RNA helicases (*dbpA*, *deaD*, *rhlE*) and GTPases (*engA*, *era*, *obgE*) which are involved in ribosome maturation at least in *E. coli* (Kaczanowska and Rydén-Aulin, 2007) were down-regulated. Besides an overall transcriptional decrease in genes related to translation, a lower transcript abundance for genes involved in transcription, and replication, recombination and repair, such as *rpoA* (DNA-directed RNA polymerase subunit alpha), *gyrA* (DNA gyrase subunit A), *fis* (DNA-binding protein Fis) and *priB* (primosomal replication protein N), was also observed. Going in hand with this, many genes required for nucleotide transport and metabolism were repressed. Several genes in the biosynthetic pathways for purines and pyrimidines were affected and transcript levels of transporters for uracil (*uraA*) and cytosine (*codB*) were reduced. Furthermore, several genes involved in flagellar biosynthesis (e.g. *flgA*, *flgB*, *flgH*, *flhBA*, *fliE*, *fliFG*) and thereby in cell motility were also decreased. Noteworthy among the functional category amino acid transport and metabolism is the down-regulation of genes involved in uptake (*potAB*, *potC*) or biosynthesis (*speC*, *speD*) of putrescine or spermidine.

When *S.* Typhimurium is allowed to adapt to acidified $NaNO_2$ for a longer period of time, more than 60% of the up-regulated genes have metabolic function. The gene displaying the greatest FC was *hdeB*, whose function is unknown and which is annotated as acid-resistance protein. Comparable to the shock response, genes involved in nitrosative stress protection under control of NsrR (*hmpA*, STM14_2185, *ygbA*, *hcp*, *yeaR-yoaG*) displayed increased transcription. Interestingly, amino acid decarboxylase systems were also found up-regulated under prolonged acidified $NaNO_2$ stress, but this time those for ornithine (*speF-potE*) and arginine (*adi*, *yjdE*). Transcription of STM14_5358, STM14_5360 and STM14_5361, which have recently been shown to encode a functional arginine deiminase (ADI) pathway in *S.* Typhimurium (Choi *et al.*, 2012), was also increased in the amino acid transport and metabolism category. The largest group of up-regulated genes comprises iron uptake and transport genes mainly in the functional categories inorganic ion transport and metabolism, and secondary metabolites biosynthesis, transport and catabolism. These include genes for the synthesis of the iron-siderophore enterobactin (*entCEBA*, *entF*), uptake of ferrous (*feoAB-yhgG*) or siderophore-bound ferric iron (*fhuADB*, *fepA*, *fepB*, *fepC*, *tonB*, *exbD*), and release of iron from bacterioferritin or siderophores (*bfd*, *fhuF*). Most of the down-regulated genes grouped mainly into the subcategories energy production and conversion and inorganic ion transport and metabolism (both metabolism), or belonged to posttranslational modification, protein turnover and chaperones (cellular processes and signaling). Strikingly, most of the gene products are involved in anaerobic respiratory pathways. Thus, genes coding for subunits of terminal reductase complexes for dimethylsulfoxid (DMSO) (*dmsAB* and two other loci putatively encoding subunits), tetrathionate (*ttrBCA*), nitrate (*narHJI*, *napFDAGHBC*) and nitrite (*nrfA*, *nrfE*) were down-regulated. Moreover, some genes involved in formation or maturation of hydrogenases (*hypBDE*) were down-regulated. Consistent with the observed up-regulation of iron import systems, transcript levels of the gene coding for the iron-storage protein *ftn* were decreased.

Another down-regulated gene shown to be iron-responsive (Bjarnason *et al.*, 2003) was *yhbU* along with its downstream-located gene *yhbV*, both coding for putative proteases.

Comparison of the stress responses to SNP and acidified $NaNO_2$ shows an overlap in up-regulation of NsrR-controlled genes, indicating that cells encounter NO under both conditions. On the other hand, differential regulation of additional genes including stress-related ones in response to acidified $NaNO_2$ supports the notion that bacteria have to cope with additional stressors under this condition.

1.2.2.2 Validation of the RNA-seq transcriptome data via qPCR

To validate the acidified $NaNO_2$ induced transcriptional changes, qPCR on four biological replicates per growth condition was performed. Genes representative for functional categories or pathways that show major deregulation by acidified $NaNO_2$ were selected for validation. For the shock response to acidified $NaNO_2$, relative transcription of six genes with increased (*adi*, *cadA*, *hdeB*, *hmpA*, *norV*, *yfiA*) and seven genes with decreased transcript abundance (*fliF*, *potB*, *purB*, *pyrE*, *rnpA*, *rplM*, *rpsH*) was analyzed. Concerning the adaptational response, a subset of eleven differentially transcribed genes, including seven up-regulated (*adi*, *fhuA*, *feoB*, *hdeB*, *hmpA*, *speF*, STM14_5361) and four down-regulated (*nrfA*, STM14_5179, *ttrC*, *yhbU*) ones, was chosen. Results obtained by qPCR showed a high correlation with the RNA-seq data for both treatments (coefficient of determination $R^2 = 0.92$ (shock response) (Figure 10A) and $R^2 = 0.96$ (adaptive response) (Figure 10B), supporting the validity and reproducibility of the RNA-seq data.

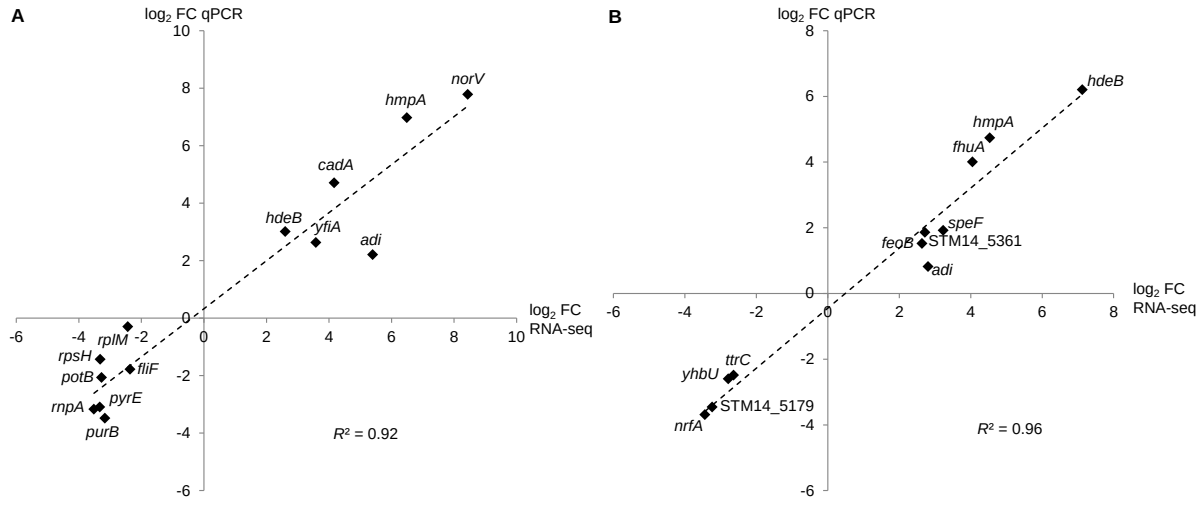

Figure 10: qPCR validation of the acidified $NaNO_2$ stress RNA-seq data of *S.* Typhimurium for selected differentially expressed genes.
Relative transcription of genes found differentially regulated in the RNA-seq analysis of (A) the shock or (B) the adaptive response of *S.* Typhimurium to acidified $NaNO_2$ were examined with qPCR. 16S rRNA (A) or *ampD* (B) was used as reference gene. Mean log_2 FC of four independent qPCR experiments were plotted against the respective log_2 FC determined by RNA-seq. The coefficient of determination R^2 was calculated in Microsoft Excel.

1.2.2.3 Construction and growth analysis of a *hdeB* deletion mutant

The gene *hdeB*, which is annotated as acid-resistance protein, was up-regulated upon acidified $NaNO_2$ shock (log_2 FC 2.60 and 3.01 by RNA-seq and qPCR analysis, respectively) and was the gene most strongly induced in the adaptive response to $NaNO_2$ (log_2 FC 7.12 and 6.20). To analyze if the *hdeB* gene product might protect *S.* Typhimurium from acidified $NaNO_2$-mediated stress, a strain lacking *hdeB* (Δ*hdeB*) was constructed. Growth of Δ*hdeB* in LB pH 5.5 with different concentrations of $NaNO_2$ (0, 50, 100 and 150 mg/l) at 24°C was analyzed compared to the WT using a Bioscreen C (Figure 11). However, no growth differences between Δ*hdeB* and the WT were detected. It cannot be ruled out, that Δ*hdeB* might still be important to withstand acidified $NaNO_2$ stress under conditions not tested by this experimental set-up.

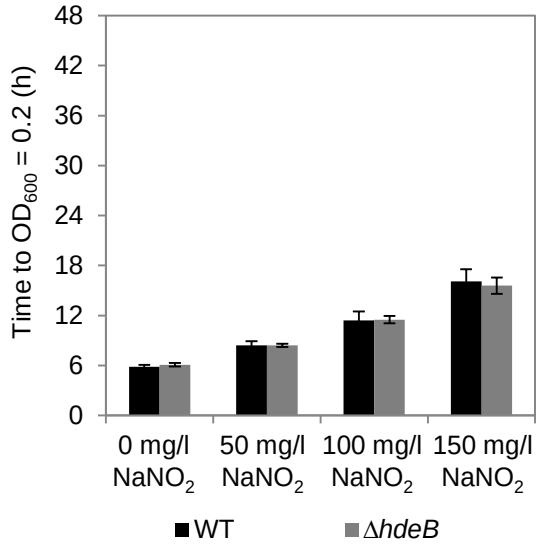

Figure 11: Impact of $NaNO_2$ on growth of *S.* Typhimurium 14028 WT and the deletion mutant Δ*hdeB* under acidic conditions.
S. Typhimurium 14028 WT (black column) and Δ*hdeB* (grey column) were grown in LB pH 5.5 in the presence of 0, 50, 100 or 150 mg/l $NaNO_2$ with agitation at 24°C under aerobic conditions in a Bioscreen C. The time the strains needed to reach an OD_{600} = 0.2 (h) in dependence of the $NaNO_2$ concentration was analyzed. Columns represent mean values ± SD from three independent experiments including duplicates.

1.2.3 Screening of an insertion mutant library for NO- and acidified $NaNO_2$-sensitive phenotypes

Proteins or enzymes might help *S.* Typhimurium to withstand NO or acidified nitrite stress without being differentially transcribed under these stress conditions. To identify such protective systems, a *S.* Typhimurium insertion mutant library constructed by insertion-duplication-mutagenesis (IDM) (Knuth *et al.*, 2004; Klumpp and Fuchs, 2007) was screened for mutants that were sensitive towards NO or acidified $NaNO_2$. In these mutants, the vector pIDM1 is randomly inserted in the chromosome due to homologous recombination between cloned chromosomal fragments and the respective gene loci.

The insertion prohibits the expression of functional proteins. Due to the temperature-sensitive replication of pIDM1 in Gram-negative bacteria, the insertion is stable at 37°C and growth analysis was performed at this temperature.

NO sensitivity was assessed by growing mutants without or with 40 µM SNP in neutral LB pH 7. In a first approach, the growth of 1114 insertion mutants was analyzed, of which 49 displayed a putative NO-sensitive phenotype. So far, 14 out of these 49 mutants were again checked in a second experiment, which confirmed the NO sensitivity of seven mutants. The insertion loci of six of the latter were determined by amplifying and sequencing the respective chromosomal fragment in pIDM1 (Schürch, 2012), which was retrieved by growing cells at a permissive temperature for vector replication. Table 13 summarizes the results of the sequence analysis.

Table 13: Identification of affected genes in NO-sensitive insertion mutants

number of mutants	14028 identifier	gene name	product	phenotype confirmed by deletion mutant
4	STM14_2883	*pta*	phosphate acetyltransferase	Yes[1]
1	STM14_2172	*treA*	trehalase	No[1]
1	STM14_2241	*pphA*	serine/threonine protein phosphatase 1	No

[1] (Schürch, 2012)

In four mutants, the phosphate acetyltransferase, encoded by the *pta* gene, was affected by the insertion. Pta, together with acetate kinase AckA, reversibly interconverts acetyl coenzyme A (acetyl-CoA) and acetate via the high energy intermediate acetyl phosphate (acetyl-P) (Forrester and Foster, 2012a, 2012b). The genes *treA* and *pphA* were identified each in one mutant.

Insertion mutagenesis might not only disrupt the gene at the insertion site, but might also have polar effects on surrounding genes. Hence, the observed phenotypes might not unequivocally be attributed to inactivation of the gene identified (Link *et al.*, 1997). Moreover, direct comparison with the WT strain is not possible, since pIDM1 is rapidly lost from the WT strain at non-permissive temperature (Fuchs *et al.*, 2006). To validate the findings of the insertion mutant screening, non-polar deletion mutants were constructed in *treA*, *pphA* and *pta* and growth of the deletion mutants at 37°C in LB pH 7 with SNP (0, 40, 80, 150 µM) was analyzed and compared with that of the WT strain in three independent experiments by Lisa Schürch (Schürch, 2012). A slightly higher sensitivity to NO was observed for Δ*pta* compared to the WT (Schürch, 2012) (data not shown). On the contrary, there were no greater differences between Δ*treA* or Δ*pphA* and the WT with regard to their SNP sensitivity (data not shown).

In trans complementation mutant Δ*pta*-comp as well as the *pta* deleted strain Δ*pta* pBAD/HisA(Tet^R) and control strain WT pBAD/HisA(Tet^R) were constructed to investigate if the growth defect could be restored by provision of *pta*. In the complemented mutant Δ*pta*-comp, expression of *pta* was driven from the P_{BAD} promoter on vector pBAD/HisA(Tet^R) by addition of 0.002% arabinose. However, complementation was already observed without the addition of arabinose, suggesting that even low levels of *pta* expressed from P_{BAD} in LB broth are sufficient (data not shown).

Growth of Δ*pta* pBAD/HisA(Tet^R) was delayed compared with the WT pBAD/HisA(Tet^R) even in the absence of SNP in LB pH 7 (Figure 12). Addition of increasing concentrations of SNP affected the AUC of Δ*pta* pBAD/HisA(Tet^R) proportionally stronger as it affected the WT pBAD/HisA(Tet^R) (Figure 12D). This effect was largely abrogated in the complemented strain Δ*pta*-comp, indicating that, indeed, the lack of *pta* was responsible for the observed growth differences.

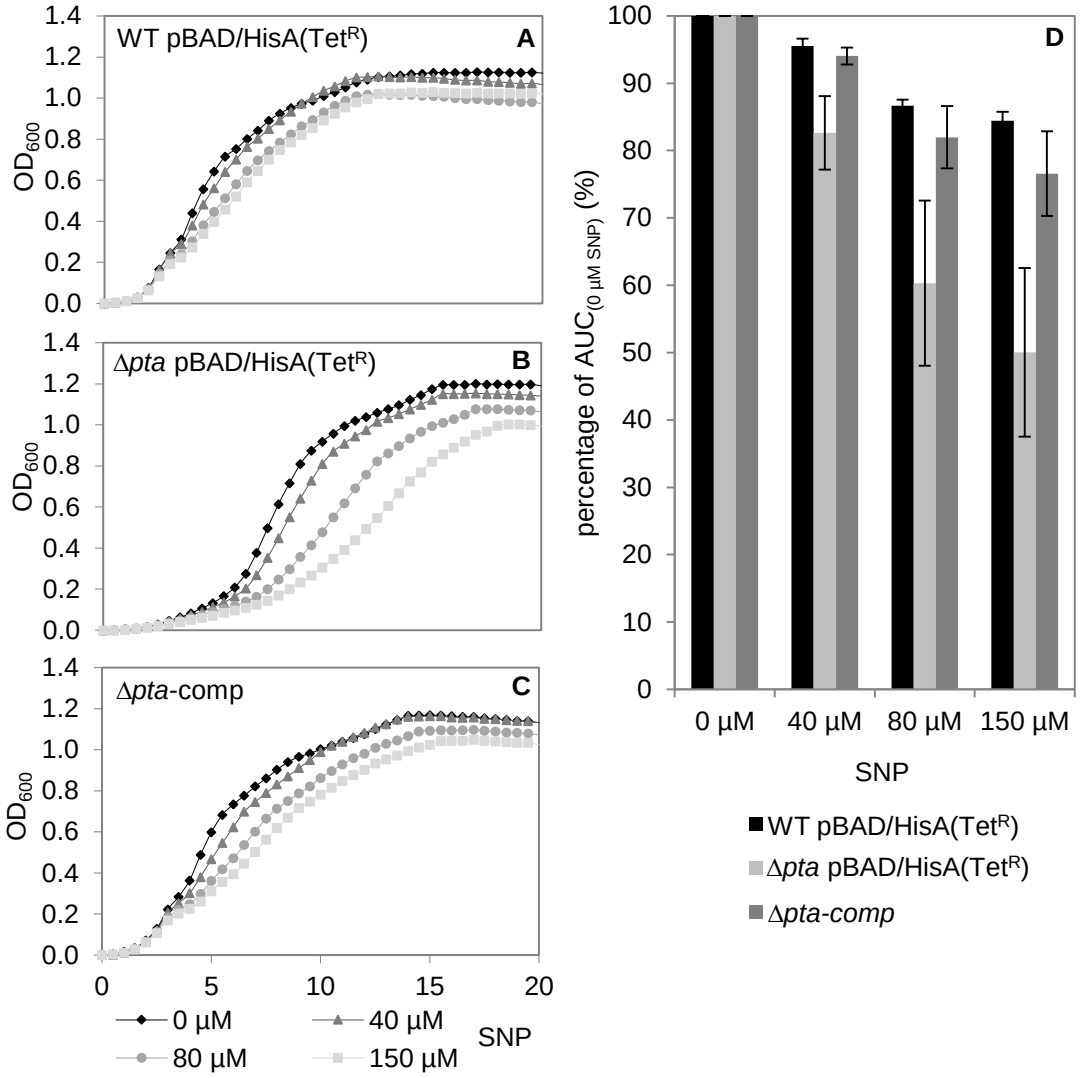

Figure 12: Impact of SNP on growth of *S.* Typhimurium WT pBAD/HisA(Tet^R), Δ*pta* pBAD/HisA(Tet^R) and complemented Δ*pta*-comp.
(A) Representative growth curves recorded in a Bioscreen C at 37°C of *S.* Typhimurium (A) WT pBAD/HisA(Tet^R), (B) Δ*pta* pBAD/HisA(Tet^R) and (c) Δ*pta*-comp in LB pH 7 + 0.002% arabinose + 17.5 mg/l tetracycline in the presence of 0, 40, 80 or 150 µM SNP. (D) The percentage of the AUC with SNP relative to the AUC without SNP (AUC_{+SNP}/AUC_{-SNP}) at 20 h was calculated for the different concentrations of SNP. Columns depict mean ± SD from three independent experiments.

Acidified $NaNO_2$ sensitivity was investigated by comparing growth of the insertion mutants in LB pH 5.5 in the absence or presence of 150 mg/l $NaNO_2$. 3031 insertion mutants were tested in a primary screening, which resulted in the identification of 111 mutants with a putative acidified $NaNO_2$-sensitive phenotype.

To date, growth of 68 of these 111 conspicuous insertion mutants was re-tested in a second experiment, confirming the nitrite sensitivity for 27 of these mutants. The insertion loci of 19 of the latter were identified and are listed in Table 14.

Table 14: Identification of affected genes in acidified $NaNO_2$-sensitive insertion mutants

number of mutants	14028 identifier	gene name	product	phenotype confirmed by deletion mutant
5	STM14_3138	*cadA*	lysine decarboxylase 1	Yes
4	STM14_4652	*pstS*	phosphate transporter subunit	ND[a]
1	STM14_0185	*lpdA*	dihydrolipoamide dehydrogenase	ND
1	STM14_1666	*sufD*	cysteine desulfurase activator complex subunit SufD	ND
1	STM14_2505	*cobS*	cobalamin synthase	No
1	STM14_2519	*cbiE*	cobalt-precorrin-6Y C(5)-methyltransferase	No[1]
1	STM14_2883	*pta*	phosphate acetyltransferase	Yes[1]
1	STM14_3066	*ppk*	polyphosphate kinase	Inconclusive[b]
1	STM14_4150	*fusA*	elongation factor G	ND
	STM14_0104	*kefC*	glutathione-regulated potassium-efflux system protein KefC	
1	STM14_4562/ STM14_4563	-/ -	putative periplasmic protein / phosphotransferase system mannitol/fructose-specific IIA component	ND
1	STM14_4638	*trmE*	tRNA modification GTPase TrmE	ND
1	STM14_4677	*trkD*	potassium transport protein Kup	ND

[1] (Schürch, 2012)
[a] ND, not determined
[b] Results of the deletion mutant were inconsistent between five independent experiments.

Sequence analysis revealed that the gene *cadA* was targeted by insertion in five independent mutants, indicating that the library contains some redundancies. *CadA* encodes an inducible lysine decarboxylase and constitutes an operon together with the upstream located *cadB*, which codes for a lysine/cadaverine antiporter (Park *et al.*, 1996). Strikingly, *cadA* and *cadB* were found to be strongly induced upon acidified $NaNO_2$ shock in the RNA-seq analysis (log_2 FC 4.17 and 4.81, respectively) (Table A 1) and up-regulation of *cadA* was verified by qPCR (log_2 FC 4.71) (Figure 10A). Besides *cadA*, the disruption of two independent gene loci connected to phosphate uptake and storage, *pstS* (four mutants) and *ppk* (one mutant), which encode a component of a high affinity phosphate-specific transport (Pst) system and a polyphosphate kinase involved in polyphosphate (poly P) synthesis, respectively, resulted in nitrite-sensitive phenotypes. In addition, one of the four NO-sensitive insertion mutants in the *pta* gene was also found to be sensitive to acidified nitrite. The other genes identified encode proteins functioning in cobalamin (coenzyme B_{12}) biosynthesis (*cbiE*, *cobS*), Fe-S cluster assembly/repair (*sufD*), central metabolism (*lpdA*), tRNA modification (*trmE*) and potassium transport (*trkD*). In one mutant, the site of insertion could not be unambiguously identified, since the fragment was composed of sequences of both *fusA* and *kefC*.

To validate the findings of the insertion mutant screening, non-polar *cadA*, *cobS*, *cbiE* and *ppk* deletion mutants were constructed.

Growth of these deletion mutants along with Δ*pta* at 37°C in LB pH 5.5 with $NaNO_2$ (0, 50, 100, 150 mg/l) was analyzed and compared with that of the WT strain in three independent experiments.

A slightly higher sensitivity to acidified $NaNO_2$, apparent in a retarded onset of growth, was observed for Δ*pta* compared to the WT (Schürch, 2012) and Δ*cadA* phenocopied the respective insertion mutant in that its growth was delayed in the presence of acidified $NaNO_2$ (data not shown). On the contrary, there were no greater differences between Δ*cobS* or Δ*cbiE* and the WT with regard to their acidified $NaNO_2$ sensitivity. Inconsistent results, however, were obtained for Δ*ppk* and further growth experiments are necessary to be able to draw sound conclusions (Table 14).

In trans complementation of *pta* and *cadA* was performed to verify that the lack of the respective proteins resulted in the observed growth retardation of Δ*pta* and Δ*cadA* in the presence of nitrite.

In trans expression of *pta* in Δ*pta*-comp resulted in growth comparable to or even slightly better than that of the WT pBAD/HisA(Tet^R) in acidic medium with $NaNO_2$ at 37°C (Figure 13). To the contrary, Δ*pta* pBAD/HisA(Tet^R) displayed an increased lag phase with higher $NaNO_2$ concentrations, which was reproducibly observed, albeit with varying length, throughout the three independent experiments.

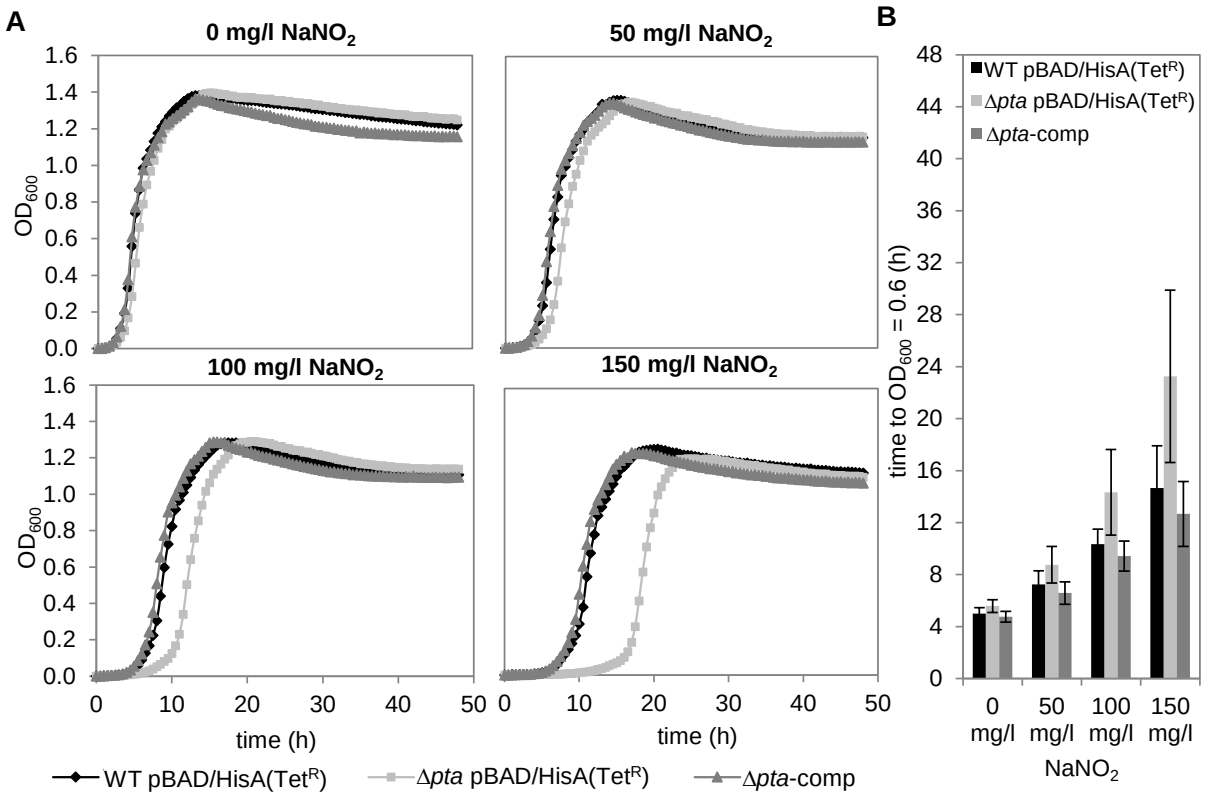

Figure 13: Impact of acidified $NaNO_2$ on growth of *S.* Typhimurium WT pBAD/HisA(Tet^R), Δ*pta* pBAD/HisA(Tet^R) and complemented Δ*pta*-comp.

(A) Representative growth curves recorded in a Bioscreen C at 37°C of *S.* Typhimurium WT pBAD/HisA(Tet^R) (diamond, black), Δ*pta* pBAD/HisA(Tet^R) (square, light grey) and Δ*pta*-comp (triangle, grey) in LB pH 5.5 + 0.002% arabinose + 17.5 mg/l tetracycline in the presence of 0, 50, 100 or 150 mg/l $NaNO_2$. (B) Time required for each strain to reach OD_{600} = 0.6 (half-maximum OD_{600}) in dependence of the $NaNO_2$ concentrations. The data represent mean values ± SD from three independent experiments including duplicates.

In trans complementation mutant Δ*cadA*-comp was constructed. The *cadA* gene was expressed from its own promoter on vector pBR322. Growth analysis of the complementation mutant Δ*cadA*-comp, the *cadA* in frame deletion mutant Δ*cadA* pBR322 and the WT pBR322 at 37°C (data not shown) and 24°C (Figure 14) confirmed that the phenotype observed due to lack of *cadA* could be successfully complemented by provision of *cadA in trans*. Whereas growth in LB pH 5.5 + 150 mg/l ampicillin without $NaNO_2$ is quite similar for WT pBR322, Δ*cadA* pBR322 and Δ*cadA*-comp, Δ*cadA* pBR322 displayed an increasing growth delay with increasing concentrations of $NaNO_2$ (50, 100, 150 mg/l). This effect was relieved in Δ*cadA*-comp.

In conclusion, CadA and Pta might protect S. Typhimurium during acidified nitrite-mediated stress, while Pta might also play some role under NO stress at neutral conditions. Since only one mutant was sensitive to both SNP and acidified nitrite, the results further indicate that additional reactive derivatives of acidified nitrite besides NO might contribute to the antibacterial effect.

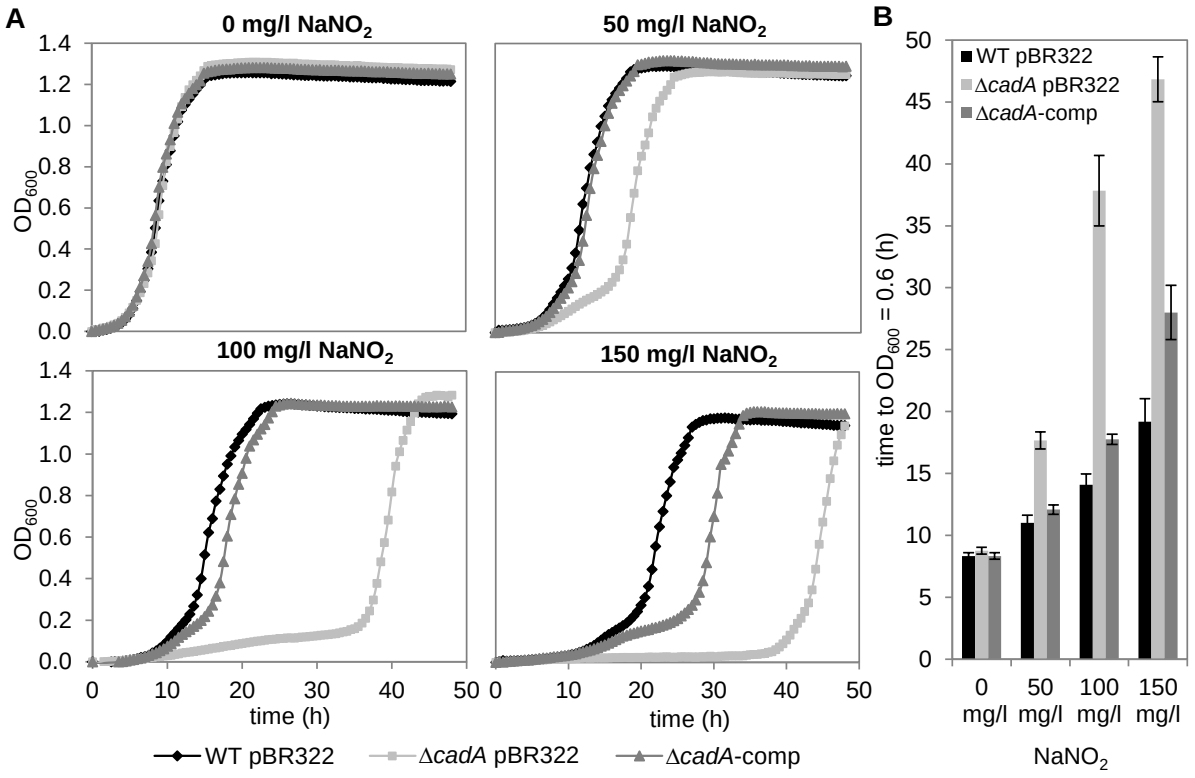

Figure 14: Impact of acidified $NaNO_2$ on growth of *S.* Typhimurium WT pBR322, Δ*cadA* pBR322 and complemented Δ*cadA*-comp.
(A) Representative growth curves recorded in a Bioscreen C at 24°C of *S.* Typhimurium WT pBR322 (diamond, black), Δ*cadA* pBR322 (square, light grey) and Δ*cadA*-comp (triangle, grey) in LB pH 5.5 + 150 mg/l ampicillin in the presence of 0, 50, 100 or 150 mg/l $NaNO_2$. (B) Time required for each strain to reach OD_{600} = 0.6 (half-maximum OD_{600}) in dependence of the $NaNO_2$ concentrations. The data represent mean values ± SD from three independent experiments including duplicates.

1.2.4 Influence of $NaNO_2$ on the intracellular pH of *S.* Typhimurium at acidic pH

The NO and acidified nitrite transcriptional responses overlap in up-regulation of NsrR target genes including the NO-detoxifying HmpA, indicating that, indeed, bacteria are exposed to NO that is formed from acidic nitrite. However, the acidified $NaNO_2$ shock and adaptive responses, especially the induction of acid tolerance systems, implicate that additional reactive compounds impose stress on the cells. The strong growth defect of the CadA deletion mutant exposed to acidified $NaNO_2$ despite a functional HmpA further supports reaction mechanisms independent of the action of NO. Based on these data, it was speculated that acidified nitrite activated transcription of the *cadBA* operon by somehow lowering the intracellular pH (pH_i). The influence of $NaNO_2$ on the pH_i of *S.* Typhimurium in dependence of the pH of the medium was analyzed. For pH_i measurements, strain WT pEGFP was used which constitutively expresses the pH-sensitive GFP derivative EGFP from a plasmid (see II2.2.8). Spectral intensity of EGFP decreases with lowered pH, thus rendering it suitable to measure pH_i changes non-invasively (Kneen *et al.*, 1998). Fluorescence emission scans from 500 - 580 nm of WT pEGFP in LB pH 5.5 or neutral LB were recorded before (ctrl) and directly after addition of 150 mg/l $NaNO_2$. Without added $NaNO_2$, fluorescence spectra of WT pEGFP under both pH values were similar with the expected peak at about 510 nm but a slightly lower intensity at pH 5.5 (Figure 15A) compared to neutral pH (Figure 15B). However, addition of $NaNO_2$ to pH 5.5 resulted in a marked decrease in the fluorescence intensity around the EGFP emission peak, whereas it had no influence at neutral pH. Addition of the same volume of H_2O as a control also did not alter the fluorescence spectra at either pH. Furthermore, addition of 150 mg/l $NaNO_2$ did not change the external pH of the medium (data not shown). These data indicate that $NaNO_2$ when added to LB broth acidified to pH 5.5 with lactic acid elicits a decrease in the pH_i of *S.* Typhimurium, which might constitute an additional mode of action of its inhibitory effect.

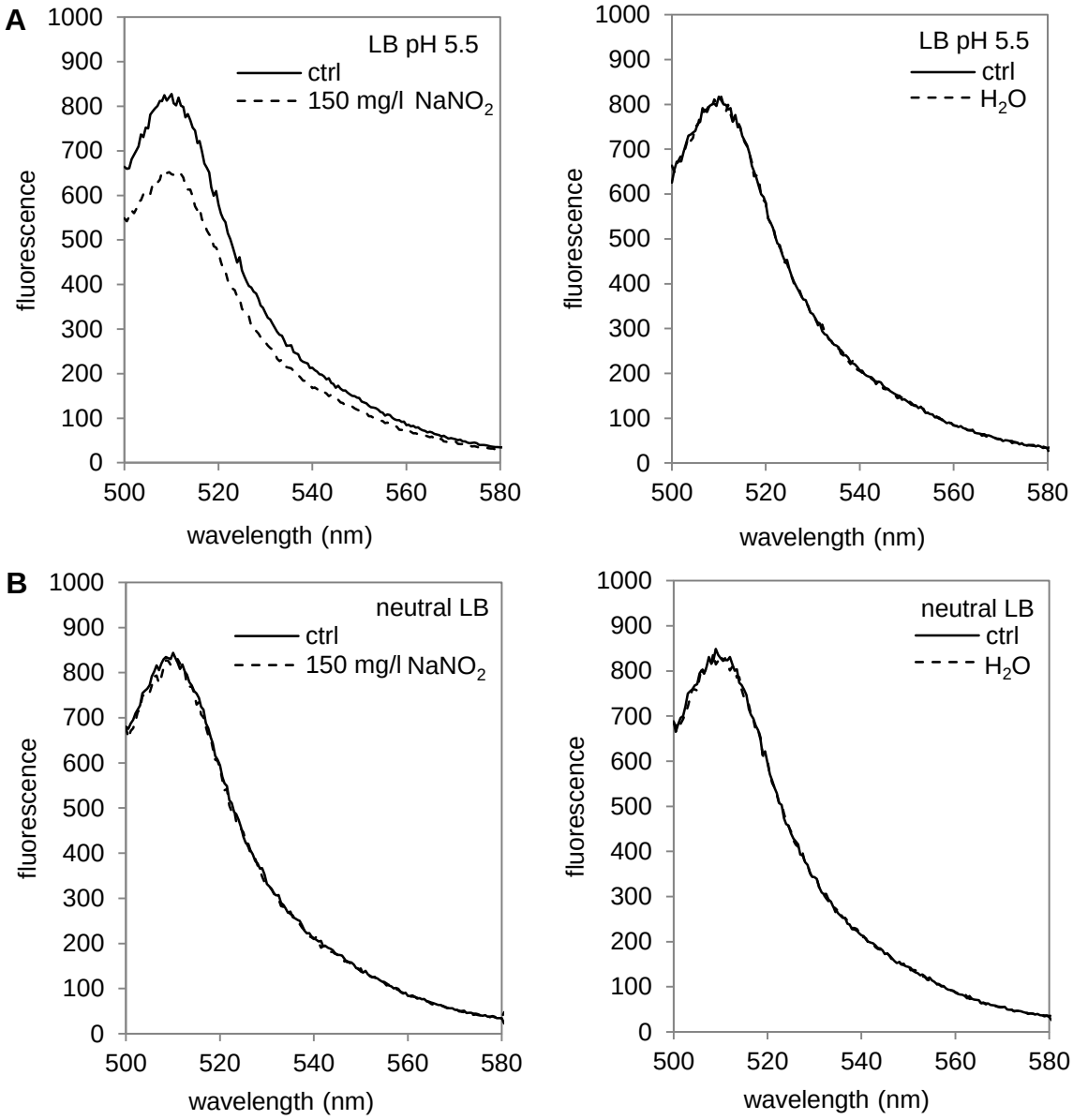

Figure 15: Effect of acidified $NaNO_2$ on the intracellular pH of *S.* Typhimurium.
Fluorescence emission spectra of WT pEGFP in (A) LB pH 5.5 or (B) neutral LB before (ctrl) and immediately after addition of 150 mg/l $NaNO_2$ (left) or H_2O (right). Representative spectra of three independent experiments are shown.

1.3 Transcriptome of *S.* Typhimurium under raw-sausage like conditions with and without $NaNO_2$

In the production of raw sausages, nitrite is thought to be critical especially in the first days of ripening, when other hurdles such as acidity or drying have yet to develop. Indeed, growth of *S.* Typhimurium at this stage is inhibited in nitrite-cured sausages compared to sausages produced without $NaNO_2$ (Figure 5A). In the first three ripening days, the concentration of $NaNO_2$ rapidly goes down from an initial 150 mg/kg to about 10 - 30 mg/kg (Figure 5D). At the same time, the pH drops from about 5.8 to 5.2 and the water activity slightly decreases (Figure 5B and 5C). If the residual nitrite still contributes to the

microbial safety of the product is unclear. To answer this question, the influence of $NaNO_2$ on the transcriptome of *S.* Typhimurium in an *in vitro* meat broth system simulating conditions on ripening day 0 (RD0, day of production) and ripening day 3 (RD3) was assessed. 150 mg/l $NaNO_2$, corresponding to the ingoing amount on RD0, and 30 mg/l, reflecting the highest residual amount on RD3, were used, respectively. To come as close as possible to the natural product, further parameters such as the additives glucose and sodium ascorbate on RD0 and the different pH values and NaCl concentrations (to mimic the decrease in water activity) on RD0 and RD3 were considered (see Table 10). Besides investigating the effect of $NaNO_2$, the transcriptional profiles of cultures from RD0 and RD3 without $NaNO_2$ were compared to find possible explanations for the growth to no-growth transition observed in the sausages between these days. Hence, four cultures cultivated under the respective conditions (RD0, RD0 + 150 mg/l $NaNO_2$, RD3, RD3 + 30 mg/l $NaNO_2$) for 1 h were sampled. To get an overview of the sample relations, a plot based on multidimensional scaling (MDS) was produced (Figure 16). Samples from RD0 and RD3, irrespective of the presence of $NaNO_2$, were clearly separated on the x-axis (dimension 1), indicating that the variation is due to the different media types simulating the different ripening days. On the contrary, RD0 and RD0 + 150 mg/l $NaNO_2$ (RD0.150N) are discriminated on the y-axis, suggesting that dimension 2 corresponds to the effect of $NaNO_2$. The samples RD3 and RD3 + 30 mg/l $NaNO_2$ (RD3.30N) cluster quite close together, reflecting a high similarity of these two samples.

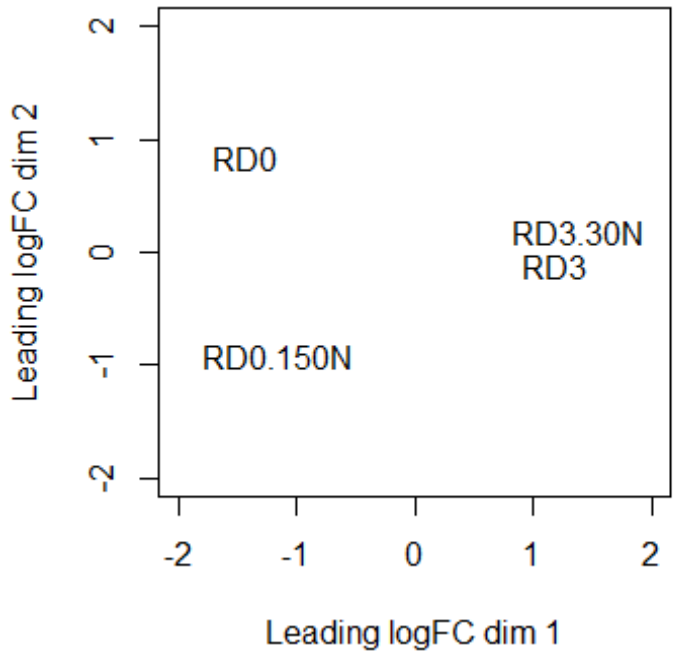

Figure 16: MDS plot of the RD0 and RD3 RNA-seq data with and without $NaNO_2$.
The MDS plot was produced based on the filtered (cpm ≥ 10 in at least one library) and TMM normalized samples using edgeR. Distances correspond to leading log_2 FC between each pair of samples.

The nitrite-treated cultures were compared to the respective control cultures and the control cultures of both ripening days were compared against each other. Results are summarized in Table 15.

Table 15: Overview of the RNA-seq pairwise comparisons of RD0 and RD3 conditions with and without $NaNO_2$

Pairwise comparison	Number of tested genes ≥ 10 cpm (% of 5416)	Number of differentially regulated genes (BH-adjusted p-value < 0.05)	
		up	down
RD0 + 150 mg/l $NaNO_2$ vs RD0	3491 (64.5%)	14	36
RD3 + 30 mg/l $NaNO_2$ vs RD3	3252 (60.0%)	0	0
RD3 vs RD0	3528 (65.1%)	265	307

1.3.1 Effect of $NaNO_2$ on *S.* Typhimurium under conditions simulating ripening day 0 (RD0) and ripening day 3 (RD3)

In total, the transcription of 50 genes was affected by the presence of 150 mg/l $NaNO_2$ on RD0, with a higher number of down-regulated than up-regulated genes (Table 15). The genes are listed according to their COGs class in appendix Table A 5 (up-regulated genes) and Table A 6 (down-regulated genes).

The genes displaying the greatest transcriptional increase in response to $NaNO_2$ were *norV* (log_2 FC 7.6) and *norW* (log_2 FC 8.7), coding for the NO-detoxifying flavorubredoxin and its associated oxidoreductase, respectively. Both are under positive control of the NO-responsive regulator NorR. Considerably higher mRNA levels were also detected for *soxS* (DNA-binding transcriptional regulator SoxS, log_2 FC 4.4) and *copA* (copper exporting ATPase, log_2 FC 4.2), the gene products of which are involved in the responses to redox-cycling compounds and copper stress, respectively. Besides *copA*, transcript abundance of *cueO*, coding for a multicopper oxidase associated with maintaining intracellular copper homeostasis (Tucker *et al.*, 2010), was elevated (log_2 FC 2.5). Transcription of *ytfE*, the product of which has been shown to be involved in the repair of Fe-S clusters damaged by oxidative or nitrosative stress (Justino *et al.*, 2007; Crack *et al.*, 2016), and seven genes involved in iron acquisition (*entCE*, *fepB*, *cirA*, *fes*, *yqjH*, *ydiE*) increased 6- to 9-fold upon growth with $NaNO_2$.

On the contrary, most of the down-regulated genes were associated with the functional category energy production and conversion. The gene products are involved in citrate fermentation (*citCDEF*) and nitrate/nitrite respiration (*narGHJI*, *narK*, *nirD*) or form the formate hydrogen lyase complex (*fdhF*, *hyc* operon). Few genes of other functional categories displayed lower mRNA levels, such as those coding for the nucleoid-associated protein Fis (*fis*), an uracil transporter (*uraA*) and for the NrdD subunit (*nrdD*) of the anaerobic ribonucleotide reductase NrdDE, which provides dNTPs for DNA replication (Partridge *et al.*, 2009).

Interestingly, less genes were found to be differentially expressed in response to $NaNO_2$ in RD0 simulating broth compared to LB broth. Some overlap was detected both with the shock response (up-regulation of *norVW* and *ytfE*, down-regulation of *fis*, *uraA* and *nrdD*) and the adaptation response (up-regulation of iron-acquisition systems, down-regulation of *nar* genes) to acidified nitrite in LB.

On the other hand, increased transcription of copper resistance systems and the lower transcript levels of citrate utilization genes was observed specifically on RD0 with added $NaNO_2$.

In contrast to the situation on RD0, no significantly (BH-adjusted p-value < 0.05) regulated genes were detected in response to 30 mg/l $NaNO_2$ on RD3 (Table 15). This indicates that this low $NaNO_2$ concentration is not sufficient to perturb transcription of *S.* Typhimurium. Consequently, it seems unlikely that the residual $NaNO_2$ on RD3 might still contribute to the microbial safety of the product.

1.3.2 Comparison of the transcriptional profiles of *S.* Typhimurium under RD0 and RD3 conditions

In short-ripened spreadable sausages produced without nitrite, *S.* Typhimurium cfu/g meat increase on ripening days 0 and 1 but stay constant from day 3 on (Figure 5A). Hence, it seems that growth conditions on RD0 are quite favorable and deteriorate during ripening, becoming quite disadvantageous on RD3. To shed light on the reasons for the observed growth cessation of *S.* Typhimurium on RD3, the transcriptomes of cultures grown under conditions simulating RD0 and RD3 were assessed and compared against each other.

Of 3528 genes (cpm ≥ 10, 65.1% of all CDS) that were subjected to differential gene expression analysis, 265 genes displayed increased and 307 decreased transcript abundances on RD3 compared to RD0 (Table 15). The genes were grouped according to their COGs category and are listed in appendix Table A 7 and Table A 8. An overview of the distribution of the differentially regulated genes according to their COGs categories is given in Figure 17.

Genes not assigned to any COG made up the largest single groups among the up- (29.2%) and down- (18.7%) regulated genes, respectively. Concerning categories associated with metabolism, different pathways within the single classes showed a transcriptional increase under one condition or the other.

Under RD0 conditions, higher mRNA abundance was detected for genes of the cytochrome *o* ubiquinol oxidase complex (*cyoABC*), membrane-bound nitrate reductase (*narGHJI*), cytoplasmic nitrite reductase (*nirB*), formate-hydrogen-lyase complex (*hyc* operon, *fdhF*), and citrate lyase (*citCDEF*), which are involved in the energy metabolism of the cell. To the contrary, transcript levels of genes encoding enzymes of the citritc acid cycle (*acnB*, *kgd*, *sucBCD*, *sdhAB*, *fumA*), sulfur compound-reducing enzyme systems (tetrathionate (*ttrBCA*), thiosulfate (*phsAB*), sulfite (*asrABC*)), DMSO reductase (*dmsABC*), Hya hydrogenase (STM14_2161 and STM14_2162), and the L-lactate utilization operon (*lldPRD*) were increased under RD3. In addition, the *pflF* gene, encoding a putative pyruvate formate lyase (PFL), was transcriptionally induced as was *pflE*, coding for a putative PFL activating enzyme, which was one of the most strongly up-regulated genes (log_2 FC 4.7) under RD3 conditions.

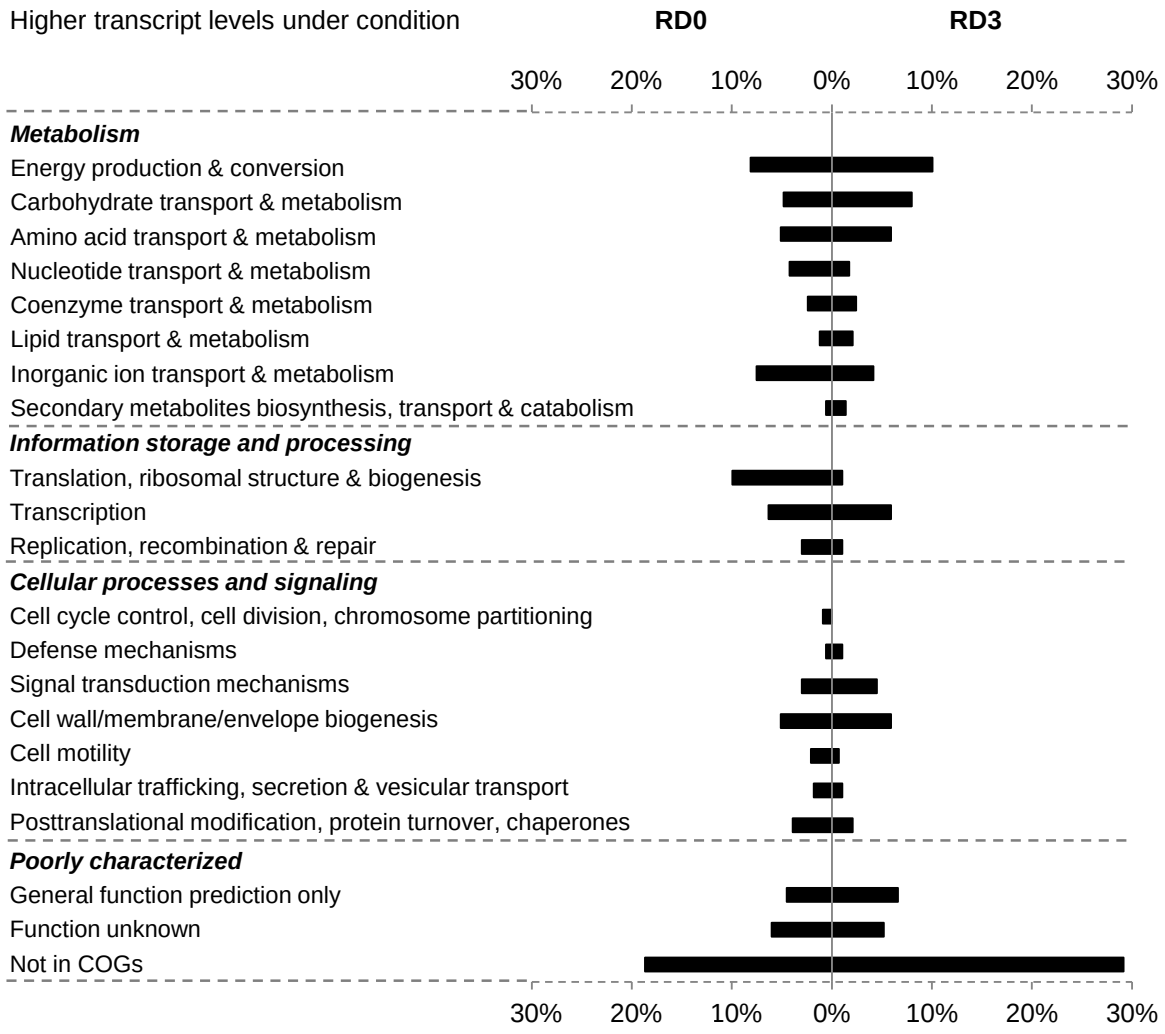

Figure 17: Overview of the differentially regulated genes under RD3 vs RD0 according to their functional category.
Genes significantly higher transcribed under RD0 or RD3 conditions in *S.* Typhimurium WT were grouped according to the NCBI COGs. Bars represent the percentage of genes with higher transcript levels in RD0 or RD3 of a given category relative to the total number of transcriptionally up-regulated genes in RD0 or RD3 among all COG categories (corresponding to 100%). Since one gene can be classified into more than one COG class, the total number of COG assignments is greater than the number of differentially expressed genes and relative percentages refer to the former.

Regarding genes in other metabolic pathways with higher transcript levels in RD0, genes involved in trehalose metabolism (*otsB*, *treF*, *treC*) and proline/glycine betaine transport (*proU*, *proWX*), in phosphate transport (*pstBACS*) and its regulation (*phoU*, *phoBR*) and the metabolism of pyrimidine and purine nucleotides had elevated transcript levels. A large group of stronger transcribed genes on RD0 further constitute those associated with translation, ribosomal structure and biogenesis (9.9%). Besides, higher mRNA abundance was found for some genes involved in the transcription and replication process, such as the DNA-binding protein Fis. Noteworthy are further those genes that displayed the most strongly elevated transcript levels in RD0 compared to RD3 apart from those connected to energy metabolism. These are involved in different stress response pathways and include *cadA* (lysine decarboxylase, $\log_2$ FC -5.65), *hmpA* (flavohemoglobin, -4.14), *cpxP* (repressor CpxP, -5.22) and

marR/marA (DNA-binding transcriptional repressor MarR/DNA binding transcriptional activator MarA, -5.63/-5.15).

In RD3, several sugar transport and utilization genes are up-regulated, such as the mannose PTS system and mannitol-specific PTS transporter and dehydrogenase (*manXYZ*, *mtlAD*). Concerning amino acid transport and metabolism, serine metabolic genes (*sdaCB*) and an aspartate-ammonia lyase encoding gene (*aspA*) were stronger transcribed under RD3 compared to RD0 amongst others. Two out of three genes in the functional category translation, ribosomal structure and biogenesis, *yfiA* (translation inhibitor protein RaiA) and *rmf* (ribosome modulation factor), are associated with resting ribosomes. Furthermore, several stress-related systems, such as four genes of the phage shock protein operon (*pspABCD*), which is induced by extracytoplasmic stress (Darwin, 2005), and several proteins annotated as universal stress proteins (*ynaF* (*uspF*), *ydaA* (*uspE*), *yecG* (*uspC*), *ybdQ*), displayed elevated transcript levels (about 5 - 15-fold). Another example is *adi*, encoding an arginine decarboxylase involved in acid resistance, for which mRNA levels were about 3.5 times higher in RD3 than in RD0.

1.3.3 Validation of RNA-seq transcriptome data under RD0 and RD3 conditions via qPCR

Differentially expressed genes were detected in RD0 in response to $NaNO_2$ and considerably more, when RD0 and RD3 cultures were compared against each other. To confirm the transcriptional changes observed by RNA-seq, 22 genes were analyzed by qPCR. Of these, considering a BH-adjusted p-value < 0.05, seven were differentially transcribed under both conditions, two were affected by $NaNO_2$, and thirteen responded specifically to RD3 conditions. qPCR was performed on three biological replicates for each condition. Cultures grown under RD3 + 30 mg/l $NaNO_2$ were also tested to check the unchanged transcriptional profile compared to RD3. mRNA expression for the three conditions (RD0 + 150 mg/l $NaNO_2$, RD3, RD3 + 30 mg/l $NaNO_2$) was calculated relative to the mRNA expression of the RD0 reference condition, which was set 100% and compared with the respective RNA-seq data, which were calculated based on the cpm in each condition. For ease of comparison, the genes were grouped into the categories “energy metabolism”, “stress response”, “transcription / DNA synthesis / translation” and “other functions”, and results are shown in Figure 18.

Two different groups of genes associated with the energy metabolism of the cell are distinguishable according to their regulation. The first one comprises genes *narG*, *nirB*, *fdhF*, *hycC* and *citC*, which were down-regulated both by $NaNO_2$ and RD3 conditions compared to RD0 (Figure 18A). A 4-fold decrease in *nirB* transcript levels under acidified $NaNO_2$ stress under RD0 was measured in the RNA-seq analysis, but the adjusted p-value 0.13 did not pass the set significance filter (< 0.05). However, qPCR confirmed the lower transcript abundance of *narG*, *nirB*, *fdhF*, *hycC* and *citC* both in response to $NaNO_2$ (% mRNA relative to RD0 ± SE: 20.2 ± 7.3%, 39.3 ± 5.9%, 13.9 ± 2.8%, 8.5 ± 2.3%, 3.6 ± 2.1%) and RD3 (4.5 ± 1.5%, 4.2 ± 0.7%, 6.4 ± 2.4%, 5.1 ± 1.0%, 0.6 ± 0.2%). Furthermore, analysis of the mRNA levels in RD3 + 30 mg/l $NaNO_2$ confirmed only minor changes in transcription compared to RD3.

The second group of genes comprises *sdhB*, *lldD*, *phsA*, *asrB*, *dmsA* and *ttrA* (Figure 18B). Trancription of these genes was not affected by $NaNO_2$ or they were too lowly transcribed (cpm < 10 for *lldD* and *ttrA*) under RD0 conditions, both without or with $NaNO_2$, and were therefore not analyzed for differential gene expression using edgeR. To the contrary, growth under RD3 conditions increased their transcript levels about 3.7- to 7.0-fold compared to growth in RD0 medium in the RNA-seq analysis. Transcriptional trends, meaning no difference in response to $NaNO_2$ and up-regulation under RD3 conditions, were confirmed for all genes except for *ttrA*, for which rather an opposite regulation in RD3 medium was found by qPCR.

The genes *fis*, *nrdD* and *yfiA* were chosen as representatives of the group "transcription / DNA synthesis / translation" (Figure 18C). The transcriptome analysis revealed a negative effect of both $NaNO_2$ and RD3 conditions on *fis* and *nrdD* transcription, whereas *yfiA* mRNA levels were not affected by $NaNO_2$ but increased in RD3. qPCR results corroborated these findings.

Relative transcription of six stress-related genes was determined, the gene products of which are involved in the responses to nitrosative (*norV*, *hmpA*, *ytfE*), oxidative (*soxS*, *ytfE*) and acid stress (*cadA*, *adi*), and which showed different expression patterns to acidified $NaNO_2$ stress in RD0 and to RD3 (Figure 18D). *NorV*, *ytfE* and *soxS* were up-regulated upon $NaNO_2$ exposure and at least tendentially down-regulated (*soxS* adjusted p-value 0.24) during growth under RD3 conditions. *HmpA* and *cadA* mRNA levels stayed constant irrespective of the presence of $NaNO_2$ under RD0, but were strongly down-regulated upon RD3 growth. *Adi* was not differentially transcribed in response to $NaNO_2$, but its mRNA was more abundant in RD3 than in RD0 broth. The qPCR data confirmed these different transcriptional patterns.

In addition, relative transcription of genes, *pflE* and *aspA*, which belong to the COGs categories posttranslational modification, protein turnover, chaperones, and amino acid transport and metabolism, respectively, was analyzed by qPCR. *PflE* mRNA was found to be only lowly expressed (cpm < 10) on RD0 conditions with or without $NaNO_2$ in the RNA-seq data. RNA-seq data revealed higher transcript abundances of both genes on RD3 relative to RD0, which were validated by qPCR (Figure 18E).

Regarding the RD3 vs RD0 comparison in general, there was a trend towards greater FC values among the down-regulated genes and lower FC values among the up-regulated genes determined by qPCR compared to RNA-seq. Nevertheless, the direction of the transcriptional change was the same for both methods. Taken together, the qPCR results were in good agreement with those of the RNA-seq analysis, indicating a high validity and reproducibility of the data.

In summary, it can be stated that the ingoing amount of 150 mg/l $NaNO_2$ has an impact on *S.* Typhimurium on RD0, but not the residual amount of nitrite *per se* on RD3. Common to all transcriptomic responses is a NO-specific response, but differences between the transcriptomic profiles in acidic LB and under RD0 conditions indicate that probably other inhibitory nitrite-derived compounds or action mechanisms are involved.

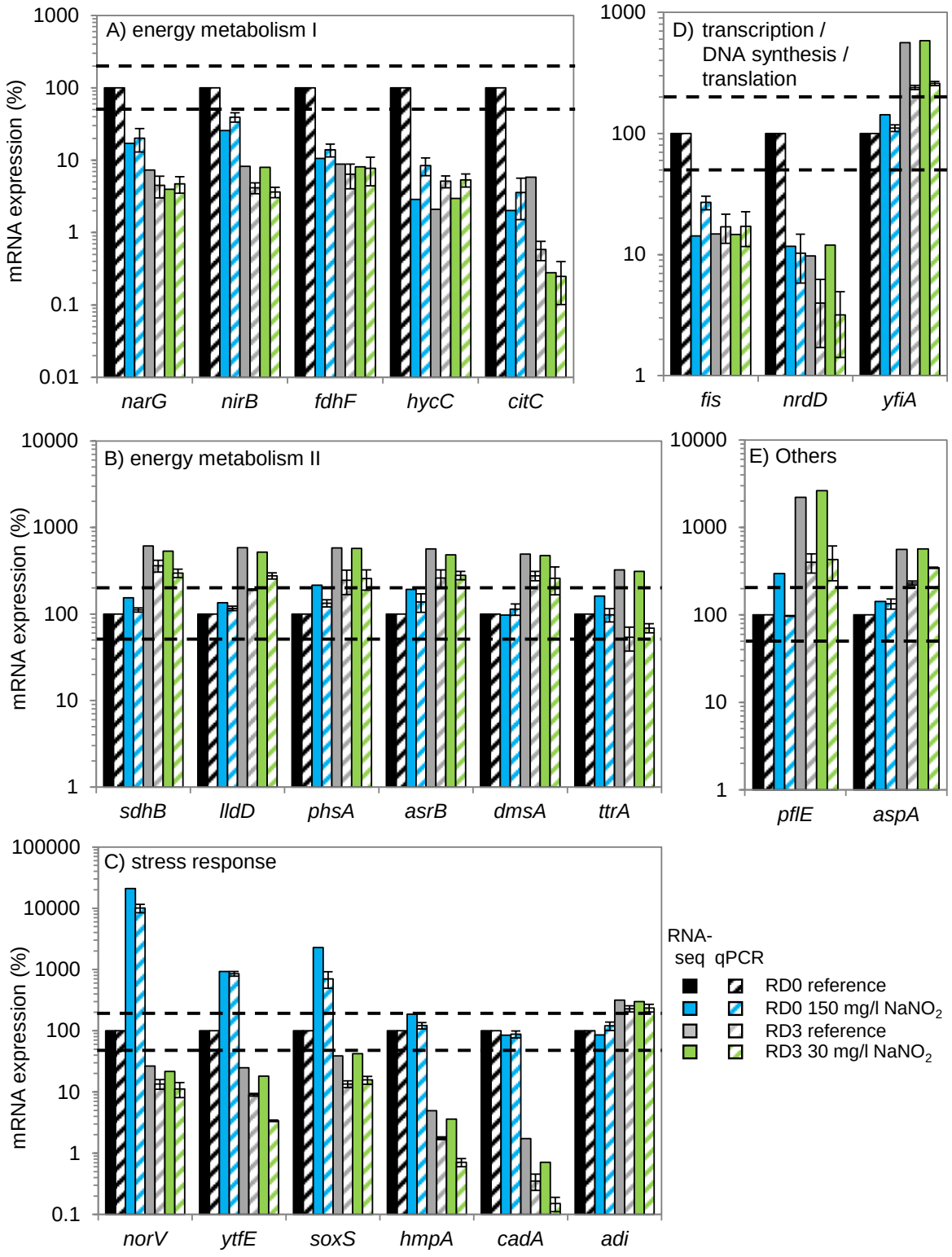

Figure 18: qPCR validation of genes differentially transcribed in *S.* Typhimurium under raw-sausage like conditions.

Shown is the mRNA expression (%) of genes associated with energy metabolism (A, B), transcription / DNA synthesis / translation (C), stress response (D) or other functions (E) determined by RNA-seq (filled) or qPCR (shaded) under the following raw-sausage like conditions: RD0 (black), RD0 + 150 mg/l $NaNO_2$ (blue), RD3 (grey), RD3 + 30 mg/l $NaNO_2$ (green). 16S rRNA was used as the normalization control gene. Fold-changes were calculated relative to RD0 as reference condition and converted to percent mRNA expression from RD0, which was set 100%. A 2-fold change in mRNA expression (%), corresponding to 200% and 50%, is indicated by black dashed lines. qPCR columns represent the mean ± SE of three independent biological experiments. RNA-seq relative expression values (hatched columns) were calculated based on cpm.

2 Enterohemorrhagic *E. coli* (EHEC)

Raw sausages are considered possible risk products not only for salmonellosis, but also for infections caused by EHEC. Whereas addition of $NaNO_2$ to a short-ripened spreadable sausage effectively prohibited growth of *Salmonella* spp. in the first ripening days, it did not influence survival of EHEC, which showed no initial multiplication in this foodstuff (Kabisch, 2014). Insight into how EHEC is affected on the molecular level by this curing agent on the one hand, and might protect itself from acidified $NaNO_2$ on the other hand, might help to better understand the situation in raw sausages. For this purpose, the global transcriptional changes of EHEC exposed to acidified $NaNO_2$ were assessed.

2.1 Transcriptional response of EHEC to acidified nitrite

The influence of NO on regulation of Shiga toxin synthesis (Vareille *et al.*, 2007) and expression of virulence genes encoded on the LEE pathogenicity island (Branchu *et al.*, 2014) has been investigated; however, the global transcriptional response of EHEC to NO or RNS has not been reported so far. Hence, transcriptional profiling via RNA-sequencing of EHEC exposed to $NaNO_2$ in acidic LB pH 5.5 was performed under two different experimental set-ups. In the first one, we sought to identify the shock response to acidified $NaNO_2$ by sampling cells as early as 10 min after addition of 150 mg/l $NaNO_2$ and comparing them with an analogously grown reference culture without nitrite. In the second set-up, transcriptomic changes were investigated after prolonged exposure to $NaNO_2$, namely, when the untreated reference culture had reached an $OD_{600} = 1.50 \pm 0.05$. At this time point, the sample culture endured acidified nitrite stress for about 1 h and had hardly resumed growth.

2.1.1 Shock response of EHEC to acidified nitrite

Of the 5385 genes annotated as protein-coding on the EHEC genome and virulence plasmid pO157, 2791 (51.8%) genes passed the cpm filtering for the pairwise comparison of the 10 min $NaNO_2$ shocked culture vs the respective reference culture. Of these, only 47 genes were differentially (BH-adjusted p-value < 0.05) regulated in response to nitrite, with 22 being annotated as hypothetical proteins. 20 genes were found to be up-regulated (Table A 9) and 27 to be down-regulated (Table A 10).

Genes under control of the dedicated NO-responsive regulators NorR (*norVsW*) and NsrR (*hmpA*, *ytfE*, *ygbA*, *ybjW* (*hcp*)) were most strongly induced upon an acidified $NaNO_2$ shock. Three genes (*ybiJ*, *ycfR*, *yhcN*) encoding members of the YhcN family (Rudd *et al.*, 1998) also showed substantially higher transcript abundances. Furthermore, *ndh* (NADH dehydrogenase) and *ldhA* (D-lactate dehydrogenase), the gene products of which are involved in the energy metabolism of the cell, were up-regulated.

Regarding the down-regulated genes, eight gene products respectively were associated with the COG category “transcription” or were not assigned to any COG. Among the first category, *cspA* and *cspE*, both coding for cold-shock proteins, were down-regulated. An example for the second category is *bssR*.

The BssR protein has an ascribed role in the regulation of biofilm formation in *E. coli* (Domka *et al.*, 2006). The gene displaying the strongest decrease (log_2 FC -4.06) in transcript abundance was *secG*, encoding an auxiliary component of the Sec protein translocation pathway (Borisov *et al.*, 2015).

2.1.2 Comparison of the 10 min and 1 h (OD_{600} = 1.5) reference cultures

To gain insight into the time course of the response to acidified nitrite, treatment time was prolonged beyond 10 min and cells from the reference and $NaNO_2$ treated culture were collected when the reference culture reached an OD_{600} = 1.5. However, differential gene expression analysis revealed that a high number of genes involved in anaerobic metabolism displayed lower transcript levels in the acidified $NaNO_2$ treated culture (data not shown). By comparing cpm values of all four conditions tested, it was realized that cpm values of this group of genes were higher only in the OD_{600} = 1.5 reference culture compared to the other cultures, which showed comparable lower cell numbers. Since cpm of these genes were also lower in the 10 min reference culture, it was unlikely that the observed regulation of these genes was solely attributable to the effect of nitrite. It might also be due to differences in the optical density of the cultures. To investigate the effect possibly imposed by the different culture densities, the transcriptomes of the 10 min and the 1 h reference cultures were compared.

For this pairwise comparison, filtering of genes with less than 10 cpm resulted in 2955 (54.9%) genes that were then subjected to differential gene expression analysis. The longer incubation time resulted in higher transcript levels of 129 genes and lower transcript levels of 60 genes. Lists of these genes sorted by their COGs class is provided in Table A 11 (up-regulated genes) and Table A 12 (down-regulated genes).

Most of the up-regulated genes are connected to anaerobic metabolism within the COGs category energy (Figure 19). These comprise genes for the electron-donating sn-glycerol-3-phosphate (*glpA*, *glpC*) and formate (*fdnGHI*) dehydrogenases and hydrogenase 2 (*hybA*), and the terminal reductases for the anaerobic respiration of DMSO (*dmsABC*), nitrate (*narGHJI*, *napFDAGHBC*), nitrite (*nirBD*, *nrfA*) and fumarate (*frdABCD*). Most of these genes are classified into the functional group of energy production and conversion, which comprises most of the up-regulated genes of all COG categories (20%). Furthermore, some genes coding for accessory proteins involved in maturation of cytochrome *c* (*ccmE*) or of catalytically active hydrogenases (*hypAB*, *hypD*) displayed increased transcript levels. These fall into the category posttranslational modification, protein turnover and chaperones. The operon *nikABCDE*, coding for a nickel transport system, also was strongly up-regulated in the 1 h reference culture as were *narK* and *focA*, which encode transporters for nitrate/nitrite and formate, respectively. Additionally, several genes encoding proteins involved in uptake of alternative carbon sources (e.g. maltose) and the transport and metabolism of amino acids (e.g. threonine) and peptides (e.g. *pepT*), or participating in the purine (*guaB*, *purK*, *purF*, *purC*, *purL*, *purDH* genes) and pyrimidine (*pyrE*, *pyrIB*) biosynthetic pathways were up-regulated.

Concerning the down-regulated genes, most of them are involved in siderophore-mediated iron uptake. They are distributed among diverse COGs. Amongst others, lower mRNA abundance was found for genes involved in enterobactin biosynthesis and export (*entCEB*, *entF*, *ybdA* (*entS*)) as well as uptake of ferric enterobactin (*fep* operon, *tonB-exbBD*). Besides genes involved in iron homeostasis, some genes of the aerobic energy metabolism were down-regulated such as the subunit II of the cytochrome *o* ubiquinol oxidase (*cyoA*) and two genes for enzymes of the citric acid cycle (*gltA*, citrate synthase; *sdhC*, subunit of the succinate dehydrogenase complex).

Since regulation of these groups of genes was quite similar when comparing the two nitrite-free reference cultures and the 1 h nitrite-treated vs the 1 h reference culture (data not shown), it seems that the latter comparison is indeed biased by an additional factor apart from $NaNO_2$ that might have been introduced by the different culture densities at harvest. Therefore, the 10 min reference culture was considered a more suitable reference for evaluating the response of EHEC to a 1 h acidified nitrite exposure.

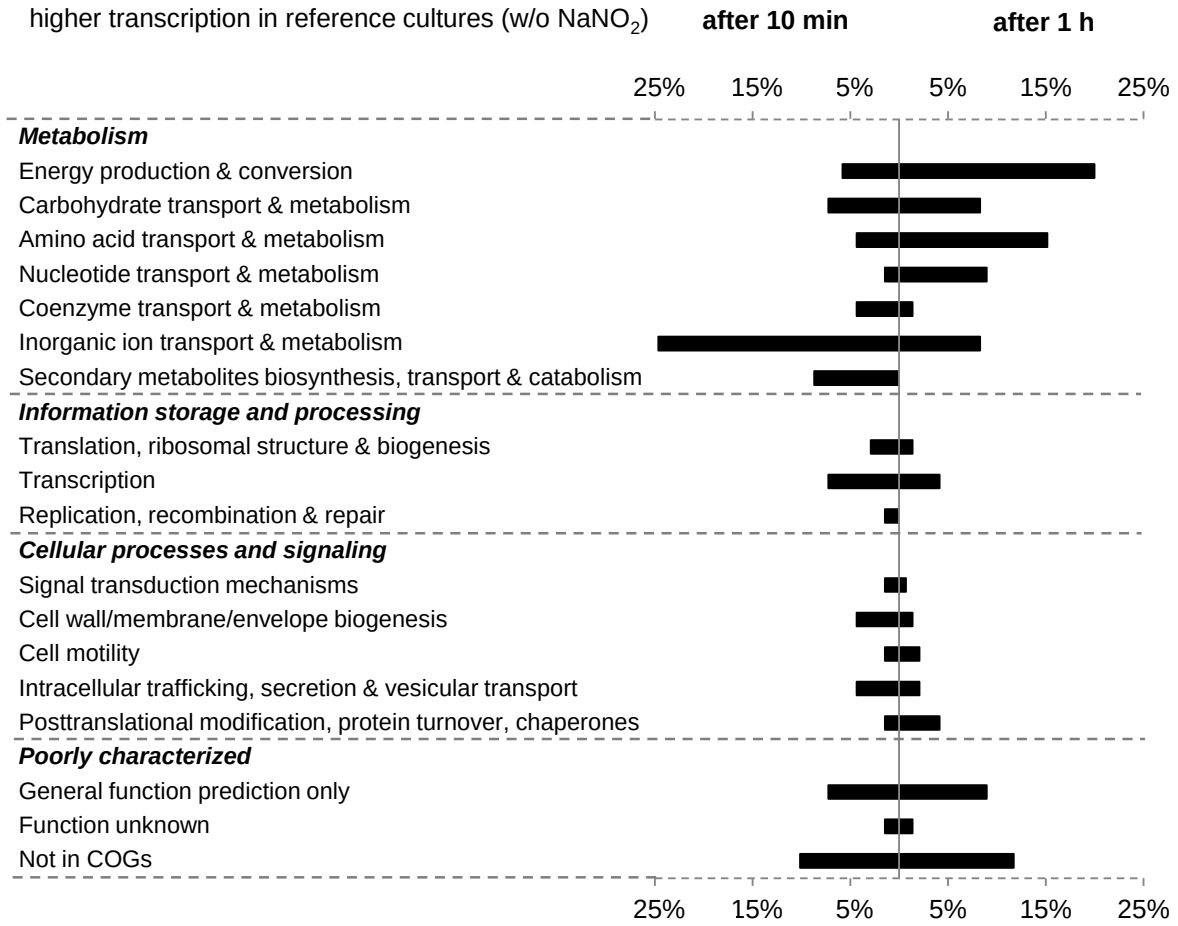

Figure 19: Overview of the differentially regulated genes in EHEC in the 1 h vs 10 min reference cultures without $NaNO_2$.

Genes significantly up-regulated in EHEC EDL933 WT 1 h or 10 min reference cultures were grouped according to the NCBI COGs. Bars represent the percentage of genes with higher transcript levels in the 1 h or 10 min reference cultures of a given category relative to the total number of transcriptionally up-regulated genes in the 1 h or 10 min reference cultures among all COG categories (corresponding to 100%). Since one gene can be classified into more than one COG class, the total number of COG assignments is greater than the number of differentially expressed genes and relative percentages refer to the former.

2.1.3 Transcriptional response of EHEC to a 1 h acidified nitrite exposure

The response of EHEC to a 1 h acidified nitrite exposure was analyzed. For the pairwise comparison of the treated culture and the 10 min reference culture without nitrite, 3012 genes (55.9% of all genes annotated as protein coding) with at least 10 cpm in one condition were investigated for differential regulation in response to $NaNO_2$. Indeed, 309 (5.7%) and 421 (7.8%) of these genes showed higher and lower mRNA abundances in the presence of $NaNO_2$, respectively. An overview according to the COGs classification is given in Figure 20 and gene lists are provided in Table A 9 (up-regulated genes) and Table A 10 (down-regulated genes).

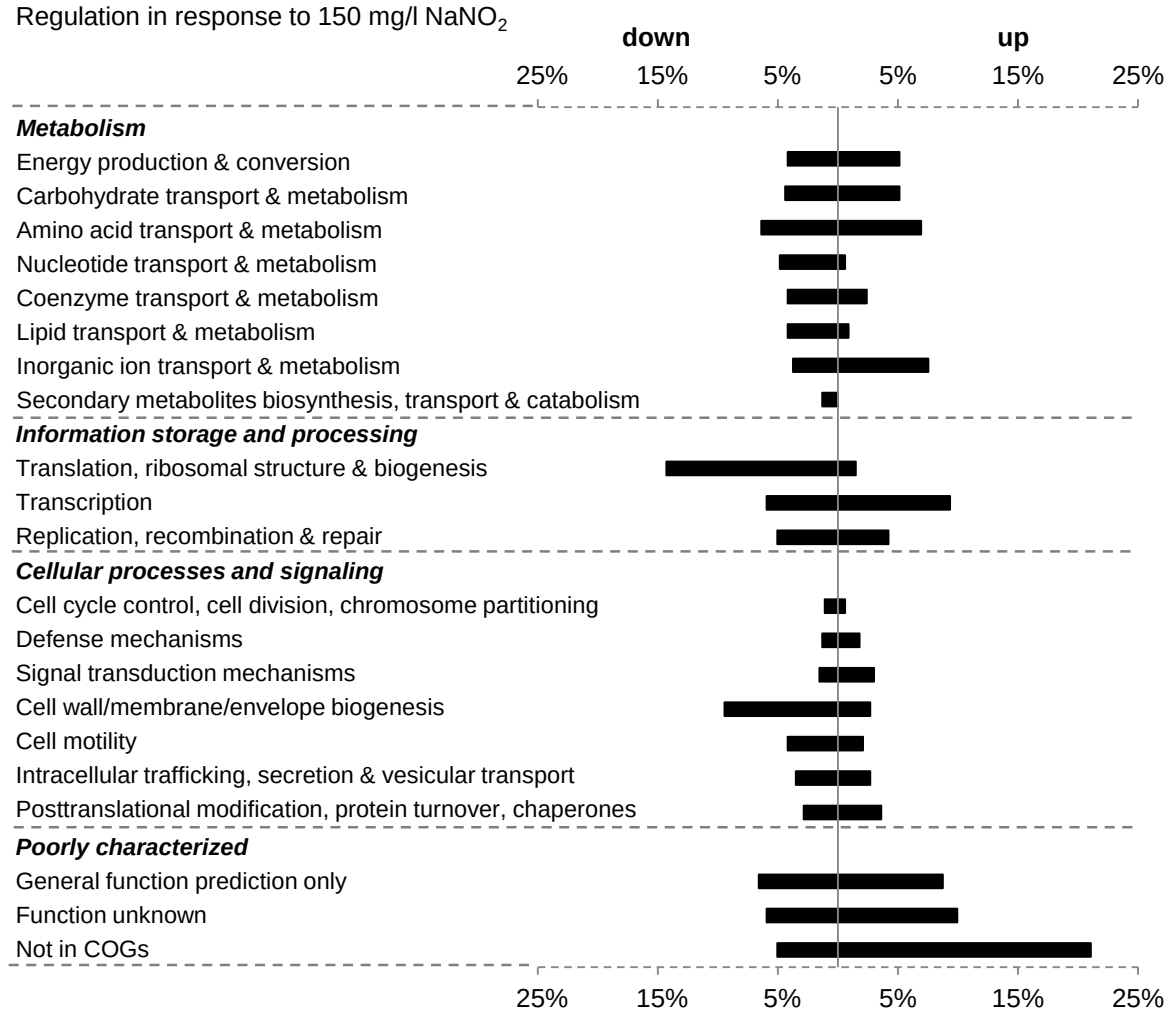

Figure 20: Overview of the differentially regulated genes in EHEC exposed for 1 h to acidified $NaNO_2$ according to their functional category.
Genes significantly up- or down-regulated in EHEC EDL933 WT grown for 1 h with 150 mg/l $NaNO_2$ at acidic pH were grouped according to the NCBI COGs. Bars represent the percentage of genes with increased or decreased transcription of a given category relative to the total number of up- or down-regulated genes among all COG categories (corresponding to 100%). Since one gene can be classified into more than one COG class, the total number of COG assignments is greater than the number of differentially expressed genes and relative percentages refer to the former.

The highest proportion of up-regulated genes (40%) are only poorly characterized, with about half of these genes (21%) even not assigned to any COG category (Figure 20). All genes that were transcriptionally induced after 10 min, were still up-regulated after 1 h. As with the shock response, described target genes under control of the dedicated NO sensors NsrR (*hmpA*, *ytfE*, *hcp-hcr*, *ygbA*, *yeaR*) and NorR (*norVsW*) showed elevated transcript levels. Strikingly, mRNA levels of both transcriptional regulators were also higher (*yjeB* (*nsrR*), $\log_2$ FC 2.26; *ygaA* (*norR*), $\log_2$ FC 2.11). Apart from these two direct NO-sensing regulators, several other genes functionally operating in transcription regulation were up-regulated, including those of the superoxide stress regulon, *soxS* and *soxR*, and *yhiX* (*gadX*), encoding an activator of the glutamate-dependent acid resistance system (Schouten and Weiss, 1999). Two genes encoding glutamate decarboxylase isoenzymes (*gadA*, *gadB*) were also up-regulated. In addition, several other stress-related genes were activated upon acidified nitrite stress. These include several paralogs of the universal stress proteins (*uspA*, *ydaA* (*uspE*), *yecG* (*uspC*), *yiiT* (*uspD*), *yhiO* (*uspB*)), small heat shock chaperones encoding genes *ibpA* and *ibpB*, and genes of the Suf system (*sufC*, *ynhE* (*sufB*), *sufA*), which mediates Fe-S cluster biogenesis under oxidative stress and iron starvation (Groote *et al.*, 1996). In addition, three genes were up-regulated that encode ribosome modulation factor (*rmf*), the YfiA protein (*yfiA*) and hibernation promoting factor (*hpf*), which inactivate ribosomes upon entry into stationary phase.

Concerning the down-regulated genes, those within the functional category translation, ribosomal structure and biogenesis constituted the largest group (14.3%). Hence, lower mRNA levels were detected for genes coding for 50S (e.g. *rpmA*, *rplU*) and 30S ribosomal proteins (e.g. *rpsT*, *rplQ*), different aminoacyl tRNA synthetases (e.g. *cysS*, *glnS*, *asnC*, *tyrS*), or enzymes participating in the translation process (initiation (*infA*), elongation (*efp*), termination (*prfA*, *prfB*, *prfC*)). In addition to the translational machinery, genes involved in transcription and replication, recombination and repair were down-regulated, such as *fis* (Fis family transcriptional regulator), *nusA* (transcription elongation factor nusA) or *gyrA* (DNA gyrase subunit A). Besides these crucial processes in cell growth, several metabolic pathways were negatively affected by a 1 h acidified $NaNO_2$ exposure. As such, genes involved in nucleotide transport and metabolism, including genes of the pyrimidine and purine biosynthetic and salvage pathways, fatty acid synthesis (*accA*, *accD*, *accB*, *fabA*, *fabH*, *fabI*) and coenzyme biosynthesis such as that of coenzyme A (*coaD*, *dfp* (*coaBC*), *coaA*) displayed decreased transcript levels. Concerning the amino acid metabolism and transport category, mRNA levels of glutamine uptake (*glnPQ*) and synthesis genes (*glnA*) as well as transcript abundance of a regulatory protein sensing the intracellular glutamine status (*glnB*) were lower compared to the nitrite-free culture. Besides glutamine, serine uptake (*sdaC*) and metabolism (*sdaA*, *sdaB*, *serB*) and different transporter genes (e.g. two subunits of the spermidine ABC transporter (*potAB*)) were negatively affected. A switch in energy generation was indicated by lower transcription of subunits of the ATP-synthase complex (*atpBEFHA*, *atpI*) and the *ackA-pta* pathway.

A 1 h acidified nitrite exposure repressed flagellar genes (*flgA*, *flgBCDEFG*, *flhBA*, *fliE*, *fliF/J*, *fliMN/PQR*) and genes involved in cell wall/membrane/envelope biogenesis, in particular several genes functioning in LPS biosynthesis (e.g. *lpxAB*, *lpxK*, *waaL*, *waaQ*, *rfaFC*) and peptidoglycan metabolism (e.g. *mrcA*, *dacA*, *mltB*).

In conclusion, considerable transcriptomic changes were induced upon a 1 h acidified $NaNO_2$ treatment of EHEC.

2.1.4 qPCR validation of the RNA-seq data of EHEC under acidified $NaNO_2$ stress

qPCR was performed to validate the $NaNO_2$ induced transcriptional changes in EHEC after a 10 min shock or after 1 h observed by RNA-seq. For each growth condition, three biological replicates were analyzed. Concerning the shock response to acidified $NaNO_2$, five up-regulated (*hmpA*, *ldhA*, *yhcN*, *ytfE*, Z3658) and four down-regulated (*bssR*, *cspA*, *secG*, *tdk*) genes were selected. For the 1 h response, those same genes that were still differentially regulated in the $NaNO_2$-treated culture compared to the control culture (all but *bssR*) were tested along with seven additional genes representing different COGs: *atpB* (energy production and conversion), *fabA* (lipid transport and metabolism), *fliF* (cell motility/intracellular trafficking, secretion, and vesicular transport), *pyrD* (nucleotide transport and metabolism), *rimM* (translation, ribosomal structure and biogenesis), *waaL* (cell wall/membrane/envelope biogenesis) displayed lower transcript levels while *gadX* (transcription) mRNA expression was higher in the presence of $NaNO_2$. Log_2 FC of all genes determined by qPCR showed a high correlation with the RNA-seq data for the 10 min acidified $NaNO_2$ stress response (R^2 = 0.97) (Figure 21A). Concerning the 1 h response (Figure 21B), qPCR results generally confirmed the directionality of regulation (R^2 = 0.87). However, results were inconsistent between the three replicates for genes *atpB* (log_2 FC 0.24, -1.45 and -0.72), *cspA* (log_2 FC 0.61, -3.11 and -0.42) and *secG* (log_2 FC 0.68, -1.77 and -0.01) and there was a greater variation in the magnitude of regulation determined by qPCR vs RNA-seq compared to the shock response. Nevertheless, validity and reproducibility of the RNA-seq data were confirmed by qPCR for both treatments.

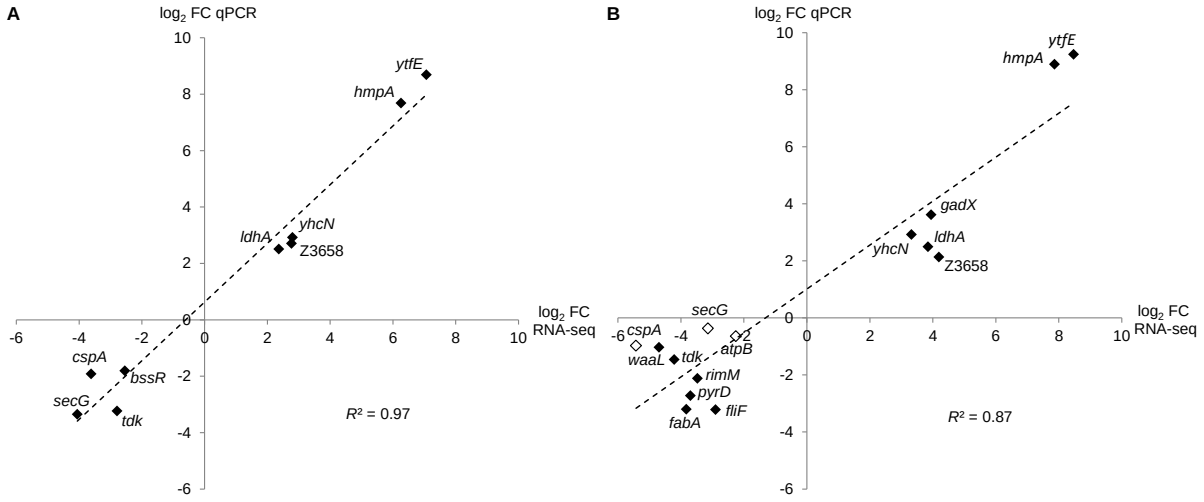

Figure 21: qPCR validation of acidified $NaNO_2$ stress RNA-seq data of EHEC for selected differentially expressed genes.
Relative transcription of genes found by RNA-seq to be differentially regulated in EHEC in response to (A) a 10 min or (B) a 1 h exposure to acidified $NaNO_2$ were examined with qPCR. 16S rRNA was used as a reference gene. Mean log_2 FC of three independent qPCR experiments were plotted against the respective log_2 FC determined by RNA-seq. Open symbols indicate an inconsistent regulation among the qPCR replicates. The coefficient of determination R^2 was calculated in Microsoft Excel.

2.2 Phenotypic characterization of deletion mutants Δ*hmpA* and Δ*nrfA* under food-related conditions

The RNA-seq and qPCR data clearly showed that EHEC mounts an adaptive response to acidified $NaNO_2$. Protection might be mediated by NO detoxification via HmpA, since transcription of the respective gene was found to be strongly induced after a 10 min (log_2 FC RNA-seq 6.26 / qPCR 7.69) and 1 h (7.86 / 8.90) exposure to acidified $NaNO_2$. Although transcription of the gene encoding the periplasmic cytochrome *c* nitrite reductase NrfA was unchanged under our experimental conditions, it might still contribute to coping with NO stress in raw sausages. On the other hand, despite displaying the greatest transcriptional change upon acidified $NaNO_2$ treatment (log_2 FC 10.95 and 12.35 after 10 min and 1 h, respectively) in our study, a protective role of the truncated flavorubredoxin encoded by the *norVs* gene in strain EDL933, which is missing the FMN-binding flavodoxin domain (Gardner *et al.*, 2002; Perna *et al.*, 2001), is rather questionable. It was found to lack NO reductase activity (Shimizu *et al.*, 2012). For this reason, it was refrained from constructing a *norVs* deletion strain. Instead, the focus was laid on HmpA and NrfA and their possible contribution to protecting EHEC against acidified $NaNO_2$-mediated stress in raw sausages.

First, growth of isogenic deletion mutants Δ*hmpA* and Δ*nrfA* was analyzed in LB pH 5.5 in the absence (0 mg/l) or presence of different concentrations of $NaNO_2$ (50, 100 and 150 mg/l) both under high (Figure 22A, B) and reduced (Figure 22C, D) O_2 levels.

With increasing concentrations of $NaNO_2$, the lag phase of the WT and Δ*nrfA* mutant increased. Whereas they needed about 6 h to reach an OD_{600} = 0.2, it took them on average 10.5 h, 16.0 - 16.5 h and 27 h when 50 mg/l, 100 mg/l and 150 mg/l $NaNO_2$, respectively, were added (Figure 22A). Similarly, biomass produced by 47 h as indicated by the AUC decreased with increasing concentrations of $NaNO_2$ (Figure 22B). To the contrary, a concentration as low as 50 mg/l $NaNO_2$ already strongly delayed growth of Δ*hmpA* (Figure 22A). At 100 mg/l and 150 mg/l $NaNO_2$, growth of Δ*hmpA* was weakly or no longer detectable within the time frame (47 h) of the experiment. Principally the same results were obtained under microaerobic conditions (Figure 22C, D).

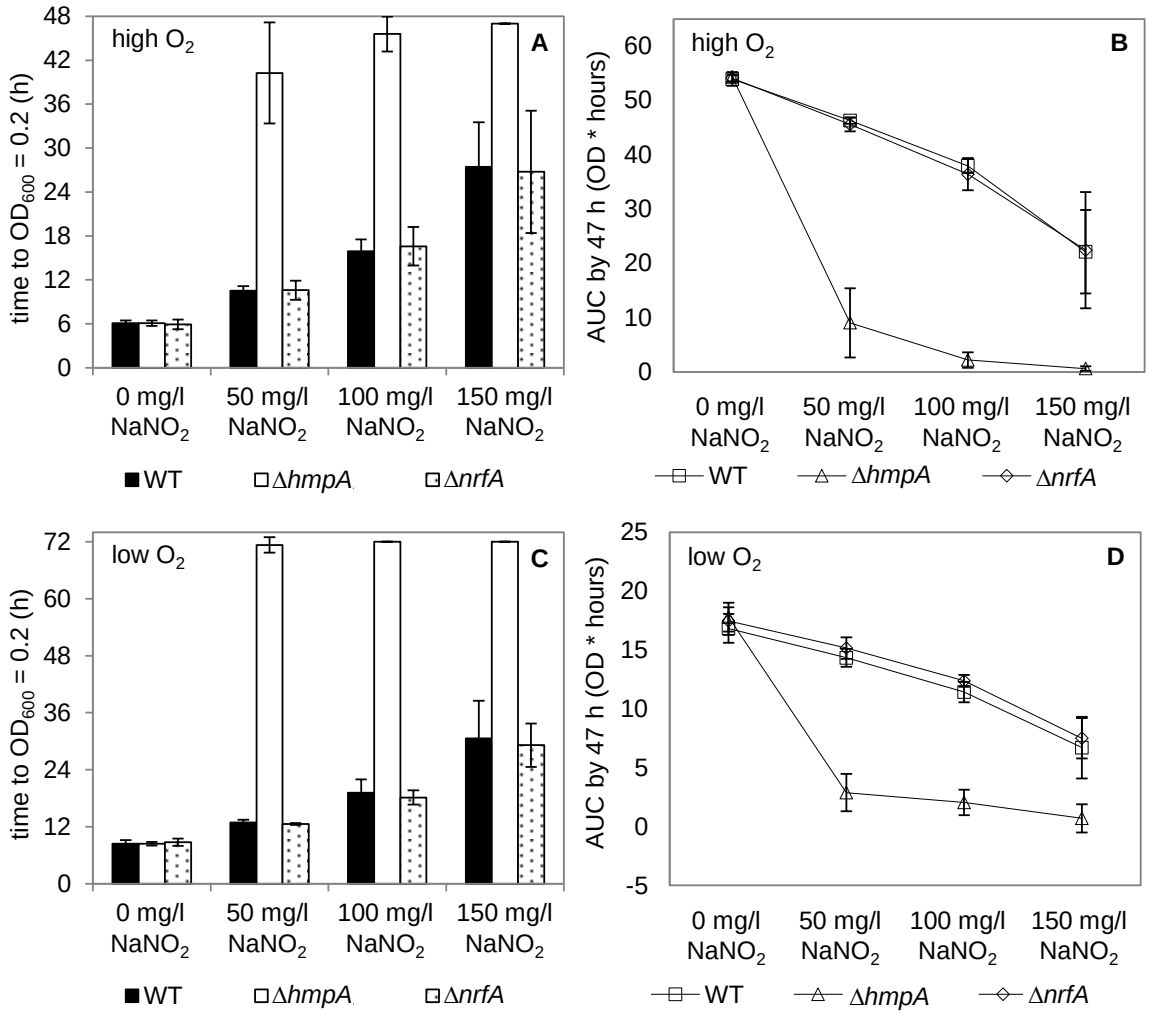

Figure 22: Impact of $NaNO_2$ on growth of EHEC EDL933 WT and the deletion mutants Δ*hmpA* and Δ*nrfA* under acidic conditions.
EHEC EDL933 WT and deletion mutants were grown in LB pH 5.5 in the presence of 0, 50, 100 or 150 mg/l $NaNO_2$ with agitation at 24°C under aerobic (A, B) or micro-aerobic conditions (C, D) in a Bioscreen C. Depicted are mean values ± SD from three independent experiments including duplicates. A, C: Time the EHEC EDL933 WT (black), Δ*hmpA* (white) and Δ*nrfA* (dotted) cultures needed to reach OD_{600} = 0.2 (h) in dependence of the $NaNO_2$ concentration. B, D: AUC after 47 h in dependence of the $NaNO_2$ concentration for cultures of EHEC EDL933 WT (square), Δ*hmpA* (triangle) and Δ*nrfA* (diamond).

Since the *in vitro* growth studies indicated that HmpA might be a good candidate for protecting EHEC from acidified $NaNO_2$ stress also in raw sausages, our cooperation partners conducted challenge studies in short-ripened spreadable sausages produced with 0 or 150 mg/l $NaNO_2$ to compare the growth kinetics of WT, Δ*hmpA* and Δ*nrfA* (Figure 23). Addition of $NaNO_2$ to the meat did not substantially influence survival of any of the strains. EHEC cfu/g meat stayed constant during the ripening period in both types of sausages. Furthermore, no differences were detected between the growth kinetics of the mutants Δ*hmpA* and Δ*nrfA* compared to the WT. Contrary to the *in vitro* growth assays, Δ*hmpA* was no more sensitive than the WT to $NaNO_2$ in short-ripened spreadable sausages.

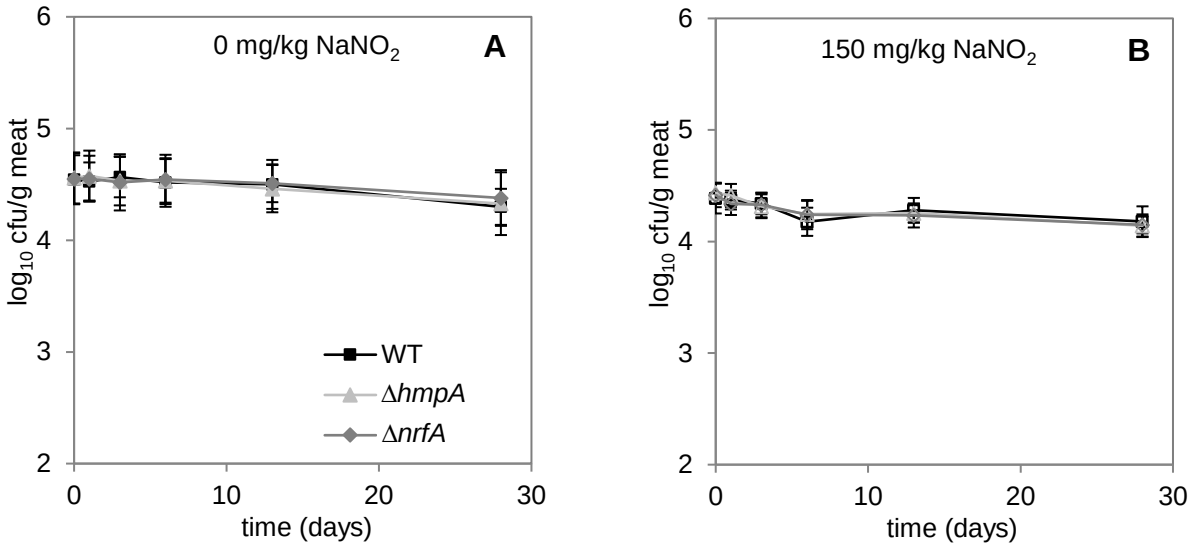

Figure 23: Impact of $NaNO_2$ on survival of EHEC EDL933 WT and deletion mutants in *hmpA* and *nrfA* in short-ripened spreadable sausages.
Numbers of EHEC EDL933 WT (square), Δ*hmpA* (triangle) and Δ*nrfA* (diamond) were determined in short-ripened spreadable sausages produced without $NaNO_2$ (A) or cured with 150 mg/kg $NaNO_2$ (B). Three different sausages per batch were sampled in duplicate on days 0, 1, 3, 6, 13 and 28. Cfu/g meat was determined via cell count on sorbitol MacConkey agar plates. Values represent the mean ± SD from three biologically independent experiments. Data were kindly provided by Rohtraud Pichner (MRI Kulmbach).

3 Plant extracts as potential curing salt substitutes

Plant extracts might constitute promising alternatives for the conventional nitrite or nitrate curing salts. First, nitrate-rich plant extracts represent a natural nitrate reservoir, which in combination with a nitrate-reducing starter culture results in the production of sausages with the desired traditional properties (Sebranek and Bacus, 2007a). Second, plants are rich in secondary metabolites that might be beneficial to the curing process (e.g. as antioxidants) and might possess antimicrobial activity (Cowan, 1999). Including potent plant extracts in the recipe might allow reducing the amount of synthetic nitrite or nitrate added. To ensure the microbiological safety of the products with reduced levels of or even without nitrite or nitrate, thorough investigations on the effectiveness of plant extracts as curing salt substitutes are essential.

3.1 Effect of different plant extracts on growth of *S.* Typhimurium and EHEC

The effects of powder or liquid extracts from six different plants (celery, chili, balm mint, mustard seed, nettle leaves, elderflower) on the growth of *S.* Typhimurium 14028 and EHEC EDL933 in RD0 broth at 24°C was tested in a Bioscreen C. The maximum concentrations recommended by the suppliers for use in food production were applied. Growth curves were compared to cultures grown with 150 mg/l $NaNO_3$, 150 mg/l $NaNO_2$ or without additives. Two independent experiments were performed for the plant extracts except for the celery extract, which was tested seven times.

150 mg/l of the traditional curing agent $NaNO_2$ retarded growth of both *S.* Typhimurium 14028 (Figure 24A) and EHEC EDL933 (Figure 25A). This is in agreement with the observed inhibitory action of $NaNO_2$ against *S.* Typhimurium on the first ripening days in the challenge assays. A suitable plant extract was claimed that substituted for the inhibitory action of $NaNO_2$ against *Salmonella* and could additionally provide phytochemical compounds active against EHEC, which are not susceptible to $NaNO_2$ *in situ*.

A decrease in the maximum culture density was observed for both *S.* Typhimurium and EHEC grown with celery extract (Figure 24C and Figure 25C). Growth was not delayed in the beginning, but ceased at a lower optical density compared to the control culture. This reduction of the maximum optical density is presumably not due to the nitrate present in the celery extract, since 150 mg/l $NaNO_3$ *per se* did not negatively affect growth of *S.* Typhimurium (Figure 24B) and EHEC (Figure 25B).

The strongest effect was observed for the chili infusion. Growth of both *S.* Typhimurium (Figure 24D) and EHEC (Figure 25D) was slowed and stopped at a lower culture density compared to the control cultures. Since the chili infusion additionally contains citric acid, it cannot be excluded that the growth inhibition observed is mediated by this organic acid or by a combined action of both ingredients.

A slightly reduced growth rate at higher optical densities was detected for EHEC grown in the presence of balm mint powder (Figure 25E). This effect, however, was not observed with the liquid extract (data not shown). Concerning *S.* Typhimurium, results from two independent experiments did not support an inhibitory effect on growth (data not shown).

No or negligible inhibitory effects on the growth behavior of both bacteria were detected for the mustard seed, elderflower and both powder and liquid extracts from nettle leaves (data not shown).

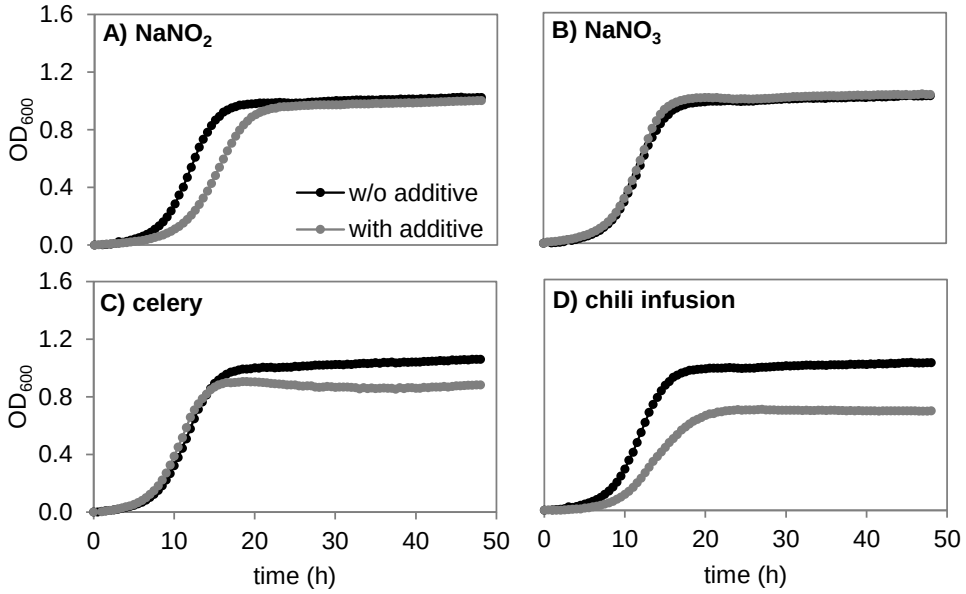

Figure 24: Effect of nitrite, nitrate, celery extract and chili infusion on *in vitro* growth of *S.* Typhimurium 14028 WT.

Growth of the *S.* Typhimurium 14028 WT in RD0 broth without additives (black line) or with additives (grey line) at 24°C was recorded over 48 h in a Bioscreen C. Representative growth curves from at least two independent experiments illustrating the impact of (A) 150 mg/l $NaNO_2$, (B) 150 mg/l $NaNO_3$, (C) 10 g/l celery extract and (D) 100 ml/l chili infusion on growth are shown.

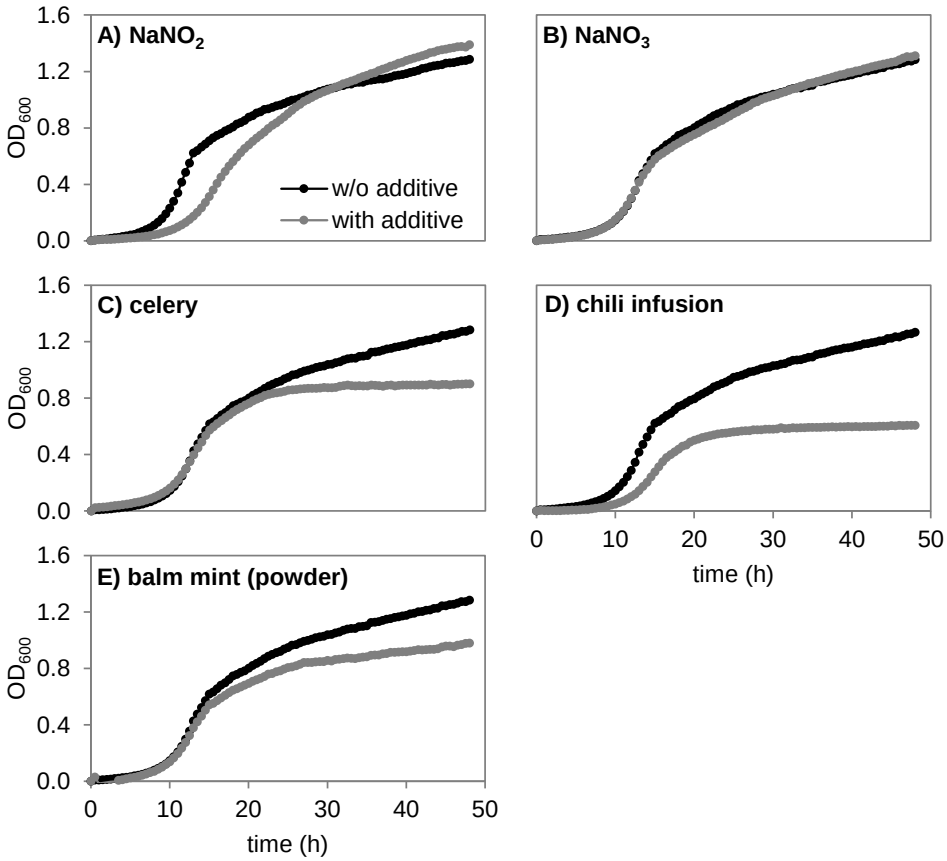

Figure 25: Effect of nitrite, nitrate, celery extract, chili infusion and balm mint powder on *in vitro* growth of EHEC EDL933 WT.

Growth of the EHEC EDL933 WT in RD0 broth without additives (black line) or with additives (grey line) at 24°C was recorded over 48 h in a Bioscreen C. Representative growth curves from at least two independent experiments illustrating the impact of (A) 150 mg/l $NaNO_2$, (B) 150 mg/l $NaNO_3$, (C) 10 g/l celery extract, (D) 100 ml/l chili infusion and (E) 3 g/l balm mint (powder) on growth are shown.

3.2 Transcriptomic response of *S.* Typhimurium to celery extract vs nitrate

The *in vitro* results and challenge experiments with salami-type sausages (Rohtraud Pichner, personal communication) suggested that the celery extract, apart from nitrate, might contain a natural antimicrobial compound that is active on *S.* Typhimurium (and EHEC *in vitro*). Assuming the antimicrobial effect is indeed ascribed to a phytochemical, and given the described actions of these compounds on bacterial cells so far (e.g. membrane disruption, see I5), one would expect to observe changes in the transcriptome in response to these stresses.

Hence, to get a hint to the molecular mechanism of the antimicrobial action of celery extract, the transcriptome of *S.* Typhimurium exposed anaerobically for 1 h to either 10 g/l celery extract or 70 mg/l KNO_3 in RD0 broth was analyzed and compared to the respective reference culture without additives. 10 g/l of celery extract was used since this corresponds to the concentration for use in raw sausage production (10 g/kg meat) recommended by the supplier, and 70 mg/l KNO_3 in turn matches the amount of nitrate in 10 g/l celery extract, as determined by our cooperation partners in Kulmbach. In the celery- and the nitrate-exposed cultures, only four genes, respectively, were differentially transcribed (adjusted p-value < 0.5) compared to the reference culture. These were *norVW*, *uhpT* and *narK* in response to celery and *norVW*, *ytfE* and *narG* in response to KNO_3 (Table 16). Considering a less stringent p-value < 0.15, transcription levels of all eight genes up-regulated in the presence of KNO_3 were also enhanced in the celery-cultivated culture. For reasons of comparison, the differential regulation of these genes to 150 mg/l $NaNO_2$ is also included in Table 16. The greatest fold-changes under both conditions were observed for genes *norV* and *norW*, encoding the NO reductase flavorubredoxin and its associated oxido-reductase, respectively. Furthermore, the Fe-S cluster repair protein encoding gene *ytfE* was up-regulated. Not surprisingly, genes associated with nitrate respiration displayed higher transcript levels, namely those coding for the membrane-bound nitrate reductase (*nar* operon (*narGHIJ*)) and a nitrate/nitrite antiporter (*narK*). The only gene that showed increased transcription in response to celery but not to nitrate was *uhpT*, which encodes a sugar phosphate antiporter. Differential transcription of *uhpT* for the pairwise comparison KNO_3 vs reference was not computed since counts did not pass the cpm filter of 10, but the cpm were similar for both conditions. When the transcriptional response of these genes to celery/KNO_3 vs $NaNO_2$ was compared, the up-regulation of *norVW* and *ytfE* was even more pronounced compared to the control culture, but the *nar* operon and *narK* were oppositely regulated, displaying decreased transcription under $NaNO_2$.

Table 16: Differentially transcribed genes in response to celery and nitrate
Log_2 FC with a BH-adjusted p-value < 0.05 are shown in bold. – indicates that the gene did not pass the cpm cutoff for the respective pairwise comparison. Transcription of the genes in response to 150 mg/l $NaNO_2$ is also shown for comparison.

			10 g/l celery vs reference		70 mg/l KNO_3 vs reference		150 mg/l $NaNO_2$ vs reference	
14028 identifier	Gene name	Product	log_2 FC	p-value (BH-adjusted)	log_2 FC	p-value (BH-adjusted)	log_2 FC	p-value (BH-adjusted)
STM14_2129	*narI*	nitrate reductase 1 subunit gamma	2.73	0.06	2.71	0.07	**-2.79**	**0.01**
STM14_2130	*narJ*	nitrate reductase 1 subunit delta	2.63	0.08	2.54	0.11	**-2.67**	**0.01**
STM14_2131	*narH*	nitrate reductase 1 subunit beta	2.51	0.10	2.63	0.07	**-2.73**	**0.01**
STM14_2132	*narG*	nitrate reductase 1 subunit alpha	2.60	0.08	**2.81**	**0.05**	**-2.65**	**0.01**
STM14_2134	*narK*	nitrite extrusion protein	**3.15**	**7.62E-03**	2.66	0.07	**-2.52**	**0.02**
STM14_3431	*norV*	anaerobic nitric oxide reductase flavorubredoxin	**3.18**	**7.62E-03**	**4.34**	**1.12E-05**	**7.61**	**3.70E-15**
STM14_3432	*norW*	nitric oxide reductase	**4.60**	**5.24E-06**	**5.77**	**2.28E-09**	**8.71**	**4.80E-18**
STM14_4568	*uhpT*	sugar phosphate antiporter	**3.29**	**7.62E-03**	-	-	-	-
STM14_5283	*ytfE*	cell morphogenesis/cell wall metabolism regulator	2.50	0.10	**2.84**	**0.05**	**3.11**	**1.56E-03**

To analyze the validity of these findings, qPCR was performed on three biological replicates of each condition. Relative transcription of selected genes *narG*, *narK*, *norV*, *ytfE* and *uhpT* obtained by qPCR confirmed the RNA-seq data (Figure 26). Concerning *uhpT*, no differential transcription was observed in response to KNO_3 or $NaNO_2$ compared to the reference, consistent with the equal RNA-seq cpm for these conditions (data not shown).

In conclusion, the transcriptional response to celery extract and KNO_3 overlapped with the exception of the *uhpT* gene, which was induced exclusively by the celery extract.

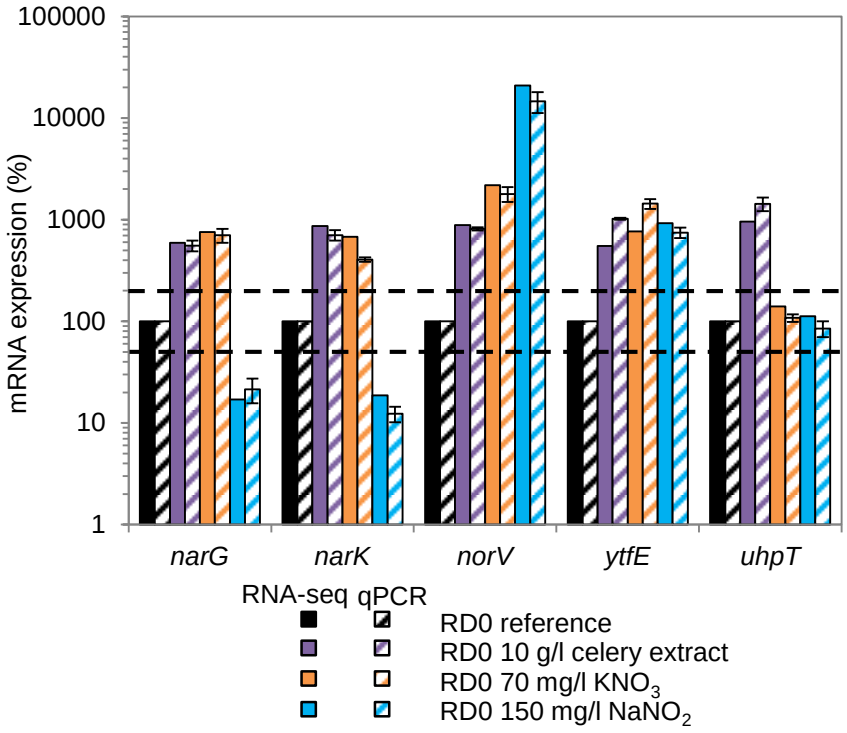

Figure 26: Effect of celery, nitrate and nitrite on the transcription of selected genes in culture broth simulating RD0.
The transcription level of genes *narG*, *narK*, *norV*, *ytfE* and *uhpT* in cultures incubated anaerobically for 1 h at 24°C in RD0 broth with 10 g/l celery (violett), 70 mg/l KNO_3 (orange) and 150 mg/l $NaNO_2$ (blue) relative to a reference culture without additives (black) was determined by RNA-seq (filled columns) and qPCR (hatched columns). Fold-changes were calculated relative to RD0 as reference condition and converted to percent mRNA expression from RD0 (set 100%). A 2-fold change in mRNA expression (%), corresponding to 200% and 50%, is indicated by black dashed lines. RNA-seq relative expression values (hatched columns) were calculated based on cpm. For qPCR, 16S rRNA was used as the normalization control gene and columns represent the mean ± SE of three independent biological experiments.

IV Discussion

1 Contribution of NO-detoxifying enzymes in protecting *S.* Typhimurium from acidified $NaNO_2$-derived stress *in vitro* and in raw-ripened spreadable sausages

Despite using $NaNO_2$ in meat curing for centuries, the mechanisms by which nitrite and its reactive derivatives, most importantly NO, inhibit growth of pathogenic bacteria besides *Clostridium botulinum* have gained surprisingly little attention. Due to the crucial role of NO as an effector of the host immune response, research with particular focus on pathogenesis of *S.* Typhimurium unraveled the contribution of NO detoxification in combating nitrosative stress and served as a starting point for this study. By assaying the *in vitro* and *in situ* growth and survival of *S.* Typhimurium 14028 deletion mutants Δ*hmpA*, Δ*norV* and Δ*nrfA*, encoding the NO-detoxifying enzymes flavohemoglobin, flavorubredoxin and cytochrome *c* nitrite reductase, respectively, this study has shed light on the contribution of these systems to the nitrosative stress defense of *S.* Typhimurium in raw sausages.

HmpA has been shown to be the key enzyme conferring protection from growth inhibition by acidified nitrite in LA-acidified LB broth pH 5.5 under both aerobic and micro-aerobic conditions at 24°C (see Figure 4), which is in agreement with earlier studies performed at 37°C (Crawford and Goldberg, 1998). Transcription data further confirmed a strong up-regulation of *hmpA* transcription in the presence of acidified $NaNO_2$ (see Figure 3). However, challenge experiments with short-ripened spreadable sausages failed to reveal a higher sensitivity of any of the mutants compared to the WT (see Figure 5), indicating that none of the NO-detoxifying systems is solely responsible for protection against nitrite-induced stress in raw sausages.

The discrepancy in the nitrite sensitivity of the HmpA mutant *in vitro* and *in situ* might be explained by the more complex growth matrix of the sausages compared to LB broth. NO derived from nitrite reacts with various components in the meat, including myoglobins, thiol groups of proteins or free radical intermediates in lipid oxidation (see Figure 1). Moreover, curing additives such as the reductant ascorbate or higher salt concentrations influence the reactivity of nitrite in the meat matrix (reviewed in Cammack *et al*., 1999; Skibsted, 2011). Hence, it is conceivable that these competitive reactions during the curing process scavenge free NO released from acidified nitrite, resulting in different nitrosating species, which might not be subject to removal by HmpA (McCollister *et al.*, 2007; Song *et al.*, 2013).

Raw sausages certainly comprise a distinct growth environment compared to laboratory LB broth. Nutrient composition (reviewed in Pereira and Vicente, 2013), texture, O_2 dispersion, and competition with the starter cultures are just some noteworthy differences. These differences might result in distinct metabolic flexibilities to circumvent nitrosative stress in raw sausages vs. LB broth. Fratamico *et al.* (2011) compared the transcriptomes of *E. coli* O157:H7 cultured in ground beef extract vs. TSB broth and found significant changes in the transcription of 128 genes. It has been reported previously that the susceptibility of *S.* Typhimurium to nitrosative stress depends on the growth condition. Sensitivity of strains mutated in NO-detoxifying enzymes is more pronounced (Park *et al.*, 2011) or only detectable

(Gardner *et al.*, 2002) in minimal media in contrast to rich media such as LB, since NO-sensitive metabolic pathways, e.g. TCA cycle to supply precursors of amino acids (Richardson *et al.*, 2011), are required under the former condition. What is more, all three systems HmpA, NorV and NrfA can contribute more or less to NO detoxification in particular environments, as deduced from single, double and triple deletion mutants exposed to NO under different growth conditions (Mills *et al.*, 2008). This possibility is further supported by the *in vitro* growth analysis of double mutants and the triple mutant under acidified $NaNO_2$ stress in this study, showing an interplay of both HmpA and NorV in protecting *S.* Typhimurium against the growth inhibitory effect of acidified nitrite (see Figure 6). Thus, the conditions in raw sausages might permit NO detoxification by the combined action of two or even all three of these systems. Investigating the growth kinetics of the strain lacking all three enzymes in raw sausages might provide further information on their contribution, if any, to survival of nitrite-derived stress in raw sausages.

2 The transcriptional response of *S.* Typhimurium to SNP-derived NO and acidified $NaNO_2$ under conditions related to raw sausage ripening

There is evidence supporting the view that there are still uncharacterized mechanisms for reduction of, or protection against NO (Arkenberg *et al.*, 2011; Cole, 2012, Vine and Cole, 2011a, 2011b). Alternative pathways other than, or additional to, NO detoxification via HmpA, NorV and NrfA might also help *S.* Typhimurium withstand nitrite-related stress in raw sausages.

2.1 The transcriptome of S. Typhimurium in response to SNP-derived NO

Given the central role of NO, the transcriptome of *S.* Typhimurium to SNP-derived NO at neutral pH was assessed first. The five genes found to be up-regulated are all members of the regulon of the NO responsive regulator NsrR, which has been implicated in nitrosative stress resistance in *S.* Typhimurium (Karlinsey *et al.*, 2012). NO inactivates NsrR, thereby relieving transcriptional repression of target genes (Tucker *et al.*, 2008a) including the NO-detoxifying HmpA (Karlinsey *et al.*, 2012). A regulon member of particular interest is the hybrid cluster protein Hcp with its associated oxidoreductase Hcr, whose function remained controversial for some time (Almeida *et al.*, 2006; Wolfe *et al.*, 2002). A more recent study indicates a supportive role in aerobic NO detoxification and resistance to NO-mediated inhibition of aerobic respiration (Karlinsey *et al.*, 2012). However, lack of Hcp did not result in diminished growth in the presence of the NO-releasing compound Spermine-NONOate (Karlinsey *et al.*, 2012). Similarly, growth studies of a *hcp* single deletion mutant (Δ*hcp*) performed in our laboratory revealed, that Δ*hcp* was no more sensitive to SNP-derived NO or acidified $NaNO_2$ under aerobic conditions as compared to the WT (Schürch, 2012) (data not shown). Observations in *E. coli* further support a role of Hcp in the anaerobic management of endogenous nitrosative stress (Cole, 2012; Seth *et al.*, 2012) and in protection against the nitrosating agent *S*-nitrosoglutathione (GSNO) (Seth *et al.*, 2012). In agreement, it was recently demonstrated that Hcp and its reductase Hcr reduce NO with high affinity under anaerobic

conditions (Wang *et al.*, 2016). A role for some other NsrR-regulated genes in supporting growth during nitrosative stress *in vitro* and *in vivo* has further been demonstrated in *S.* Typhimurium (Karlinsey *et al.*, 2012); yet, the exact functions of some such as YgbA or STM1808 remain to be characterized.

2.2 The acidified $NaNO_2$ stress response – protection provided by the lysine decarboxylase CadA and evidence for intracellular acidification as a novel mode of the antibacterial action of acidified $NaNO_2$

Apart from NO, other reactive nitrogen species with antimicrobial potential arise from nitrite (Cammack *et al.*, 1999) under the mildly acidic condition in the meat. To gain further insight into the antimicrobial action of $NaNO_2$ under conditions relevant for food and to identify critical determinants in the protective response of this organism, the shock and adaptive response of *S.* Typhimurium to $NaNO_2$ acidified by lactic acid at an ambient temperature of 24°C was analyzed.

The NsrR regulon implicated in nitrosative stress protection (Karlinsey *et al.*, 2012) was found to be strongly induced in both the immediate and continuous response to acidified $NaNO_2$ stress. This is consistent with the SNP transcriptome data and with previous studies in *S.* Typhimurium using NO donor compounds (Richardson *et al.*, 2011; Bourret *et al.*, 2008), underlining the importance of NO arising from acidified $NaNO_2$. To the contrary, transcriptional activation of *norV*, encoding the NO-reducing flavorubredoxin (Mills *et al.*, 2005), was observed after 10 min but not after prolonged exposure. This might be due to oscillations in *norV* mRNA levels under aerobic conditions as previously reported for *E. coli* (Mukhopadhyay *et al.*, 2004). Besides this direct response to nitrosative stress, several other stress-related genes were induced, including acid resistance genes, such as *cadBA*, *adi* and *yjdE* (Zhao and Houry, 2010), and genes related to DNA damage like *ogt* (Yamada *et al.*, 1995) and *dps* (Calhoun and Kwon, 2011). The shock response was further characterized by down-regulation of the translational machinery and genes involved in transcription and replication, which comprise crucial physiological processes. This trend was also observed in previous studies investigating the NO stress response of S. Typhimurium (Bourret *et al.*, 2008; Richardson *et al.*, 2011) and might be a non-specific consequence of the reduced growth rate following addition of 150 mg/l $NaNO_2$ (see Figure 8). Obviously, inducing stress tolerance and reducing cell growth promotes survival of *S.* Typhimurium subjected to harsh acidified $NaNO_2$ stress.

The transcriptional changes observed in the adaptive response mainly comprise genes involved in iron homeostasis and anaerobic respiration. The decreased transcription of the latter group of genes is consistent with previous studies investigating the response to NO stress in *S.* Typhimurium (Richardson *et al.*, 2011) and further in *E. coli*, albeit under anaerobic conditions (Justino *et al.*, 2005; Pullan *et al.*, 2007). Differential regulation was mainly ascribed to inactivation of the regulator FNR, which regulates many genes in response to O_2 availability (Spiro and Guest, 1990; Fink *et al.*, 2007) and whose Fe-S cluster is nitrosylated by NO (Crack *et al.*, 2008). Under the culture density investigated (OD_{600} = 1.5), cells might have experienced some O_2 shortage that was sufficient to induce FNR regulation, such as

observed by Richardson *et al.* (2011). The other large group of genes found deregulated under prolonged acidified $NaNO_2$ exposure were iron-responsive genes, which are subjected to regulation by Fur (Bjarnason *et al.*, 2003; Troxell *et al.*, 2011). Under iron-replete conditions, dimeric Fe^{2+}-bound Fur binds to consensus DNA sequences and represses transcription of iron-uptake systems (Escolar *et al.*, 1999). Upon nitrosylation Fe-Fur loses its DNA-binding activity (D'Autreaux *et al.*, 2002), resulting in derepression of target genes involved in iron acquisition, as observed in our RNA-seq data as well as in other studies (Richardson *et al.*, 2011; Mukhopadhyay *et al.*, 2004; Pullan *et al.*, 2007). The transcriptional changes observed might therefore merely be a coincidental consequence of inactivation of FNR and Fur by NO arising from acidified $NaNO_2$. To the contrary, derepression of NsrR-regulated genes may provide a physiological benefit by alleviating the nitrosative stress on the cells.

An unexpected finding was the up-regulation of inducible amino acid decarboxylases and the respective amino acid/polyamine antiporters, which are crucial constituents of the acid stress response in enteropathogenic bacteria (Zhao and Houry, 2010). Whereas the decarboxylation systems for lysine (*cadA*, *cadB*) and ornithine (*speF*, *potE*) were induced in response to acidified $NaNO_2$ shock and continuous stress, respectively, the arginine decarboxylase system (*adi*, *yjdE*) was up-regulated under both conditions. The amino acid decarboxylases are known to be induced by low pH (Zhao and Houry, 2010), and each was shown to confer more or less to acid resistance under different conditions in *S.* Typhimurium (Viala *et al.*, 2011; Alvarez-Ordóñez *et al.*, 2010). Since increased transcription of inducible amino acid decarboxylases has never been observed in bacteria exposed to NO under neutral pH, this response is presumably specific to acidified $NaNO_2$ stress. The physiological role of CadA in protection against acidified $NaNO_2$ stress is supported by the impaired growth of the deletion mutant Δ*cadA* pBR322 in the presence of $NaNO_2$ (see Figure 14). Interestingly, *Salmonella* CadA protein levels of a strain, missing the three major up-regulated proteins (HmpA, YtfE, Hcp), were found to be elevated under RNS stress in mice (Burton *et al.*, 2014). In uropathogenic *E. coli* (UPEC), the lysine decarboxylase system has been demonstrated to be involved in protection against nitrosative stress elicited by acidified $NaNO_2$ (Bower and Mulvey, 2006). Mutations in either *cadC*, encoding the transcriptional activator, *cadA* or *cadB* resulted in increased sensitivity towards acidified $NaNO_2$ (Bower and Mulvey, 2006). There are several possible explanations how CadA might contribute to nitrosative stress protection. First, the polyamine cadaverine is produced upon decarboxylation of lysine. Bower and Mulvey (2006) found that exogenous supplementation with cadaverine or other polyamines rescued growth of the cadaverine-deficient deletion mutants, arguing for polyamines as the mediator of the protective effect. Preliminary supplementation studies with cadaverine, spermidine and putrescine, however, did not stimulate growth of *S.* Typhimurium WT and Δ*cadA* exposed to acidified $NaNO_2$ stress (data not shown). Besides protection by cadaverine, the end product of lysine decarboxylation, postulated so far, our data indicate that the pH-homeostatic function of the lysine decarboxylase system itself (Park *et al.*, 1996) might account for protection against acidified $NaNO_2$ stress. Decarboxylation of lysine to the polyamine cadaverine consumes an intracellular proton, and the basic cadaverine is

subsequently exported in exchange for extracellular lysine via the antiporter (Park *et al.*, 1996). Both reactions contribute to pH-homeostasis and local buffering of the extracellular medium. However, this would imply that acidified $NaNO_2$ would somehow perturb the intracellular pH of *S.* Typhimurium in the first place. Indeed, measurement of the pH_i in *S.* Typhimurium via a pH-sensitive GFP derivative indicated intracellular acidification upon addition of 150 mg/l $NaNO_2$ to mildly acidic LB medium, but not to neutral medium (see Figure 15). Imposing intracellular acid stress on bacteria might provide an additional mechanism of the inhibitory action of acidified nitrite, which has previously been reported for yeasts (Mortensen *et al.*, 2008). The effector of the intracellular acidification might be nitrous acid that is supposed to form upon acidification of nitrite. Nitrous acid as a weak acid might diffuse across the membrane and dissociate in the neutral cytoplasm, thereby releasing a proton (Lambert and Stratford, 1999). Lysine decarboxylase might provide a mechanism to neutralize these protons. Furthermore, pH buffering of the surrounding environment might decrease the rate of NO and RNS formation from nitrite, thereby indirectly contributing to nitrosative stress protection by diminishing the growth inhibitory effects of these species.

In conclusion, the lysine decarboxylase CadA is shown to play an important role in protecting *S.* Typhimurium against acidified $NaNO_2$-mediated stress. Furthermore, to our knowledge, this study provides first evidence that intracellular acidification might additionally contribute to the antibacterial action of acidified $NaNO_2$ in foodstuff.

2.3 Putative systems involved in NO and acidified $NaNO_2$ tolerance of *S.* Typhimurium

The transcriptome data and the screening of the insertion mutant library provided some hints to additional systems that could play a role in acidified nitrite resistance.

The gene *hdeB*, annotated as acid-resistance protein, displayed higher transcript levels following a 10 min acidified $NaNO_2$ shock and had the strongest transcriptional increase after acidified $NaNO_2$ adaptation in *S.* Typhimurium. Nevertheless, deletion of HdeB did not influence growth in the presence of acidified $NaNO_2$ compared to the WT (see Figure 11). In *E. coli*, HdeB encodes an acid stress chaperone that, along with HdeA, protects periplasmic proteins against extreme acid stress (< pH 4) by preventing their aggregation, and further assists in solubilization of mixed protein-chaperone aggregates during recovery from acid stress at neutral pH (Kern *et al.*, 2007; Malki *et al.*, 2008; Dahl *et al.*, 2015). On the contrary, EHEC O157:H7 is not dependent on these acid stress chaperones but seems to have evolved other acid defense strategies (Carter *et al.*, 2012). Unlike *E. coli*, genes coding for HdeA and HdeB are absent in *S.* Typhimurium (Hong *et al.*, 2012), but it harbors the aforementioned STM14_1885 gene, which is annotated as *hdeB*. Recently SEN1493, the homologue of STM14_1885 in *S.* Enteritidis Nal^R, was found to be induced in tryptic soy broth grown *S.* Enteritidis upon acidification to pH 5.5 with HCl (Joerger *et al.*, 2012). A follow-up study confirmed that it contributed to *S.* Enteritidis survival at pH 2 following pre-exposure at pH 5.5 (Joerger and Choi, 2015). However, since serovar-specific differences in gene expression and function of the *hdeB*-like locus were found (Joerger *et al.*, 2012;

Joerger and Choi, 2015), it remains to be determined if up-regulation of *hdeB* in response to acidified $NaNO_2$ primes cells to resist subsequent stresses or may merely be a coincidental consequence of the intracellular acidification in *S.* Typhimurium (see Figure 15).

Screening of an insertion mutant library provided some evidence regarding not necessarily inducible systems that might influence the resistance of *S.* Typhimurium to acidified $NaNO_2$-derived stress. Since the library covers about 62% of the *S.* Typhimurium genome (Knuth, 2004) and only part of it was screened, this approach does not claim to be exhaustive. Indeed, HmpA, lack of which results in a strong acidified $NaNO_2$-sensitive phenotype (see Figure 4), was not identified. Nevertheless, the screen provided some interesting hints that deserve further consideration.

Interestingly, *lpdA*, coding for lipoamide dehydrogenase, an essential component of the pyruvate and α-ketoglutarate dehydrogenase complexes and the glycine cleavage multi-enzyme system (Perham, 2000), was identified as insertion site in a nitrite-susceptible mutant. This mutant grew slower even in the absence of stress (data not shown). Richardson and colleagues (2011) claimed that LpdA is a key target of NO in the TCA cycle of *S.* Typhimurium, and that more than 50% of the transcriptional changes are due to LpdA inhibition. An improper functioning TCA cycle would explain the slower growth rate even in the absence of stress. Why lack of *lpdA* renders *S.* Typhimurium even more sensitive to acidified $NaNO_2$, however, remains to be elucidated.

An increased sensitivity to acidified $NaNO_2$ in the absence of a functional SufD protein, which is required for iron acquisition during Fe-S cluster formation (Saini *et al.*, 2010), is quite feasible. The Suf system is most important in Fe-S cluster biosynthesis under stress conditions such as iron limitation and oxidative stress in *E. coli* (Outten *et al.*, 2004; Jang and Imlay, 2010). Up-regulation of at least *sufA*, the first gene of the *suf* operon, under nitrosative stress was observed in different bacteria (Justino *et al.*, 2005; Pullan *et al.*, 2007; Bower *et al.*, 2009; Richardson *et al.*, 2011) and also in this study, implying also a function under this stress condition.

Strikingly, three genes involved in phosphate management of the cell, namely *pstS*, *ppk* and *pta* (Wanner, 1996), were identified to be disrupted by plasmid-insertion in acidified $NaNO_2$ sensitive mutants. The *pta* insertion strain additionally displayed enhanced sensitivity to NO under neutral conditions.

The PstS protein is part of the ABC-type phosphate-specific transport (Pst) system responsible for high affinity uptake of periplasmic inorganic phosphate (P_i). The Pst system belongs to the phosphate (Pho) regulon, that is controlled by the PhoR/PhoB two-component regulation system in response to environmental P_i limitation and plays a key role in phosphate homeostasis (Wanner, 1993, 1996). Moreover, the Pst system is a negative regulator of the Pho regulon when P_i is in excess (Wanner, 1996). The *ppk* gene encodes a polyphosphate kinase that catalyzes the reversible synthesis of poly P from the terminal phosphate of ATP (Kornberg *et al.*, 1999). Poly P serves both as a phosphate and as an energy reservoir amongst others, and has been implicated in responses to adverse environmental conditions (Kornberg *et al.*, 1999). *Pta* codes for the phosphate acetyltransferase that together with acetate kinase

AckA forms the Pta-AckA pathway: Pta catalyzes the reversible interconversion of acetyl-CoA and P_i to the high-energy intermediate acetyl-P, while AckA reversibly converts acetyl-P and ADP to acetate and ATP (Rose *et al.*, 1954). This pathway functions in energy generation via substrate-level phosphorylation during anaerobic mixed-acid fermentation and aerobic growth on excess glucose or glycolytic intermediates (Wolfe, 2005). Acetyl-P can also activate the PhoB response regulator independent of the signal transduction from its cognate histidine kinase PhoR (Wanner and Wilmes-Riesenberg, 1992; Kim *et al.*, 1996). A functional PhoB, in turn, is essential for the accumulation of poly P in *E. coli* (Rao *et al.*, 1998). Several lines of evidence link phosphate management to stress responses and virulence. Lamarche *et al.* (2008) nicely summarizes the impact of the Pho regulon on the production of poly P, the stringent response alarmone guanosine tetraphosphate (ppGpp) and the alternative sigma factor RpoS, all of which are necessary for proper adaptation to stressful environmental conditions, including nutrient-limitation and heat, osmotic or acid stress (Kornberg *et al.*, 1999). As such, *S.* Typhimurium *ppk* mutants were found to grow poorly on weak organic acids (Price-Carter *et al.*, 2005), and displayed a disrupted ATP homeostasis, reduced *rpoS* expression and virulence attenuation (McMeechan *et al.*, 2007). Following this line of reasoning, the necessity of a proper phosphate management could be expanded to acidified $NaNO_2$ stress as well, which is in agreement with the transcriptome data that indicate stringent control as response to this stress. However, further experiments investigating the growth of the respective deletion mutants and using defined levels of added phosphate are necessary to support this hypothesis.

With regard to Pta, disruption of which rendered *S.* Typhimurium more sensitive to both SNP-derived NO and acidified $NaNO_2$, the lack of its metabolic function might provide an alternative explanation. The *pta* deletion strain displayed an increased lag phase and slower growth in neutral LB pH 7 even without NO (see Figure 12), but grew essentially as the WT strain in LB pH 5.5 without $NaNO_2$ (see Figure 13). This observation might be explained by the lower steady state level of Pta under acidic conditions (Wolfe, 2005). In line with the need for metabolic flexibility to overcome inhibition of LpdA in key enzymes of the TCA cycle (Richardson *et al.*, 2011), a properly functioning Pta-AckA pathway might serve as an additional route to generate either acetyl-CoA or ATP during conditions of NO as well as acidified $NaNO_2$ stress.

3 Transcriptional profiling of *S.* Typhimurium in meat extract broth simulating conditions of RD0 and RD3

3.1 $NaNO_2$ evokes a transcriptional response only on RD0

The transcriptome studies in LB broth provided a first insight into the response of *S.* Typhimurium to SNP-derived NO and acidified $NaNO_2$. Given the fact, that raw sausages are a complex matrix with additional ingredients such as glucose, NaCl and sodium ascorbate, subsequent studies to unravel the molecular impact of $NaNO_2$ were consequentially performed in meat extract broths mimicking the

conditions on RD0 (pH 5.8, added sodium ascorbate, glucose, NaCl and 150 mg/l $NaNO_2$, anaerobic) and RD3 (pH 5.2, 30 mg/l $NaNO_2$, more NaCl to simulate lower a_w, anaerobic).

Whereas 150 mg/l $NaNO_2$ on RD0 obviously imposed stress on *S.* Typhimurium as indicated by up-regulation of stress-related genes, the residual 30 mg/l $NaNO_2$ present in raw sausages on RD3 did not evoke transcriptional changes (see Table 15).

The up-regulation of the *norVW* operon and of *ytfE* are in agreement with the well-defined roles of the encoded proteins in anaerobic NO detoxification (Gomes *et al.*, 2002; Mills *et al.*, 2005) and repair of Fe-S clusters damaged by nitrosative stress (Justino *et al.*, 2007; Vine *et al.*, 2010), respectively. However, acidified $NaNO_2$ does not only induce a directed response to NO stress, but further activates systems involved in protection against oxidative stress (*soxS*) and copper stress (*copA*, *cueO*). The SoxRS system regulates the defense to oxidative stress mediated by redox-cycling compounds (Gu and Imlay, 2011). Upon oxidation of the [2Fe-2S] cluster of SoxR, it switches on transcription of the *soxS* gene, encoding the transcriptional regulator SoxS, which in turn activates target genes necessary for resistance (Nunoshiba *et al.*, 1992; Pomposiello and Demple, 2000). However, SoxR is also activated by nitrosylation of the Fe-S cluster which was found to occur both *in vivo* and *in vitro* (Ding and Demple, 2000), and concomitantly, *soxS* was found to be induced in *E. coli*, UPEC and *S.* Typhimurium by NO or sources of NO including acidified $NaNO_2$ also in several other studies (Justino *et al.*, 2005; Pullan *et al.*, 2007; Mukhopadhyay *et al.*, 2004; Bower *et al.*, 2009; Richardson *et al.*, 2011). If a stronger transcription of SoxS serves a physiological role, maybe in counteracting the production of the highly cytotoxic peroxynitrite that can be formed in the presence of both NO and superoxide (Fukuto *et al.*, 2000), remains to be determined, since SoxRS target gene transcription was not enhanced in most cases as in our study.

On the contrary, there is some evidence for a protective function of copper homeostatic systems under nitrosative stress. In *S.* Typhimurium, the Cue system comprising the copper exporting ATPase CopA and the multicopper oxidase CueO (also known as CuiD), protect the cytoplasm and periplasm from copper induced damage, respectively, and are necessary for copper tolerance both under aerobic and anaerobic conditions (Espariz *et al.*, 2007). Excess copper is poisonous to the cell, since it damages dehydratases containing Fe-S clusters by displacement of the iron atoms (Macomber and Imlay, 2009). These shared targets of copper and NO might exacerbate the stress on the cells. Direct evidence in protection from nitrosative stress was provided by a *copA* deletion strain of *Neisseria gonorrhoeae*, which displayed increased sensitivity to nitrite and NO in the presence of copper (Djoko *et al.*, 2012). The authors argued, that copper ions which drive cycling between NO and *S*-nitrosothiols (Singh *et al.*, 1996) may potentiate RNS-mediated killing. Similarly, in *Helicobacter pylori*, the copper-ion responsive two-component regulation system CdrRS and the copper resistance determinant A encoded by *cdrA*, were found to function in the nitrosative stress response (Hung *et al.*, 2015). Concerning Enterobacteriaceae, elevated transcript levels of *copA* in response to nitrosative stress were observed in *E. coli* and *S.* Typhimurium in previous studies, especially under conditions of low O_2 (Pullan *et al.*,

2007; Richardson *et al.*, 2011). In EHEC, *copA* mRNA levels were 4-fold increased following a 1 h exposure to acidified $NaNO_2$ in LB, a trend, however, not observed for *S.* Typhimurium in LB broth. Investigation of *S.* Typhimurium and EHEC *copA* deletion strains might provide additional information on a putative protective role of copper resistance under acidified $NaNO_2$ stress in Enterobacteriaceae.

Among the stronger transcribed genes in the presence of 150 mg/l $NaNO_2$ are several genes involved in acquisition of ferric iron. Higher transcription levels of iron-uptake systems were also observed under acidified $NaNO_2$ adaptation in LB broth and in NO-exposed *S.* Typhimurium cells in BHI (Richardson *et al.*, 2011). Inactivation of the Fe-Fur regulator by nitrosylation, resulting in derepression of target genes (D'Autreaux *et al.*, 2002), might constitute a mechanism to provide the cell with necessary iron for the repair of RNS-damaged Fe-S clusters especially when iron levels are low.

The cytoplasmic pathway for nitrate and nitrite reduction comprising Nar and Nir and the nitrate/nitrite antiporter NarK as well as the formate-hydrogenlyase complex (FHL) had lower transcript levels in the presence of nitrite. Why the reason for the former is unclear, the observed regulation of the latter might be explained by a metabolic shift between the two cultures caused by the presence of nitrite. In the absence of nitrite, glucose is metabolized via the mixed-acid fermentation pathway, resulting in the excretion of formate, which is then reimported into the cell and disproportionated into CO_2 and H_2 by FHL (Leonhartsberger *et al.*, 2002). If nitrite is available, it serves as electron acceptor of an anaerobic energy-conserving respiratory chain with the periplasmic cytochrome *c* nitrite reductase NrfA at its end, that reduces nitrite to ammonium by transferring electrons donated by formate, that is oxidized via formate dehydrogenase (reviewed by Simon, 2002). This reaction might remove formate, an obligatory signal for induction of FHL expression (Rossmann *et al.*, 1991). A different mechanism might explain the lower transcription of members of the citrate utilization operon, *cit*. Citric acid was proposed to be involved in acid resistance of *Salmonella* (Foster and Hall, 1991; Foster and Spector, 1995), and indeed, *cit* transcript levels were found to be reduced in response to acid stress in *S.* Enteritidis Nal^R and *S.* Kentucky (Joerger *et al.*, 2012). Reasoning that nitrous acid arising from acidified nitrite might cause additional acid stress, as indicated by intracellular pH measurements (see Figure 15), conservation of citrate in the cell by reducing its utilization via the *cit* operon encoded pathway might be protective.

While 150 mg/l $NaNO_2$ in RD0 induced some adaptive response in *S.* Typhimurium, 30 mg/l $NaNO_2$ in RD3 failed to do so. However, although only residual amounts of nitrite *per se* are detected in cured meats and raw sausage products (Honikel, 2008; Kabisch, 2014), it cannot be excluded that meat proteins modified by nitrite and its derivatives serve as a reservoir for NO and nitrosating agents (Skibsted, 2011) that further inhibit bacterial growth. The *in vitro* experimental design addressed the impact of residual nitrite and does not support conclusions on the possible contribution of NO-modified meat compounds to the antibacterial action in meat products.

3.2 Transcriptional response of *S.* Typhimurium to conditions on RD3 – partial overlap with that of nitrite on RD0 among massive changes

As of RD3, however, additional hurdles such as a more acidic pH and lowered a_w become more prominent. Comparing the transcriptomes of RD0 and RD3 revealed massive changes.

Interestingly, expression of some genes was affected similarly by $NaNO_2$ on RD0 and stress conditions on RD3. As such, metabolic genes involved in the cytoplasmic nitrate/nitrite reduction pathway (*narG*, *nirB*), the formate-hydrogen-lyase complex (*fdhF*, *hycC*) and citrate utilization (*cit* operon) displayed lower transcript levels. Similarly, mRNA levels of *fis* and *nrdD*, which are involved in the transcriptional regulation and provision of DNA building blocks, respectively, were decreased both by $NaNO_2$ on RD0 and on RD3 compared to RD0. This points to some overlap between the responses to nitrite-derived stress on RD0 and lower pH/higher salt stress on RD3.

Lower transcript levels of genes involved in translation and DNA synthesis indicate that RD3 conditions are unfavourable for growth compared to RD0. Some changes might reflect a response to the increased acid stress (pH 5.2 vs 5.8) by the higher amount of lactic acid on RD3. The arginine decarboxylase system, which is induced during acid adaptation at moderate acidic pH (~5.0), mediates survival of *S.* Typhimurium at pH levels as low as pH 2.3 under anaerobic conditions (Kieboom and Abee, 2006; Alvarez-Ordóñez *et al.*, 2010; Viala *et al.*, 2011). The Hya hydrogenase was found to recycle H_2 during anaerobic fermentative growth, and also to contribute to acid resistance (Zbell *et al.*, 2008; Zbell and Maier, 2009). The L-lactate utilization operon might also be induced by the higher amount of lactic acid. In addition, differential regulation of genes involved in energy metabolism was observed under the ATR in *S.* Typhimurium, involving donw-regulation of the *narGHIJ* and up-regulation of several TCA cycle genes (Ryan *et al.*, 2015). Some transcriptional changes on RD3 vs RD0 are consistent with relief from glucose-mediated catabolite repression on RD3, such as those of PFL, which supplies the citric acid cycle with acetyl-CoA formed via the conversion of pyruvate to formate under anaerobic fermentative growth conditions (Wong *et al.*, 1989), and of the thiosulfate reductase encoded by the *phs* operon (Clark and Barrett, 1987).

Stress-associated systems up-regulated on RD3 are notably the phage shock protein Psp system and several paralogs of the USP family. The Psp systems is an extracytoplasmic stress response system that helps cells to manage insults of cell membrane function, such as dissipation of the proton motive force (Joly *et al.*, 2010). *Psp*-inducing conditions identified in *S.* Typhimurium include stationary growth phase in a *rpoE* background, ionophores and protonophores, mutations in F_1F_0 ATPase and macrophage infection (summarized by Joly *et al.*, 2010). In *E. coli*, the *psp* system was proposed to play a role in stationary phase survival under nutrient- or energy-limited conditions (Weiner and Model, 1994). Similarly, energy limitation due to the lack of glucose in combination with acid and salt stress might be responsible for the observed induction in *S.* Typhimurium. The USPs are induced under different environmental stress conditions that confer growth inhibition, including DNA damage and starvation of

glucose and phosphate, and are crucial for survival and recovery of prolonged periods of growth arrest under stress conditions (Siegele, 2005). It is supposed that they have partially overlapping but distinct biological functions (Nachin *et al.*, 2005). The structure and function of YdaA (UspE) and YnaF (UspF), transcription of which was induced under RD3 conditions, were recently characterized in *S.* Typhimurium, and suggested a role of YdaA in lipid A metabolism and for YnaF in regulation of chloride ion concentration (Bangera *et al.*, 2015). Hence, up-regulation of *ynaF* might correlate with the higher salt concentration added under RD3 conditions. *YecG* (*uspC*) and *ydaA* were found to be induced upon growth arrest in *E. coli*, and induction was mediated by the stringent response alarmone ppGpp (Gustavsson *et al.*, 2002). Accordingly, the transcriptomic data support a transition of *S.* Typhimurium to a growth arrested state under RD3 conditions, consistent with the data in short-ripened sausages (see Figure 5).

4 The acidifed $NaNO_2$ stress response of EHEC – common features and differences in relation to *S.* Typhimurium

One aim of this study was to shed light on the differential impact of nitrite on *S.* Typhimurium and EHEC in short-ripened spreadable sausages (Kabisch, 2014). Whereas 150 mg/l $NaNO_2$ prevented the initial multiplication of *S.* Typhimurium, it did not influence kinetics of EHEC. However, EHEC did not grow whatsoever in short-ripened spreadable sausages irrespective of the addition of $NaNO_2$.

Regarding the transcriptional response in LB pH 5.5, less genes were affected by a 10 min acidified $NaNO_2$ shock in EHEC compared to *S.* Typhimurium (47 vs 301 genes). Common to both bacteria is the strong induction of members of the NO-responsive NsrR and NorR regulons, including the NO-detoxifying flavohemoglobin HmpA and flavorubredoxin NorV. Given the fact, that the truncated NorVs protein of EHEC strain EDL933 is not functional (Shimizu *et al.*, 2012), up-regulation of the *norVsW* genes is not expected to be of physiological significance. Transcriptional induction of NsrR and NorR target genes is consistent with other transcriptome studies of *S.* Typhimurium, *E. coli* and UPEC in response to NO, GNSO and/or acidified nitrite (Bourret *et al.*, 2008; Mukhopadhyay *et al.*, 2004; Justino *et al.*, 2005; Pullan *et al.*, 2007; Bower *et al.*, 2009), underlining the importance of the regulon members in mediating a directed protective response to NO stress. Some common trends are observed between the acidified $NaNO_2$ shock response of *S.* Typhimurium and the 1 h response of EHEC. As such, *nrdH*, *qor*, *sufA* and members of the universal stress protein (USP) family, *yhiO* (*uspB*), *ybdQ* (*uspG*) and *yecG* (*uspC*), had higher transcript levels in nitrite-treated cultures. In contrast, flagellar genes, the translational machinery and genes involved in the synthesis of nucleotides are down-regulated in response to a 10 min acidified $NaNO_2$ shock in *S.* Typhimurium and to a 1 h exposure in EHEC. This transcription pattern combines those of the stringent stress response induced by nutrient-limitation (Durfee *et al.*, 2008; Traxler *et al.*, 2008) and the general stress response mediated by RpoS (Dong and Schellhorn, 2009; Patten *et al.*, 2004), both of which are initiated upon growth arrest of cells (Chang *et al.*, 2002). From this it can be concluded, that the transient growth arrest caused by massive acidified

$NaNO_2$ stress elicits stringent control of high-energy cellular processes such as ribosome biosynthesis and motility and regulation of stress-related genes in both *S.* Typhimurium and EHEC. This is in agreement with an earlier study of the response of *S.* Typhimurium to NO stress under extremely acidic conditions (Bourret *et al.*, 2008). The Gram-positive bacterium *Listeria monocytogenes*, which lacks NO-detoxifying enzymes, was also found to mount a general stress response under severe acidified $NaNO_2$ stress (Müller-Herbst *et al.*, 2016). However, it is important to keep in mind that these changes are observed more quickly upon $NaNO_2$ addition in *S.* Typhimurium compared to EHEC, and seem to be reversed at the adaptive response of *S.* Typhimurium. If this might be due to the non-functional NorVs and concomitantly higher levels of NO and derived RNS in EHEC, is not known. However, in contrast to the NO detoxification machinery, this general stress response seems to be of a transient nature in *S.* Typhimurium to enable cells to survive harsh NO or RNS shock and is reversed once the stress level is reduced.

Addition of $NaNO_2$ to EHEC cultures grown under acidic conditions, also triggers acid protective systems, although different ones compared to *S.* Typhimurium. The genes *gadA* and *gadB* encoding the two isoforms of glutamate decarboxylase, which converts glutamate to γ-aminobutyrate thereby consuming one intracellular proton, were found to be up-regulated. This decarboxylase system is missing from *S.* Typhimurium (Zhao and Houry, 2010). In addition, *gadX*, coding for a positive regulator of the Gad system (Tramonti *et al.*, 2002), displayed elevated transcript levels. Interestingly, induction of *gadX* by NO has been observed in EHEC before (Branchu *et al.*, 2014) and the identification of a NsrR binding site in UPEC (Spiro *et al.*, 2015) might suggest a direct regulation via NsrR also in EHEC.

A striking difference in the transcriptional profiles is the higher transcription of genes that have been associated with biofilm growth in the presence of acidified $NaNO_2$ in EHEC vs *S.* Typhimurium, with many of them being among those genes with the greatest fold-changes. Twelve genes that were found to be up-regulated during biofilm growth of asymptomatic bacteriuria *E. coli* strains, also displayed elevated transcript levels after a 10 min and/or 1 h exposure of EHEC to acidified $NaNO_2$ (*ybiJ*, *ycfR* (*bhsA*), *yhcN*, *ibpA*, *ibpB*, *asnA*, *yhaK*, *glgS*, *grxA*, *yhhW*, *pdhR*, *yfiD*) (Hancock and Klemm, 2007; Hancock *et al.*, 2010). In addition, *tnaA*, encoding tryptophanase, and *yjfO* (*bsmA*), which influence biofilm formation in *E. coli* (Di Martino *et al.*, 2002; Weber *et al.*, 2010), were also found to be up-regulated in EHEC after 1 h treatment with acidified $NaNO_2$. Stressful conditions have been shown to induce biofilm growth of bacteria, and biofilms in turn render bacteria more resistant to various stresses (Landini, 2009). From this it could be speculated that biofilm formation might be a strategy employed by EHEC to withstand growth-arresting acidified $NaNO_2$ stress. Given the fact, that NO has been described as a potent mediator of biofilm dispersal of several bacteria including EHEC (Marvasi *et al.*, 2014; Barraud *et al.*, 2006), this hypothesis clearly awaits further investigation.

Among those genes up-regulated both in biofilms and in response to acidified nitrite stress by EHEC, there are several members of the YhcN/DUF1471 family, which comprises a conserved group of low-molecular-weight proteins in Enterobacteriaceae (Rudd *et al.*, 1998). Strikingly, *ybiJ*, *ycfR* and *yhcN*,

which displayed increased mRNA levels in EHEC exposed to acidified $NaNO_2$, were previously observed among the strongest up-regulated genes in two studies investigating the NO stress response of *S.* Typhimurium in brain-heart-infusion medium and EG medium pH 4.4 (Richardson *et al.*, 2011; Bourret *et al.*, 2008), but the authors did not elaborate on this since it was not in the focus of their studies. On the contrary, these genes were not found to be differentially regulated in response to acidified $NaNO_2$ in *S.* Typhimurium in this study and in UPEC (Bower *et al.*, 2009), which could be due to the choice of growth medium (BHI/EG medium vs LB) or the level of nitrosative stress (NO derived from NO donor Spermine/NONOate vs acidified $NaNO_2$ for different time intervals). Interestingly, YhcN family homologues of *Yersinia pestis* were found to be induced by mildly acidic pH, and contributed to acid resistance and biofilm formation *in vitro* (Vadyvaloo *et al.*, 2015). Members of this family function not only in biofilm formation but were found to transcriptionally respond to and protect against multiple stresses, including cytoplasmic acidification, acid, hydrogen peroxide, and heat treatment (Weber *et al.*, 2010; Lee *et al.*, 2010; Kannan *et al.*, 2008). YbiJ, YhcN and YcfR therefore constitute promising candidates that deserve further investigation regarding their putative role in resistance to acidified $NaNO_2$ stress, especially in the context of raw sausage ripening.

The transcriptome of the culture initially intended to serve as reference culture for the adaptive response of EHEC (harvested at $OD_{600} = 1.5$) turned out to be unsuitable. Since anaerobic pathways were primarily found to be higher transcribed, this points to O_2 shortage at $OD_{600} = 1.5$ with concomitant activation of these pathways by FNR (Spiro and Guest, 1990). A comparable expression profile was found in EHEC between 3 and 4 h of growth in glucose minimal medium, which correlated with a strong reduction in dissolved O_2 in the medium (Bergholz *et al.*, 2007). Hence, it is important to keep in mind that a well-conceived experimental setup is crucial to avoid such undesired effects.

Considering a putative contribution of NO-detoxifying systems in the context of raw sausages, analogous results to those of *S.* Typhimurium were obtained. Transcription of *hmpA* increased upon nitrite treatment and HmpA protected EHEC from acidified $NaNO_2$-dependent growth inhibition *in vitro*, but was dispensable in $NaNO_2$-cured short-ripened spreadable sausages. Lack of NrfA did not alter *in vitro* growth and *in situ* survival of EHEC. This supports the notion of other mechanisms to cope with nitrite stress in raw sausage products.

5 Plant extracts with antibacterial action as potential nitrite substitutes

Plant extracts constitute promising nitrite substitutes in natural curing, since they provide a nitrate reservoir that can be converted to nitrite by suitable nitrate-reducing starter cultures (Sebranek and Bacus, 2007a). In addition, plant extracts contain bioactive phytochemicals that might exert antimicrobial properties (Cowan, 1999), thereby allowing reduction of added nitrate or nitrite to levels sufficient to just obtain the desired chemical properties such as color and flavor (Sebranek and Bacus, 2007b).

In vitro growth assays performed here-in along with assessment of the visual and sensory properties of prototype sausages (performed by cooperation partners from the MRI Kulmbach), argued for the celery extract as suitable candidate. Addition of celery extract resulted in a measurable lower optical culture density of both *S.* Typhimurium and EHEC *in vitro* (see Figure 24 and Figure 25) and resulted in a faster cfu reduction of *S.* Typhimurium in celery-produced salami-type sausages compared to nitrate-cured ones (Rohtraud Pichner, personal communication), pointing to an antibacterial compound in the extract. RNA-seq data revealed that genes encoding the membrane-bound NarGHJI nitrate reductase and the nitrate/nitrite antiporter NarK were activated both by nitrate and celery extract, indicating that celery is indeed a source of nitrate that is subsequently reduced to nitrite, which is then exported in exchange for new nitrate. Since NarGHJI is the main producer of endogenous NO in *S.* Typhimurium (Gilberthorpe and Poole, 2008; Rowley *et al.*, 2012), transcriptional up-regulation of the main anaerobic NO detoxification system, NorVW (Mills *et al.*, 2008), and the YtfE protein for repair of NO-modified Fe-S clusters is consequential. A comparable transcription pattern for *narGHJI*, *narK* and *norV* was reported under nitrate-rich conditions in minimal medium with glycerol (Rowley *et al.*, 2012).

Although the *in vitro* Bioscreen growth assays and *in situ* challenge assays both supported a nitrate-independent, antibacterial effect of celery extract, the RNA-seq data of nitrate- and celery-cultivated *S.* Typhimurium contradict this idea. Only one gene, *uhpT*, displayed higher transcript levels in response to celery vs nitrate. UhpT encodes a P_i-linked hexose phosphate antiport carrier, which is controlled by external glucose 6-phosphate via the UhpABC regulatory system (Sonna *et al.*, 1988; Island *et al.*, 1992; Verhamme *et al.*, 2002). Reasoning that phytochemicals profoundly impact bacterial physiology, e.g. by disrupting cell membrane integrity (Negi, 2012), and that, as a consequence, the antibacterial action of bioactive compounds should be deducible from the transcriptional response (Rosamond and Allsop, 2000; Hutter *et al.*, 2004), there must be other reasons for the observed effects of celery extract on growth of *S.* Typhimurium and EHEC *in vitro* and *in situ*. While the different experimental set-up relating to the culture volume and O_2 availability between the growth assays in the Bioscreen and the RNA-seq cultures might provide an explanation for the discrepancy observed *in vitro*, the different amount of nitrate provided as KNO_3 (150 mg/kg) or via the celery extract (70 mg/kg) (Rohtraud Pichner, personal communication) could account for the observed faster reduction of *Salmonella* in celery- compared to nitrate-produced sausages. Higher concentrations of nitrate might favour growth of nitrate-reducing staphylococci over lactic acid bacteria, resulting in less production of lactic acid, as indicated by the higher pH measured in nitrate-cured sausages (Rohtraud Pichner, personal communication). Moreover, nitrate and nitrite reducing capacities under certain conditions have also been reported for meat-borne lactic acid bacteria (Hammes *et al.*, 1990; Brooijmans *et al.*, 2009). The higher nitrate content might fuel nitrate and/or nitrite respiratory metabolism, resulting in less acid production and a different pH profile compared to strict fermentative growth. The higher pH might in turn favor survival of *Salmonella*. Challenge experiments using the same ingoing amount of nitrate provided via authentic nitrate or celery extract could shed light on this issue.

6 Conclusion and data transfer to raw sausage products

Single well-characterized NO-detoxifying systems HmpA, NorV, and NrfA are subordinate in the response of *S.* Typhimurium and EHEC to the curing agent $NaNO_2$ in short-ripened spreadable sausages. The lysine decarboxylase CadA was found to protect against acidified $NaNO_2$ stress in *S.* Typhimurium *in vitro*, and cytoplasmic pH measuremements support intracellular acidification, presumably via HNO_2, as a possible additional mode of the antibacterial action. This goes in hand with the transcriptional up-regulation of systems associated with the acid response, including different amino acid decarboxylases in both *S.* Typhimurium and EHEC and members of the YhcN family in EHEC. This induction of acid stress systems is especially interesting with respect to the raw sausage product, since it could render cells more resistant to subsequent acid stress (Foster and Hall, 1991), which is an important hurdle during later stages of ripening (Leistner and Gorris, 1995). In addition, insertion mutant analysis and transcriptome data hint to some link of proper phosphate management, copper tolerance and biofilm formation with the acidified $NaNO_2$ tolerance of *S.* Typhimurium and EHEC, respectively. Whereas the *S.* Typhimurium transcriptomic data in LB pH 5.5 and the RD0 and RD3 meat extract broths fit well to the observation of the challenge assays, the EHEC *in vitro* growth and transcriptome data seem to contrast the *in situ* data, where no effect on survival of EHEC is observed (see Figure 23). EHEC even mount a stronger and sustained general stress response to acidified $NaNO_2$ compared to *S.* Typhimurium, and even need more time to resume growth. However, it should be kept in mind that the general stress response is induced by different kinds of stress, including starvation and acid stress, and results in cross-protection against a wide range of stressful treatments (Battesti *et al.*, 2011). EHEC do not grow in short-ripened spreadable sausages even in absence of $NaNO_2$, which indicates adverse conditions that might evoke the general stress response for survival. This is also consistent with the transcriptome data of *S.* Typhimurium under RD0 and RD3 conditions, with stress genes known to be associated with growth-arrested cells being more strongly transcribed. Given the fact that acidified $NaNO_2$ targets cellular processes of actively growing cells (respiration, replication, Fe-S clusters of metabolic enzymes) (see I3), and that slowly growing cells such as those in stationary phase have been shown to be resistant to diverse stresses (Rees *et al.*, 1995; Dodd and Aldsworth, 2002), the initial conditions might induce cross-protection also against $NaNO_2$ in EHEC. This might provide an explanation for the differential impact of $NaNO_2$ on *S.* Typhimurium and EHEC in short-ripened spreadable sausages.

In conclusion, this study provided some novel aspects in the response of *S.* Typhimurium and EHEC to the curing agent nitrite and its antimicrobial action under food-related aspects. The observation that a lower nitrate level at an acidic pH is more efficient in reducing *Salmonella* than a twice-as high nitrate concentration at a less acidic pH, sustains the importance of a well-considered and empirically tested combination of different hurdles for the microbiological safety of raw sausages. Moreover, the results from this study indicate that several different systems are involved in the nitrite stress response of these Gram-negative bacteria. The discrepancy between the *in vitro* and *in situ* data from the Δ*hmpA* mutant

suggest that the plethora of systems might be able to compensate loss of each other in the product and effectively combat the nitrite-derived stress. This additionally highlights the necessity to combine different kinds of hurdles in the production process.

The complexity of nitrite chemistry in meat and its diverse interactions with meat components and additives cannot be adequately mimicked *in vitro*. That *in situ* studies are feasible was recently demonstrated by Vermassen *et al.* (2014), who analyzed the transcriptome and nitrosative stress response of the starter culture *Staphylococcus xylosus*. Future work should aim at investigating also food-borne pathogenic bacteria directly in the product.

References

Abnet, C. C. (2007). Carcinogenic food contaminants. *Cancer Invest*. 25(3): 189–196.

Almeida, C. C., Romão, C. V., Lindley, P. F., Teixeira, M., and Saraiva, L. M. (2006). The role of the hybrid cluster protein in oxidative stress defense. *J. Biol. Chem*. **281**(43): 32445–32450.

Alvarez-Ordóñez, A., Fernández, A., Bernardo, A., and López, M. (2010). Arginine and lysine decarboxylases and the acid tolerance response of *Salmonella* Typhimurium. *Int. J. Food Microbiol.* **136**(3): 278–282.

Arkenberg, A., Runkel, S., Richardson, D. J., and Rowley, G. (2011). The production and detoxification of a potent cytotoxin, nitric oxide, by pathogenic enteric bacteria. *Biochem. Soc. Trans*. **39**(6): 1876–1879.

Baer, A. A., Miller, M. J., and Dilger, A. C. (2013). Pathogens of Interest to the Pork Industry: A Review of Research on Interventions to Assure Food Safety. *Comprehensive Reviews in Food Science and Food Safety*. **12**(2): 183–217.

Bang, I.-S., Liu, L., Vazquez-Torres, A., Crouch, M.-L., Stamler, J. S., and Fang, F. C. (2006). Maintenance of nitric oxide and redox homeostasis by the *salmonella* flavohemoglobin hmp. *J. Biol. Chem.* **281**(38): 28039–28047.

Bangera, M., Panigrahi, R., Sagurthi, S. R., Savithri, H. S., and Murthy, M. R. N. (2015). Structural and functional analysis of two universal stress proteins YdaA and YnaF from *Salmonella typhimurium*: possible roles in microbial stress tolerance. *Journal of structural biology*. **189**(3): 238–250.

Barraud, N., Hassett, D. J., Hwang, S.-H., Rice, S. A., Kjelleberg, S., and Webb, J. S. (2006). Involvement of nitric oxide in biofilm dispersal of *Pseudomonas aeruginosa*. *Journal of Bacteriology*. **188**(21): 7344–7353.

Battesti, A., Majdalani, N., and Gottesman, S. (2011). The RpoS-mediated general stress response in *Escherichia coli*. *Annual review of microbiology*. **65**: 189–213.

Benjamin, N., O'Driscoll, F., Dougall, H., Duncan, C., Smith, L., Golden, M., and McKenzie, H. (1994). Stomach NO synthesis. *Nature*. **368**(6471): 502.

Benjamini, Y., and Hochberg, Y. (1995). Controlling the False Discovery Rate: A Practical and Powerful Approach to Multiple Testing. *Journal of the Royal Statistical Society. Series B (Methodological)*. **57**(1): 289–300.

Bergan, J., Dyve Lingelem, A. B., Simm, R., Skotland, T., and Sandvig, K. (2012). Shiga toxins. *Toxicon : official journal of the International Society on Toxinology*. **60**(6): 1085–1107.

Bergholz, T. M., Wick, L. M., Qi, W., Riordan, J. T., Ouellette, L. M., and Whittam, T. S. (2007). Global transcriptional response of *Escherichia coli* O157:H7 to growth transitions in glucose minimal medium. *BMC microbiology*. **7**: 97.

Beutin, L., Miko, A., Krause, G., Pries, K., Haby, S., Steege, K., and Albrecht, N. (2007). Identification of human-pathogenic strains of Shiga toxin-producing *Escherichia coli* from food by a combination of serotyping and molecular typing of Shiga toxin genes. *Appl Environ Microbiol*. **73**(15): 4769–4775.

Birzele, B., Djordjević, S., and Krämer, J. (2005). A study of the role of different nitrite concentrations on human pathogenic bacteria in fresh spreadable ham and onion sausage. *Food Control*. **16**(8): 695–699.

Bjarnason, J., Southward, C. M., and Surette, M. G. (2003). Genomic profiling of iron-responsive genes in *Salmonella enterica* serovar typhimurium by high-throughput screening of a random promoter library. *J. Bacteriol.* **185**(16): 4973–4982.

Blanco, M., Blanco, J. E., Mora, A., Dahbi, G., Alonso, M. P., Gonzalez, E. A., Bernardez, M. I., and Blanco, J. (2004). Serotypes, Virulence Genes, and Intimin Types of Shiga Toxin (Verotoxin)-Producing *Escherichia coli* Isolates from Cattle in Spain and Identification of a New Intimin Variant Gene (eae-). *Journal of Clinical Microbiology*. **42**(2): 645–651.

Blankenberg, D., Kuster, G. von, Coraor, N., Ananda, G., Lazarus, R., Mangan, M., Nekrutenko, A., and Taylor, J. (2010). Galaxy: a web-based genome analysis tool for experimentalists. *Curr Protoc Mol Biol*. **19**: Unit 19.10.1–21.

Bodenmiller, D. M., and Spiro, S. (2006). The *yjeB* (*nsrR*) gene of *Escherichia coli* encodes a nitric oxide-sensitive transcriptional regulator. *J. Bacteriol.* **188**(3): 874–881.

Boerlin, P., McEwen, S. A., Boerlin-Petzold, F., Wilson, J. B., Johnson, R. P., and Gyles, C. L. (1999). Associations between virulence factors of Shiga toxin-producing *Escherichia coli* and disease in humans. *Journal of Clinical Microbiology*. **37**(3): 497–503.

Bolivar, F., Rodriguez, R. L., Greene, P. J., Betlach, M. C., Heyneker, H. L., Boyer, H. W., Crosa, J. H., and Falkow, S. (1977). Construction and characterization of new cloning vehicles. II. A multipurpose cloning system. *Gene*. **2**(2): 95–113.

Bonamore, A., and Boffi, A. (2008). Flavohemoglobin: structure and reactivity. *IUBMB Life*. **60**(1): 19–28.

Borisov, V. B., Forte, E., Konstantinov, A. A., Poole, R. K., Sarti, P., and Giuffre, A. (2004). Interaction of the bacterial terminal oxidase cytochrome *bd* with nitric oxide. *FEBS Lett*. **576**(1-2): 201–204.

Borisov, V. B., Forte, E., Siletsky, S. A., Sarti, P., and Giuffrè, A. (2015). Cytochrome *bd* from *Escherichia coli* catalyzes peroxynitrite decomposition. *Biochimica et biophysica acta*. **1847**(2): 182–188.

Bourret, T. J., Porwollik, S., McClelland, M., Zhao, R., Greco, T., Ischiropoulos, H., Vázquez-Torres, A., and Aballay, A. (2008). Nitric Oxide Antagonizes the Acid Tolerance Response that Protects *Salmonella* against Innate Gastric Defenses. *PLoS ONE*. **3**(3): e1833.

Bower, J. M., Gordon-Raagas, H. B., and Mulvey, M. A. (2009). Conditioning of uropathogenic *Escherichia coli* for enhanced colonization of host. *Infect. Immun.* **77**(5): 2104–2112.

Bower, J. M., and Mulvey, M. A. (2006). Polyamine-mediated resistance of uropathogenic *Escherichia coli* to nitrosative stress. *J. Bacteriol.* **188**(3): 928–933.

Branchu, P., Matrat, S., Vareille, M., Garrivier, A., Durand, A., Crépin, S., Harel, J., Jubelin, G., and Gobert, A. P. (2014). NsrR, GadE, and GadX interplay in repressing expression of the *Escherichia coli* O157:H7 LEE pathogenicity island in response to nitric oxide. *PLoS Pathog.* **10**(1): e1003874.

Brooijmans, R. J. W., Vos, W. M. de, and Hugenholtz, J. (2009). *Lactobacillus plantarum* WCFS1 electron transport chains. *Applied and Environmental Microbiology*. **75**(11): 3580–3585.

Browning, D. F., Lee, D. J., Spiro, S., and Busby, S. J. W. (2010). Down-regulation of the *Escherichia coli* K-12 *nrf* promoter by binding of the NsrR nitric oxide-sensing transcription repressor to an upstream site. *Journal of Bacteriology*. **192**(14): 3824–3828.

Bryan, N. S., Alexander, D. D., Coughlin, J. R., Milkowski, A. L., and Boffetta, P. (2012). Ingested nitrate and nitrite and stomach cancer risk: An updated review. *Food and Chemical Toxicology*. **50**(10): 3646–3665.

Burney, S., Caulfield, J. L., Niles, J. C., Wishnok, J. S., and Tannenbaum, S. R. (1999). The chemistry of DNA damage from nitric oxide and peroxynitrite. *Mutation research*. **424**(1-2): 37–49.

Burton, N. A., Schürmann, N., Casse, O., Steeb, A. K., Claudi, B., Zankl, J., Schmidt, A., and Bumann, D. (2014). Disparate Impact of Oxidative Host Defenses Determines the Fate of *Salmonella* during Systemic Infection in Mice. *Cell Host & Microbe*. **15**(1): 72–83.

Bustin, S. A. (2000). Absolute quantification of mRNA using real-time reverse transcription polymerase chain reaction assays. *J. Mol. Endocrinol.* **25**(2): 169–193.

Calhoun, L. N., and Kwon, Y. M. (2011). The ferritin-like protein Dps protects *Salmonella enterica* serotype Enteritidis from the Fenton-mediated killing mechanism of bactericidal antibiotics. *Int. J. Antimicrob. Agents*. **37**(3): 261–265.

Callaway, T. R., Edrington, T. S., Anderson, R. C., Byrd, J. A., and Nisbet, D. J. (2008). Gastrointestinal microbial ecology and the safety of our food supply as related to *Salmonella*. *J. Anim. Sci*. **86**(14 Suppl): E163-72.

Cammack, R., Joannou, C. L., Cui, X. Y., Torres, M. C., Maraj, S. R., and Hughes, M. N. (1999). Nitrite and nitrosyl compounds in food preservation. *Biochim Biophys Acta*. **1411**(2-3): 475–488.

Carter, M. Q., Louie, J. W., Fagerquist, C. K., Sultan, O., Miller, W. G., and Mandrell, R. E. (2012). Evolutionary silence of the acid chaperone protein HdeB in enterohemorrhagic *Escherichia coli* O157:H7. *Applied and Environmental Microbiology*. **78**(4): 1004–1014.

Carver, T., Harris, S. R., Berriman, M., Parkhill, J., and McQuillan, J. A. (2012). Artemis: an integrated platform for visualization and analysis of high-throughput sequence-based experimental data. *Bioinformatics*. **28**(4): 464–469.

CDC (1995). *Escherichia coli* O157:H7 outbreak linked to commercially distributed dry-cured salami--Washington and California, 1994. *MMWR Morb Mortal Wkly Rep*. **44**(9): 157–160.

Chakravortty, D., and Hensel, M. (2003). Inducible nitric oxide synthase and control of intracellular bacterial pathogens. *Microbes Infect*. **5**(7): 621–627.

Chan, R. K., Botstein, D., Watanabe, T., and Ogata, Y. (1972). Specialized transduction of tetracycline resistance by phage P22 in *Salmonella typhimurium*. II. Properties of a high-frequency-transducing lysate. *Virology*. **50**(3): 883–898.

Chang, D.-E., Smalley, D. J., and Conway, T. (2002). Gene expression profiling of *Escherichia coli* growth transitions: an expanded stringent response model. *Molecular Microbiology*. **45**(2): 289–306.

Choi, Y., Choi, J., Groisman, E. A., Kang, D.-H., Shin, D., and Ryu, S. (2012). Expression of STM4467-encoded arginine deiminase controlled by the STM4463 regulator contributes to *Salmonella enterica* serovar Typhimurium virulence. *Infect. Immun.* **80**(12): 4291–4297.

Chung, H. J., Bang, W., and Drake, M. A. (2006). Stress Response of *Escherichia coli*. *Comp Rev Food Sci Food Safety*. **5**(3): 52–64.

Clark, M. A., and Barrett, E. L. (1987). The *phs* gene and hydrogen sulfide production by *Salmonella typhimurium*. *Journal of Bacteriology*. **169**(6): 2391–2397.

Coburn, B., Grassl, G. A., and Finlay, B. B. (2007). *Salmonella*, the host and disease: a brief review. *Immunology and cell biology*. **85**(2): 112–118.

Cole, J. (1996). Nitrate reduction to ammonia by enteric bacteria: redundancy, or a strategy for survival during oxygen starvation? *FEMS microbiology letters*. **136**(1): 1–11.

Cole, J. A. (2012). Legless pathogens: how bacterial physiology provides the key to understanding pathogenicity. *Microbiology (Reading, Engl.)*. **158**(Pt 6): 1402–1413.

Corker, H., and Poole, R. K. (2003). Nitric oxide formation by *Escherichia coli*. Dependence on nitrite reductase, the NO-sensing regulator Fnr, and flavohemoglobin Hmp. *J. Biol. Chem.* **278**(34): 31584–31592.

Cowan, M. M. (1999). Plant products as antimicrobial agents. *Clinical microbiology reviews*. **12**(4): 564–582.

Crack, J. C., Le Brun, N. E., Thomson, A. J., Green, J., and Jervis, A. J. (2008). Reactions of nitric oxide and oxygen with the regulator of fumarate and nitrate reduction, a global transcriptional regulator, during anaerobic growth of *Escherichia coli*. *Meth. Enzymol.* **437**: 191–209.

Crack, J. C., Munnoch, J., Dodd, E. L., Knowles, F., Al Bassam, M. M., Kamali, S., Holland, A. A., Cramer, S. P., Hamilton, C. J., Johnson, M. K., Thomson, A. J., Hutchings, M. I., and Le Brun, N. E. (2015). NsrR from *Streptomyces coelicolor* Is a Nitric Oxide-sensing [4Fe-4S] Cluster Protein with a Specialized Regulatory Function. *J. Biol. Chem.* **290**(20): 12689–12704.

Crack, J. C., Svistunenko, D. A., Munnoch, J., Thomson, A. J., Hutchings, M. I., and Le Brun, N. E. (2016). Differentiated, promoter-specific response of 4Fe-4S NsrR DNA-binding to reaction with nitric oxide. *The Journal of biological chemistry*.

Crawford, M. J., and Goldberg, D. E. (1998). Role for the *Salmonella* flavohemoglobin in protection from nitric oxide. *J Biol Chem*. **273**(20): 12543–12547.

Cruz-Ramos, H., Crack, J., Wu, G., Hughes, M. N., Scott, C., Thomson, A. J., Green, J., and Poole, R. K. (2002). NO sensing by FNR: regulation of the *Escherichia coli* NO-detoxifying flavohaemoglobin, Hmp. *EMBO J.* **21**(13): 3235–3244.

Dahl, J.-U., Koldewey, P., Salmon, L., Horowitz, S., Bardwell, J. C. A., and Jakob, U. (2015). HdeB functions as an acid-protective chaperone in bacteria. *The Journal of biological chemistry*. **290**(1): 65–75.

Darwin, A. J. (2005). The phage-shock-protein response. *Molecular Microbiology*. **57**(3): 621–628.

Datsenko, K. A., and Wanner, B. L. (2000). One-step inactivation of chromosomal genes in *Escherichia coli* K-12 using PCR products. *Proc. Natl. Acad. Sci. U.S.A.* **97**(12): 6640–6645.

D'Autreaux, B., Touati, D., Bersch, B., Latour, J.-M., and Michaud-Soret, I. (2002). Direct inhibition by nitric oxide of the transcriptional ferric uptake regulation protein via nitrosylation of the iron. *Proc. Natl. Acad. Sci. U.S.A.* **99**(26): 16619–16624.

D'Autréaux, B., Tucker, N. P., Dixon, R., and Spiro, S. (2005). A non-haem iron centre in the transcription factor NorR senses nitric oxide. *Nature*. **437**(7059): 769–772.

Delhalle, L., Saegerman, C., Farnir, F., Korsak, N., Maes, D., Messens, W., De, S. L., De, Z. L., and Daube, G. (2009). *Salmonella* surveillance and control at post-harvest in the Belgian pork meat chain. *Food Microbiol*. **26**(3): 265–271.

Denicola, A., Souza, J. M., Radi, R., and Lissi, E. (1996). Nitric oxide diffusion in membranes determined by fluorescence quenching. *Arch. Biochem. Biophys.* **328**(1): 208–212.

Di Martino, P., Merieau, A., Phillips, R., Orange, N., and Hulen, C. (2002). Isolation of an *Escherichia coli* strain mutant unable to form biofilm on polystyrene and to adhere to human pneumocyte cells: involvement of tryptophanase. *Canadian journal of microbiology*. **48**(2): 132–137.

Ding, H., and Demple, B. (2000). Direct nitric oxide signal transduction via nitrosylation of iron-sulfur centers in the SoxR transcription activator. *Proceedings of the National Academy of Sciences of the United States of America*. **97**(10): 5146–5150.

Djoko, K. Y., Franiek, J. A., Edwards, J. L., Falsetta, M. L., Kidd, S. P., Potter, A. J., Chen, N. H., Apicella, M. A., Jennings, M. P., and McEwan, A. G. (2012). Phenotypic characterization of a *copA* mutant of *Neisseria gonorrhoeae* identifies a link between copper and nitrosative stress. *Infection and Immunity*. **80**(3): 1065–1071.

Dodd, C. E. R., and Aldsworth, T. G. (2002). The importance of RpoS in the survival of bacteria through food processing. *International Journal of Food Microbiology*. **74**(3): 189–194.

Domka, J., Lee, J., and Wood, T. K. (2006). YliH (BssR) and YceP (BssS) regulate *Escherichia coli* K-12 biofilm formation by influencing cell signaling. *Appl Environ Microbiol*. **72**(4): 2449–2459.

Dong, T., and Schellhorn, H. E. (2009). Global effect of RpoS on gene expression in pathogenic *Escherichia coli* O157:H7 strain EDL933. *BMC Genomics*. **10**: 349.

Dourou, D., Porto-Fett, A. C., Shoyer, B., Call, J. E., Nychas, G. J., Illg, E. K., and Luchansky, J. B. (2009). Behavior of *Escherichia coli* O157:H7, *Listeria monocytogenes*, and *Salmonella* in teewurst, a raw spreadable sausage. *Int J Food Microbiol*. **130**(3): 245–250.

Duan, X., Yang, J., Ren, B., Tan, G., and Ding, H. (2009). Reactivity of nitric oxide with the [4Fe-4S] cluster of dihydroxyacid dehydratase from *Escherichia coli*. *The Biochemical journal*. **417**(3): 783–789.

Durfee, T., Hansen, A.-M., Zhi, H., Blattner, F. R., and Jin, D. J. (2008). Transcription profiling of the stringent response in *Escherichia coli*. *J. Bacteriol.* **190**(3): 1084–1096.

EFSA (European Food Safety Authority). European Centre for Disease Prevention and Control (2015). The European Union Summary Report on Trends and Sources of Zoonoses, Zoonotic Agents and Food-borne Outbreaks in 2014. *EFSA Journal*. **13**(12): 4329.

Eriksson, S., Lucchini, S., Thompson, A., Rhen, M., and Hinton, J. C. (2003). Unravelling the biology of macrophage infection by gene expression profiling of intracellular *Salmonella enterica*. *Mol Microbiol*. **47**(1): 103–118.

Escolar, L., Pérez-Martín, J., and Lorenzo, V. de (1999). Opening the iron box: transcriptional metalloregulation by the Fur protein. *J. Bacteriol.* **181**(20): 6223–6229.

Espariz, M., Checa, S. K., Audero, M. E., Pontel, L. B., and Soncini, F. C. (2007). Dissecting the *Salmonella* response to copper. *Microbiology (Reading, England)*. **153**(Pt 9): 2989–2997.

European Commission (2005). Commission Regulation (EC) No. 2073/2005 of 15 November 2005 on microbiological criteria for foodstuffs. *Official Journal of the European Union*. **L338**: 1–26.

European Parliament, C. o. t. E. U. (2006). Directive 2006/52/EC of the European Parliament and of the Council of 5 July 2006 amending Directive 95/2/EC on food additives other than colours and sweeteners and Directive 94/35/EC on sweeteners for use in foodstuffs. http://eur-lex.europa.eu/legal-content/EN/TXT/PDF/?uri=CELEX:32006L0052&rid=2.

Fabrega, A., and Vila, J. (2013). *Salmonella enterica* serovar Typhimurium skills to succeed in the host: virulence and regulation. *Clinical microbiology reviews*. **26**(2): 308–341.

Fang, F. C. (1997). Perspectives series: host/pathogen interactions. Mechanisms of nitric oxide-related antimicrobial activity. *J. Clin. Invest*. **99**(12): 2818–2825.

Fang, F. C. (2004). Antimicrobial reactive oxygen and nitrogen species: concepts and controversies. *Nat Rev Microbiol*. **2**(10): 820–832.

Federal Ministry of Food and Agriculture (2010). Deutsches Lebensmittelbuch. Leitsätze für Fleisch und Fleischerzeugnisse. http://www.bmelv.de/SharedDocs/Downloads/Ernaehrung/Lebensmittelbuch /LeitsaetzeFleisch.pdf?__blob=publicationFile.

Ferens, W. A., and Hovde, C. J. (2010). *Escherichia coli* O157:H7: Animal Reservoir and Sources of Human Infection. *Foodborne Pathog Dis*.

Filenko, N., Spiro, S., Browning, D. F., Squire, D., Overton, T. W., Cole, J., and Constantinidou, C. (2007). The NsrR regulon of *Escherichia coli* K-12 includes genes encoding the hybrid cluster protein and the periplasmic, respiratory nitrite reductase. *J Bacteriol*. **189**(12): 4410–4417.

Fink, R. C., Evans, M. R., Porwollik, S., Vazquez-Torres, A., Jones-Carson, J., Troxell, B., Libby, S. J., McClelland, M., and Hassan, H. M. (2007). FNR is a global regulator of virulence and anaerobic metabolism in *Salmonella enterica* serovar Typhimurium (ATCC 14028s). *J. Bacteriol.* **189**(6): 2262–2273.

Finlay, B. B., Ruschkowski, S., and Dedhar, S. (1991). Cytoskeletal rearrangements accompanying *Salmonella* entry into epithelial cells. *Journal of cell science*. **99 (Pt 2)**: 283–296.

Forrester, M. T., and Foster, M. W. (2012a). Protection from nitrosative stress. A central role for microbial flavohemoglobin. *Free Radical Biology and Medicine*. **52**(9): 1620–1633.

Forrester, M. T., and Foster, M. W. (2012b). Response to "Is flavohemoglobin a nitric oxide dioxygenase? ". *Free Radical Biology and Medicine*. **53**(5): 1211–1212.

Foster, J. W., and Hall, H. K. (1991). Inducible pH homeostasis and the acid tolerance response of *Salmonella typhimurium*. *Journal of Bacteriology*. **173**(16): 5129–5135.

Foster, J. W., and Spector, M. P. (1995). How *Salmonella* survive against the odds. *Annu Rev Microbiol*. **49**: 145–174.

Fratamico, P. M., Wang, S., Yan, X., Zhang, W., and Li, Y. (2011). Differential gene expression of *E. coli* O157:H7 in ground beef extract compared to tryptic soy broth. *J. Food Sci*. **76**(1): M79-87.

Fuchs, T. M., Klumpp, J., and Przybilla, K. (2006). Insertion-duplication mutagenesis of *Salmonella enterica* and related species using a novel thermosensitive vector. *Plasmid*. **55**(1): 39–49.

Fukuto, J. M., Cho, J. Y., and Switzer, C. H. (2000). The Chemical Properties of Nitric Oxide and Related Nitrogen Oxides. In: Nitric oxide. Biology and pathobiology. 1st ed., pp. 23–40. Ignarro, L. J., Ed., Academic Press, San Diego.

Gardner, A. M., and Gardner, P. R. (2002). Flavohemoglobin detoxifies nitric oxide in aerobic, but not anaerobic, *Escherichia coli*. Evidence for a novel inducible anaerobic nitric oxide-scavenging activity. *J. Biol. Chem.* **277**(10): 8166–8171.

Gardner, A. M., Gessner, C. R., and Gardner, P. R. (2003). Regulation of the nitric oxide reduction operon (*norRVW*) in Escherichia coli. Role of NorR and sigma54 in the nitric oxide stress response. *J. Biol. Chem.* **278**(12): 10081–10086.

Gardner, A. M., Helmick, R. A., and Gardner, P. R. (2002). Flavorubredoxin, an inducible catalyst for nitric oxide reduction and detoxification in *Escherichia coli*. *J. Biol. Chem*. **277**(10): 8172–8177.

Gardner, P. R., Costantino, G., Szabó, C., and Salzman, A. L. (1997). Nitric oxide sensitivity of the aconitases. *The Journal of biological chemistry*. **272**(40): 25071–25076.

Gardner, P. R., Gardner, A. M., Martin, L. A., and Salzman, A. L. (1998). Nitric oxide dioxygenase: an enzymic function for flavohemoglobin. *Proc. Natl. Acad. Sci. U.S.A.* **95**(18): 10378–10383.

Gentleman, R. C., Carey, V. J., Bates, D. M., Bolstad, B., Dettling, M., Dudoit, S., Ellis, B., Gautier, L., Ge, Y., Gentry, J., Hornik, K., Hothorn, T., Huber, W., Iacus, S., Irizarry, R., Leisch, F., Li, C., Maechler, M., Rossini, A. J., Sawitzki, G., Smith, C., Smyth, G., Tierney, L., Yang, J. Y. H., and Zhang, J. (2004). Bioconductor: open software development for computational biology and bioinformatics. *Genome Biol.* **5**(10): R80.

Gilberthorpe, N. J., Lee, M. E., Stevanin, T. M., Read, R. C., and Poole, R. K. (2007). NsrR: a key regulator circumventing *Salmonella enterica* serovar Typhimurium oxidative and nitrosative stress *in vitro* and in IFN-gamma-stimulated J774.2 macrophages. *Microbiology (Reading, Engl.)*. **153**(Pt 6): 1756–1771.

Gilberthorpe, N. J., and Poole, R. K. (2008). Nitric oxide homeostasis in *Salmonella typhimurium*: roles of respiratory nitrate reductase and flavohemoglobin. *J. Biol. Chem.* **283**(17): 11146–11154.

Glass, K. A., Loeffelholz, J. M., Ford, J. P., and Doyle, M. P. (1992). Fate of *Escherichia coli* O157:H7 as affected by pH or sodium chloride and in fermented, dry sausage. *Appl Environ Microbiol*. **58**(8): 2513–2516.

Goecks, J., Nekrutenko, A., Taylor, J., and Galaxy Team, T. (2010). Galaxy: a comprehensive approach for supporting accessible, reproducible, and transparent computational research in the life sciences. *Genome Biol*. **11**(8): R86.

Gomes, C. M., Giuffrè, A., Forte, E., Vicente, J. B., Saraiva, L. M., Brunori, M., and Teixeira, M. (2002). A novel type of nitric-oxide reductase. *Escherichia coli* flavorubredoxin. *J. Biol. Chem.* **277**(28): 25273–25276.

Gomes, C. M., Vicente, J. B., Wasserfallen, A., and Teixeira, M. (2000). Spectroscopic studies and characterization of a novel electron-transfer chain from *Escherichia coli* involving a flavorubredoxin and its flavoprotein reductase partner. *Biochemistry*. **39**(51): 16230–16237.

Gordon, M. A. (2008). *Salmonella* infections in immunocompromised adults. *The Journal of infection*. **56**(6): 413–422.

Gould, L. H., Demma, L., Jones, T. F., Hurd, S., Vugia, D. J., Smith, K., Shiferaw, B., Segler, S., Palmer, A., Zansky, S., and Griffin, P. M. (2009). Hemolytic Uremic Syndrome and Death in Persons with *Escherichia coli* O157. H7 Infection, Foodborne Diseases Active Surveillance Network Sites, 2000–2006. *CLIN INFECT DIS*. **49**(10): 1480–1485.

Groote, M. A. de, Testerman, T., Xu, Y., Stauffer, G., and Fang, F. C. (1996). Homocysteine antagonism of nitric oxide-related cytostasis in *Salmonella typhimurium*. *Science (New York, N.Y.)*. **272**(5260): 414–417.

Gu, M., and Imlay, J. A. (2011). The SoxRS response of *Escherichia coli* is directly activated by redox-cycling drugs rather than by superoxide. *Molecular Microbiology*. **79**(5): 1136–1150.

Gustavsson, N., Diez, A., and Nystrom, T. (2002). The universal stress protein paralogues of *Escherichia coli* are co-ordinately regulated and co-operate in the defence against DNA damage. *Mol Microbiol*. **43**(1): 107–117.

Haldane, J. (1901). The Red Colour of Salted Meat. *The Journal of hygiene*. **1**(1): 115–122.

Hammer, K. A., Carson, C. F., and Riley, T. V. (1999). Antimicrobial activity of essential oils and other plant extracts. *J Appl Microbiol*. **86**(6): 985–990.

Hammes, W. P., Bantleon, A., and Min, S. (1990). Lactic acid bacteria in meat fermentation. *FEMS microbiology letters*. **87**(1-2): 165–174.

Hanahan, D. (1983). Studies on transformation of *Escherichia coli* with plasmids. *J. Mol. Biol.* **166**(4): 557–580.

Hancock, V., and Klemm, P. (2007). Global gene expression profiling of asymptomatic bacteriuria *Escherichia coli* during biofilm growth in human urine. *Infection and Immunity*. **75**(2): 966–976.

Hancock, V., Vejborg, R. M., and Klemm, P. (2010). Functional genomics of probiotic *Escherichia coli* Nissle 1917 and 83972, and UPEC strain CFT073: comparison of transcriptomes, growth and biofilm formation. *Molecular genetics and genomics: MGG*. **284**(6): 437–454.

Haraga, A., Ohlson, M. B., and Miller, S. I. (2008). *Salmonellae* interplay with host cells. *Nat Rev Microbiol*. **6**(1): 53–66.

Hausladen, A., Gow, A., and Stamler, J. S. (2001). Flavohemoglobin denitrosylase catalyzes the reaction of a nitroxyl equivalent with molecular oxygen. *Proc. Natl. Acad. Sci. U.S.A.* **98**(18): 10108–10112.

Hausladen, A., Gow, A. J., and Stamler, J. S. (1998). Nitrosative stress: metabolic pathway involving the flavohemoglobin. *Proc Natl Acad Sci U S A*. **95**(24): 14100–14105.

Hausladen, A., and Stamler, J. S. (2012). Is the flavohemoglobin a nitric oxide dioxygenase? *Free Radical Biology and Medicine*. **53**(5): 1209–1210.

Hayashi, T., Makino, K., Ohnishi, M., Kurokawa, K., Ishii, K., Yokoyama, K., Han, C. G., Ohtsubo, E., Nakayama, K., Murata, T., Tanaka, M., Tobe, T., Iida, T., Takami, H., Honda, T., Sasakawa, C., Ogasawara, N., Yasunaga, T., Kuhara, S., Shiba, T., Hattori, M., and Shinagawa, H. (2001). Complete genome sequence of enterohemorrhagic *Escherichia coli* O157:H7 and genomic comparison with a laboratory strain K-12. *DNA Res.* **8**(1): 11–22.

Hjertqvist, M., Luzzi, I., Lofdahl, S., Olsson, A., Radal, J., and Andersson, Y. (2006). Unusual phage pattern of *Salmonella* Typhimurium isolated from Swedish patients and Italian salami. *Euro Surveill.* **11**(2): E060209.3.

Hohmann, E. L. (2001). Nontyphoidal salmonellosis. *Clinical infectious diseases: an official publication of the Infectious Diseases Society of America*. **32**(2): 263–269.

Holyoake, L. V., Hunt, S., Sanguinetti, G., Cook, G. M., Howard, M. J., Rowe, M. L., Poole, R. K., and Shepherd, M. (2016). CydDC-mediated reductant export in *Escherichia coli* controls the transcriptional wiring of energy metabolism and combats nitrosative stress. *The Biochemical journal*. **473**(6): 693–701.

Hong, W., Wu, Y. E., Fu, X., and Chang, Z. (2012). Chaperone-dependent mechanisms for acid resistance in enteric bacteria. *Trends in Microbiology*. **20**(7): 328–335.

Honikel, K. O. (2008). The use and control of nitrate and nitrite for the processing of meat products. *Meat Science*. **78**(1-2): 68–76.

Hord, N. G., Tang, Y., and Bryan, N. S. (2009). Food sources of nitrates and nitrites: the physiologic context for potential health benefits. *The American journal of clinical nutrition*. **90**(1): 1–10.

Humphrey, T. (2004). Science and society. *Salmonella*, stress responses and food safety. *Nat Rev Micro*. **2**(6): 504–509.

Hung, C.-L., Cheng, H.-H., Hsieh, W.-C., Tsai, Z. T.-Y., Tsai, H.-K., Chu, C.-H., Hsieh, W.-P., Chen, Y.-F., Tsou, Y., Lai, C.-H., and Wang, W.-C. (2015). The CrdRS two-component system in *Helicobacter pylori* responds to nitrosative stress. *Molecular Microbiology*. **97**(6): 1128–1141.

Hutchings, M. I., Mandhana, N., and Spiro, S. (2002). The NorR protein of *Escherichia coli* activates expression of the flavorubredoxin gene *norV* in response to reactive nitrogen species. *J. Bacteriol.* **184**(16): 4640–4643.

Hutter, B., Schaab, C., Albrecht, S., Borgmann, M., Brunner, N. A., Freiberg, C., Ziegelbauer, K., Rock, C. O., Ivanov, I., and Loferer, H. (2004). Prediction of mechanisms of action of antibacterial compounds by gene expression profiling. *Antimicrobial agents and chemotherapy*. **48**(8): 2838–2844.

Hyduke, D. R., Jarboe, L. R., Tran, L. M., Chou, K. J., and Liao, J. C. (2007). Integrated network analysis identifies nitric oxide response networks and dihydroxyacid dehydratase as a crucial target in *Escherichia coli*. *Proc Natl Acad Sci U S A*. **104**(20): 8484–8489.

Island, M. D., Wei, B. Y., and Kadner, R. J. (1992). Structure and function of the *uhp* genes for the sugar phosphate transport system in *Escherichia coli* and *Salmonella typhimurium*. *Journal of Bacteriology*. **174**(9): 2754–2762.

Jang, S., and Imlay, J. A. (2010). Hydrogen peroxide inactivates the *Escherichia coli* Isc iron-sulphur assembly system, and OxyR induces the Suf system to compensate. *Molecular Microbiology*. **78**(6): 1448–1467.

Jarvik, T., Smillie, C., Groisman, E. A., and Ochman, H. (2009). Short-Term Signatures of Evolutionary Change in the *Salmonella enterica* Serovar Typhimurium 14028 Genome. *Journal of Bacteriology*. **192**(2): 560–567.

Jia, W., and Cole, J. A. (2005). Nitrate and nitrite transport in *Escherichia coli*. *Biochemical Society transactions*. **33**(Pt 1): 159–161.

Jia, W., Tovell, N., Clegg, S., Trimmer, M., and Cole, J. (2009). A single channel for nitrate uptake, nitrite export and nitrite uptake by *Escherichia coli* NarU and a role for NirC in nitrite export and uptake. *The Biochemical journal*. **417**(1): 297–304.

Jira, W. (2004). Chemische Vorgänge beim Pökeln und Räuchern. Teil 1: Pökeln = Chemical reactions of curing and smoking. Part 1: Curing. *Fleischwirtschaft*. **84**(5): 235–239.

Joerger, R. D., and Choi, S. (2015). Contribution of the *hdeB*-like gene (SEN1493) to survival of *Salmonella enterica* enteritidis Nal(R) at pH 2. *Foodborne Pathogens and Disease*. **12**(4): 353–359.

Joerger, R. D., Sartori, C., Frye, J. G., Turpin, J. B., Schmidt, C., McClelland, M., and Porwollik, S. (2012). Gene expression analysis of *Salmonella enterica* Enteritidis Nal(R) and *Salmonella enterica* Kentucky 3795 exposed to HCl and acetic acid in rich medium. *Foodborne Pathogens and Disease*. **9**(4): 331–337.

Joly, N., Engl, C., Jovanovic, G., Huvet, M., Toni, T., Sheng, X., Stumpf, M. P. H., and Buck, M. (2010). Managing membrane stress: the phage shock protein (Psp) response, from molecular mechanisms to physiology. *FEMS microbiology reviews*. **34**(5): 797–827.

Justino, M. C., Almeida, C. C., Teixeira, M., and Saraiva, L. M. (2007). *Escherichia coli* di-iron YtfE protein is necessary for the repair of stress-damaged iron-sulfur clusters. *J Biol Chem*. **282**(14): 10352–10359.

Justino, M. C., Vicente, J. B., Teixeira, M., and Saraiva, L. M. (2005). New genes implicated in the protection of anaerobically grown *Escherichia coli* against nitric oxide. *J. Biol. Chem.* **280**(4): 2636–2643.

Kabisch, J. (2014). Mikrobiologische Sicherheit von Rohwurstprodukten. Wirkung von Natriumnitrit auf Lebensmittelinfektionserreger. Doctoral dissertation. Technical University of Munich. URN: http://nbn-resolving.de/urn/ resolver.pl? urn:nbn:de:bvb:91-diss-20141015-1182797-0-6.

Kaczanowska, M., and Rydén-Aulin, M. (2007). Ribosome biogenesis and the translation process in *Escherichia coli*. *Microbiol. Mol. Biol. Rev.* **71**(3): 477–494.

Kannan, G., Wilks, J. C., Fitzgerald, D. M., Jones, B. D., Bondurant, S. S., and Slonczewski, J. L. (2008). Rapid acid treatment of *Escherichia coli*: transcriptomic response and recovery. *BMC microbiology*. **8**: 37.

Kaper, J. B., Nataro, J. P., and Mobley, H. L. (2004). Pathogenic *Escherichia coli*. *Nat Rev Microbiol*. **2**(2): 123–140.

Karlinsey, J. E., Bang, I.-S., Becker, L. A., Frawley, E. R., Porwollik, S., Robbins, H. F., Thomas, V. C., Urbano, R., McClelland, M., and Fang, F. C. (2012). The NsrR regulon in nitrosative stress resistance of *Salmonella enterica* serovar Typhimurium. *Mol. Microbiol.* **85**(6): 1179–1193.

Kern, R., Malki, A., Abdallah, J., Tagourti, J., and Richarme, G. (2007). *Escherichia coli* HdeB is an acid stress chaperone. *Journal of Bacteriology*. **189**(2): 603–610.

Kieboom, J., and Abee, T. (2006). Arginine-dependent acid resistance in *Salmonella enterica* serovar Typhimurium. *J. Bacteriol.* **188**(15): 5650–5653.

Kim, S. K., Wilmes-Riesenberg, M. R., and Wanner, B. L. (1996). Involvement of the sensor kinase EnvZ in the in vivo activation of the response-regulator PhoB by acetyl phosphate. *Molecular Microbiology*. **22**(1): 135–147.

Kim, S. O., Orii, Y., Lloyd, D., Hughes, M. N., and Poole, R. K. (1999). Anoxic function for the *Escherichia coli* flavohaemoglobin (Hmp): reversible binding of nitric oxide and reduction to nitrous oxide. *FEBS Lett*. **445**(2-3): 389–394.

Klumpp, J., and Fuchs, T. M. (2007). Identification of novel genes in genomic islands that contribute to *Salmonella typhimurium* replication in macrophages. *Microbiology (Reading, Engl.)*. **153**(Pt 4): 1207–1220.

Kneen, M., Farinas, J., Li, Y., and Verkman, A. S. (1998). Green fluorescent protein as a noninvasive intracellular pH indicator. *Biophys. J.* **74**(3): 1591–1599.

Knuth, K. (2004). Identifizierung von essentiellen Genen in *Salmonella typhimurium* und *Listeria monocytogenes* durch Genom-weite Insertions-Duplikations-Mutagenese. Doctoral dissertation. University of Würzburg. URN: urn:nbn:de:bvb:20-opus-10003

Knuth, K., Niesalla, H., Hueck, C. J., and Fuchs, T. M. (2004). Large-scale identification of essential *Salmonella* genes by trapping lethal insertions. *Mol. Microbiol*. **51**(6): 1729–1744.

Kornberg, A., Rao, N. N., and Ault-Riche, D. (1999). Inorganic polyphosphate: a molecule of many functions. *Annual review of biochemistry*. **68**: 89–125.

Kulasekara, B. R., Jacobs, M., Zhou, Y., Wu, Z., Sims, E., Saenphimmachak, C., Rohmer, L., Ritchie, J. M., Radey, M., McKevitt, M., Freeman, T. L., Hayden, H., Haugen, E., Gillett, W., Fong, C., Chang, J., Beskhlebnaya, V., Waldor, M. K., Samadpour, M., Whittam, T. S., Kaul, R., Brittnacher, M., and Miller, S. I. (2009). Analysis of the genome of the *Escherichia coli* O157:H7 2006 spinach-associated outbreak isolate indicates candidate genes that may enhance virulence. *Infect. Immun.* **77**(9): 3713–3721.

Lamarche, M. G., Wanner, B. L., Crepin, S., and Harel, J. (2008). The phosphate regulon and bacterial virulence: a regulatory network connecting phosphate homeostasis and pathogenesis. *FEMS microbiology reviews*. **32**(3): 461–473.

Lambert, R. J., and Stratford, M. (1999). Weak-acid preservatives: modelling microbial inhibition and response. *J. Appl. Microbiol.* **86**(1): 157–164.

Landini, P. (2009). Cross-talk mechanisms in biofilm formation and responses to environmental and physiological stress in *Escherichia coli*. *Research in microbiology*. **160**(4): 259–266.

Landry, A. P., Duan, X., Huang, H., and Ding, H. (2011). Iron-sulfur proteins are the major source of protein-bound dinitrosyl iron complexes formed in *Escherichia coli* cells under nitric oxide stress. *Free Radic. Biol. Med.* **50**(11): 1582–1590.

Landstorfer, R., Simon, S., Schober, S., Keim, D., Scherer, S., and Neuhaus, K. (2014). Comparison of strand-specific transcriptomes of enterohemorrhagic *Escherichia coli* O157:H7 EDL933 (EHEC) under eleven different environmental conditions including radish sprouts and cattle feces. *BMC Genomics*. **15**(1): 353.

Langmead, B., Trapnell, C., Pop, M., and Salzberg, S. L. (2009). Ultrafast and memory-efficient alignment of short DNA sequences to the human genome. *Genome Biol*. **10**(3): R25.

Lee, J., Hiibel, S. R., Reardon, K. F., and Wood, T. K. (2010). Identification of stress-related proteins in *Escherichia coli* using the pollutant cis-dichloroethylene. *Journal of applied microbiology*. **108**(6): 2088–2102.

Leistner, L. (2000). Basic aspects of food preservation by hurdle technology. *Int J Food Microbiol*. **55**(1-3): 181–186.

Leistner, L., and Gorris, L. G. (1995). Food preservation by hurdle technology. *Trends in Food Science & Technology*. **6**(2): 41–46.

Leonhartsberger, S., Korsa, I., and Bock, A. (2002). The molecular biology of formate metabolism in enterobacteria. *Journal of molecular microbiology and biotechnology*. **4**(3): 269–276.

Lepoivre, M., Fieschi, F., Coves, J., Thelander, L., and Fontecave, M. (1991). Inactivation of ribonucleotide reductase by nitric oxide. *Biochemical and biophysical research communications*. **179**(1): 442–448.

Lepoivre, M., Flaman, J. M., Bobé, P., Lemaire, G., and Henry, Y. (1994). Quenching of the tyrosyl free radical of ribonucleotide reductase by nitric oxide. Relationship to cytostasis induced in tumor cells by cytotoxic macrophages. *The Journal of biological chemistry*. **269**(34): 21891–21897.

Li, H., Handsaker, B., Wysoker, A., Fennell, T., Ruan, J., Homer, N., Marth, G., Abecasis, G., and Durbin, R. (2009). The Sequence Alignment/Map format and SAMtools. *Bioinformatics*. **25**(16): 2078–2079.

Link, A. J., Phillips, D., and Church, G. M. (1997). Methods for generating precise deletions and insertions in the genome of wild-type *Escherichia coli*: application to open reading frame characterization. *J. Bacteriol*. **179**(20): 6228–6237.

Liu, C. Y., Hsu, Y. H., Wu, M. T., Pan, P. C., Ho, C. K., Su, L., Xu, X., Li, Y., and Christiani, D. C. (2009). Cured meat, vegetables, and bean-curd foods in relation to childhood acute leukemia risk: a population based case-control study. *BMC Cancer*. **9**: 15.

Livak, K. J., and Schmittgen, T. D. (2001). Analysis of relative gene expression data using real-time quantitative PCR and the 2(-Delta Delta C(T)) Method. *Methods (San Diego, Calif.)*. **25**(4): 402–408.

Lundberg, J. O., Weitzberg, E., and Gladwin, M. T. (2008). The nitrate-nitrite-nitric oxide pathway in physiology and therapeutics. *Nature reviews. Drug discovery*. **7**(2): 156–167.

Lundberg, J. O., Weitzberg, E., Lundberg, J. M., and Alving, K. (1994). Intragastric nitric oxide production in humans: measurements in expelled air. *Gut*. **35**(11): 1543–1546.

Luzzi, I., Galetta, P., Massari, M., Rizzo, C., Dionisi, A. M., Filetici, E., Cawthorne, A., Tozzi, A., Argentieri, M., Bilei, S., Busani, L., Gnesivo, C., Pendenza, A., Piccoli, A., Napoli, P., Loffredo, L., Trinito, M. O., Santarelli, E., and Degli Ciofi Atti, M. L. (2007). An Easter outbreak of *Salmonella* Typhimurium DT 104A associated with traditional pork salami in Italy. *Euro Surveill*. **12**(4): E11-2.

MacDonald, D. M., Fyfe, M., Paccagnella, A., Trinidad, A., Louie, K., and Patrick, D. (2004). *Escherichia coli* O157:H7 outbreak linked to salami, British Columbia, Canada, 1999. *Epidemiology and infection*. **132**(2): 283–289.

Macomber, L., and Imlay, J. A. (2009). The iron-sulfur clusters of dehydratases are primary intracellular targets of copper toxicity. *Proceedings of the National Academy of Sciences of the United States of America*. **106**(20): 8344–8349.

Majowicz, S. E., Musto, J., Scallan, E., Angulo, F. J., Kirk, M., O'Brien, S. J., Jones, T. F., Fazil, A., and Hoekstra, R. M. (2010). The global burden of nontyphoidal *Salmonella* gastroenteritis. *Clin. Infect. Dis.* **50**(6): 882–889.

Majowicz, S. E., Scallan, E., Jones-Bitton, A., Sargeant, J. M., Stapleton, J., Angulo, F. J., Yeung, D. H., and Kirk, M. D. (2014). Global Incidence of Human Shiga Toxin–Producing *Escherichia coli* Infections and Deaths. A Systematic Review and Knowledge Synthesis. *Foodborne Pathogens and Disease*. **11**(6): 447–455.

Malki, A., Le, H.-T., Milles, S., Kern, R., Caldas, T., Abdallah, J., and Richarme, G. (2008). Solubilization of protein aggregates by the acid stress chaperones HdeA and HdeB. *The Journal of biological chemistry*. **283**(20): 13679–13687.

Marvasi, M., Chen, C., Carrazana, M., Durie, I. A., and Teplitski, M. (2014). Systematic analysis of the ability of Nitric Oxide donors to dislodge biofilms formed by *Salmonella enterica* and *Escherichia coli* O157:H7. *AMB Express*. **4**: 42.

Mason, M. G., Shepherd, M., Nicholls, P., Dobbin, P. S., Dodsworth, K. S., Poole, R. K., and Cooper, C. E. (2009). Cytochrome *bd* confers nitric oxide resistance to *Escherichia coli*. *Nat Chem Biol*. **5**(2): 94–96.

McCollister, B. D., Myers, J. T., Jones-Carson, J., Husain, M., Bourret, T. J., and Vázquez-Torres, A. (2007). N(2)O(3) enhances the nitrosative potential of IFNgamma-primed macrophages in response to *Salmonella*. *Immunobiology*. **212**(9-10): 759–769.

McMeechan, A., Lovell, M. A., Cogan, T. A., Marston, K. L., Humphrey, T. J., and Barrow, P. A. (2007). Inactivation of *ppk* differentially affects virulence and disrupts ATP homeostasis in *Salmonella enterica* serovars Typhimurium and Gallinarum. *Res. Microbiol*. **158**(1): 79–85.

Mead, P. S., and Griffin, P. M. (1998). *Escherichia coli* O157. H7. *The Lancet*. **352**(9135): 1207–1212.

Mensinga, T. T., Speijers, G. J., and Meulenbelt, J. (2003). Health implications of exposure to environmental nitrogenous compounds. *Toxicol Rev*. **22**(1): 41–51.

Meyer, C., Thiel, S., Ullrich, U., and Stolle, A. (2010). *Salmonella* in raw meat and by-products from pork and beef. *J. Food Prot*. **73**(10): 1780–1784.

Mills, P. C., Richardson, D. J., Hinton, J. C. D., and Spiro, S. (2005). Detoxification of nitric oxide by the flavorubredoxin of *Salmonella enterica* serovar Typhimurium. *Biochem. Soc. Trans.* **33**(Pt 1): 198–199.

Mills, P. C., Rowley, G., Spiro, S., Hinton, J. C. D., and Richardson, D. J. (2008). A combination of cytochrome *c* nitrite reductase (NrfA) and flavorubredoxin (NorV) protects *Salmonella enterica* serovar Typhimurium against killing by NO in anoxic environments. *Microbiology (Reading, Engl.)*. **154**(Pt 4): 1218–1228.

Miranda, K. M., Espey, M. G., Jourd'heuil, D., Grisham, M. B., Fukuto, J. M., Feelisch, M., and Wink, D. A. (2000). The Chemical Biology of Nitric Oxide. In: Nitric oxide. Biology and pathobiology. 1st ed., pp. 41–55. Ignarro, L. J., Ed., Academic Press, San Diego.

Moncada, S., and Higgs, A. (1993). The L-arginine-nitric oxide pathway. *N Engl J Med*. **329**(27): 2002–2012.

Moncada, S., Palmer, R. M., and Higgs, E. A. (1991). Nitric oxide: physiology, pathophysiology, and pharmacology. *Pharmacological reviews*. **43**(2): 109–142.

Mortensen, H. D., Jacobsen, T., Koch, A. G., and Arneborg, N. (2008). Intracellular pH Homeostasis Plays a Role in the Tolerance of *Debaryomyces hansenii* and *Candida zeylanoides* to Acidified Nitrite. *Applied and Environmental Microbiology*. **74**(15): 4835–4840.

Mukhopadhyay, P., Zheng, M., Bedzyk, L. A., LaRossa, R. A., and Storz, G. (2004). Prominent roles of the NorR and Fur regulators in the *Escherichia coli* transcriptional response to reactive nitrogen species. *Proc. Natl. Acad. Sci. U.S.A.* **101**(3): 745–750.

Müller-Herbst, S., Wüstner, S., Kabisch, J., Pichner, R., and Scherer, S. (2016). Acidified nitrite inhibits proliferation of *Listeria monocytogenes* - Transcriptional analysis of a preservation method. *International Journal of Food Microbiology*. **226**: 33–41.

Murphy, K. C., and Campellone, K. G. (2003). Lambda Red-mediated recombinogenic engineering of enterohemorrhagic and enteropathogenic *E. coli*. *BMC Mol. Biol.* **4**: 11.

Nachin, L., Nannmark, U., and Nystrom, T. (2005). Differential roles of the universal stress proteins of *Escherichia coli* in oxidative stress resistance, adhesion, and motility. *Journal of Bacteriology*. **187**(18): 6265–6272.

Nataro, J. P., and Kaper, J. B. (1998). Diarrheagenic *Escherichia coli*. *Clin Microbiol Rev*. **11**(1): 142–201.

Negi, P. S. (2012). Plant extracts for the control of bacterial growth: efficacy, stability and safety issues for food application. *International Journal of Food Microbiology*. **156**(1): 7–17.

Nobre, L. S., Garcia-Serres, R., Todorovic, S., Hildebrandt, P., Teixeira, M., Latour, J.-M., Saraiva, L. M., and Giuffrè, A. (2014). *Escherichia coli* RIC Is Able to Donate Iron to Iron-Sulfur Clusters. *PLoS ONE*. **9**(4): e95222.

Nunoshiba, T., Hidalgo, E., Amábile Cuevas, C. F., and Demple, B. (1992). Two-stage control of an oxidative stress regulon: the *Escherichia coli* SoxR protein triggers redox-inducible expression of the *soxS* regulatory gene. *Journal of Bacteriology*. **174**(19): 6054–6060.

Nygard, K., Lindstedt, B. A., Wahl, W., Jensvoll, L., Kjelso, C., Molbak, K., Torpdahl, M., and Kapperud, G. (2007). Outbreak of *Salmonella* Typhimurium infection traced to imported cured sausage using MLVA-subtyping. *Euro Surveill*. **12**(3): E070315.5.

Ostroff, S. M., Tarr, P. I., Neill, M. A., Lewis, J. H., Hargrett-Bean, N., and Kobayashi, J. M. (1989). Toxin Genotypes and Plasmid Profiles as Determinants of Systemic Sequelae in *Escherichia coli* O157. H7 Infections. *Journal of Infectious Diseases*. **160**(6): 994–998.

Outten, F. W., Djaman, O., and Storz, G. (2004). A *suf* operon requirement for Fe-S cluster assembly during iron starvation in *Escherichia coli*. *Molecular Microbiology*. **52**(3): 861–872.

Park, Y. K., Bearson, B., Bang, S. H., Bang, I. S., and Foster, J. W. (1996). Internal pH crisis, lysine decarboxylase and the acid tolerance response of *Salmonella typhimurium*. *Mol. Microbiol*. **20**(3): 605–611.

Park, Y. M., Lee, H. J., Jeong, J.-H., Kook, J.-K., Choy, H. E., Hahn, T.-W., and Bang, I. S. (2015). Branched-chain amino acid supplementation promotes aerobic growth of *Salmonella* Typhimurium under nitrosative stress conditions. *Archives of microbiology*. **197**(10): 1117–1127.

Park, Y. M., Park, H. J., Joung, Y. H., and Bang, I. S. (2011). Nitrosative stress causes amino acid auxotrophy in *hmp* mutant *Salmonella* Typhimurium. *Microbiol. Immunol*. **55**(10): 743–747.

Partridge, J. D., Bodenmiller, D. M., Humphrys, M. S., and Spiro, S. (2009). NsrR targets in the *Escherichia coli* genome. New insights into DNA sequence requirements for binding and a role for NsrR in the regulation of motility. *Molecular Microbiology*. **73**(4): 680–694.

Patten, C. L., Kirchhof, M. G., Schertzberg, M. R., Morton, R. A., and Schellhorn, H. E. (2004). Microarray analysis of RpoS-mediated gene expression in *Escherichia coli* K-12. *Molecular genetics and genomics: MGG*. **272**(5): 580–591.

Pereira, P. M. C. C. de, and Vicente, A. F. D. R. B. (2013). Meat nutritional composition and nutritive role in the human diet. *Meat Sci*. **93**(3): 586–592.

Perham, R. N. (2000). Swinging arms and swinging domains in multifunctional enzymes: catalytic machines for multistep reactions. *Annual review of biochemistry*. **69**: 961–1004.

Perna, N. T., Plunkett, G., Burland, V., Mau, B., Glasner, J. D., Rose, D. J., Mayhew, G. F., Evans, P. S., Gregor, J., Kirkpatrick, H. A., Pósfai, G., Hackett, J., Klink, S., Boutin, A., Shao, Y., Miller, L., Grotbeck, E. J., Davis, N. W., Lim, A., Dimalanta, E. T., Potamousis, K. D., Apodaca, J., Anantharaman, T. S., Lin, J., Yen, G., Schwartz, D. C., Welch, R. A., and Blattner, F. R. (2001). Genome sequence of *enterohaemorrhagic Escherichia coli* O157:H7. *Nature*. **409**(6819): 529–533.

Pfaffl, M. W., Horgan, G. W., and Dempfle, L. (2002). Relative expression software tool (REST) for group-wise comparison and statistical analysis of relative expression results in real-time PCR. *Nucleic Acids Res.* **30**(9): e36.

Polikanov, Y. S., Blaha, G. M., and Steitz, T. A. (2012). How Hibernation Factors RMF, HPF, and YfiA Turn Off Protein Synthesis. *Science*. **336**(6083): 915–918.

Pomposiello, P. J., and Demple, B. (2000). Identification of SoxS-regulated genes in *Salmonella enterica* serovar typhimurium. *Journal of Bacteriology*. **182**(1): 23–29.

Poock, S. R., Leach, E. R., Moir, J. W. B., Cole, J. A., and Richardson, D. J. (2002). Respiratory detoxification of nitric oxide by the cytochrome *c* nitrite reductase of *Escherichia coli*. *J. Biol. Chem.* **277**(26): 23664–23669.

Prendergast, D. M., Duggan, S. J., Gonzales-Barron, U., Fanning, S., Butler, F., Cormican, M., and Duffy, G. (2009). Prevalence, numbers and characteristics of *Salmonella* spp. on Irish retail pork. *Int J Food Microbiol*. **131**(2-3): 233–239.

Price-Carter, M., Fazzio, T. G., Vallbona, E. I., and Roth, J. R. (2005). Polyphosphate Kinase Protects *Salmonella enterica* from Weak Organic Acid Stress. *Journal of Bacteriology*. **187**(9): 3088–3099.

Pullan, S. T., Gidley, M. D., Jones, R. A., Barrett, J., Stevanin, T. M., Read, R. C., Green, J., and Poole, R. K. (2007). Nitric oxide in chemostat-cultured *Escherichia coli* is sensed by Fnr and other global regulators: unaltered methionine biosynthesis indicates lack of S nitrosation. *J. Bacteriol.* **189**(5): 1845–1855.

Rabin, R. S., and Stewart, V. (1993). Dual response regulators (NarL and NarP) interact with dual sensors (NarX and NarQ) to control nitrate- and nitrite-regulated gene expression in *Escherichia coli* K-12. *Journal of Bacteriology*. **175**(11): 3259–3268.

Rao, N. N., Liu, S., and Kornberg, A. (1998). Inorganic polyphosphate in *Escherichia coli*: the phosphate regulon and the stringent response. *Journal of Bacteriology*. **180**(8): 2186–2193.

Rees, C. E., Dodd, C. E., Gibson, P. T., Booth, I. R., and Stewart, G. S. (1995). The significance of bacteria in stationary phase to food microbiology. *International Journal of Food Microbiology*. **28**(2): 263–275.

Reid, S. D., Herbelin, C. J., Bumbaugh, A. C., Selander, R. K., and Whittam, T. S. (2000). Parallel evolution of virulence in pathogenic *Escherichia coli*. *Nature*. **406**(6791): 64–67.

Ren, B., Zhang, N., Yang, J., and Ding, H. (2008). Nitric oxide-induced bacteriostasis and modification of iron-sulphur proteins in *Escherichia coli*. *Mol. Microbiol.* **70**(4): 953–964.

Richardson, A. R., Payne, E. C., Younger, N., Karlinsey, J. E., Thomas, V. C., Becker, L. A., Navarre, W. W., Castor, M. E., Libby, S. J., and Fang, F. C. (2011). Multiple targets of nitric oxide in the tricarboxylic acid cycle of *Salmonella enterica* serovar typhimurium. *Cell Host Microbe*. **10**(1): 33–43.

Richardson, A. R., Soliven, K. C., Castor, M. E., Barnes, P. D., Libby, S. J., and Fang, F. C. (2009). The Base Excision Repair system of *Salmonella enterica* serovar typhimurium counteracts DNA damage by host nitric oxide. *PLoS Pathog.* **5**(5): e1000451.

Ridnour, L. A., Thomas, D. D., Mancardi, D., Espey, M. G., Miranda, K. M., Paolocci, N., Feelisch, M., Fukuto, J., and Wink, D. A. (2004). The chemistry of nitrosative stress induced by nitric oxide and reactive nitrogen oxide species. Putting perspective on stressful biological situations. *Biol Chem*. **385**(1): 1–10.

Riley, L. W., Remis, R. S., Helgerson, S. D., McGee, H. B., Wells, J. G., Davis, B. R., Hebert, R. J., Olcott, E. S., Johnson, L. M., Hargrett, N. T., Blake, P. A., and Cohen, M. L. (1983). Hemorrhagic colitis associated with a rare *Escherichia coli* serotype. *N. Engl. J. Med.* **308**(12): 681–685.

Robinson, M. D., McCarthy, D. J., and Smyth, G. K. (2010). edgeR: a Bioconductor package for differential expression analysis of digital gene expression data. *Bioinformatics*. **26**(1): 139–140.

Robinson, M. D., and Oshlack, A. (2010). A scaling normalization method for differential expression analysis of RNA-seq data. *Genome Biol*. **11**(3): R25.

Rodionov, D. A., Dubchak, I. L., Arkin, A. P., Alm, E. J., and Gelfand, M. S. (2005). Dissimilatory metabolism of nitrogen oxides in bacteria: comparative reconstruction of transcriptional networks. *PLoS Comput Biol*. **1**(5): e55.

Rosamond, J., and Allsop, A. (2000). Harnessing the power of the genome in the search for new antibiotics. *Science (New York, N.Y.)*. **287**(5460): 1973–1976.

Rose, I. A., Grunberg-Manago, M., Korey, S. R., and Ochoa, S. (1954). Enzymatic phosphorylation of acetate. *The Journal of biological chemistry*. **211**(2): 737–756.

Rossmann, R., Sawers, G., and Böck, A. (1991). Mechanism of regulation of the formate-hydrogenlyase pathway by oxygen, nitrate, and pH. Definition of the formate regulon. *Mol Microbiol*. **5**(11): 2807–2814.

Rowley, G., Hensen, D., Felgate, H., Arkenberg, A., Appia-Ayme, C., Prior, K., Harrington, C., Field, S. J., Butt, J. N., Baggs, E., and Richardson, D. J. (2012). Resolving the contributions of the membrane-bound and periplasmic nitrate reductase systems to nitric oxide and nitrous oxide production in *Salmonella enterica* serovar Typhimurium. *Biochem. J.* **441**(2): 755–762.

Rudd, K. E., Humphery-Smith, I., Wasinger, V. C., and Bairoch, A. (1998). Low molecular weight proteins: a challenge for post-genomic research. *Electrophoresis*. **19**(4): 536–544.

Rutherford, K., Parkhill, J., Crook, J., Horsnell, T., Rice, P., Rajandream, M. A., and Barrell, B. (2000). Artemis: sequence visualization and annotation. *Bioinformatics*. **16**(10): 944–945.

Ryan, D., Pati, N. B., Ojha, U. K., Padhi, C., Ray, S., Jaiswal, S., Singh, G. P., Mannala, G. K., Schultze, T., Chakraborty, T., and Suar, M. (2015). Global transcriptome and mutagenic analyses of the acid tolerance response of *Salmonella enterica* serovar Typhimurium. *Applied and Environmental Microbiology*. **81**(23): 8054–8065.

Saini, A., Mapolelo, D. T., Chahal, H. K., Johnson, M. K., and Outten, F. W. (2010). SufD and SufC ATPase activity are required for iron acquisition during *in vivo* Fe-S cluster formation on SufB. *Biochemistry*. **49**(43): 9402–9412.

Savage, P. J., Leong, J. M., and Murphy, K. C. (2006). Rapid Allelic Exchange in Enterohemorrhagic *Escherichia coli* (EHEC) and Other *E. coli* Using Lambda Red Recombination. *Current Protocols in Microbiology*. 00:A:5A.2:5A.2.1–5A.2.13.

Schapiro, J. M., Libby, S. J., and Fang, F. C. (2003). Inhibition of bacterial DNA replication by zinc mobilization during nitrosative stress. *Proceedings of the National Academy of Sciences of the United States of America*. **100**(14): 8496–8501.

Schmid, H., Hachler, H., Stephan, R., Baumgartner, A., and Boubaker, K. (2008). Outbreak of *Salmonella enterica* serovar Typhimurium in Switzerland, May-June 2008, implications for production and control of meat preparations. *Euro Surveill*. **13**(44): pii: 19020.

Schouten, K. A., and Weiss, B. (1999). Endonuclease V protects *Escherichia coli* against specific mutations caused by nitrous acid. *Mutation research*. **435**(3): 245–254.

Schürch, L. (2012). Weiterführende Charakterisierung der Nitrit- und Stickstoffmonoxid-Stressantwort von *Salmonella enterica* Serovar Typhimurium. Master's Thesis, unpublished.

Sebranek, J. G., and Bacus, J. N. (2007a). Natural and Organic Cured Meat Products: Regulatory, Manufacturing, Marketing, Quality and Safety Issues. *American Meat Science Association White Paper Series*. **1:** 1-15.

Sebranek, J. G., and Bacus, J. N. (2007b). Cured meat products without direct addition of nitrate or nitrite: what are the issues? *Meat Science*. **77**(1): 136–147.

Sebranek, J. G., Jackson-Davis, A. L., Myers, K. L., and Lavieri, N. A. (2012). Beyond celery and starter culture: advances in natural/organic curing processes in the United States. *Meat Science*. **92**(3): 267–273.

Seth, D., Hausladen, A., Wang, Y.-J., and Stamler, J. S. (2012). Endogenous protein S-Nitrosylation in *E. coli*: regulation by OxyR. *Science*. **336**(6080): 470–473.

Shen, S., and Fang, F. C. (2012). Integrated stress responses in *Salmonella*. *International Journal of Food Microbiology*. **152**(3): 75–81.

Shimizu, T., Tsutsuki, H., Matsumoto, A., Nakaya, H., and Noda, M. (2012). The nitric oxide reductase of enterohaemorrhagic *Escherichia coli* plays an important role for the survival within macrophages. *Mol. Microbiol.* **85**(3): 492–512.

Siegele, D. A. (2005). Universal stress proteins in *Escherichia coli*. *Journal of Bacteriology*. **187**(18): 6253–6254.

Simon, J. (2002). Enzymology and bioenergetics of respiratory nitrite ammonification. *FEMS Microbiol. Rev.* **26**(3): 285–309.

Sindelar, J. J., and Milkowski, A. L. (2012). Human safety controversies surrounding nitrate and nitrite in the diet. *Nitric Oxide*. **26**(4): 259–266.

Singh, R. J., Hogg, N., Joseph, J., and Kalyanaraman, B. (1996). Mechanism of nitric oxide release from S-nitrosothiols. *The Journal of biological chemistry*. **271**(31): 18596–18603.

Skibsted, L. H. (2011). Nitric oxide and quality and safety of muscle based foods. *Nitric Oxide*. **24**(4): 176–183.

Song, M., Husain, M., Jones-Carson, J., Liu, L., Henard, C. A., and Vázquez-Torres, A. (2013). Low-molecular-weight thiol-dependent antioxidant and antinitrosative defences in *Salmonella* pathogenesis. *Mol. Microbiol.* **87**(3): 609–622.

Sonna, L. A., Ambudkar, S. V., and Maloney, P. C. (1988). The mechanism of glucose 6-phosphate transport by *Escherichia coli*. *The Journal of biological chemistry*. **263**(14): 6625–6630.

Spek, E. J., Wright, T. L., Stitt, M. S., Taghizadeh, N. R., Tannenbaum, S. R., Marinus, M. G., and Engelward, B. P. (2001). Recombinational repair is critical for survival of *Escherichia coli* exposed to nitric oxide. *Journal of Bacteriology*. **183**(1): 131–138.

Spiro, S. (2007). Regulators of bacterial responses to nitric oxide. *FEMS Microbiol. Rev.* **31**(2): 193–211.

Spiro, S., and Guest, J. R. (1990). FNR and its role in oxygen-regulated gene expression in *Escherichia coli*. *FEMS Microbiol. Rev.* **6**(4): 399–428.

Spiro, S., Zhang, M. Q., Mehta, H. H., and Liu, Y. (2015). Genome-wide analysis of the response to nitric oxide in uropathogenic *Escherichia coli* CFT073. *Microbial Genomics*. **1**(4).

Starke, M., Richter, M., and Fuchs, T. M. (2013). The insecticidal toxin genes of *Yersinia enterocolitica* are activated by the thermolabile LTTR-like regulator TcaR2 at low temperatures. *Molecular Microbiology*. **89**(4): 596–611.

Stevanin, T. M., Ioannidis, N., Mills, C. E., Kim, S. O., Hughes, M. N., and Poole, R. K. (2000). Flavohemoglobin Hmp affords inducible protection for *Escherichia coli* respiration, catalyzed by cytochromes *bo*' or *bd*, from nitric oxide. *The Journal of biological chemistry*. **275**(46): 35868–35875.

Stevanin, T. M., Poole, R. K., Demoncheaux, E. A. G., and Read, R. C. (2002). Flavohemoglobin Hmp protects *Salmonella enterica* serovar typhimurium from nitric oxide-related killing by human macrophages. *Infect. Immun.* **70**(8): 4399–4405.

Svensson, L., Poljakovic, M., Säve, S., Gilberthorpe, N., Schön, T., Strid, S., Corker, H., Poole, R. K., and Persson, K. (2010). Role of flavohemoglobin in combating nitrosative stress in uropathogenic *Escherichia coli*--implications for urinary tract infection. *Microb. Pathog.* **49**(3): 59–66.

Tarr, P. I., Gordon, C. A., and Chandler, W. L. (2005). Shiga-toxin-producing *Escherichia coli* and haemolytic uraemic syndrome. *The Lancet*. **365**(9464): 1073–1086.

Tindall, B. J., Grimont, P. A. D., Garrity, G. M., and Euzéby, J. P. (2005). Nomenclature and taxonomy of the genus *Salmonella*. *Int. J. Syst. Evol. Microbiol.* **55**(Pt 1): 521–524.

Tramonti, A., Visca, P., Canio, M. de, Falconi, M., and Biase, D. de (2002). Functional characterization and regulation of *gadX*, a gene encoding an AraC/XylS-like transcriptional activator of the *Escherichia coli* glutamic acid decarboxylase system. *Journal of Bacteriology*. **184**(10): 2603–2613.

Traxler, M. F., Summers, S. M., Nguyen, H.-T., Zacharia, V. M., Hightower, G. A., Smith, J. T., and Conway, T. (2008). The global, ppGpp-mediated stringent response to amino acid starvation in *Escherichia coli*. *Molecular Microbiology*. **68**(5): 1128–1148.

Troxell, B., Fink, R. C., Porwollik, S., McClelland, M., and Hassan, H. M. (2011). The Fur regulon in anaerobically grown *Salmonella enterica* sv. Typhimurium: identification of new Fur targets. *BMC Microbiol.* **11**: 236.

Tucker, N. P., D'Autreaux, B., Studholme, D. J., Spiro, S., and Dixon, R. (2004). DNA Binding Activity of the *Escherichia coli* Nitric Oxide Sensor NorR Suggests a Conserved Target Sequence in Diverse Proteobacteria. *Journal of Bacteriology*. **186**(19): 6656–6660.

Tucker, N. P., Hicks, M. G., Clarke, T. A., Crack, J. C., Chandra, G., Le Brun, N. E., Dixon, R., Hutchings, M. I., and Yuan, A. (2008a). The Transcriptional Repressor Protein NsrR Senses Nitric Oxide Directly via a [2Fe-2S] Cluster. *PLoS ONE*. **3**(11): e3623.

Tucker, N. P., D'Autréaux, B., Yousafzai, F. K., Fairhurst, S. A., Spiro, S., and Dixon, R. (2008b). Analysis of the nitric oxide-sensing non-heme iron center in the NorR regulatory protein. *J. Biol. Chem.* **283**(2): 908–918.

Tucker, N. P., Le Brun, N. E., Dixon, R., and Hutchings, M. I. (2010). There's NO stopping NsrR, a global regulator of the bacterial NO stress response. *Trends in Microbiology*. **18**(4): 149–156.

Unden, G., and Bongaerts, J. (1997). Alternative respiratory pathways of *Escherichia coli*: energetics and transcriptional regulation in response to electron acceptors. *Biochimica et biophysica acta*. **1320**(3): 217–234.

Vadyvaloo, V., Viall, A. K., Jarrett, C. O., Hinz, A. K., Sturdevant, D. E., and Joseph Hinnebusch, B. (2015). Role of the PhoP-PhoQ gene regulatory system in adaptation of *Yersinia pestis* to environmental stress in the flea digestive tract. *Microbiology (Reading, England)*. **161**(6): 1198–1210.

van Loon, A. J., Botterweck, A. A., Goldbohm, R. A., Brants, H. A., van Klaveren, J. D., and van den Brandt, P. A. (1998). Intake of nitrate and nitrite and the risk of gastric cancer: a prospective cohort study. *Br. J. Cancer*. **78**(1): 129–135.

van Wonderen, J. H., Burlat, B., Richardson, D. J., Cheesman, M. R., and Butt, J. N. (2008). The nitric oxide reductase activity of cytochrome *c* nitrite reductase from *Escherichia coli*. *J. Biol. Chem.* **283**(15): 9587–9594.

Vareille, M., Sablet, T. de, Hindré, T., Martin, C., and Gobert, A. P. (2007). Nitric oxide inhibits Shiga-toxin synthesis by enterohemorrhagic *Escherichia coli*. *Proc. Natl. Acad. Sci. U.S.A.* **104**(24): 10199–10204.

Vasudevan, S. G., Armarego, W. L., Shaw, D. C., Lilley, P. E., Dixon, N. E., and Poole, R. K. (1991). Isolation and nucleotide sequence of the *hmp* gene that encodes a haemoglobin-like protein in *Escherichia coli* K-12. *Mol Gen Genet*. **226**(1-2): 49–58.

Verhamme, D. T., Postma, P. W., Crielaard, W., and Hellingwerf, K. J. (2002). Cooperativity in signal transfer through the Uhp system of *Escherichia coli*. *Journal of Bacteriology*. **184**(15): 4205–4210.

Vermassen, A., La Foye, A. de, Loux, V., Talon, R., and Leroy, S. (2014). Transcriptomic analysis of *Staphylococcus xylosus* in the presence of nitrate and nitrite in meat reveals its response to nitrosative stress. *Frontiers in microbiology*. **5**: 691.

Viala, J. P. M., Méresse, S., Pocachard, B., Guilhon, A.-A., Aussel, L., Barras, F., and Chakravortty, D. (2011). Sensing and Adaptation to Low pH Mediated by Inducible Amino Acid Decarboxylases in *Salmonella*. *PLoS ONE*. **6**(7): e22397.

Vine, C. E., and Cole, J. A. (2011a). Nitrosative stress in *Escherichia coli*: reduction of nitric oxide. *Biochem. Soc. Trans*. **39**(1): 213–215.

Vine, C. E., and Cole, J. A. (2011b). Unresolved sources, sinks, and pathways for the recovery of enteric bacteria from nitrosative stress. *FEMS Microbiol. Lett*. **325**(2): 99–107.

Vine, C. E., Justino, M. C., Saraiva, L. M., and Cole, J. (2010). Detection by whole genome microarrays of a spontaneous 126-gene deletion during construction of a *ytfE* mutant: confirmation that a *ytfE* mutation results in loss of repair of iron-sulfur centres in proteins damaged by oxidative or nitrosative stress. *Journal of microbiological methods*. **81**(1): 77–79.

Vine, C. E., Purewal, S. K., and Cole, J. A. (2011). NsrR-dependent method for detecting nitric oxide accumulation in the *Escherichia coli* cytoplasm and enzymes involved in NO production. *FEMS Microbiol. Lett*. **325**(2): 108–114.

Wang, H., and Gunsalus, R. P. (2000). The *nrfA* and *nirB* nitrite reductase operons in *Escherichia coli* are expressed differently in response to nitrate than to nitrite. *J. Bacteriol.* **182**(20): 5813–5822.

Wang, H., Tseng, C. P., and Gunsalus, R. P. (1999). The *napF* and *narG* nitrate reductase operons in *Escherichia coli* are differentially expressed in response to submicromolar concentrations of nitrate but not nitrite. *Journal of Bacteriology*. **181**(17): 5303–5308.

Wang, J., Vine, C. E., Balasiny, B. K., Rizk, J., Bradley, C. L., Tinajero-Trejo, M., Poole, R. K., Bergaust, L. L., Bakken, L. R., and Cole, J. A. (2016). The roles of the hybrid cluster protein, Hcp and its reductase, Hcr, in high affinity nitric oxide reduction that protects anaerobic cultures of *Escherichia coli* against nitrosative stress. *Molecular Microbiology*. **100**(5): 877–892.

Wanner, B. L. (1993). Gene regulation by phosphate in enteric bacteria. *Journal of cellular biochemistry*. **51**(1): 47–54.

Wanner, B. L. (1996). Phosphorus assimilation and control of the phosphate regulon. In: *Escherichia coli* and *Salmonella*. Cellular and molecular biology. 2nd ed., pp. pp. 1357–1381. Neidhardt FC, Curtiss R III, Ingraham JL, Lin ECC, Low KB Jr, Magasanik B, Reznikoff WS, Riley M, Schaechter M, Umbarger HE, Ed., ASM Press, Washington, D.C.

Wanner, B. L., and Wilmes-Riesenberg, M. R. (1992). Involvement of phosphotransacetylase, acetate kinase, and acetyl phosphate synthesis in control of the phosphate regulon in *Escherichia coli*. *Journal of Bacteriology*. **174**(7): 2124–2130.

Weber, M. M., French, C. L., Barnes, M. B., Siegele, D. A., and McLean, R. J. C. (2010). A previously uncharacterized gene, *yjfO* (*bsmA*), influences *Escherichia coli* biofilm formation and stress response. *Microbiology (Reading, England)*. **156**(Pt 1): 139–147.

Weiner, L., and Model, P. (1994). Role of an *Escherichia coli* stress-response operon in stationary-phase survival. *Proceedings of the National Academy of Sciences of the United States of America*. **91**(6): 2191–2195.

Weiss, B. (2006). Evidence for mutagenesis by nitric oxide during nitrate metabolism in *Escherichia coli*. *J. Bacteriol.* **188**(3): 829–833.

Williams, R. C., Isaacs, S., Decou, M. L., Richardson, E. A., Buffett, M. C., Slinger, R. W., Brodsky, M. H., Ciebin, B. W., Ellis, A., and Hockin, J. (2000). Illness outbreak associated with *Escherichia coli* O157:H7 in Genoa salami. E. coli O157:H7 Working Group. *CMAJ*. **162**(10): 1409–1413.

Wink, D. A., Kasprzak, K. S., Maragos, C. M., Elespuru, R. K., Misra, M., Dunams, T. M., Cebula, T. A., Koch, W. H., Andrews, A. W., Allen, J. S., and et, a. (1991). DNA deaminating ability and genotoxicity of nitric oxide and its progenitors. *Science*. **254**(5034): 1001–1003.

Wolfe, A. J. (2005). The acetate switch. *Microbiology and molecular biology reviews: MMBR*. **69**(1): 12–50.

Wolfe, M. T., Heo, J., Garavelli, J. S., and Ludden, P. W. (2002). Hydroxylamine reductase activity of the hybrid cluster protein from *Escherichia coli*. *J. Bacteriol*. **184**(21): 5898–5902.

Wong, K. K., Suen, K. L., and Kwan, H. S. (1989). Transcription of *pfl* is regulated by anaerobiosis, catabolite repression, pyruvate, and *oxrA*: *pfl*::Mu dA operon fusions of *Salmonella typhimurium*. *Journal of Bacteriology*. **171**(9): 4900–4905.

Yamada, M., Sedgwick, B., Sofuni, T., and Nohmi, T. (1995). Construction and characterization of mutants of *Salmonella typhimurium* deficient in DNA repair of O6-methylguanine. *J. Bacteriol.* **177**(6): 1511–1519.

Yu, H., Sato, E. F., Nagata, K., Nishikawa, M., Kashiba, M., Arakawa, T., Kobayashi, K., Tamura, T., and Inoue, M. (1997). Oxygen-dependent regulation of the respiration and growth of *Escherichia coli* by nitric oxide. *FEBS letters*. **409**(2): 161–165.

Zbell, A. L., and Maier, R. J. (2009). Role of the Hya hydrogenase in recycling of anaerobically produced H2 in *Salmonella enterica* serovar Typhimurium. *Appl. Environ. Microbiol*. **75**(5): 1456–1459.

Zbell, A. L., Maier, S. E., and Maier, R. J. (2008). *Salmonella enterica* serovar Typhimurium NiFe uptake-type hydrogenases are differentially expressed in vivo. *Infection and Immunity*. **76**(10): 4445–4454.

Zhao, B., and Houry, W. A. (2010). Acid stress response in enteropathogenic gammaproteobacteria: an aptitude for survival. *Biochem. Cell Biol.* **88**(2): 301–314.

List of Abbreviations

× *g*	centrifugal force
°C	degree Celsius
µ	micro-
acetyl-CoA	acetyl coenzyme A
acetyl-P	acetyl phosphate
Amp	ampicillin
ara	arabinose
ATR	acid tolerance response
AUC	area under growth curve
a_w	water activity
BAM	Binary Alignment/Map
BCAA	branched-chain amino acids
BH	Benjamini-Hochberg
bp	base pair(s)
$CaCl_2$	calcium chloride
cDNA	complementary DNA
CDS	coding sequence
cfu	colony forming units
Cm	chloramphenicol
COGs	Clusters of Orthologous Genes
cpm	counts per million (reads)
C_t	threshold cycle
DEPC	diethylpyrocarbonate
DHL agar	deoxycholate hydrogen sulfide lactose agar
DNA	deoxyribonucleic acid
DNIC	dinitrosyl complex
dNTPs	deoxynucleotid triphosphates
E	primer efficiency
EDTA	ethylenediaminetetraacetic acid
EGFP	enhanced green fluorescent protein
E_h	redox potential
EHEC	enterohemorrhagic *E. coli*
EtOH	ethanol
F	Farad
FAD	flavin adenine dinucleotide
fastq	text-based format containing the nucleotide sequence and its corresponding quality scores
FC	fold-change
FDR	false discovery rate
Fe-S	iron-sulfur
FMN	flavin mononucleotide
FRT	Flp recombination target
FTP	file transfer protocol
GFP	green fluorescent protein
GSH	glutathione
GSNO	*S*-nitrosoglutathione
h	hour(s)

HEPES	N-2-Hydroxyethyl piperazine-N'-2-ethane sulphonic acid
HNO	nitroxyl
HNO_2	nitrous acid
HUS	hemolytic uremic syndrome
ID	identifier
iNOS	inducible nitric oxide synthase
IPTG	isopropyl β-D-1-thiogalactopyranoside
k	kilo-
Kan	kanamycin
kb	kilobase
K_m	Michaelis constant
KNO_3	potassium nitrate
LA	lactic acid
LB	Luria-Bertani
LEE	locus of enterocyte effacement
LMW	low moleuclar weight
M	molar
m	milli-
MEB0	meat extract broth to simulate ripening day 0
MEB3	meat extract broth to simulate ripening day 3
MES	2-(N-Morpholino)-ethane sulphonic acid
min	minute
MRI	Max Rubner Institute
n	nano-
N_2O	nitrous oxide
N_2O_3	dinitrogen trioxide
NaCl	sodium chloride
NAD(P)H	Nicotinamide adenine dinucleotide (phosphate)
$NaNO_2$	sodium nitrite
$NaNO_3$	sodium nitrate
NCBI	National Center for Biotechnology Information
NH_4^+	ammonia
NO	nitric oxide
NO^+	nitrosonium ion
NO_2^-	nitrite
NO_3^-	nitrate
NOS	nitric oxide synthase
nt	nucleotide(s)
O_2	oxygen
O_2^-	superoxide
OD_{600}	optical density at 600 nm
$ONOO^-$/ONOOH	peroxynitrite/peroxynitrous acid
p	pico-
P_i	inorganic phosphate
PAI	pathogenicity island
PBS	phosphate buffered saline
PCR	polymerase chain reaction
poly P	polyphosphate
p-value	probability value

qPCR	quantitative PCR
^{R}	resistant
RD0	ripening day 0
RD3	ripening day 3
RNA	ribonucleic acid
RNase	ribonuclease
RNA-seq	RNA sequencing
RNS	reactive nitrogen species
rpm	revolutions per minute
rRNA	ribosomal RNA
RT	room temperature
RTE	ready-to-eat
^{S}	sensitive
S. Typhimurium	*Salmonella enterica subsp. enterica* serovar Typhimurium
SAM	Sequence Alignment/Map
SD	standard deviation
SDS	sodium dodecyl sulphate
SE	standard error
sec	second
SNP	sodium nitroprusside
SOC	super optimal broth with catabolite repression
SPI	*Salmonella* pathogenicity island
STEC	Shiga toxin-producing *E. coli*
Stx	Shiga toxin
T3SS	type three secretion system
TAE	tris-acetate-EDTA
TCA	tricarboxylic acid cycle
TE	tris-EDTA
Tet	tetracycline
T_m	melting temperature
TMM	trimmed mean of M-values
Tris	tris(hydroxymethyl)aminomethane
U	Unit
UV	ultraviolett
V	Volt
v/v	volume to volume
w/o	without
w/v	weight to volume
WT	wildtype
XLD agar	xylose lysine deoxycholate agar
σ^{54}	sigma 54
Ω	Ohm

List of Figures

List of Tables

List of Appendix Tables

Appendix

Table A 1: Up-regulated genes under acidified $NaNO_2$ shock in *S.* Typhimurium 14028 WT

COG	14028 identifier	LT2 identifier	Gene name	Product	log_2 FC	p-value (BH-adjusted)
Energy production & conversion (C)						
COG1151C	STM14_1052	STM0937	*hcp*	hydroxylamine reductase	2.90	3.21E-03
COG0247C	STM14_2821	STM2286	*glpC*	sn-glycerol-3-phosphate dehydrogenase subunit C	2.06	4.85E-02
COG1018C	STM14_3135	STM2556	*hmpA*	nitric oxide dioxygenase	6.49	4.38E-12
*COG1819GC	STM14_3344	STM2773	*iroB*	putative glycosyl transferase	2.49	1.60E-02
COG0426C	STM14_3431	STM2840	*norV*[1]	anaerobic nitric oxide reductase flavorubredoxin	8.44	8.43E-17
COG1902C	STM14_3898	STM3219	*fadH*	2,4-dienoyl-CoA reductase	2.99	1.69E-03
*COG0604CR	STM14_5103	STM4245	*qor*	quinone oxidoreductase	1.96	4.69E-02
Carbohydrate transport & metabolism (G)						
COG1440G	STM14_1594	STM1312	*celA*	PTS system N,N'-diacetylchitobiose-specific transporter subunit IIB	2.06	3.47E-02
COG1447G	STM14_1596	STM1314	*celC*	PTS system N,N'-diacetylchitobiose-specific transporter subunit IIA	2.27	1.85E-02
COG2814G	STM14_2686	STM2179	-	putative sugar transporter	2.34	4.04E-02
*COG1819GC	STM14_3344	STM2773	*iroB*	putative glycosyl transferase	2.49	1.60E-02
COG2271G	STM14_3791	STM3134	-	putative permease	3.34	3.55E-04
COG1312G	STM14_3795	STM3135	-	mannonate dehydratase	2.17	2.45E-02
COG0246G	STM14_3796	STM3136	-	putative D-mannonate oxidoreductase	2.19	2.37E-02
COG3836G	STM14_3931	STM3249	*garL*	alpha-dehydro-beta-deoxy-D-glucarate aldolase	2.32	3.37E-02
COG0524G	STM14_4272	STM3547.Sc	-	putative transcriptional regulator	2.13	3.43E-02
COG3775G	STM14_4561	STM3782	-	putative PTS system galactitol-specific enzyme IIC component	2.20	2.60E-02
*COG1762GT	STM14_4563	STM3784	-	phosphotransferase system mannitol/fructose-specific IIA component	2.34	1.36E-02
COG2814G	STM14_5161	STM4290	*proP*	proline/glycine betaine transporter	2.11	2.92E-02
*COG2610GE	STM14_5378	STM4482	*idnT*	L-idonate transport protein	3.12	3.33E-03
Amino acid transport & metabolism (E)						
COG1280E	STM14_0427	STM0365	*yahN*	putative transport protein	2.04	4.39E-02
COG3075E	STM14_2820	STM2285	*glpB*	anaerobic glycerol-3-phosphate dehydrogenase subunit B	2.97	1.23E-02
COG0531E	STM14_3137	STM2558	*cadB*	lysine/cadaverine antiporter	4.81	6.92E-07
COG1982E	STM14_3138	STM2559	*cadA*	lysine decarboxylase 1	4.17	9.28E-06
COG3104E	STM14_4321	STM3592	*yhiP*	inner membrane transporter YhiP	2.80	2.74E-03
COG0747E	STM14_4375	STM3630	*dppA*	dipeptide transport protein	3.22	4.43E-04
COG0002E	STM14_4956	STM4121	*argC*	N-acetyl-gamma-glutamyl-phosphate reductase	2.92	6.11E-03
COG0531E	STM14_5166	STM4294	*yjdE*	arginine:agmatine antiporter	4.03	1.85E-05
COG1982E	STM14_5169	STM4296	*adi*	catabolic arginine decarboxylase	5.40	3.97E-09
*COG2610GE	STM14_5378	STM4482	*idnT*	L-idonate transport protein	3.12	3.33E-03
*COG0601EP	STM14_4373	STM3629	*dppB*	dipeptide transporter permease DppB	2.30	3.32E-02
Coenzyme transport & metabolism (H)						
COG0746H	STM14_4803	STM3994	*mobA*	molybdopterin-guanine dinucleotide biosynthesis protein MobA	2.07	3.64E-02

Lipid transport & metabolism (I)						
COG1960I	STM14_0365	STM0309	*fadE*	acyl-CoA dehydrogenase	2.11	3.03E-02
COG1250I	STM14_2937	STM2388	*fadJ*	multifunctional fatty acid oxidation complex subunit alpha	2.02	3.93E-02
Inorganic ion transport & metabolism (P)						
COG1464P	STM14_0600	STM0510	*sfbA*	ABC transporter ATP-binding protein	3.00	1.63E-03
COG1135P	STM14_0601	STM0511	*sfbB*	ABC transporter ATP-binding protein	2.19	2.90E-02
COG0783P	STM14_0966	STM0831	*dps*	DNA starvation/stationary phase protection protein Dps	1.95	4.39E-02
COG3615P	STM14_1534	STM1271	*yeaR*	putative cytoplasmic protein	2.60	8.23E-03
COG3615P	STM14_2185	STM1808	-	putative cytoplasmic protein	6.67	4.38E-12
COG4771P	STM14_3348	STM2777	*iroN*	outer membrane receptor FepA	2.13	3.10E-02
*COG0601EP	STM14_4373	STM3629	*dppB*	dipeptide transporter permease DppB	2.30	3.32E-02
Secondary metabolites biosynthesis, transport & catabolism (Q)						
COG1228Q	STM14_0913	STM0787	*hutI*	imidazolonepropionase	2.31	1.77E-02
COG0412Q	STM14_4773	STM3967	*dlhH*	putative dienelactone hydrolase	2.40	2.03E-02
Translation, ribosomal structure & biogenesis (J)						
COG1544J	STM14_3266	STM2665	*yfiA*	translation inhibitor protein RaiA	3.58	7.63E-05
COG1544J	STM14_4009	STM3321	*yhbH*	putative sigma(54) modulation protein	2.02	3.64E-02
Transcription (K)						
COG2188K	STM14_0915	STM0789	*hutC*	histidine utilization repressor	2.65	9.13E-03
*COG2197TK	STM14_1526	STM1265	-	putative response regulator	1.97	4.28E-02
*COG2197TK	STM14_3463	STM2866	*sprB*	transcriptional regulator	2.34	1.40E-02
COG2207K	STM14_3465	STM2867	*hilC*	invasion regulatory protein	1.92	4.73E-02
COG2732K	STM14_4057	STM3363	*yhcO*	putative cytoplasmic protein	2.11	3.37E-02
COG2944K	STM14_4398	STM3648	*yiaG*	putative transcriptional regulator	2.73	3.42E-03
COG2944K	STM14_4557	STM3778	-	putative DNA-binding protein	2.03	4.50E-02
COG0583K	STM14_4693	STM3897	*yifA*	transcriptional regulator HdfR	2.42	1.06E-02
COG2207K	STM14_5314	STM4423	-	putative DNA-binding protein	2.81	4.35E-03
Replication, recombination & repair (L)						
COG0350L	STM14_2006	STM1659	*ogt*	O-6-alkylguanine-DNA:cysteine-protein methyltransferase	2.21	2.21E-02
Cell cycle control, cell division, chromosome partitioning (D)						
COG2846D	STM14_5283	STM4399	*ytfE*	cell morphogenesis/cell wall metabolism regulator	6.06	1.77E-10
Signal transduction mechanisms (T)						
COG0589T	STM14_0713	STM0614	*ybdQ*	putative universal stress protein	1.99	3.89E-02
*COG2197TK	STM14_1526	STM1265	-	putative response regulator	1.97	4.28E-02
COG2766T	STM14_1558	STM1285	*yeaG*	putative serine protein kinase	2.16	2.45E-02
COG0589T	STM14_2344	STM1927	*yecG*	universal stress protein UspC	2.42	1.95E-02
*COG2197TK	STM14_3463	STM2866	*sprB*	transcriptional regulator	2.34	1.40E-02
*COG0840NT	STM14_3893	STM3216	-	putative methyl-accepting chemotaxis protein	1.92	4.85E-02
*COG0840NT	STM14_4305	STM3577	*tcp*	methyl-accepting transmembrane citrate/phenol chemoreceptor	2.45	9.17E-03
*COG1762GT	STM14_4563	STM3784	-	phosphotransferase system mannitol/fructose-specific IIA component	2.34	1.36E-02
Cell motility (N)						
*COG0840NT	STM14_3893	STM3216	-	putative methyl-accepting chemotaxis protein	1.92	4.85E-02
*COG0840NT	STM14_4305	STM3577	*tcp*	methyl-accepting transmembrane citrate/phenol chemoreceptor	2.45	9.17E-03
Posttranslational modification, protein turnover, chaperones (O)						
COG0071O	STM14_1509	STM1251	-	putative molecular chaperone	2.00	3.74E-02
COG1764O	STM14_1886	STM1563	*osmC*	putative envelope protein	2.96	1.78E-03

COG0695O	STM14_3387	STM2805	*nrdH*	glutaredoxin-like protein	3.10	1.56E-03
General function prediction only (R)						
COG0446R	STM14_3432	STM2841	*norW*[1]	nitric oxide reductase	7.49	1.33E-13
COG1203R	STM14_3548	STM2944	*ygcB*	putative helicase	3.31	3.55E-04
*COG0604CR	STM14_5103	STM4245	*qor*	quinone oxidoreductase	1.96	4.69E-02
Function unknown (S)						
COG3123S	STM14_0462	STM0391	*yaiE*	hypothetical protein	2.12	3.37E-02
COG5464S	STM14_0564	STM0479	-	putative transposase	2.07	4.63E-02
COG3110S	STM14_1222	STM1077	*yccT*	hypothetical protein	3.29	4.25E-03
COG0316S	STM14_1663	STM1369	*sufA*	iron-sulfur cluster assembly scaffold protein	2.36	1.90E-02
COG2719S	STM14_2181	STM1804.S	*ycgB*	hypothetical protein	3.06	8.82E-04
COG3157S	STM14_3785	STM3131	-	putative cytoplasmic protein	2.59	1.62E-02
COG3111S	STM14_3848	STM3176	*ygiW*	putative outer membrane protein	2.03	3.66E-02
COG3237S	STM14_5097	STM4240	*yjbJ*	putative stress-response protein	1.97	4.14E-02
COG5464S	STM14_5428	STM4518	-	putative inner membrane protein	2.37	2.54E-02
Not assigned						
	STM14_0135	STM0114	*leuL*	leu operon leader peptide	3.79	3.60E-05
	STM14_0193	STM0161	*kdgT*	2-keto-3-deoxygluconate permease	2.01	4.05E-02
	STM14_0224	-	-	hypothetical protein	2.43	3.66E-02
	STM14_0383	STM0327	-	putative cytoplasmic protein	3.50	1.13E-04
	STM14_0803	STM0688	*ybfN*	putative lipoprotein	2.04	4.32E-02
	STM14_958	-	-	hypothetical protein	2.22	3.48E-02
	STM14_1060	-	-	hypothetical protein	2.53	2.47E-02
	STM14_1273	-	-	hypothetical protein	2.09	3.98E-02
	STM14_1275	STM1121	*ymdF*	putative cytoplasmic protein	2.29	1.85E-02
	STM14_1330	STM1161.S	*bssS*	biofilm formation regulatory protein BssS	2.95	1.35E-03
	STM14_1535	STM1272	*yoaG*	putative cytoplasmic protein	2.20	2.19E-02
	STM14_1593	-	-	hypothetical protein	2.14	3.08E-02
	STM14_1885	STM1562	*hdeB*	acid-resistance protein	2.60	5.30E-03
	STM14_2680	-	-	hypothetical protein	2.12	2.77E-02
	STM14_3199	-	-	hypothetical protein	4.19	5.99E-06
	STM14_3253	STM2655	-	putative cytoplasmic protein	2.24	3.43E-02
	STM14_3267	-	-	hypothetical protein	2.23	2.03E-02
	STM14_3376	-	-	hypothetical protein	2.05	3.83E-02
	STM14_3456	STM2860	*ygbA*	hypothetical protein	5.29	7.64E-09
	STM14_3630	STM3007	*ygdR*	putative peptide transport protein	2.64	4.56E-03
	STM14_3631	-	-	hypothetical protein	1.94	5.00E-02
	STM14_3749	STM3105	*yggM*	hypothetical protein	3.15	1.02E-03
	STM14_3910	STM3228	*yqjC*	hypothetical protein	1.98	4.02E-02
	STM14_3919	STM3237	*yhaL*	putative cytoplasmic protein	3.52	2.84E-03
	STM14_4278	STM3552	*yhhA*	hypothetical protein	2.52	1.67E-02
	STM14_4319	STM3590	*uspB*	universal stress protein UspB	2.26	2.03E-02
	STM14_4446	STM3688	-	putative cytoplasmic protein	3.74	4.16E-04
	STM14_4697	STM3900	*ilvL*	ilvG operon leader peptide	3.45	1.49E-04
	STM14_5259	STM4377	*aidB*	isovaleryl CoA dehydrogenase	2.64	9.13E-03
	STM14_5469	STM4552	-	putative inner membrane protein	3.80	4.19E-05

*****Genes assigned to more than one COG class

[1] Gene names according to the *E. coli* homologues

Table A 2: Down-regulated genes under acidified $NaNO_2$ shock in *S.* Typhimurium 14028 WT

COG	14028 identifier	LT2 identifier	Gene name	Product	log_2 FC	p-value (BH-adjusted)
Energy production & conversion (C)						
COG4660C	STM14_1753	STM1454	*ydgQ*	SoxR-reducing system protein RsxE	-2.41	1.38E-02
COG4659C	STM14_1754	STM1455	*ydgP*	electron transport complex protein RnfG	-2.09	3.37E-02
COG4658C	STM14_1755	STM1456	*rnfD*	electron transport complex protein RnfD	-2.65	8.27E-03
COG4656C	STM14_1756	STM1457	-	electron transport complex protein RnfC	-2.42	1.25E-02
COG2878C	STM14_1757	STM1458	*ydgM*	electron transport complex protein RnfB	-2.01	4.50E-02
COG0282C	STM14_2882	STM2337	*ackA*	acetate kinase	-2.26	1.78E-02
COG1143C	STM14_3156	STM2576	*yfhL*	putative ferredoxin	-2.86	4.25E-03
COG1032C	STM14_3839	STM3168	*ygiR*	hypothetical protein	-2.65	6.69E-03
Carbohydrate transport & metabolism (G)						
COG0524G	STM14_0578	STM0491	*gsk*	inosine-guanosine kinase	-2.79	3.58E-03
COG2814G	STM14_1016	STM0866	*mdfA*	multidrug translocase	-2.00	4.92E-02
COG2814G	STM14_1094	STM0968	*ycaD*	MFS family transporter	-4.06	6.79E-05
COG0574G	STM14_1639	STM1349	*pps*	phosphoenolpyruvate synthase	-2.35	1.26E-02
COG0483G	STM14_3124	STM2546	*suhB*	inositol monophosphatase	-3.34	2.81E-04
COG2814G	STM14_4586	STM3798	*emrD*	multidrug resistance protein D	-2.05	3.89E-02
Amino acid transport & metabolism (E)						
*COG0505EF	STM14_0077	STM0066	*carA*	carbamoyl phosphate synthase small subunit	-4.78	1.82E-06
COG1586E	STM14_0197	STM0165	*speD*	S-adenosylmethionine decarboxylase	-2.52	8.09E-03
COG1177E	STM14_1398	STM1223	*potC*	spermidine/putrescine ABC transporter membrane protein	-2.24	2.03E-02
COG1176E	STM14_1402	STM1225	*potB*	spermidine/putrescine ABC transporter membrane protein	-3.27	5.16E-04
COG3842E	STM14_1403	STM1226	*potA*	putrescine/spermidine ABC transporter ATPase	-2.44	1.08E-02
COG1605E	STM14_1531	STM1269	-	chorismate mutase	-2.79	4.10E-03
*COG0252EJ	STM14_1571	STM1294	*ansA*	asparaginase	-2.15	3.14E-02
*COG0462FE	STM14_2153	STM1780	*prsA*	ribose-phosphate pyrophosphokinase	-3.28	3.34E-04
COG0814E	STM14_2355	STM1937	*tyrP*	tyrosine-specific transport protein	-2.70	9.13E-03
COG0531E	STM14_2560	STM2068	*yeeF*	putative amino acid transport protein	-3.47	1.42E-04
COG0436E	STM14_2874	STM2331	*yfbQ*	aminotransferase AlaT	-2.12	3.08E-02
COG0814E	STM14_3650	STM3022	-	putative transport protein	-2.18	2.55E-02
COG1982E	STM14_3761	STM3114	*speC*	ornithine decarboxylase	-2.20	2.90E-02
COG0814E	STM14_4369	STM3625	*yhjV*	putative transport protein	-2.43	1.92E-02
COG0174E	STM14_4820	STM4007	*glnA*	glutamine synthetase	-2.02	3.66E-02
Nucleotide transport & metabolism (F)						
*COG0505EF	STM14_0077	STM0066	*carA*	carbamoyl phosphate synthase small subunit	-4.78	1.82E-06
COG1051F	STM14_0163	STM0137	*mutT*	nucleoside triphosphate pyrophosphohydrolase	-2.26	3.15E-02
COG0634F	STM14_0202	STM0170	*hpt*	hypoxanthine-guanine phosphoribosyltransferase	-2.46	9.13E-03
COG0528F	STM14_0259	STM0218	*pyrH*	uridylate kinase	-2.14	2.64E-02
COG0503F	STM14_0373	STM0317	*gpt*	xanthine-guanine phosphoribosyltransferase	-3.17	5.64E-04
COG0563F	STM14_0574	STM0488	*adk*	adenylate kinase	-2.43	1.01E-02
COG0167F	STM14_1200	STM1058	*pyrD*	dihydroorotate dehydrogenase 2	-2.47	9.70E-03

COG0418F	STM14_1332	STM1163	*pyrC*	dihydroorotase	-2.22	2.49E-02
COG0015F	STM14_1410	STM1232	*purB*	adenylosuccinate lyase	-3.16	6.27E-04
COG0284F	STM14_2064	STM1707	*pyrF*	orotidine 5'-phosphate decarboxylase	-2.94	2.40E-03
*COG0462FE	STM14_2153	STM1780	*prsA*	ribose-phosphate pyrophosphokinase	-3.28	3.34E-04
COG0572F	STM14_2618	STM2122	*udk*	uridine kinase	-2.68	4.56E-03
COG0034F	STM14_2909	STM2362	*purF*	amidophosphoribosyltransferase	-2.06	3.46E-02
COG2233F	STM14_3061	STM2497	*uraA*	uracil transporter	-3.94	3.88E-05
COG0150F	STM14_3064	STM2499.S	*purM*	phosphoribosylaminoimidazole synthetase	-2.13	3.15E-02
COG0519F	STM14_3075	STM2510	*guaA*	bifunctional GMP synthase/glutamine amidotransferase protein	-2.26	1.83E-02
COG0516F	STM14_3076	STM2511	*guaB*	inositol-5-monophosphate dehydrogenase	-3.80	4.19E-05
COG0207F	STM14_3617	STM3001	*thyA*	thymidylate synthase	-1.96	4.96E-02
COG1457F	STM14_4024	STM3333	*codB*	cytosine permease	-2.21	3.74E-02
COG0461F	STM14_4495	STM3733	*pyrE*	orotate phosphoribosyltransferase	-3.33	4.43E-04
COG0138F	STM14_5017	STM4176	*purH*	bifunctional phosphoribosylaminoimidazolecarboxamide formyltransferase/IMP cyclohydrolase	-2.63	9.13E-03
Coenzyme transport & metabolism (H)						
COG0262H	STM14_0106	STM0087	*folA*	dihydrofolate reductase	-2.99	3.21E-03
COG0413H	STM14_0216	STM0182	*panB*	3-methyl-2-oxobutanoate hydroxymethyltransferase	-3.18	2.97E-03
COG0301H	STM14_0503	STM0425	*thiI*	thiamine biosynthesis protein ThiI	-1.96	4.39E-02
COG2240H	STM14_1748	STM1450	*pdxY*	pyridoxamine kinase	-2.11	2.90E-02
COG2226H	STM14_2217	STM1835	*rrmA*	23S rRNA methyltransferase A	-2.81	6.11E-03
COG2227H	STM14_2318	STM1906	*yecP*	hypothetical protein	-2.13	3.15E-02
COG1477H	STM14_2796	STM2266	*apbE*	thiamine biosynthesis lipoprotein ApbE	-2.00	4.39E-02
COG0720H	STM14_3554	STM2949	*ptpS*	putative 6-pyruvoyl tetrahydrobiopterin synthase	-4.04	1.84E-04
COG1072H	STM14_4975	STM4139	*coaA*	pantothenate kinase	-2.08	3.15E-02
Lipid transport & metabolism (I)						
COG0764I	STM14_1211	STM1067	*fabA*	3-hydroxydecanoyl-ACP dehydratase	-2.71	3.86E-03
COG1607I	STM14_2099	STM1736	*yciA*	acyl-CoA thioester hydrolase	-2.58	1.57E-02
COG1835I	STM14_2758	STM2232	*oafA*	O-antigen acetylase	-3.04	8.65E-04
Inorganic ion transport & metabolism (P)						
COG0306P	STM14_4318	STM3589	*pitA*	low-affinity phosphate transporter	-2.41	1.13E-02
Secondary metabolites biosynthesis, transport & catabolism (Q)						
COG1021Q	STM14_0694	STM0596	*entE*	enterobactin synthase subunit E	-2.02	4.06E-02
Translation, ribosomal structure & biogenesis (J)						
COG0268J	STM14_0052	STM0043	*rpsT*	30S ribosomal protein S20	-2.54	6.69E-03
COG0809J	STM14_0478	STM0404	*queA*	S-adenosylmethionine--tRNA ribosyltransferase-isomerase	-2.31	1.95E-02
*COG0513LKJ	STM14_0951	STM0820	*rhlE*	ATP-dependent RNA helicase RhlE	-3.54	2.75E-04
COG0621J	STM14_0996	STM0852	*yliG*	putative FeS oxidoreductase	-3.90	4.19E-05
COG0361J	STM14_1075	STM0953	*infA*	translation initiation factor IF-1	-3.55	9.21E-05
COG0539J	STM14_1110	STM0981	*rpsA*	30S ribosomal protein S1	-2.15	2.45E-02
COG0482J	STM14_1412	STM1234.S	*trmU*	tRNA (5-methyl aminomethyl-2-thiouridylate)-methyltransferase	-1.96	4.63E-02
*COG0252EJ	STM14_1571	STM1294	*ansA*	asparaginase	-2.15	3.14E-02
COG0016J	STM14_1624	STM1337	*pheS*	phenylalanyl-tRNA synthetase subunit alpha	-2.73	3.93E-03
*COG0513LKJ	STM14_2001	STM1655	*dbpA*	ATP-dependent RNA helicase DbpA	-2.11	4.28E-02
COG0023J	STM14_2063	STM1706	*yciH*	translation initiation factor Sui1	-3.04	2.40E-03

COG1187J	STM14_2082	STM1719	*yciL*	23S rRNA pseudouridylate synthase B	-2.80	4.25E-03
COG0144J	STM14_2237	STM1850	*yebU*	rRNA (cytosine-C(5)-)-methyltransferase RsmF	-2.66	9.13E-03
COG0018J	STM14_2322	STM1909	*argS*	arginyl-tRNA synthetase	-2.27	1.78E-02
COG0231J	STM14_2733	STM2211.S	*yeiP*	elongation factor P	-2.36	1.31E-02
COG2890J	STM14_2934	STM2385	*yfcB*	N5-glutamine S-adenosyl-L-methionine-dependent methyltransferase	-2.21	2.21E-02
COG0336J	STM14_3277	STM2674	*trmD*	tRNA (guanine-N(1)-)-methyltransferase	-2.35	1.25E-02
COG0806J	STM14_3278	STM2675	*rimM*	16S rRNA-processing protein	-2.52	7.25E-03
COG0828J	STM14_3886	STM3209	*rpsU*	30S ribosomal protein S21	-4.78	1.11E-07
COG2813J	STM14_3899	STM3220	*ygjO*	putative methyltransferase	-2.24	2.03E-02
*COG0513LKJ	STM14_3962	STM3280.S	*deaD*	ATP-dependent RNA helicase DeaD	-2.49	9.58E-03
COG0184J	STM14_3966	STM3283	*rpsO*	30S ribosomal protein S15	-2.60	5.31E-03
COG0211J	STM14_3990	STM3303	*rpmA*	50S ribosomal protein L27	-2.16	2.32E-02
COG0261J	STM14_3991	STM3304	*rplU*	50S ribosomal protein L21	-2.64	4.56E-03
COG0102J	STM14_4037	STM3345	*rplM*	50S ribosomal protein L13	-2.43	9.46E-03
COG0042J	STM14_4082	STM3384	*yhdG*	tRNA-dihydrouridine synthase B	-3.18	4.68E-04
COG0203J	STM14_4117	STM3414	*rplQ*	50S ribosomal protein L17	-2.14	2.51E-02
COG0522J	STM14_4119	STM3416	*rpsD*	30S ribosomal protein S4	-2.33	1.31E-02
COG0100J	STM14_4120	STM3417	*rpsK*	30S ribosomal protein S11	-2.06	3.24E-02
COG1841J	STM14_4125	STM3422	*rpmD*	50S ribosomal protein L30	-1.97	4.07E-02
COG0098J	STM14_4126	STM3423	*rpsE*	30S ribosomal protein S5	-2.27	1.67E-02
COG0256J	STM14_4127	STM3424	*rplR*	50S ribosomal protein L18	-2.32	1.36E-02
COG0097J	STM14_4128	STM3425	*rplF*	50S ribosomal protein L6	-2.55	6.41E-03
COG0096J	STM14_4129	STM3426	*rpsH*	30S ribosomal protein S8	-3.32	2.75E-04
COG0199J	STM14_4130	STM3427.S	*rpsN*	30S ribosomal protein S14	-3.19	4.43E-04
COG0094J	STM14_4131	STM3428	*rplE*	50S ribosomal protein L5	-2.66	4.25E-03
COG0198J	STM14_4132	STM3429	*rplX*	50S ribosomal protein L24	-2.46	9.13E-03
COG0185J	STM14_4139	STM3436	*rpsS*	30S ribosomal protein S19	-2.35	1.26E-02
COG0090J	STM14_4140	STM3437	*rplB*	50S ribosomal protein L2	-2.01	3.66E-02
COG0089J	STM14_4141	STM3438	*rplW*	50S ribosomal protein L23	-2.45	9.13E-03
COG0088J	STM14_4142	STM3439	*rplD*	50S ribosomal protein L4	-2.35	1.25E-02
COG0087J	STM14_4143	STM3440	*rplC*	50S ribosomal protein L3	-2.41	1.01E-02
COG0051J	STM14_4144	STM3441	*rpsJ*	30S ribosomal protein S10	-3.08	6.95E-04
COG0049J	STM14_4151	STM3447	*rpsG*	30S ribosomal protein S7	-2.49	8.23E-03
COG0267J	STM14_4489	STM3727	*rpmG*	50S ribosomal protein L33	-3.09	6.80E-04
COG0227J	STM14_4490	STM3728	*rpmB*	50S ribosomal protein L28	-2.38	1.13E-02
COG0689J	STM14_4496	STM3734	*rph*	ribonuclease PH	-2.86	2.40E-03
COG0230J	STM14_4634	STM3839	*rpmH*	50S ribosomal protein L34	-2.33	1.31E-02
COG0594J	STM14_4635	STM3840	*rnpA*	ribonuclease P	-3.52	1.08E-04
COG0080J	STM14_4986	STM4149	*rplK*	50S ribosomal protein L11	-2.15	2.45E-02
COG0360J	STM14_5275	STM4391	*rpsF*	30S ribosomal protein S6	-3.38	2.16E-04
COG0238J	STM14_5277	STM4393	*rpsR*	30S ribosomal protein S18	-3.66	5.61E-05
COG2813J	STM14_5473	STM4556	*rsmC*	16S ribosomal RNA m2G1207 methyltransferase	-2.50	9.74E-03
COG4108J	STM14_5478	STM4560	*prfC*	peptide chain release factor 3	-2.43	1.06E-02
Transcription (K)						
*COG0553KL	STM14_0116	STM0096	*hepA*	ATP-dependent helicase HepA	-2.09	3.46E-02
COG1278K	STM14_0732	STM0629	*cspE*	cold shock protein CspE	-3.42	1.65E-04
*COG0513LKJ	STM14_0951	STM0820	*rhlE*	ATP-dependent RNA helicase RhlE	-3.54	2.75E-04
COG1609K	STM14_1727	STM1430	*purR*	DNA-binding transcriptional repressor PurR	-2.33	1.69E-02
*COG0513LKJ	STM14_2001	STM1655	*dbpA*	ATP-dependent RNA helicase DbpA	-2.11	4.28E-02

COG4776K	STM14_2056	STM1702	*rnb*	exoribonuclease II	-2.25	1.89E-02
COG1414K	STM14_3742	STM3098	-	putative transcriptional regulator	-2.07	4.85E-02
*COG0513LKJ	STM14_3962	STM3280.S	*deaD*	ATP-dependent RNA helicase DeaD	-2.49	9.58E-03
*COG2901KL	STM14_4083	STM3385	*fis*	DNA-binding protein Fis	-3.85	2.71E-05
COG0202K	STM14_4118	STM3415	*rpoA*	DNA-directed RNA polymerase subunit alpha	-1.98	4.03E-02
Replication, recombination & repair (L)						
*COG0553KL	STM14_0116	STM0096	*hepA*	ATP-dependent helicase HepA	-2.09	3.46E-02
*COG0513LKJ	STM14_0951	STM0820	*rhlE*	ATP-dependent RNA helicase RhlE	-3.54	2.75E-04
COG0116L	STM14_1204	STM1061	*ycbY*	23S rRNA m(2)G2445 methyltransferase	-2.48	1.01E-02
COG0188L	STM14_2804	STM2272	*gyrA*	DNA gyrase subunit A	-2.04	3.46E-02
*COG2901KL	STM14_4083	STM3385	*fis*	DNA-binding protein Fis	-3.85	2.71E-05
COG3344L	STM14_4641	STM3846.s	-	putative reverse transcriptase	-2.47	9.13E-03
COG2965L	STM14_5276	STM4392	*priB*	primosomal replication protein N	-2.88	1.83E-03
*COG0513LKJ	STM14_2001	STM1655	*dbpA*	ATP-dependent RNA helicase DbpA	-2.11	4.28E-02
*COG0513LKJ	STM14_3962	STM3280.S	*deaD*	ATP-dependent RNA helicase DeaD	-2.49	9.58E-03
Signal transduction mechanisms (T)						
COG3109T	STM14_2233	STM1846	*proQ*	putative solute/DNA competence effector	-2.47	9.13E-03
Cell wall/membrane/envelope biogenesis (M)						
COG0768M	STM14_0148	STM0122	*ftsI*	division specific transpeptidase	-2.22	1.95E-02
COG0463M	STM14_0651	STM0558	*yfdH*	putative glycosyltransferase	-4.37	3.91E-05
COG3137M	STM14_1611	STM1327	*ydiY*	putative outer membrane protein	-3.74	4.75E-05
COG0768M	STM14_2324	STM1910	-	putative penicillin-binding protein	-2.53	1.06E-02
COG4623M	STM14_3147	STM2567	*yfhD*	putative transglycosylase	-2.34	1.38E-02
COG0463M	STM14_5055	STM4205	-	putative phage glycosyltransferase	-3.24	4.46E-04
COG1346M	STM14_5138	STM4272	-	putative inner membrane protein	-2.38	1.57E-02
Cell motility (N)						
*COG1261NO	STM14_1343	STM1173	*flgA*	flagellar basal body P-ring biosynthesis protein FlgA	-2.77	5.12E-03
COG1815N	STM14_1345	STM1174	*flgB*	flagellar basal body rod protein FlgB	-2.02	3.72E-02
COG2063N	STM14_1351	STM1180	*flgH*	flagellar basal body L-ring protein	-2.78	4.56E-03
*COG1298NU	STM14_2327	STM1913	*flhA*	flagellar biosynthesis protein FlhA	-2.13	3.08E-02
*COG1377NU	STM14_2328	STM1914	*flhB*	flagellar biosynthesis protein FlhB	-2.60	9.13E-03
*COG1677NU	STM14_2388	STM1968	*fliE*	flagellar hook-basal body protein FliE	-2.89	5.93E-03
*COG1766NU	STM14_2390	STM1969	*fliF*	flagellar MS-ring protein	-2.36	1.26E-02
COG1536N	STM14_2391	STM1970	*fliG*	flagellar motor switch protein G	-2.02	3.72E-02
Intracellular trafficking, secretion, & vesicular transport (U)						
COG0848U	STM14_0868	STM0746	*tolR*	colicin uptake protein TolR	-2.03	3.66E-02
*COG1298NU	STM14_2327	STM1913	*flhA*	flagellar biosynthesis protein FlhA	-2.13	3.08E-02
*COG1377NU	STM14_2328	STM1914	*flhB*	flagellar biosynthesis protein FlhB	-2.60	9.13E-03
*COG1677NU	STM14_2388	STM1968	*fliE*	flagellar hook-basal body protein FliE	-2.89	5.93E-03
*COG1766NU	STM14_2390	STM1969	*fliF*	flagellar MS-ring protein	-2.36	1.26E-02
COG1314U	STM14_3976	STM3293	*secG*	preprotein translocase subunit SecG	-1.98	4.03E-02
COG0706U	STM14_4637	STM3842	*yidC*	putative inner membrane protein translocase component YidC	-2.78	2.75E-03
COG0805U	STM14_4781	STM3975	*tatC*	TatABCE protein translocation system subunit	-2.05	3.46E-02
COG0690U	STM14_4984	STM4147	*secE*	preprotein translocase subunit SecE	-2.14	2.77E-02
Posttranslational modification, protein turnover, chaperones (O)						
COG1067O	STM14_1212	STM1068	*lonH*	putative protease	-2.26	1.89E-02
*COG1261NO	STM14_1343	STM1173	*flgA*	flagellar basal body P-ring biosynthesis protein FlgA	-2.77	5.12E-03
COG1214O	STM14_2202	STM1820	*yeaZ*	putative molecular chaperone	-2.43	1.87E-02
COG0826O	STM14_2634	STM2136	*yegQ*	putative protease	-3.38	5.08E-04

General function prediction only (R)						
COG1054R	STM14_1324	STM1156	*yceA*	hypothetical protein	-2.65	4.93E-03
COG2915R	STM14_1411	STM1233	*ycfC*	hypothetical protein	-2.54	8.96E-03
COG4106R	STM14_2317	STM1905	*yecO*	putative SAM-dependent methyltransferase	-2.45	1.08E-02
COG1160R	STM14_3089	STM2519	*engA*	GTP-binding protein EngA	-2.38	1.23E-02
COG0820R	STM14_3097	STM2525	*yfgB*	hypothetical protein	-2.62	5.19E-03
COG1159R	STM14_3160	STM2580	*era*	GTP-binding protein Era	-2.33	1.38E-02
COG0536R	STM14_3988	STM3301	*obgE*	GTPase ObgE	-2.47	9.46E-03
COG2252R	STM14_4646	STM3851.S	*yieG*	putative xanthine/uracil permease family protein	-2.07	4.03E-02
COG2252R	STM14_5133	STM4268	*yjcD*	hypothetical protein	-2.15	4.39E-02
COG1380R	STM14_5137	STM4271	-	LrgA family protein	-2.14	3.44E-02
Function unknown (S)						
COG1576S	STM14_0749	STM0641	*ybeA*	SPOUT methyltransferase superfamily protein	-2.15	3.74E-02
COG0799S	STM14_0750	STM0642	*ybeB*	hypothetical protein	-2.64	9.73E-03
COG1376S	STM14_977	STM0837	*ybiS*	hypothetical protein	-2.82	2.64E-03
COG1944S	STM14_1101	STM0975	*ycaO*	putative cytoplasmic protein	-3.12	7.68E-04
COG3781S	STM14_1845	STM1527	-	putative inner membrane protein	-2.64	6.09E-03
COG2983S	STM14_2190	STM1811	*ycgN*	hypothetical protein	-2.18	3.15E-02
COG3101S	STM14_2930	STM2381	*yfcM*	putative cytoplasmic protein	-1.92	4.97E-02
COG2990S	STM14_3352	STM2781	*virK*	virulence protein	-3.38	2.76E-04
COG2862S	STM14_3818	STM3153	*yqhA*	hypothetical protein	-2.21	2.52E-02
COG3036S	STM14_4114	STM3411	-	putative cytoplasmic protein	-1.96	4.85E-02
COG2860S	STM14_4502	STM3738	-	putative inner membrane protein	-2.61	7.47E-03
COG0759S	STM14_4636	STM3841	-	hypothetical protein	-3.31	4.43E-04
COG3085S	STM14_4694	STM3898	*yifE*	hypothetical protein	-1.92	4.77E-02
COG2246S	STM14_5056	STM4206	-	putative phage glucose translocase	-2.33	2.32E-02
COG3242S	STM14_5246	STM4365	*yjeT*	putative inner membrane protein	-2.07	4.04E-02
Not assigned						
	STM14_0296	-	-	hypothetical protein	-5.68	2.21E-09
	STM14_0731	STM0628	*pagP*	palmitoyl transferase for Lipid A	-2.90	3.53E-03
	STM14_1076	STM0954	-	putative inner membrane protein	-3.21	4.40E-04
	STM14_1493	STM1242	*envE*	putative envelope protein	-3.49	8.10E-04
	STM14_1760	STM1461.S	*ydgT*	oriC-binding nucleoid-associated protein	-2.14	2.89E-02
	STM14_1982	STM1638	-	putative SAM-dependent methyltransferase	-2.25	2.72E-02
	STM14_2366	-	-	putative inner membrane protein	-2.57	6.92E-03
	STM14_2367	STM1949	*yecF*	hypothetical protein	-1.97	4.05E-02
	STM14_2489	STM2005	-	putative endoprotease	-4.86	5.54E-06
	STM14_2562	-	-	hypothetical protein	-4.22	5.54E-06
	STM14_2881	-	-	hypothetical protein	-2.14	2.78E-02
	STM14_3146	STM2566	-	hypothetical protein	-2.55	1.83E-02
	STM14_3353	-	-	hypothetical protein	-2.65	5.55E-03
COG5653	STM14_3354	STM2782	*mig-14*	putative transcriptional activator	-2.25	1.85E-02
	STM14_3467	STM2868	*orgC*	putative cytoplasmic protein	-2.30	2.03E-02
	STM14_3468	STM2869	*orgB*	needle complex export protein	-2.70	4.25E-03
	STM14_3732	STM3089	*yqgD*	putative inner membrane protein	-2.22	2.10E-02
	STM14_4633	-	-	hypothetical protein	-2.39	2.11E-02
	STM14_4640	STM3845	-	putative inner membrane protein	-2.10	2.95E-02
	STM14_4797	-	-	hypothetical protein	-5.59	2.69E-09
	STM14_4898	-	-	hypothetical protein	-2.25	3.06E-02
	STM14_4970	-	-	hypothetical protein	-5.49	3.97E-09

	STM14_5054	STM4204	-	putative inner membrane protein	-2.85	2.50E-03
	STM14_5196	-	-	hypothetical protein	-3.02	1.66E-03

*****Genes assigned to more than one COG class

Table A 3: Up-regulated genes under acidified $NaNO_2$ adaptation in *S.* Typhimurium 14028 WT

COG	14028 identifier	LT2 identifier	Gene name	Product	log_2 FC	p-value (BH-adjusted)
Energy production & conversion (C)						
COG1151C	STM14_1052	STM0937	*hcp*	hydroxylamine reductase	3.38	2.74E-04
COG1018C	STM14_3135	STM2556	*hmpA*	nitric oxide dioxygenase	4.53	1.62E-06
Carbohydrate transport & metabolism (G)						
COG1129G	STM14_4899	STM4074	*ego*	putative ABC-type aldose transport system ATPase component	2.89	2.88E-03
COG1172G	STM14_4900	STM4075	*ydeY*	putative sugar transport protein	2.74	5.86E-03
COG1172G	STM14_4901	STM4076	*ydeZ*	putative sugar transport protein	2.92	2.61E-03
COG1879G	STM14_4902	STM4077	*yneA*	putative sugar transport protein	2.34	2.42E-02
COG1830G	STM14_4903	STM4078	*yneB*	aldolase	2.15	4.66E-02
Amino acid transport & metabolism (E)						
COG0531E	STM14_0817	STM0700	*potE*	putrescine transporter	3.40	2.60E-04
COG1982E	STM14_0818	STM0701	*speF*	ornithine decarboxylase	3.23	5.40E-04
COG2502E	STM14_4674	STM3877	*asnA*	asparagine synthetase AsnA	2.15	4.66E-02
COG0531E	STM14_5166	STM4294	*yjdE*	arginine:agmatine antiporter	3.59	1.97E-04
COG1982E	STM14_5169	STM4296	*adi*	catabolic arginine decarboxylase	2.81	4.01E-03
COG0078E	STM14_5358	STM4465	-	ornithine carbamoyltransferase	3.56	1.97E-04
COG0549E	STM14_5360	STM4466	-	carbamate kinase	2.89	4.80E-03
COG2235E	STM14_5361	STM4467	-	arginine deiminase	2.72	5.86E-03
Coenzyme transport & metabolism (H)						
*COG1120PH	STM14_0688	STM0590	*fepC*	iron-enterobactin transporter ATP-binding protein	4.50	7.64E-06
*COG1169HQ	STM14_0693	STM0595	*entC*	isochorismate synthase	3.42	4.84E-04
Lipid transport & metabolism (I)						
*COG1028IQR	STM14_0696	STM0598	*entA*	2,3-dihydroxybenzoate-2,3-dehydrogenase	4.57	7.64E-06
Inorganic ion transport & metabolism (P)						
COG1629P	STM14_0228	STM0191	*fhuA*	ferrichrome outer membrane transporter	4.05	1.04E-05
COG0614P	STM14_0230	STM0193	*fhuD*	iron-hydroxamate transporter substrate-binding subunit	4.18	1.53E-05
COG0609P	STM14_0231	STM0194	*fhuB*	iron-hydroxamate transporter permease subunit	4.46	5.57E-06
COG4771P	STM14_0682	STM0585	*fepA*	outer membrane receptor FepA	2.40	1.97E-02
*COG1120PH	STM14_0688	STM0590	*fepC*	iron-enterobactin transporter ATP-binding protein	4.50	7.64E-06
COG4592P	STM14_0692	STM0594	*fepB*	iron-enterobactin transporter periplasmic binding protein	2.24	4.27E-02
COG3615P	STM14_1534	STM1271	*yeaR*	putative cytoplasmic protein	3.37	2.87E-04
COG3615P	STM14_2185	STM1808	-	putative cytoplasmic protein	4.41	5.57E-06
COG4771P	STM14_2713	STM2199	*cirA*	colicin I receptor	2.37	2.74E-02
COG0803P	STM14_3458	STM2861	*sitA*	putative periplasmic binding protein	2.67	7.65E-03
COG2906P	STM14_4147	STM3444	*bfd*	bacterioferritin-associated ferredoxin	4.72	7.45E-07
COG1918P	STM14_4221	STM3505	*feoA*	ferrous iron transport protein A	2.87	3.61E-03
COG0370P	STM14_4222	STM3506	*feoB*	ferrous iron transport protein B	2.64	7.57E-03

Secondary metabolites biosynthesis, transport & catabolism (Q)						
COG1020Q	STM14_0686	STM0588	*entF*	enterobactin synthase subunit F	3.03	1.75E-03
*COG1169HQ	STM14_0693	STM0595	*entC*	isochorismate synthase	3.42	4.84E-04
COG1021Q	STM14_0694	STM0596	*entE*	enterobactin synthase subunit E	3.52	2.74E-04
COG1535Q	STM14_0695	STM0597	*entB*	2,3-dihydro-2,3-dihydroxybenzoate synthetase	5.58	1.23E-07
*COG1028IQR	STM14_0696	STM0598	*entA*	2,3-dihydroxybenzoate-2,3-dehydrogenase	4.57	7.64E-06
COG0179Q	STM14_2684	STM2177	-	putative flutathione S-transferase	2.62	1.21E-02
Transcription (K)						
*COG2197TK	STM14_3463	STM2866	*sprB*	transcriptional regulator	2.46	1.48E-02
COG2207K	STM14_3465	STM2867	*hilC*	invasion regulatory protein	2.21	3.85E-02
Defense mechanisms (V)						
COG0841V	STM14_2626	STM2128	*yegO*	multidrug efflux system subunit MdtC	2.34	2.83E-02
Signal transduction mechanisms (T)						
*COG2197TK	STM14_3463	STM2866	*sprB*	transcriptional regulator	2.46	1.48E-02
Cell wall/membrane/envelope biogenesis (M)						
COG0810M	STM14_2100	STM1737	*tonB*	transporter	2.67	8.01E-03
COG2222M	STM14_4331	STM3601	-	putative phosphosugar isomerase	2.27	3.47E-02
Intracellular trafficking, secretion, & vesicular transport (U)						
COG0848U	STM14_3824	STM3158	*exbD*	biopolymer transport protein ExbD	2.19	4.24E-02
General function prediction only (R)						
*COG1028IQR	STM14_0696	STM0598	*entA*	2,3-dihydroxybenzoate-2,3-dehydrogenase	4.57	7.64E-06
COG3467R	STM14_0816	STM0699	-	putative cytoplasmic protein	3.44	2.60E-04
COG4114R	STM14_5466	STM4550	*fhuF*	ferric hydroximate transport ferric iron reductase	2.62	1.04E-02
Function unknown (S)						
COG3391S	STM14_1918	STM1586	-	hypothetical protein	2.28	2.89E-02
COG2128S	STM14_3385	STM2804	-	putative cytoplasmic protein	3.32	6.83E-04
COG1917S	STM14_4895	STM4071	-	putative mannose-6-phosphate isomerase	2.31	2.89E-02
Not assigned						
	STM14_0227	-	-	hypothetical protein	3.75	4.88E-05
	STM14_0819	-	-	hypothetical protein	2.21	3.85E-02
	STM14_1535	STM1272	*yoaG*	putative cytoplasmic protein	3.03	1.38E-03
	STM14_1885	STM1562	*hdeB*	acid-resistance protein	7.12	1.78E-13
	STM14_2227	STM1841	-	hypothetical protein	2.55	1.12E-02
	STM14_2269	STM1868A	-	lytic enzyme	3.17	7.45E-04
	STM14_2270	-	-	hypothetical protein	3.29	4.18E-04
	STM14_2271	-	-	hypothetical protein	4.24	7.82E-06
	STM14_3456	STM2860	*ygbA*	hypothetical protein	4.20	7.64E-06
	STM14_4223	STM3507	*yhgG*	putative cytoplasmic protein	2.82	5.37E-03

*Genes assigned to more than one COG class

Table A 4: Down-regulated genes under acidified $NaNO_2$ adaptation in *S.* Typhimurium 14028 WT

COG	14028 identifier	LT2 identifier	Gene name	Product	log_2 FC	p-value (BH-adjusted)
Energy production & conversion (C)						
COG0243C	STM14_1089	STM0964	*dmsA*	anaerobic dimethyl sulfoxide reductase subunit A	-2.75	4.94E-03
COG0437C	STM14_1090	STM0965	*dmsB*	anaerobic dimethyl sulfoxide reductase subunit B	-4.56	1.04E-05
COG0243C	STM14_1677	STM1383	*ttrA*	tetrathionate reductase complex subunit A	-3.88	2.38E-05
COG0437C	STM14_1679	STM1385	*ttrB*	tetrathionate reductase complex subunit B	-2.19	4.10E-02
COG0437C	STM14_1893	STM1569	*fdnH*	formate dehydrogenase-N beta subunit	-2.84	3.75E-03
COG2181C	STM14_2129	STM1761	*narI*	nitrate reductase 1 subunit gamma	-2.54	1.12E-02
COG2180C	STM14_2130	STM1762	*narJ*	nitrate reductase 1 subunit delta	-2.51	1.21E-02
COG1140C	STM14_2131	STM1763	*narH*	nitrate reductase 1 subunit beta	-2.61	7.95E-03
COG3005C	STM14_2784	STM2255	*napC*	cytochrome *c*-type protein NapC	-3.97	1.53E-05
COG3043C	STM14_2785	STM2256	*napB*	diheme cytochrome *c*550	-4.31	5.57E-06
COG0348C	STM14_2786	STM2257	*napH*	quinol dehydrogenase membrane component	-3.73	5.57E-05
COG0437C	STM14_2787	STM2258	*napG*	quinol dehydrogenase periplasmic component	-4.34	1.04E-05
COG0243C	STM14_2788	STM2259	*napA*	nitrate reductase	-3.26	4.84E-04
COG4231C	STM14_2790	STM2261	*napF*	ferredoxin-type protein	-2.51	1.21E-02
COG0243C	STM14_3103	STM2530	-	putative anaerobic dimethylsulfoxide reductase	-2.71	8.23E-03
COG0243C	STM14_5178	STM4305.S	-	putative anaerobic dimethylsulfoxide reductase subunit A	-2.51	1.26E-02
COG0437C	STM14_5179	STM4306	-	putative anaerobic dimethylsulfoxide reductase subunit B	-3.23	8.77E-04
Carbohydrate transport & metabolism (G)						
COG3414G	STM14_2888	STM2343	-	putative cytoplasmic protein	-2.32	3.85E-02
Amino acid transport & metabolism (E)						
COG0747E	STM14_1515	STM1255	-	putative ABC transporter periplasmic binding protein	-2.28	2.89E-02
*COG0601EP	STM14_1516	STM1256	-	putative ABC transporter protein	-2.34	2.53E-02
*COG1173EP	STM14_1517	STM1257	-	putative ABC transporter protein	-2.45	1.75E-02
*COG1124EP	STM14_1519	STM1259	-	ABC transporter ATP-binding protein	-2.71	6.49E-03
Inorganic ion transport & metabolism (P)						
*COG0601EP	STM14_1516	STM1256	-	putative ABC transporter protein	-2.34	2.53E-02
*COG1173EP	STM14_1517	STM1257	-	putative ABC transporter protein	-2.45	1.75E-02
*COG1124EP	STM14_1519	STM1259	-	ABC transporter ATP-binding protein	-2.71	6.49E-03
COG3301P	STM14_1678	STM1384	*ttrC*	tetrathionate reductase complex subunit C	-2.63	7.70E-03
COG1528P	STM14_2353	STM1935	*ftn*	ferritin	-2.81	3.75E-03
COG3062P	STM14_2789	STM2260	*napD*	assembly protein for periplasmic nitrate reductase	-2.94	2.51E-03
COG1118P	STM14_3716	STM3075	-	putative ABC-type cobalt transport system ATP-binding component	-2.52	1.93E-02
COG1858P	STM14_4612	STM3820	-	putative cytochrome *c* peroxidase	-2.61	8.01E-03
COG0376P	STM14_4936	STM4106	*katG*	hydroperoxidase	-2.38	1.97E-02

COG3303P	STM14_5143	STM4277	*nrfA*	cytochrome *c* nitrite reductase	-3.44	2.60E-04
Transcription (K)						
*COG0378OK	STM14_3451	STM2855	*hypB*	hydrogenase nickel incorporation protein HypB	-2.50	1.33E-02
*COG3604KT	STM14_3455	STM2859	*fhlA*	formate hydrogen-lyase transcriptional activator	-2.20	4.28E-02
Signal transduction mechanisms (T)						
*COG3604KT	STM14_3455	STM2859	*fhlA*	formate hydrogen-lyase transcriptional activator	-2.20	4.28E-02
Cell wall/membrane/envelope biogenesis (M)						
COG3047M	STM14_2095	STM1732	*ompW*	outer membrane protein W	-2.30	2.78E-02
Cell motility (N)						
*COG3188NU	STM14_2653	STM2150	*stcC*	putative outer membrane protein	-2.55	1.26E-02
*COG3539NU	STM14_2655	STM2152	*stcA*	putative fimbrial-like protein	-3.72	5.44E-05
Intracellular trafficking, secretion & vesicular transport (U)						
*COG3188NU	STM14_2653	STM2150	*stcC*	putative outer membrane protein	-2.55	1.26E-02
*COG3539NU	STM14_2655	STM2152	*stcA*	putative fimbrial-like protein	-3.72	5.44E-05
Posttranslational modification, protein turnover, chaperones (O)						
COG4133O	STM14_2783	STM2254	*ccmA_1*	cytochrome *c* biogenesis protein CcmA	-3.11	2.52E-03
*COG0378OK	STM14_3451	STM2855	*hypB*	hydrogenase nickel incorporation protein HypB	-2.50	1.33E-02
COG0409O	STM14_3453	STM2857	*hypD*	putative hydrogenase formation protein	-2.18	4.66E-02
COG0309O	STM14_3454	STM2858	*hypE*	putative hydrogenase formation protein	-2.97	3.19E-03
COG0826O	STM14_3956	STM3274	*yhbU*	putative protease	-2.78	4.70E-03
COG0826O	STM14_3957	STM3275.S	*yhbV*	putative protease	-3.51	2.12E-04
COG1138O	STM14_5147	STM4281	*nrfE*	formate-dependent nitrite reductase	-2.94	4.57E-03
COG1180O	STM14_5484	STM4565	*yjjW*	pyruvate formate lyase-activating enzyme	-2.31	3.81E-02
General function prediction only (R)						
COG1123R	STM14_1518	STM1258	-	ABC transporter ATP-binding protein	-3.18	8.66E-04
COG2962R	STM14_3601	STM2986.Sc	-	putative integral membrane protein	-2.64	7.65E-03
COG1661R	STM14_3712	STM3071	-	putative DNA-binding protein	-2.82	4.57E-03
COG0375R	STM14_3808	STM3144	*hypA_2*	hydrogenase nickel incorporation protein HybF	-2.25	4.48E-02
COG3381R	STM14_5181	STM4308	-	putative anaerobic dehydrogenase component	-3.24	8.34E-04
Function unknown (S)						
COG1584S	STM14_0009	STM0009	*yaaH*	hypothetical protein	-2.62	1.22E-02
Not assigned						
	STM14_1092	-	-	hypothetical protein	-2.48	2.17E-02
	STM14_2354	STM1936	*yecH*	putative cytoplasmic protein	-2.32	2.89E-02
	STM14_2652	STM2149	*stcD*	putative outer membrane lipoprotein	-2.46	1.82E-02
	STM14_3211	-	-	hypothetical protein	-2.59	8.23E-03
	STM14_3713	STM3072	-	putative inner membrane protein	-2.77	4.84E-03
	STM14_5485	STM4566	*yjjI*	hypothetical protein	-2.22	3.85E-02

*Genes assigned to more than one COG class

Table A 5: Up-regulated genes in response to 150 mg/l $NaNO_2$ on RD0 in *S.* Typhimurium 14028 WT

COG	14028 identifier	LT2 identifier	Gene name	Product	log_2 FC	p-value (BH-adjusted)
Energy production & conversion (C)						
COG0426C	STM14_3431	STM2840	*norV*[1]	anaerobic nitric oxide reductase flavorubredoxin	7.61	3.70E-15
Coenzyme transport & metabolism (H)						
*COG1169HQ	STM14_0693	STM0595	*entC*	isochorismate synthase	2.74	9.59E-03
Inorganic ion transport & metabolism (P)						
COG2217P	STM14_0586	STM0498	*copA*	copper exporting ATPase	4.20	4.01E-06
COG4592P	STM14_0692	STM0594	*fepB*	iron-enterobactin transporter periplasmic binding protein	3.20	1.13E-03
COG4771P	STM14_2713	STM2199	*cirA*	colicin I receptor	2.87	5.15E-03
COG2382P	STM14_0684	STM0586	*fes*	enterobactin/ferric enterobactin esterase	2.86	7.89E-03
COG4256P	STM14_1634	STM1346	*ydiE*	hypothetical protein	2.78	9.02E-03
COG2375P	STM14_3891	STM3214	*yqjH*	putative transporter	2.60	1.51E-02
Secondary metabolites biosynthesis, transport & catabolism (Q)						
*COG1169HQ	STM14_0693	STM0595	*entC*	isochorismate synthase	2.74	9.59E-03
COG1021Q	STM14_0694	STM0596	*entE*	enterobactin synthase subunit E	2.81	8.23E-03
COG2132Q	STM14_0200	STM0168	*cueO*	multicopper oxidase	2.50	2.38E-02
Transcription						
COG2207K	STM14_5127	STM4265	*soxS*	DNA-binding transcriptional regulator SoxS	4.41	1.15E-06
Cell cycle control, cell division, chromosome partitioning (D)						
COG2846D	STM14_5283	STM4399	*ytfE*	cell morphogenesis/cell wall metabolism regulator	3.11	1.56E-03
General function prediction only (R)						
COG0446R	STM14_3432	STM2841	*norW*	nitric oxide reductase	8.71	4.80E-18
not assigned						
-	STM14_5469	STM4552	-	putative inner membrane protein	3.29	6.64E-04

*Genes assigned to more than one COG class

[1] Gene names according to the *E. coli* homologues

Table A 6: Down-regulated genes in response to 150 mg/l $NaNO_2$ on RD0 in *S.* Typhimurium 14028 WT

COG	14028 identifier	LT2 identifier	Gene name	Product	log_2 FC	p-value (BH-adjusted)
Energy production & conversion (C)						
COG3051C	STM14_0722	STM0621	*citF*	citrate lyase subunit alpha/citrate-ACP transferase	-3.52	2.96E-04
COG3052C	STM14_0724	STM0623	*citD*	citrate lyase subunit gamma	-7.27	7.13E-11
COG3053C	STM14_0725	STM0624	*citC*	citrate lyase synthetase	-5.72	9.67E-10
COG2181C	STM14_2129	STM1761	*narI*	nitrate reductase 1 subunit gamma	-2.79	9.15E-03
COG2180C	STM14_2130	STM1762	*narJ*	nitrate reductase 1 subunit delta	-2.67	1.37E-02
COG1140C	STM14_2131	STM1763	*narH*	nitrate reductase 1 subunit beta	-2.73	9.59E-03
COG5013C	STM14_2132	STM1764	*narG*	nitrate reductase 1 subunit alpha	-2.65	1.32E-02
COG1142C	STM14_3436	STM2843	*hydN*	electron transport protein HydN	-4.86	9.79E-08
COG0680C	STM14_3439	STM2845	*hycI*	hydrogenase 3 maturation protease	-2.44	3.80E-02
COG3260C	STM14_3441	STM2847	*hycG*	hydrogenase	-3.50	3.97E-04
COG1143C	STM14_3442	STM2848	*hycF*	formate hydrogenlyase complex iron-sulfur subunit	-3.78	8.06E-05
COG3261C	STM14_3443	STM2849	*hycE*	hydrogenase 3 large subunit	-3.01	2.64E-03
COG0650C	STM14_3444	STM2850	*hycD*	hydrogenase 3 membrane subunit	-4.15	9.87E-06

COG1142C	STM14_3446	STM2852	*hycB*	hydrogenase-3 iron-sulfur subunit	-5.04	6.85E-08
*COG0651CP	STM14_3445	STM2851	*hycC*	formate hydrogenlyase subunit 3	-5.21	2.31E-08
Carbohydrate transport & metabolism (G)						
COG2301G	STM14_0723	STM0622	*citE*	citrate lyase subunit beta	-5.36	8.54E-08
Nucleotide transport & metabolism (F)						
COG2233F	STM14_3061	STM2497	*uraA*	uracil transporter	-3.06	3.91E-03
COG1328F	STM14_5343	STM4452	*nrdD*	anaerobic ribonucleoside triphosphate reductase	-3.19	1.13E-03
Inorganic ion transport & metabolism (P)						
COG2223P	STM14_2134	STM1765	*narK*	nitrite extrusion protein	-2.52	2.45E-02
*COG0651CP	STM14_3445	STM2851	*hycC*	formate hydrogenlyase subunit 3	-5.21	2.31E-08
*COG2146PR	STM14_4184	STM3475	*nirD*	nitrite reductase small subunit	-2.52	2.43E-02
Translation, ribosomal structure & biogenesis (J)						
COG0042J	STM14_4082	STM3384	*yhdG*	tRNA-dihydrouridine synthase B	-2.57	1.73E-02
Transcription (K)						
*COG2901KL	STM14_4083	STM3385	*fis*	DNA-binding protein Fis	-2.91	4.00E-03
Replication, recombination & repair (L)						
*COG2901KL	STM14_4083	STM3385	*fis*	DNA-binding protein Fis	-2.91	4.00E-03
Cell wall/membrane/envelope biogenesis (M)						
COG3203M	STM14_1848	STM1530	-	putative outer membrane protein	-2.33	4.70E-02
Posttranslational modification, protein turnover, chaperones (O)						
COG0068O	STM14_3434	STM2842	*hypF*	hydrogenase maturation protein	-3.03	2.71E-03
COG0826O	STM14_3956	STM3274	*yhbU*	putative protease	-2.43	4.53E-02
General function prediction only (R)						
COG0375R	STM14_3450	STM2854	*hypA_1*	hydrogenase nickel incorporation protein	-3.91	2.78E-05
*COG2146PR	STM14_4184	STM3475	*nirD*	nitrite reductase small subunit	-2.52	2.43E-02
COG3383R	STM14_5155	STM4285	*fdhF*	formate dehydrogenase	-3.34	5.33E-04
Function unknown (S)						
COG3691S	STM14_2939	STM2390	*yfcZ*	putative cytoplasmic protein	-2.43	3.20E-02
not assigned						
-	STM14_1238	STM1092	*orfX*	putative cytoplasmic protein	-5.23	9.79E-08
-	STM14_1564	-	-	hypothetical protein	-2.39	4.42E-02
-	STM14_2745	-	-	bicyclomycin/multidrug efflux system protein	-3.17	1.14E-03
-	STM14_3437	-	-	hypothetical protein	-2.73	1.40E-02
-	STM14_3440	STM2846	*hycH*	hydrogenase 3 large subunit processing protein	-3.15	2.24E-03
-	STM14_3447	-	-	hypothetical protein	-5.18	2.31E-08
-	STM14_3448	STM2853	*hycA*	formate hydrogenlyase regulatory protein HycA	-5.65	9.67E-10
-	STM14_3449	-	-	hypothetical protein	-5.98	8.79E-10

*Genes assigned to more than one COG class

Table A 7: Genes with increased transcript levels on RD3 compared to RD0 in *S.* Typhimurium 14028 WT

COG	14028 identifier	LT2 identifier	Gene name	Product	$\log_2$ FC	p-value (BH-adjusted)
Energy production & conversion (C)						
COG0371C	STM14_0701	STM0602	*ybdH*	hypothetical protein	2.05	2.22E-02
COG1053C	STM14_0853	STM0734	*sdhA*	succinate dehydrogenase flavoprotein subunit	1.92	3.25E-02
COG0479C	STM14_0854	STM0735	*sdhB*	succinate dehydrogenase iron-sulfur subunit	2.82	1.40E-03
COG0567C	STM14_0855	STM0736	*kgd*	alpha-ketoglutarate decarboxylase	2.48	4.69E-03

COG0508C	STM14_0856	STM0737	*sucB*	dihydrolipoamide acetyltransferase	2.27	1.02E-02
COG0045C	STM14_0857	STM0738	*sucC*	succinyl-CoA synthetase subunit beta	1.96	2.88E-02
COG0074C	STM14_0858	STM0739	*sucD*	succinyl-CoA synthetase subunit alpha	2.20	1.30E-02
COG1882C	STM14_984	STM0843	*pflF*	putative pyruvate formate lyase	2.94	9.33E-04
COG2025C	STM14_1003	STM0856	-	putative electron transfer protein alpha subunit	3.08	5.41E-04
COG0243C	STM14_1089	STM0964	*dmsA*	anaerobic dimethyl sulfoxide reductase subunit A	2.50	4.54E-03
COG0437C	STM14_1090	STM0965	*dmsB*	anaerobic dimethyl sulfoxide reductase subunit B	2.67	2.74E-03
COG0243C	STM14_1677	STM1383	*ttrA*	tetrathionate reductase complex subunit A	1.89	4.04E-02
COG0437C	STM14_1679	STM1385	*ttrB*	tetrathionate reductase complex subunit B	2.89	1.59E-03
COG1951C	STM14_1770	STM1468	*fumA*	fumarase A	2.18	1.39E-02
COG1740C	STM14_2161	STM1786	-	hydrogenase-1 small subunit	2.12	1.71E-02
COG0374C	STM14_2162	STM1787	-	hydrogenase 1 large subunit	1.99	2.60E-02
COG1969C	STM14_2163	STM1788	-	hydrogenase 1 b-type cytochrome subunit	2.27	1.02E-02
COG1271C	STM14_2167	STM1792	-	putative cytochrome oxidase subunit I	2.02	2.44E-02
COG1294C	STM14_2168	STM1793	-	putative cytochrome oxidase subunit II	2.42	6.05E-03
COG0437C	STM14_2554	STM2064	*phsB*	thiosulfate reductase electron transport protein	2.30	1.03E-02
COG0243C	STM14_2555	STM2065	*phsA*	thiosulfate reductase	2.74	2.21E-03
*COG4577QC	STM14_3013	STM2455	*eutK*	putative carboxysome structural protein	2.38	8.20E-03
*COG0543HC	STM14_3127	STM2549	*asrB*	anaerobic sulfite reductase subunit B	2.70	2.38E-03
COG2221C	STM14_3128	STM2550	*asrC*	anaerobic sulfide reductase	2.27	1.04E-02
COG0680C	STM14_3810	STM3146	*hybD*	hydrogenase 2 maturation endopeptidase	1.81	4.68E-02
COG1979C	STM14_3831	STM3164	*yqhD*	putative alcohol dehydrogenase	1.88	3.76E-02
COG1012C	STM14_4438	STM3680	*aldB*	aldehyde dehydrogenase B	2.31	9.20E-03
COG1620C	STM14_4451	STM3692	*lldP*	L-lactate permease	2.01	3.04E-02
COG1304C	STM14_4453	STM3694	*lldD*	L-lactate dehydrogenase	2.75	2.21E-03
Carbohydrate transport & metabolism (G)						
COG0235G	STM14_0120	STM0101	*araD*	L-ribulose-5-phosphate 4-epimerase	2.63	4.13E-03
COG2814G	STM14_0384	STM0328.s	-	putative permease	2.16	1.60E-02
COG2301G	STM14_1001	STM0854	-	putative cytoplasmic protein	3.35	1.75E-04
COG2814G	STM14_1335	STM1166	*yceL*	multidrug resistance protein MdtH	1.96	3.16E-02
COG3444G	STM14_2212	STM1830	*manX*	mannose-specific enzyme IIAB	2.85	1.26E-03
COG3715G	STM14_2213	STM1831	*manY*	mannose-specific enzyme IIC	1.99	2.57E-02
COG3716G	STM14_2214	STM1832	*manZ*	mannose-specific PTS system protein IID	2.33	8.48E-03
COG0469G	STM14_2296	STM1888	*pykA*	pyruvate kinase	1.80	4.84E-02
*COG0451MG	STM14_2583	STM2089	*rfbJ*	CDP-abequose synthase	2.64	2.80E-03
*COG0451MG	STM14_2585	STM2091	*rfbG*	CDP glucose 4,6-dehydratase	1.83	4.32E-02
COG2814G	STM14_2815	STM2280	-	putative permease	1.83	4.49E-02
COG2814G	STM14_4029	STM3338	*nanT*	putative sialic acid transporter	2.07	2.05E-02
COG0524G	STM14_4330	STM3600	-	putative sugar kinase	2.66	2.74E-03

COG2213G	STM14_4443	STM3685	*mtlA*	mannitol-specific enzyme IIABC component	2.44	5.78E-03
COG0246G	STM14_4444	STM3686	*mtlD*	mannitol-1-phosphate 5-dehydrogenase	2.13	1.67E-02
*COG1762GT	STM14_4563	STM3784	-	phosphotransferase system mannitol/fructose-specific IIA component	2.49	6.05E-03
COG1879G	STM14_4681	STM3884	*rbsB*	D-ribose transporter subunit RbsB	1.81	4.60E-02
COG0235G	STM14_4864	STM4045	*rhaD*	rhamnulose-1-phosphate aldolase	2.32	9.55E-03
COG1172G	STM14_4901	STM4076	*ydeZ*	putative sugar transport protein	2.35	9.91E-03
COG1879G	STM14_4902	STM4077	*yneA*	putative sugar transport protein	3.12	6.32E-04
COG1830G	STM14_4903	STM4078	*yneB*	aldolase	2.73	2.35E-03
COG2731G	STM14_5363	STM4468	*yjgK*	putative cytoplasmic protein	1.99	3.30E-02
*COG2610GE	STM14_5378	STM4482	*idnT*	L-idonate transport protein	2.35	9.08E-03
Amino acid transport & metabolism (E)						
COG0289E	STM14_0075	STM0064	*dapB*	dihydrodipicolinate reductase	2.06	2.22E-02
*COG0458EF	STM14_0078	STM0067	*carB*	carbamoyl phosphate synthase large subunit	2.11	1.92E-02
COG1280E	STM14_0427	STM0365	*yahN*	putative transport protein	1.83	4.60E-02
*COG0834ET	STM14_0773	STM0665	*gltI*	glutamate and aspartate transporter subunit	2.08	1.97E-02
COG0531E	STM14_0817	STM0700	*potE*	putrescine transporter	1.88	3.78E-02
COG4690E	STM14_1240	STM1094	*pipD*	pathogenicity island-encoded protein D	2.51	4.61E-03
COG0665E	STM14_2179	STM1803	*dadA*	D-amino acid dehydrogenase small subunit	2.10	1.93E-02
*COG0493ER	STM14_2693	STM2186	-	putative oxidoreductase	3.39	1.39E-04
COG4303E	STM14_3016	STM2458	*eutB*	ethanolamine ammonia-lyase heavy chain	1.97	2.96E-02
COG0814E	STM14_3581	STM2970	*sdaC*	putative serine transport protein	3.08	5.68E-04
COG1760E	STM14_3582	STM2971	*sdaB*	L-serine dehydratase/L-threonine deaminase 2	2.65	2.80E-03
COG1003E	STM14_3687	STM3053	*gcvP*	glycine dehydrogenase	2.26	1.05E-02
COG2502E	STM14_4674	STM3877	*asnA*	asparagine synthetase AsnA	2.91	1.02E-03
*COG0059EH	STM14_4706	STM3909	*ilvC*	ketol-acid reductoisomerase	2.20	1.36E-02
COG1982E	STM14_5169	STM4296	*adi*	catabolic arginine decarboxylase	1.87	3.89E-02
COG1027E	STM14_5202	STM4326	*aspA*	aspartate ammonia-lyase	2.69	2.34E-03
*COG2610GE	STM14_5378	STM4482	*idnT*	L-idonate transport protein	2.35	9.08E-03
Nucleotide transport & metabolism (F)						
*COG0458EF	STM14_0078	STM0067	*carB*	carbamoyl phosphate synthase large subunit	2.11	1.92E-02
COG1957F	STM14_0769	STM0661	*rihA*	ribonucleoside hydrolase 1	3.48	1.40E-04
COG0167F	STM14_2694	STM2187	*yeiA*	dihydropyrimidine dehydrogenase	2.87	1.15E-03
COG2820F	STM14_4774	STM3968	*udp*	uridine phosphorylase	2.35	7.96E-03
COG0044F	STM14_5419	STM4512	*iadA*	isoaspartyl dipeptidase	2.08	1.97E-02
Coenzyme transport & metabolism (H)						
COG2243H	STM14_2512	STM2024	*cbiL*	cobalt-precorrin-2 C(20)-methyltransferase	2.59	4.69E-03
COG4822H	STM14_2513	STM2025	*cbiK*	vitamin B12 biosynthetic protein	2.01	2.76E-02
COG2073H	STM14_2516	STM2028	*cbiG*	cobalamin biosynthesis protein CbiG	2.18	1.56E-02
*COG0543HC	STM14_3127	STM2549	*asrB*	anaerobic sulfite reductase subunit B	2.70	2.38E-03
*COG0059EH	STM14_4706	STM3909	*ilvC*	ketol-acid reductoisomerase	2.20	1.36E-02
COG3201H	STM14_4709	STM3911	-	putative inner membrane protein	2.05	2.50E-02
COG0340H	STM14_4974	STM4138	*birA*	biotin--protein ligase	2.12	1.71E-02

Lipid transport & metabolism (I)						
COG1024I	STM14_0083	STM0070	*caiD*	carnitinyl-CoA dehydratase	3.01	8.89E-04
COG1250I	STM14_2937	STM2388	*fadJ*	multifunctional fatty acid oxidation complex subunit alpha	1.80	4.82E-02
*COG1028IQR	STM14_3003	STM2445	*ucpA*	short chain dehydrogenase	2.87	1.15E-03
COG2084I	STM14_3930	STM3248	*garR*	tartronate semialdehyde reductase	2.22	1.50E-02
COG0439I	STM14_4077	STM3380	*accC*	acetyl-CoA carboxylase biotin carboxylase subunit	1.81	4.56E-02
COG0365I	STM14_5141	STM4275	*acs*	acetyl-CoA synthetase	1.88	4.48E-02
Inorganic ion transport & metabolism (P)						
COG3119P	STM14_0100	STM0084	-	putative sulfatase	2.02	2.44E-02
*COG3678UNTP	STM14_0362	STM0307	-	VirG-like protein	2.16	1.61E-02
COG1464P	STM14_0600	STM0510	*sfbA*	ABC transporter ATP-binding protein	1.86	4.43E-02
COG1135P	STM14_0601	STM0511	*sfbB*	ABC transporter ATP-binding protein	1.94	3.41E-02
COG2011P	STM14_0602	STM0512	*sfbC*	putative ABC transporter permease	2.23	1.31E-02
COG1528P	STM14_2353	STM1935	*ftn*	ferritin	1.85	4.06E-02
COG1930P	STM14_2510	STM2022	*cbiN*	cobalt transport protein CbiN	2.17	1.91E-02
COG0310P	STM14_2511	STM2023	*cbiM*	cobalt transport protein CbiM	2.24	1.40E-02
COG2897P	STM14_3106	STM2533	*sseA*	3-mercaptopyruvate sulfurtransferase	2.02	2.51E-02
COG1858P	STM14_4612	STM3820	-	putative cytochrome *c* peroxidase	2.61	3.38E-03
COG0376P	STM14_4936	STM4106	*katG*	hydroperoxidase	1.93	3.26E-02
*COG3678UNTP	STM14_5013	STM4172	*zraP*	zinc resistance protein	2.84	1.59E-03
Secondary metabolites biosynthesis, transport & catabolism (Q)						
COG3127Q	STM14_0596	STM0508	*ybbP*	putative inner membrane protein	1.87	3.99E-02
COG2050Q	STM14_1660	STM1366	-	hypothetical protein	2.01	2.67E-02
*COG1028IQR	STM14_3003	STM2445	*ucpA*	short chain dehydrogenase	2.87	1.15E-03
*COG4577QC	STM14_3013	STM2455	*eutK*	putative carboxysome structural protein	2.38	8.20E-03
Translation, ribosomal structure & biogenesis (J)						
COG3130J	STM14_1210	STM1066	*rmf*	ribosome modulation factor	1.79	4.84E-02
*COG1208MJ	STM14_2586	STM2092	*rfbF*	glucose-1-phosphate cytidylyltransferase	1.92	3.27E-02
COG1544J	STM14_3266	STM2665	*yfiA*	translation inhibitor protein RaiA	2.69	2.34E-03
Transcription						
COG3710K	STM14_0019	STM0017	-	hypothetical protein	2.45	6.19E-03
COG0583K	STM14_0038	STM0030	-	putative transcriptional regulator	3.30	2.42E-04
COG0583K	STM14_0049	STM0040	*nhaR*	transcriptional activator NhaR	1.83	4.45E-02
COG0583K	STM14_0887	STM0763.s	-	transcriptional regulator	2.48	4.82E-03
*COG1983KT	STM14_2038	STM1688	*pspC*	DNA-binding transcriptional activator PspC	3.24	2.52E-04
*COG1842KT	STM14_2040	STM1690	*pspA*	phage shock protein PspA	3.56	7.00E-05
COG1278K	STM14_2220	STM1837	*cspC*	cold shock-like protein CspC	2.55	3.93E-03
COG0583K	STM14_2816	STM2281	-	putative transcriptional regulator	2.46	7.40E-03
COG1309K	STM14_4087	STM3389	*envR*	DNA-binding transcriptional regulator EnvR	2.48	5.33E-03
COG2909K	STM14_4234	STM3515	*malT*	transcriptional regulator MalT	3.13	4.23E-04
COG3722K	STM14_4445	STM3687	*mtlR*	mannitol repressor protein	1.88	4.04E-02
COG2186K	STM14_4452	STM3693	*lldR*	DNA-binding transcriptional repressor LldR	3.52	1.37E-04
COG2944K	STM14_4557	STM3778	-	putative DNA-binding protein	1.92	3.39E-02
COG2188K	STM14_4564	STM3785	-	putative regulatory protein	3.34	2.11E-04
COG2207K	STM14_5188	STM4315	-	putative DNA-binding protein	2.19	1.39E-02

COG0583K	STM14_5418	STM4511	*yjiE*	putative DNA-binding transcriptional regulator	2.52	4.23E-03
COG3933K	STM14_5448	STM4534	-	putative transcriptional regulator	2.16	1.58E-02
Replication, recombination & repair (L)						
COG3145L	STM14_2794	STM2264	*alkB*	DNA repair system protein	1.87	4.32E-02
COG1518L	STM14_3542	STM2938	-	putative cytoplasmic protein	2.05	2.36E-02
COG3449L	STM14_3847	STM3175	-	putative regulatory protein	1.98	2.78E-02
Defense mechanisms (V)						
COG0842V	STM14_4313	STM3585	*yhhJ*	putative ABC transport protein	1.83	4.65E-02
COG1131V	STM14_4314	STM3586.S	*yhiH*	putative ABC-type multidrug transport system ATPase component	1.85	4.15E-02
COG1566V	STM14_4315	STM3587	*yhiI*	hypothetical protein	1.85	4.35E-02
Signal transduction mechanisms (T)						
*COG3678UNTP	STM14_0362	STM0307	-	VirG-like protein	2.16	1.61E-02
COG0589T	STM14_0713	STM0614	*ybdQ*	putative universal stress protein	3.25	2.48E-04
*COG0834ET	STM14_0773	STM0665	*gltI*	glutamate and aspartate transporter subunit	2.08	1.97E-02
COG2200T	STM14_1632	STM1344	*ydiV*	hypothetical protein	2.29	1.02E-02
COG4191T	STM14_1680	STM1386	*ttrS*	sensory histidine kinase	2.39	7.22E-03
COG0589T	STM14_1997	STM1652	*ynaF*	putative universal stress protein	3.86	1.45E-05
COG0589T	STM14_2008	STM1661	*ydaA*	universal stress protein UspE	2.30	9.41E-03
*COG1983KT	STM14_2038	STM1688	*pspC*	DNA-binding transcriptional activator PspC	3.24	2.52E-04
*COG1842KT	STM14_2040	STM1690	*pspA*	phage shock protein PspA	3.56	7.00E-05
COG0589T	STM14_2344	STM1927	*yecG*	universal stress protein UspC	3.57	7.58E-05
*COG1762GT	STM14_4563	STM3784	-	phosphotransferase system mannitol/fructose-specific IIA component	2.49	6.05E-03
*COG3678UNTP	STM14_5013	STM4172	*zraP*	zinc resistance protein	2.84	1.59E-03
COG1966T	STM14_5445	STM4532	*yjiY*	putative carbon starvation protein	2.68	2.55E-03
Cell wall/membrane/envelope biogenesis (M)						
COG0768M	STM14_0148	STM0122	*ftsI*	division specific transpeptidase	2.08	1.97E-02
COG3248M	STM14_0489	STM0413	*tsx*	nucleoside channel	2.82	1.45E-03
COG3203M	STM14_1898	STM1572	*nmpC*	putative outer membrane porin	2.38	7.04E-03
COG3047M	STM14_2095	STM1732	*ompW*	outer membrane protein W	2.97	8.15E-04
COG0787M	STM14_2178	STM1802	*dadX*	alanine racemase	2.35	8.55E-03
COG0836M	STM14_2578	STM2084	*rfbM*	mannose-1-phosphate guanylyltransferase	2.01	2.45E-02
COG0438M	STM14_2580	STM2086	*rfbU*	mannosyl transferase	2.19	1.36E-02
COG0463M	STM14_2581	STM2087	*rfbV*	abequosyltransferase	2.60	3.17E-03
*COG0451MG	STM14_2583	STM2089	*rfbJ*	CDP-abequose synthase	2.64	2.80E-03
COG0399M	STM14_2584	STM2090	*rfbH*	CDP-6-deoxy-D-xylo-4-hexulose-3-dehydrase	2.25	1.08E-02
*COG0451MG	STM14_2585	STM2091	*rfbG*	CDP glucose 4,6-dehydratase	1.83	4.32E-02
*COG1208MJ	STM14_2586	STM2092	*rfbF*	glucose-1-phosphate cytidylyltransferase	1.92	3.27E-02
COG3203M	STM14_2797	STM2267	*ompC*	outer membrane porin protein C	1.82	4.53E-02
*COG4948MR	STM14_3568	STM2960	*gudD*	d-glucarate dehydratase	1.83	4.78E-02
COG2222M	STM14_4331	STM3601	-	putative phosphosugar isomerase	2.52	4.29E-03
*COG1538MU	STM14_5119	STM4259	-	putative ABC exporter outer membrane component	2.45	5.64E-03
COG0845M	STM14_5120	STM4260	-	cation efflux pump	1.92	3.31E-02
Intracellular trafficking, secretion, & vesicular transport (U)						
*COG3678UNTP	STM14_0362	STM0307	-	VirG-like protein	2.16	1.61E-02
*COG3678UNTP	STM14_5013	STM4172	*zraP*	zinc resistance protein	2.84	1.59E-03

*COG1538MU	STM14_5119	STM4259	-	putative ABC exporter outer membrane component	2.45	5.64E-03
Cell motility						
*COG3678UNTP	STM14_0362	STM0307	-	VirG-like protein	2.16	1.61E-02
*COG3678UNTP	STM14_5013	STM4172	*zraP*	zinc resistance protein	2.84	1.59E-03
Posttranslational modification, protein turnover, chaperones (O)						
COG0450O	STM14_0707	STM0608	*ahpC*	alkyl hydroperoxide reductase subunit C	1.93	3.20E-02
COG3634O	STM14_0708	STM0609	*ahpF*	alkyl hydroperoxide reductase F52a subunit	1.99	2.61E-02
COG1180O	STM14_985	STM0844	*pflE*	putative pyruvate formate lyase activating enzyme	4.66	7.43E-07
COG0695O	STM14_1023	STM0872	*grxA*	glutaredoxin	2.10	1.86E-02
COG0625O	STM14_1749	STM1451	*gst*	glutathionine S-transferase	2.95	9.00E-04
COG0298O	STM14_3807	STM3143	*hybG*	hydrogenase 2 accessory protein HypG	1.86	4.04E-02
General function prediction only (R)						
COG0663R	STM14_0082	STM0069	*caiE*	carnitine operon protein CaiE	2.49	6.24E-03
COG1123R	STM14_991	STM0848	*yliA*	glutathione transporter ATP-binding protein	2.63	3.09E-03
COG3302R	STM14_1091	STM0966	*dmsC*	anaerobic dimethyl sulfoxide reductase subunit C	2.45	5.93E-03
COG1216R	STM14_2579	STM2085	*rfbN*	rhamnosyl transferase	2.20	1.30E-02
COG2244R	STM14_2582	STM2088	*rfbX*	putative O-antigen transferase	2.64	2.80E-03
COG1380R	STM14_2688	STM2181	*yohJ*	hypothetical protein	1.92	3.35E-02
*COG0493ER	STM14_2693	STM2186	-	putative oxidoreductase	3.39	1.39E-04
*COG1028IQR	STM14_3003	STM2445	*ucpA*	short chain dehydrogenase	2.87	1.15E-03
COG3445R	STM14_3243	STM2646	*yfiD*	autonomous glycyl radical cofactor GrcA	2.18	1.40E-02
COG1203R	STM14_3548	STM2944	*ygcB*	putative helicase	2.19	1.34E-02
*COG4948MR	STM14_3568	STM2960	*gudD*	d-glucarate dehydratase	1.83	4.78E-02
COG1611R	STM14_3578	STM2969	*ygdH*	putative nucleotide binding protein	1.86	3.99E-02
COG1487R	STM14_3663	STM3033	-	plasmid maintenance protein	1.91	3.39E-02
COG1279R	STM14_3706	STM3066	*yggA*	arginine exporter protein	1.98	2.78E-02
COG3529R	STM14_4160	STM3456	*yheV*	putative cytoplasmic protein	1.80	4.87E-02
COG2704R	STM14_4329	STM3599	-	anaerobic C4-dicarboxylate transporter	2.80	1.58E-03
COG0431R	STM14_4645	STM3850	*yieF*	putative oxidoreductase	2.32	9.11E-03
COG0456R	STM14_5027	STM4181	*yjaB*	hypothetical protein	1.79	4.97E-02
COG2704R	STM14_5201	STM4325	*dcuA*	anaerobic C4-dicarboxylate transporter	2.60	3.27E-03
Function unknown (S)						
COG4890S	STM14_0863	STM0742	*ybgT*	putative outer membrane lipoprotein	2.19	1.36E-02
COG1357S	STM14_1233	STM1088	*pipB*	secreted effector protein	2.26	1.08E-02
COG3055S	STM14_1293	STM1130	-	putative inner membrane protein	3.60	6.72E-05
COG4718S	STM14_1471	STM2593	-	phage tail component M-like protein	2.05	2.28E-02
COG3228S	STM14_2485	STM2001	*yeeI*	putative inner membrane protein	2.54	4.23E-03
COG4456S	STM14_3664	STM3034	-	putative virulence-associated protein	2.07	1.98E-02
COG3111S	STM14_3848	STM3176	*ygiW*	putative outer membrane protein	2.09	1.89E-02
COG5426S	STM14_4273	STM3548	-	putative cytoplasmic protein	2.03	2.45E-02
COG5464S	STM14_4542	STM3766	-	putative cytoplasmic protein	2.09	2.28E-02
COG3084S	STM14_4804	STM3995	*yihD*	putative cytoplasmic protein	1.79	4.87E-02
COG3738S	STM14_4937	STM4107	*yijF*	hypothetical protein	2.02	2.64E-02

COG5510S	STM14_5216	STM4336	*ecnB*	entericidin B membrane lipoprotein	1.93	3.23E-02
COG3811S	STM14_5401	STM4501	-	hypothetical protein	2.34	9.06E-03
COG5464S	STM14_5428	STM4518	-	putative inner membrane protein	2.07	2.21E-02
COG3610S	STM14_5460	STM4545	-	hypothetical protein	2.02	2.57E-02
not assigned						
-	STM14_0001	STM0001	*thrL*	thr operon leader peptide	2.28	9.86E-03
-	STM14_0076	-	-	hypothetical protein	2.32	9.42E-03
-	STM14_0081	STM0068	*caiF*	DNA-binding transcriptional activator CaiF	3.18	3.79E-04
-	STM14_0119	STM0100	-	putative cytoplasmic protein	2.97	8.15E-04
-	STM14_0383	STM0327	-	putative cytoplasmic protein	2.43	5.78E-03
-	STM14_0403	-	-	hypothetical protein	2.65	2.88E-03
-	STM14_0424	STM0362	-	putative cytoplasmic protein	2.62	3.29E-03
-	STM14_0454	STM0384	*psiF*	hypothetical protein	2.55	3.93E-03
-	STM14_0597	-	-	hypothetical protein	2.95	1.09E-03
-	STM14_0768	STM0660	-	putative cytoplasmic protein	2.44	6.19E-03
-	STM14_0859	-	-	hypothetical protein	1.93	3.54E-02
-	STM14_0864	-	-	hypothetical protein	2.52	4.32E-03
-	STM14_0897	-	-	hypothetical protein	2.03	2.28E-02
-	STM14_974	-	-	hypothetical protein	3.03	6.32E-04
-	STM14_998	STM0853	*bssR*	biofilm formation regulatory protein BssR	2.07	2.00E-02
-	STM14_999	-	-	hypothetical protein	3.31	2.13E-04
-	STM14_1000	-	-	hypothetical protein	4.87	2.49E-07
-	STM14_1002	STM0855	-	putative electron transfer protein beta subunit	3.13	4.29E-04
-	STM14_1092	-	-	hypothetical protein	2.71	2.74E-03
-	STM14_1197	STM1055	-	hypothetical protein	1.94	3.11E-02
-	STM14_1270	STM1117	*agp*	glucose-1-phosphatase/inositol phosphatase	2.64	2.95E-03
-	STM14_1282	-	-	hypothetical protein	1.93	3.20E-02
-	STM14_1554	-	-	hypothetical protein	2.19	1.43E-02
-	STM14_1555	-	-	salivary secreted protein	2.19	1.43E-02
-	STM14_1771	-	-	fumarase A	2.26	1.29E-02
-	STM14_1912	STM1583	-	putative cytoplasmic protein	2.01	2.45E-02
-	STM14_1922	-	-	hypothetical protein	2.41	8.55E-03
-	STM14_1932	-	-	hypothetical protein	2.27	1.02E-02
-	STM14_1933	-	-	hypothetical protein	2.64	2.80E-03
-	STM14_1939	-	-	hypothetical protein	2.62	3.46E-03
-	STM14_1940	STM1602	*sifB*	secreted effector protein	2.58	3.93E-03
-	STM14_2009	STM1662	*ynaJ*	putative inner membrane protein	1.98	2.66E-02
-	STM14_2037	STM1687	*pspD*	peripheral inner membrane phage-shock protein	2.54	4.13E-03
-	STM14_2039	STM1689	*pspB*	phage shock protein B	3.87	1.45E-05
-	STM14_2151	-	-	hypothetical protein	4.38	5.32E-06
-	STM14_2155	STM1782	*ychH*	hypothetical protein	3.04	6.32E-04
-	STM14_2166	STM1791	-	putative hydrogenase-1 protein	2.00	2.63E-02
-	STM14_2169	STM1794	-	hypothetical protein	2.73	2.16E-03
-	STM14_2221	STM1838	*yobF*	putative cytoplasmic protein	2.87	1.15E-03
-	STM14_2238	-	-	hypothetical protein	1.94	3.16E-02
-	STM14_2239	STM1851	-	putative cytoplasmic protein	1.81	4.71E-02

-	STM14_2242	STM1854	-	putative inner membrane protein	2.18	1.42E-02
-	STM14_2269	STM1868A	-	lytic enzyme	2.31	1.17E-02
-	STM14_2270	-	-	hypothetical protein	2.39	8.09E-03
-	STM14_2352	STM1934	-	putative outer membrane lipoprotein	1.92	4.00E-02
-	STM14_2359	STM1941	-	putative inner membrane protein	2.67	2.74E-03
-	STM14_2428	-	-	hypothetical protein	2.05	2.26E-02
-	STM14_2637	STM2138	-	putative cytoplasmic protein	4.32	1.18E-06
-	STM14_2656	STM2153	*yehE*	putative outer membrane protein	2.37	7.44E-03
-	STM14_2854	-	-	hypothetical protein	2.71	2.99E-03
-	STM14_2951	STM2400	-	putative inner membrane protein	2.06	2.15E-02
-	STM14_3056	-	-	hypothetical protein	2.64	3.85E-03
-	STM14_3126	STM2548	*asrA*	anaerobic sulfide reductase	2.97	8.89E-04
-	STM14_3166	STM2585	-	transposase-like protein	1.88	3.80E-02
-	STM14_3267	-	-	hypothetical protein	2.66	2.74E-03
-	STM14_3353	-	-	hypothetical protein	2.08	2.44E-02
-	STM14_3466	-	-	hypothetical protein	1.93	3.41E-02
-	STM14_3541	STM2937	*ygbF*	hypothetical protein	3.53	8.26E-05
-	STM14_3543	STM2939	*ygcH*	putative cytoplasmic protein	1.90	3.97E-02
-	STM14_3544	STM2940	-	putative cytoplasmic protein	1.98	3.16E-02
-	STM14_3545	STM2941	*yghJ*	putative cytoplasmic protein	2.57	3.98E-03
-	STM14_3546	STM2942	-	putative transposase	3.59	9.18E-05
-	STM14_3547	STM2943	-	putative cytoplasmic protein	2.85	1.65E-03
-	STM14_3830	-	-	hypothetical protein	2.36	8.97E-03
-	STM14_3860	-	-	hypothetical protein	2.25	1.21E-02
-	STM14_3871	STM3197	*glgS*	glycogen synthesis protein GlgS	3.55	7.37E-05
-	STM14_3884	-	-	hypothetical protein	2.07	2.02E-02
-	STM14_4085	STM3387	*yhdU*	hypothetical protein	1.83	4.48E-02
-	STM14_4277	-	-	hypothetical protein	2.03	2.47E-02
-	STM14_4278	STM3552	*yhhA*	hypothetical protein	2.10	1.87E-02
-	STM14_4519	STM3752	-	putative cytoplasmic protein	3.18	3.79E-04
-	STM14_4696	-	-	hypothetical protein	1.94	3.59E-02
-	STM14_4708	-	-	cyclic nucleotide-binding domain-containing protein	2.19	1.55E-02
-	STM14_4741	STM3940	-	putative inner membrane protein	2.24	1.43E-02
-	STM14_5019	-	-	hypothetical protein	3.22	4.23E-04
-	STM14_5045	STM4196	-	putative cytoplasmic protein	3.19	5.21E-04
-	STM14_5117	STM4257	-	hypothetical protein	1.84	4.35E-02
-	STM14_5118	STM4258	-	putative methyl-accepting chemotaxis protein	2.16	1.57E-02
-	STM14_5129	-	-	hypothetical protein	2.25	1.08E-02
-	STM14_5203	-	-	hypothetical protein	2.48	4.69E-03
-	STM14_5259	STM4377	*aidB*	isovaleryl CoA dehydrogenase	2.10	1.97E-02
-	STM14_5431	STM4520	-	putative cytoplasmic protein	2.28	1.27E-02
-	STM14_5469	STM4552	-	putative inner membrane protein	2.20	1.34E-02
-	STM14_5596	PSLT076	*traY*	conjugative transfer: oriT nicking	2.32	9.01E-03

*Genes assigned to more than one COG class

Table A 8: Genes with decreased transcript levels on RD3 compared to RD0 in *S.* Typhimurium 14028 WT

COG	14028 identifier	LT2 identifier	Gene name	Product	log_2 FC	p-value (BH-adjusted)
Energy production & conversion (C)						
COG1845C	STM14_0521	STM0441	*cyoC*	cytochrome o ubiquinol oxidase subunit III	-1.79	5.00E-02
COG0843C	STM14_0522	STM0442	*cyoB*	cytochrome o ubiquinol oxidase subunit I	-2.20	1.32E-02
COG1622C	STM14_0523	STM0443	*cyoA*	cytochrome o ubiquinol oxidase subunit II	-2.50	4.39E-03
COG3051C	STM14_0722	STM0621	*citF*	citrate lyase subunit alpha/citrate-ACP transferase	-2.98	9.33E-04
COG3052C	STM14_0724	STM0623	*citD*	citrate lyase subunit gamma	-5.68	1.97E-08
COG3053C	STM14_0725	STM0624	*citC*	citrate lyase synthetase	-3.90	1.45E-05
COG1018C	STM14_1051	STM0936	*hcr*	HCP oxidoreductase	-3.46	9.80E-05
*COG4232OC	STM14_1267	STM1114	*scsB*	suppression of copper sensitivity protein	-1.99	3.64E-02
COG1062C	STM14_1968	STM1627	-	alcohol dehydrogenase class III	-2.57	3.76E-03
COG2181C	STM14_2129	STM1761	*narI*	nitrate reductase 1 subunit gamma	-1.87	4.45E-02
COG2180C	STM14_2130	STM1762	*narJ*	nitrate reductase 1 subunit delta	-3.00	9.33E-04
COG1140C	STM14_2131	STM1763	*narH*	nitrate reductase 1 subunit beta	-3.32	2.14E-04
COG5013C	STM14_2132	STM1764	*narG*	nitrate reductase 1 subunit alpha	-3.57	7.56E-05
COG0282C	STM14_2882	STM2337	*ackA*	acetate kinase	-2.06	2.06E-02
COG1018C	STM14_3135	STM2556	*hmpA*	nitric oxide dioxygenase	-4.14	3.19E-06
COG1143C	STM14_3156	STM2576	*yfhL*	putative ferredoxin	-4.52	7.98E-07
COG1142C	STM14_3436	STM2843	*hydN*	electron transport protein HydN	-7.37	1.70E-13
COG3260C	STM14_3441	STM2847	*hycG*	hydrogenase	-3.70	7.00E-05
COG1143C	STM14_3442	STM2848	*hycF*	formate hydrogenlyase complex iron-sulfur subunit	-3.39	2.07E-04
COG3261C	STM14_3443	STM2849	*hycE*	hydrogenase 3 large subunit	-2.26	1.06E-02
COG0650C	STM14_3444	STM2850	*hycD*	hydrogenase 3 membrane subunit	-4.52	9.99E-07
*COG0651CP	STM14_3445	STM2851	*hycC*	formate hydrogenlyase subunit 3	-5.37	7.93E-09
COG1142C	STM14_3446	STM2852	*hycB*	hydrogenase-3 iron-sulfur subunit	-6.55	5.82E-11
COG0716C	STM14_3677	STM3045	*fldB*	flavodoxin FldB	-1.80	4.97E-02
COG1251C	STM14_4183	STM3474	*nirB*	nitrite reductase large subunit	-3.40	1.40E-04
COG0578C	STM14_4246	STM3526	*glpD*	glycerol-3-phosphate dehydrogenase	-1.90	3.45E-02
COG0716C	STM14_4672	STM3875	*mioC*	flavodoxin	-3.54	7.63E-05
Carbohydrate transport & metabolism (G)						
COG2814G	STM14_0450	STM0382	-	putative permease	-2.45	6.19E-03
COG0524G	STM14_0578	STM0491	*gsk*	inosine-guanosine kinase	-2.58	4.13E-03
COG2301G	STM14_0723	STM0622	*citE*	citrate lyase subunit beta	-8.10	1.36E-10
COG2814G	STM14_1321	STM1154	*yceE*	drug efflux system protein MdtG	-2.30	9.91E-03
COG2814G	STM14_1725	STM1428	*ydhC*	inner membrane transport protein YdhC	-3.04	6.32E-04
COG1877G	STM14_2346	STM1929	*otsB*	trehalose-6-phosphate phosphatase	-1.82	4.51E-02
COG1299G	STM14_2721	STM2204	*fruA*	PTS system fructose-specific transporter subunit IIBC	-2.06	2.17E-02
COG1105G	STM14_2722	STM2205	*fruK*	1-phosphofructokinase	-2.06	2.14E-02
COG4668G	STM14_2723	STM2206	*fruF*	bifunctional fructose-specific PTS IIA/HPr protein	-2.56	3.96E-03
COG0483G	STM14_3124	STM2546	*suhB*	inositol monophosphatase	-4.13	3.19E-06
COG2814G	STM14_3395	STM2812	-	putative inner membrane protein	-2.56	4.22E-03

COG2814G	STM14_3400	STM2815	*emrB*	putative multidrug transport protein	-1.80	4.81E-02
COG1626G	STM14_4334	STM3603	*treF*	trehalase	-2.06	2.07E-02
COG2814G	STM14_4555	STM3776	*nepI*	ribonucleoside transporter	-2.09	2.44E-02
COG2814G	STM14_5161	STM4290	*proP*	proline/glycine betaine transporter	-3.46	9.80E-05
COG0366G	STM14_5345	STM4453	*treC*	trehalose-6-phosphate hydrolase	-2.12	2.28E-02
Amino acid transport & metabolism (E)						
COG0066E	STM14_0131	STM0110	*leuD*	isopropylmalate isomerase small subunit	-2.87	1.53E-03
COG0065E	STM14_0132	STM0111	*leuC*	isopropylmalate isomerase large subunit	-2.16	1.69E-02
COG1114E	STM14_0473	STM0399	*brnQ*	branched-chain amino acid transporter	-2.38	7.22E-03
*COG0111HE	STM14_1299	STM1135	*ycdW*	putative oxidoreductase	-2.34	1.04E-02
COG1125E	STM14_1802	STM1491	-	proline/glycine betaine transport system	-3.27	2.27E-04
COG1174E	STM14_1803	STM1492	-	putative ABC transporter permease	-3.31	2.07E-04
COG1174E	STM14_1805	STM1494	-	putative transport system permease component	-4.20	2.84E-06
*COG0462FE	STM14_2153	STM1780	*prsA*	ribose-phosphate pyrophosphokinase	-2.64	2.80E-03
COG0814E	STM14_2355	STM1937	*tyrP*	tyrosine-specific transport protein	-2.34	9.73E-03
COG0531E	STM14_2560	STM2068	*yeeF*	putative amino acid transport protein	-2.98	9.07E-04
COG0531E	STM14_3137	STM2558	*cadB*	lysine/cadaverine antiporter	-2.71	2.21E-03
COG1982E	STM14_3138	STM2559	*cadA*	lysine decarboxylase 1	-5.65	5.69E-10
COG3104E	STM14_3139	STM2560	*yjdL*	putative di-/tripeptide transport protein	-7.30	4.65E-14
COG4176E	STM14_3392	STM2810	*proW*	glycine betaine transporter membrane protein	-2.93	9.28E-04
COG2113E	STM14_3393	STM2811	*proX*	glycine betaine transporter periplasmic subunit	-5.63	5.74E-10
COG0814E	STM14_3961	STM3279	*mtr*	tryptophan permease	-3.13	5.70E-04
COG3977E	STM14_4421	STM3665	*avtA*	valine--pyruvate transaminase	-2.14	1.70E-02
Nucleotide transport & metabolism (F)						
COG0634F	STM14_0202	STM0170	*hpt*	hypoxanthine-guanine phosphoribosyltransferase	-2.37	7.39E-03
COG0528F	STM14_0259	STM0218	*pyrH*	uridylate kinase	-2.39	6.88E-03
COG0503F	STM14_0373	STM0317	*gpt*	xanthine-guanine phosphoribosyltransferase	-2.93	1.02E-03
COG0503F	STM14_0568	STM0483	*apt*	adenine phosphoribosyltransferase	-3.54	7.82E-05
COG0283F	STM14_1109	STM0980	*cmk*	cytidylate kinase	-2.65	2.74E-03
*COG0462FE	STM14_2153	STM1780	*prsA*	ribose-phosphate pyrophosphokinase	-2.64	2.80E-03
COG0572F	STM14_2618	STM2122	*udk*	uridine kinase	-1.99	2.75E-02
COG0209F	STM14_2812	STM2277	*nrdA*	ribonucleotide-diphosphate reductase subunit alpha	-3.15	3.99E-04
COG0208F	STM14_2813	STM2278	*nrdB*	ribonucleotide-diphosphate reductase subunit beta	-2.36	8.09E-03
COG2233F	STM14_3061	STM2497	*uraA*	uracil transporter	-3.23	6.86E-04
COG0519F	STM14_3075	STM2510	*guaA*	bifunctional GMP synthase/glutamine amidotransferase protein	-2.08	1.94E-02
COG0516F	STM14_3076	STM2511	*guaB*	inositol-5-monophosphate dehydrogenase	-2.91	1.02E-03
COG0504F	STM14_3558	STM2953	*pyrG*	CTP synthetase	-2.04	2.23E-02

COG1328F	STM14_5343	STM4452	*nrdD*	anaerobic ribonucleoside triphosphate reductase	-3.15	4.11E-04
Coenzyme transport & metabolism (H)						
COG0301H	STM14_0503	STM0425	*thiI*	thiamine biosynthesis protein ThiI	-2.00	2.59E-02
COG0321H	STM14_0741	STM0635.S	*lipB*	lipoyltransferase	-3.00	7.84E-04
*COG0111HE	STM14_1299	STM1135	*ycdW*	putative oxidoreductase	-2.34	1.04E-02
COG0373H	STM14_2147	STM1777	*hemA*	glutamyl-tRNA reductase	-2.42	6.06E-03
COG1179H	STM14_3602	STM2987	*ygdL*	hypothetical protein	-1.93	3.31E-02
COG1539H	STM14_3882	STM3206	*folB*	bifunctional dihydroneopterin aldolase/dihydroneopterin triphosphate 2'-epimerase	-2.94	1.32E-03
COG0452H	STM14_4492	STM3730	*dfp*	bifunctional phosphopantothenoylcysteine decarboxylase/phosphopantothenate synthase	-1.89	3.64E-02
COG1575H	STM14_4918	STM4090	*menA*	1,4-dihydroxy-2-naphthoate octaprenyltransferase	-1.88	3.86E-02
Lipid transport & metabolism (I)						
COG0764I	STM14_1211	STM1067	*fabA*	3-hydroxydecanoyl-ACP dehydratase	-3.04	6.32E-04
COG1947I	STM14_2150	STM1779	*ipk*	4-diphosphocytidyl-2-C-methyl-D-erythritol kinase	-2.35	8.56E-03
*COG0318IQ	STM14_2199	STM1818	*fadD*	long-chain-fatty-acid--CoA ligase	-2.48	5.08E-03
COG0777I	STM14_2914	STM2366	*accD*	acetyl-CoA carboxylase subunit beta	-2.21	1.30E-02
Inorganic ion transport & metabolism (P)						
COG1629P	STM14_0228	STM0191	*fhuA*	ferrichrome outer membrane transporter	-2.34	8.64E-03
COG2076P	STM14_1791	STM1482	*ydgF*	multidrug efflux system protein MdtJ	-3.44	1.24E-04
COG2076P	STM14_1792	STM1483	*ydgE*	multidrug efflux system protein MdtI	-4.27	6.41E-06
COG0038P	STM14_1801	STM1490	-	putative voltage-gated ClC-type chloride channel ClcB	-4.15	1.91E-05
COG1275P	STM14_1947	STM1609	*tehA*	potassium-tellurite ethidium and proflavin transporter	-2.27	1.03E-02
COG3546P	STM14_2094	STM1731	-	putative catalase	-2.51	4.38E-03
COG2223P	STM14_2134	STM1765	*narK*	nitrite extrusion protein	-3.56	9.80E-05
COG0387P	STM14_2141	STM1771	*chaA*	calcium/sodium:proton antiporter	-2.35	8.64E-03
COG0659P	STM14_2154	STM1781	*ychM*	putative sulfate transporter YchM	-3.06	6.86E-04
COG3615P	STM14_2185	STM1808	-	putative cytoplasmic protein	-2.14	1.58E-02
COG4531P	STM14_2300	STM1891	*znuA*	high-affinity zinc transporter periplasmic protein	-2.36	7.80E-03
COG4536P	STM14_3284	STM2679	*yfjD*	hypothetical protein	-2.33	9.23E-03
*COG0651CP	STM14_3445	STM2851	*hycC*	formate hydrogenlyase subunit 3	-5.37	7.93E-09
COG0803P	STM14_3458	STM2861	*sitA*	putative periplasmic binding protein	-2.06	2.26E-02
COG1121P	STM14_3459	STM2862	*sitB*	putative ATP-binding protein	-2.14	1.79E-02
*COG2146PR	STM14_4184	STM3475	*nirD*	nitrite reductase small subunit	-3.15	5.41E-04
COG2116P	STM14_4186	STM3476	*nirC*	nitrite transporter NirC	-3.05	1.32E-03
COG0370P	STM14_4222	STM3506	*feoB*	ferrous iron transport protein B	-2.69	2.34E-03
COG0704P	STM14_4648	STM3853	*phoU*	transcriptional regulator PhoU	-2.12	1.73E-02
COG1117P	STM14_4649	STM3854	*pstB*	phosphate transporter subunit	-2.42	6.24E-03
COG0581P	STM14_4650	STM3855	*pstA*	phosphate transporter permease subunit	-1.96	2.92E-02
COG0573P	STM14_4651	STM3856	*pstC*	phosphate transporter permease subunit	-2.60	3.38E-03
COG0226P	STM14_4652	STM3857	*pstS*	phosphate transporter subunit	-2.81	1.49E-03

*COG3678UNTP	STM14_4883	STM4060	*cpxP*	repressor CpxP	-5.22	7.30E-09
COG2824P	STM14_5159	STM4289	*phnA*	hypothetical protein	-4.63	2.49E-07
Secondary metabolites biosynthesis, transport & catabolism (Q)						
*COG0318IQ	STM14_2199	STM1818	*fadD*	long-chain-fatty-acid--CoA ligase	-2.48	5.08E-03
COG2050Q	STM14_4758	STM3956	*yigI*	hypothetical protein	-1.86	4.83E-02
Translation, ribosomal structure & biogenesis (J)						
COG0268J	STM14_0052	STM0043	*rpsT*	30S ribosomal protein S20	-3.00	7.16E-04
COG0024J	STM14_0255	STM0215	*map*	methionine aminopeptidase	-1.85	4.11E-02
COG0809J	STM14_0478	STM0404	*queA*	S-adenosylmethionine--tRNA ribosyltransferase-isomerase	-2.38	8.09E-03
*COG0513LKJ	STM14_951	STM0820	*rhlE*	ATP-dependent RNA helicase RhlE	-3.19	3.79E-04
COG0621J	STM14_996	STM0852	*yliG*	putative FeS oxidoreductase	-2.30	1.06E-02
COG0482J	STM14_1412	STM1234.S	*trmU*	tRNA (5-methyl aminomethyl-2-thiouridylate)-methyltransferase	-1.79	4.92E-02
COG0216J	STM14_2146	STM1776	*prfA*	peptide chain release factor 1	-1.91	3.55E-02
COG0231J	STM14_2733	STM2211.S	*yeiP*	elongation factor P	-2.53	4.58E-03
COG1187J	STM14_2747	STM2222	*rsuA*	16S rRNA pseudouridylate synthase A	-2.28	1.02E-02
COG0336J	STM14_3277	STM2674	*trmD*	tRNA (guanine-N(1)-)-methyltransferase	-1.90	3.52E-02
COG0806J	STM14_3278	STM2675	*rimM*	16S rRNA-processing protein	-2.52	4.23E-03
COG0564J	STM14_3573	STM2964	*yqcB*	tRNA pseudouridine synthase C	-1.88	4.53E-02
*COG0513LKJ	STM14_3962	STM3280.S	*deaD*	ATP-dependent RNA helicase DeaD	-2.44	5.60E-03
COG0184J	STM14_3966	STM3283	*rpsO*	30S ribosomal protein S15	-2.25	1.06E-02
COG0858J	STM14_3968	STM3285	*rbfA*	ribosome-binding factor A	-1.80	4.82E-02
COG0532J	STM14_3969	STM3286	*infB*	translation initiation factor IF-2	-2.10	1.83E-02
COG1534J	STM14_3983	STM3298.S	*yhbY*	RNA-binding protein YhbY	-2.05	2.15E-02
COG0211J	STM14_3990	STM3303	*rpmA*	50S ribosomal protein L27	-1.95	2.98E-02
COG0261J	STM14_3991	STM3304	*rplU*	50S ribosomal protein L21	-2.00	2.56E-02
COG0042J	STM14_4082	STM3384	*yhdG*	tRNA-dihydrouridine synthase B	-3.24	2.52E-04
COG0144J	STM14_4111	STM3408	*sun*	16S rRNA methyltransferase B	-1.97	2.93E-02
COG0090J	STM14_4140	STM3437	*rplB*	50S ribosomal protein L2	-2.01	2.45E-02
COG0089J	STM14_4141	STM3438	*rplW*	50S ribosomal protein L23	-2.53	4.19E-03
COG0088J	STM14_4142	STM3439	*rplD*	50S ribosomal protein L4	-2.46	5.12E-03
COG0087J	STM14_4143	STM3440	*rplC*	50S ribosomal protein L3	-2.26	1.03E-02
COG0051J	STM14_4144	STM3441	*rpsJ*	30S ribosomal protein S10	-2.72	2.20E-03
COG0048J	STM14_4152	STM3448	*rpsL*	30S ribosomal protein S12	-1.79	4.90E-02
COG0227J	STM14_4490	STM3728	*rpmB*	50S ribosomal protein L28	-1.80	4.73E-02
COG0689J	STM14_4496	STM3734	*rph*	ribonuclease PH	-3.34	2.05E-04
COG0230J	STM14_4634	STM3839	*rpmH*	50S ribosomal protein L34	-2.58	3.39E-03
COG0594J	STM14_4635	STM3840	*rnpA*	ribonuclease P	-2.97	8.22E-04
COG2269J	STM14_5224	STM4344	*yjeA*	lysyl-tRNA synthetase	-1.82	4.51E-02
COG0360J	STM14_5275	STM4391	*rpsF*	30S ribosomal protein S6	-2.52	4.31E-03
Transcription (K)						
COG2186K	STM14_0182	STM0151	*pdhR*	transcriptional regulator PdhR	-1.87	3.88E-02
*COG0745TK	STM14_0470	STM0397	*phoB*	transcriptional regulator PhoB	-2.84	1.35E-03
COG1309K	STM14_0676	STM0580	-	putative regulatory protein	-2.17	1.43E-02
COG4977K	STM14_0678	STM0581	-	putative regulatory protein	-3.52	7.77E-05
COG0583K	STM14_0739	STM0634	*ybeF*	putative DNA-binding transcriptional regulator	-2.20	1.40E-02
*COG0513LKJ	STM14_951	STM0820	*rhlE*	ATP-dependent RNA helicase RhlE	-3.19	3.79E-04
COG1321K	STM14_975	STM0835	-	manganese transport regulator MntR	-2.21	1.43E-02

COG1309K	STM14_1276	STM1122	*ycdC*	putative transcriptional repressor	-3.02	6.93E-04
*COG2747KNU	STM14_1342	STM1172	*flgM*	anti-sigma-28 factor FlgM	-2.49	4.60E-03
*COG2197TK	STM14_1526	STM1265	-	putative response regulator	-2.35	7.90E-03
COG2207K	STM14_1837	STM1519.S	*marA*	DNA-binding transcriptional activator MarA	-5.15	1.02E-08
COG1846K	STM14_1838	STM1520	*marR*	DNA-binding transcriptional repressor MarR	-5.63	5.90E-10
*COG2197TK	STM14_2403	STM1982	*rcsA*	colanic acid capsular biosynthesis activation protein A	-2.40	7.39E-03
COG0583K	STM14_2873	STM2330	*lrhA*	NADH dehydrogenase transcriptional repressor	-2.30	9.23E-03
COG1846K	STM14_3397	STM2813	*emrR*	transcriptional repressor MprA	-2.68	2.40E-03
COG1414K	STM14_3742	STM3098	-	putative transcriptional regulator	-3.49	2.62E-04
*COG0513LKJ	STM14_3962	STM3280.S	*deaD*	ATP-dependent RNA helicase DeaD	-2.44	5.60E-03
COG0195K	STM14_3970	STM3287	*nusA*	transcription elongation factor NusA	-2.27	1.02E-02
*COG2901KL	STM14_4083	STM3385	*fis*	DNA-binding protein Fis	-2.55	3.93E-03
COG0789K	STM14_5195	STM4320	-	putative regulatory protein	-1.99	2.61E-02
COG1609K	STM14_5348	STM4455	*treR*	trehalose repressor	-3.00	8.22E-04
Replication, recombination & repair (L)						
*COG0513LKJ	STM14_951	STM0820	*rhlE*	ATP-dependent RNA helicase RhlE	-3.19	3.79E-04
COG0550L	STM14_2075	STM1714	*topA*	DNA topoisomerase I	-2.23	1.16E-02
*COG0494LR	STM14_3038	STM2477	*yffH*	putative pyrophosphohydrolase	-2.29	9.91E-03
COG0593L	STM14_3060	STM2496	*yfgE*	DNA replication initiation factor	-2.74	2.32E-03
COG0358L	STM14_3887	STM3210	*dnaG*	DNA primase	-1.91	3.44E-02
*COG0513LKJ	STM14_3962	STM3280.S	*deaD*	ATP-dependent RNA helicase DeaD	-2.44	5.60E-03
*COG2901KL	STM14_4083	STM3385	*fis*	DNA-binding protein Fis	-2.55	3.93E-03
COG2965L	STM14_5276	STM4392	*priB*	primosomal replication protein N	-2.09	1.92E-02
COG3050L	STM14_5475	STM4557	*holD*	DNA polymerase III subunit psi	-3.03	8.89E-04
COG4974L	STM14_5554	PSLT031	*rsdB*	resolvase	-1.98	2.79E-02
Cell cycle control, cell division, chromosome partitioning (D)						
COG0445D	STM14_4671	STM3874	*gidA*	tRNA uridine 5-carboxymethylaminomethyl modification protein GidA	-1.82	4.54E-02
COG2846D	STM14_5283	STM4399	*ytfE*	cell morphogenesis/cell wall metabolism regulator	-1.81	4.83E-02
COG1192D	STM14_5575	PSLT052	*parA*	plasmid partition protein A	-2.51	4.34E-03
Defense mechanisms						
COG1566V	STM14_1740	STM1442	*ydhJ*	putative multidrug resistance efflux pump	-2.16	1.75E-02
COG1566V	STM14_3399	STM2814	*emrA*	multidrug resistance secretion protein	-2.30	9.41E-03
Signal transduction mechanisms (T)						
*COG0745TK	STM14_0470	STM0397	*phoB*	transcriptional regulator PhoB	-2.84	1.35E-03
COG5002T	STM14_0471	STM0398	*phoR*	phosphate regulon sensor protein	-2.75	2.01E-03
*COG2197TK	STM14_1526	STM1265	-	putative response regulator	-2.35	7.90E-03
*COG2197TK	STM14_2403	STM1982	*rcsA*	colanic acid capsular biosynthesis activation protein A	-2.40	7.39E-03
COG0642T	STM14_2802	STM2271	*rcsC*	hybrid sensory kinase in two-component regulatory system with RcsB and YojN	-2.48	5.16E-03
COG3026T	STM14_3232	STM2638	*rseB*	periplasmic negative regulator of sigmaE	-1.86	4.07E-02
COG3103T	STM14_3879	STM3203	*ygiM*	putative signal transduction protein	-1.86	4.21E-02

*COG0840NT	STM14_3893	STM3216	-	putative methyl-accepting chemotaxis protein	-2.13	1.67E-02
COG2200T	STM14_4346	STM3611	*yhjH*	EAL domain-containing protein	-2.61	3.17E-03
*COG3678UNTP	STM14_4883	STM4060	*cpxP*	repressor CpxP	-5.22	7.30E-09
Cell wall/membrane/envelope biogenesis (M)						
COG0741M	STM14_0305	STM0260	*dniR*	membrane-bound lytic murein transglycosylase D	-2.28	1.01E-02
COG1686M	STM14_0744	STM0637	*dacA*	D-alanyl-D-alanine carboxypeptidase	-2.84	1.31E-03
COG1560M	STM14_1323	STM1155	*htrB*	lipid A biosynthesis lauroyl acyltransferase	-2.36	8.52E-03
COG1732M	STM14_1804	STM1493	-	putative ABC transporter periplasmic component	-4.59	3.02E-07
COG3203M	STM14_1848	STM1530	-	putative outer membrane protein	-4.25	1.86E-06
COG3017M	STM14_2149	STM1778	*lolB*	outer membrane lipoprotein LolB	-2.04	2.38E-02
COG0739M	STM14_2299	STM1890	*yebA*	hypothetical protein	-2.22	1.21E-02
COG3765M	STM14_2573	STM2079	*wzzB*	lipopolysaccharide O-antigen chain length regulator	-2.15	1.53E-02
COG1089M	STM14_2604	STM2109	*gmd*	GDP-D-mannose dehydratase	-3.51	2.84E-04
COG3206M	STM14_2611	STM2116	*wzc*	tyrosine kinase	-2.60	4.92E-03
*COG4948MR	STM14_2807	STM2273	-	putative dehydratase	-2.60	3.39E-03
COG1560M	STM14_2953	STM2401	*ddg*	lipid A biosynthesis palmitoleoyl acyltransferase	-2.17	1.56E-02
COG2951M	STM14_3420	STM2831	*mltB*	murein hydrolase B	-2.34	9.21E-03
COG2821M	STM14_3603	STM2988	*mltA*	murein transglycosylase A	-2.19	1.39E-02
COG0860M	STM14_3606	STM2991	*amiC*	N-acetylmuramoyl-L-alanine amidase	-1.88	3.88E-02
COG2027M	STM14_3986	STM3300	*dacB*	D-alanyl-D-alanine carboxypeptidase	-1.89	3.78E-02
COG0859M	STM14_4484	STM3723	*rfaQ*	lipopolysaccharide core biosynthesis protein	-1.99	2.59E-02
Cell motility						
*COG3418NUO	STM14_1341	STM1171	*flgN*	putative FlgK/FlgL export chaperone	-2.52	4.23E-03
*COG2747KNU	STM14_1342	STM1172	*flgM*	anti-sigma-28 factor FlgM	-2.49	4.60E-03
COG1360N	STM14_2337	STM1922	*motB*	flagellar motor protein MotB	-1.94	3.09E-02
COG1291N	STM14_2338	STM1923	*motA*	flagellar motor protein MotA	-2.37	7.39E-03
*COG0840NT	STM14_3893	STM3216	-	putative methyl-accepting chemotaxis protein	-2.13	1.67E-02
*COG3539NU	STM14_4387	STM3640	*lpfA*	long polar fimbrial protein A precursor	-2.38	7.35E-03
*COG3678UNTP	STM14_4883	STM4060	*cpxP*	repressor CpxP	-5.22	7.30E-09
Intracellular trafficking, secretion, & vesicular transport (U)						
*COG3418NUO	STM14_1341	STM1171	*flgN*	putative FlgK/FlgL export chaperone	-2.52	4.23E-03
*COG2747KNU	STM14_1342	STM1172	*flgM*	anti-sigma-28 factor FlgM	-2.49	4.60E-03
COG1314U	STM14_3976	STM3293	*secG*	preprotein translocase subunit SecG	-2.86	1.19E-03
*COG3539NU	STM14_4387	STM3640	*lpfA*	long polar fimbrial protein A precursor	-2.38	7.35E-03
COG1826U	STM14_4779	STM3973	*tatA*	twin argininte translocase protein A	-2.10	1.82E-02
*COG3678UNTP	STM14_4883	STM4060	*cpxP*	repressor CpxP	-5.22	7.30E-09
Posttranslational modification, protein turnover, chaperones (O)						
COG0542O	STM14_0319	STM0272	-	putative chaperone ATPase	-2.94	1.31E-03
COG0544O	STM14_0529	STM0447	*tig*	trigger factor	-2.29	9.58E-03
*COG4232OC	STM14_1267	STM1114	*scsB*	suppression of copper sensitivity protein	-1.99	3.64E-02

*COG3418NUO	STM14_1341	STM1171	*flgN*	putative FlgK/FlgL export chaperone	-2.52	4.23E-03
COG1214O	STM14_2202	STM1820	*yeaZ*	putative molecular chaperone	-3.75	4.26E-05
COG0826O	STM14_2634	STM2136	*yegQ*	putative protease	-2.09	1.93E-02
COG0443O	STM14_3114	STM2539	*hscA*	chaperone protein HscA	-1.91	3.37E-02
COG0068O	STM14_3434	STM2842	*hypF*	hydrogenase maturation protein	-2.77	2.08E-03
COG0652O	STM14_4179	STM3472	*ppiA*	peptidyl-prolyl cis-trans isomerase A	-2.54	4.13E-03
COG0071O	STM14_4599	STM3808.S	*ibpB*	heat shock chaperone IbpB	-1.95	3.02E-02
COG0071O	STM14_4600	STM3809.S	*ibpA*	heat shock protein IbpA	-2.50	4.57E-03
COG5405O	STM14_4920	STM4092	*hslV*	ATP-dependent protease peptidase subunit	-2.53	4.23E-03
COG0545O	STM14_5281	STM4397	*fklB*	peptidyl-prolyl cis-trans isomerase	-1.91	3.77E-02
General function prediction only (R)						
COG0656R	STM14_0300	STM0255	*dkgB*	2,5-diketo-D-gluconate reductase B	-2.75	2.21E-03
COG0488R	STM14_978	STM0838	*ybiT*	putative ABC transporter ATPase component	-2.28	9.91E-03
COG2915R	STM14_1411	STM1233	*ycfC*	hypothetical protein	-1.85	4.26E-02
COG3083R	STM14_2754	STM2228	*yejM*	putative hydrolase	-2.05	2.15E-02
*COG4948MR	STM14_2807	STM2273	-	putative dehydratase	-2.60	3.39E-03
COG0622R	STM14_2893	STM2347	*yfcE*	phosphodiesterase	-2.19	1.40E-02
*COG0494LR	STM14_3038	STM2477	*yffH*	putative pyrophosphohydrolase	-2.29	9.91E-03
COG4137R	STM14_3283	STM2678	*corE*	hypothetical protein	-3.01	8.22E-04
COG3950R	STM14_3310	STM2746	-	putative ATPase	-2.08	1.97E-02
COG2916R	STM14_3377	STM2799	*stpA*	DNA binding protein	-2.83	1.32E-03
COG0325R	STM14_3744	STM3100	*yggS*	hypothetical protein	-3.01	8.15E-04
COG1811R	STM14_3764	STM3115	*yqgA*	putative inner membrane protein	-2.60	3.38E-03
*COG2146PR	STM14_4184	STM3475	*nirD*	nitrite reductase small subunit	-3.15	5.41E-04
COG3383R	STM14_5155	STM4285	*fdhF*	formate dehydrogenase	-3.30	2.07E-04
COG0456R	STM14_5476	STM4558	*rimI*	ribosomal-protein-alanine N-acetyltransferase	-2.80	1.88E-03
Function unknown (S)						
COG2315S	STM14_0675	STM0579	*ybdF*	hypothetical protein	-2.31	9.44E-03
COG2921S	STM14_0743	STM0636	*ybeD*	hypothetical protein	-2.89	1.07E-03
COG0799S	STM14_0750	STM0642	*ybeB*	hypothetical protein	-2.23	1.36E-02
COG1376S	STM14_977	STM0837	*ybiS*	hypothetical protein	-2.20	1.38E-02
COG3226S	STM14_1020	STM0869	-	putative regulatory protein	-1.83	4.94E-02
COG2990S	STM14_1057	STM0940	*ybjX*	VirK-like protein	-1.92	3.31E-02
COG1944S	STM14_1101	STM0975	*ycaO*	putative cytoplasmic protein	-2.00	2.59E-02
COG3304S	STM14_1219	STM1074	*yccF*	hypothetical protein	-3.13	9.09E-04
COG3781S	STM14_1845	STM1527	-	putative inner membrane protein	-2.22	1.40E-02
COG1937S	STM14_1969	STM1628	-	putative cytoplasmic protein	-1.88	4.26E-02
COG3685S	STM14_2092	STM1729	*yciF*	putative cytoplasmic protein	-2.27	1.02E-02
COG3685S	STM14_2093	STM1730	*yciE*	putative cytoplasmic protein	-2.44	5.72E-03
COG3094S	STM14_2144	STM1774	*sirC*	putative transcriptional regulator	-2.17	1.53E-02
COG2975S	STM14_3112	STM2537	*yfhJ*	hypothetical protein	-1.84	4.36E-02
COG2128S	STM14_3385	STM2804	-	putative cytoplasmic protein	-2.65	4.31E-03
COG4125S	STM14_3648	STM3021	-	putative inner membrane protein	-3.81	3.86E-05
COG0762S	STM14_3745	STM3101	*yggT*	putative integral membrane protein	-2.29	1.02E-02
COG0779S	STM14_3971	STM3288	*yhbC*	hypothetical protein	-2.71	2.21E-03
COG1289S	STM14_4058	STM3364	*yhcP*	p-hydroxybenzoic acid efflux subunit AaeB	-2.12	1.85E-02
COG0759S	STM14_4636	STM3841	-	hypothetical protein	-3.06	6.32E-04

not assigned						
-	STM14_0186	-	-	hypothetical protein	-2.82	2.56E-03
-	STM14_0187	STM0155	-	putative outer membrane protein	-3.52	3.24E-04
-	STM14_0242	-	-	hypothetical protein	-2.46	8.43E-03
-	STM14_0296	-	-	hypothetical protein	-2.51	4.39E-03
-	STM14_0321	-	-	putative cytoplasmic protein	-2.88	2.08E-03
-	STM14_0677	-	-	hypothetical protein	-3.79	2.06E-05
-	STM14_0731	STM0628	*pagP*	palmitoyl transferase for Lipid A	-2.74	2.34E-03
-	STM14_0738	-	-	hypothetical protein	-2.63	2.98E-03
-	STM14_0811	STM0695	*ybfE*	LexA regulated protein	-2.76	2.35E-03
-	STM14_0925	-	-	hypothetical protein	-2.19	1.40E-02
-	STM14_940	STM0810	-	putative inner membrane protein	-2.43	9.36E-03
-	STM14_1076	STM0954	-	putative inner membrane protein	-2.21	1.28E-02
-	STM14_1202	STM1059	*ycbW*	putative cytoplasmic protein	-1.79	4.98E-02
-	STM14_1446	-	-	putative bacteriophage protein	-2.92	1.09E-03
-	STM14_1564	-	-	hypothetical protein	-1.99	2.93E-02
-	STM14_1760	STM1461.S	*ydgT*	oriC-binding nucleoid-associated protein	-3.48	1.06E-04
-	STM14_1790	-	-	hypothetical protein	-2.56	4.31E-03
-	STM14_1836	STM1518	*marB*	hypothetical protein	-3.70	3.67E-05
-	STM14_2020	STM1673	-	putative outer membrane lipoprotein	-2.53	4.39E-03
-	STM14_2076	-	-	hypothetical protein	-3.17	4.11E-04
-	STM14_2077	STM1715	*yciN*	hypothetical protein	-1.84	4.21E-02
-	STM14_2276	-	-	hypothetical protein	-2.94	1.10E-03
-	STM14_2366	-	-	putative inner membrane protein	-2.58	4.81E-03
-	STM14_2367	STM1949	*yecF*	hypothetical protein	-1.86	4.07E-02
-	STM14_2833	STM2296	*ais*	aluminum-inducible protein	-2.51	6.23E-03
-	STM14_2881	-	-	hypothetical protein	-3.37	1.70E-04
-	STM14_3236	-	-	hypothetical protein	-2.01	3.06E-02
-	STM14_3311	STM2747	-	putative cytoplasmic protein	-2.02	2.37E-02
-	STM14_3394	-	-	hypothetical protein	-5.30	2.03E-07
-	STM14_3437	-	-	hypothetical protein	-4.08	3.57E-05
-	STM14_3440	STM2846	*hycH*	hydrogenase 3 large subunit processing protein	-2.15	2.00E-02
-	STM14_3447	-	-	hypothetical protein	-7.59	1.52E-13
-	STM14_3448	STM2853	*hycA*	formate hydrogenlyase regulatory protein HycA	-7.74	1.40E-14
-	STM14_3449	-	-	hypothetical protein	-7.80	4.29E-13
-	STM14_3500	STM2901	-	putative cytoplasmic protein	-1.87	4.15E-02
-	STM14_3536	STM2932	*ygbE*	hypothetical protein	-1.88	4.23E-02
-	STM14_3822	STM3156	-	putative cytoplasmic protein	-1.91	3.51E-02
-	STM14_3965	-	-	hypothetical protein	-2.02	2.44E-02
-	STM14_4053	-	-	hypothetical protein	-2.71	2.40E-03
-	STM14_4055	STM3361	*yhcN*	putative outer membrane protein	-2.97	8.15E-04
-	STM14_4056	STM3362	-	hypothetical protein	-2.90	1.02E-03
-	STM14_4092	STM3392	*yhdV*	putative outer membrane lipoprotein	-2.21	1.32E-02
-	STM14_4093	-	-	hypothetical protein	-2.89	1.59E-03
-	STM14_4163	-	-	hypothetical protein	-2.08	2.57E-02
-	STM14_4178	STM3471	*yhfG*	hypothetical protein	-1.87	4.11E-02
-	STM14_4220	-	-	hypothetical protein	-2.06	2.49E-02
-	STM14_4223	STM3507	*yhgG*	putative cytoplasmic protein	-2.33	9.60E-03
-	STM14_4400	STM3650	-	hypothetical protein	-2.18	1.43E-02
-	STM14_4581	-	-	hypothetical protein	-5.26	1.97E-08

-	STM14_4601	-	-	hypothetical protein	-2.65	2.80E-03
-	STM14_4633	-	-	hypothetical protein	-2.00	2.67E-02
-	STM14_4640	STM3845	-	putative inner membrane protein	-2.42	6.23E-03
-	STM14_4797	-	-	hypothetical protein	-2.62	3.14E-03
-	STM14_4970	-	-	hypothetical protein	-2.60	3.39E-03
-	STM14_5123	STM4263	*yjcB*	putative inner membrane protein	-1.84	4.34E-02
-	STM14_5150	-	-	hypothetical protein	-2.61	3.87E-03
-	STM14_5154	-	-	hypothetical protein	-1.91	3.97E-02
-	STM14_5162	-	-	hypothetical protein	-3.35	1.65E-04
-	STM14_5196	-	-	hypothetical protein	-4.51	2.82E-06
-	STM14_5274	STM4390	-	putative cytoplasmic protein	-2.05	2.27E-02
-	STM14_5495	STM4575	-	putative outer membrane protein	-1.82	4.54E-02
-	STM14_5570	PSLT047	-	putative cytoplasmic protein	-2.55	4.29E-03

*Genes assigned to more than one COG class

Table A 9: Up-regulated genes in response to an acidified $NaNO_2$ 10 min shock or 1 h exposure in EHEC EDL933 WT

				10 min		1 h	
COG	EDL933 identifier	Gene	Product	log_2 FC	p-value (BH-adjusted)	log_2 FC	p-value (BH-adjusted)
Energy production & conversion (C)							
COG1018C	Z1106	-	HCP oxidoreductase			7.46	1.14E-11
COG1151C	Z1107	*ybjW*	hydroxylamine reductase	5.46	1.78E-07	7.14	2.33E-12
COG0348C	Z1409	*yccM*	hypothetical protein			3.41	1.77E-03
COG1252C	Z1748	*ndh*	NADH dehydrogenase	3.13	1.61E-03	4.01	5.16E-06
COG1454C	Z2016	*adhE*	bifunctional acetaldehyde-CoA/alcohol dehydrogenase			1.99	2.06E-02
*COG1052CHR	Z2329	*ldhA*	D-lactate dehydrogenase	2.36	3.86E-02	3.84	1.07E-05
COG4117C	Z2697	*ydhU*	hypothetical protein			2.35	2.11E-02
*COG0473CE	Z2843	*yeaU*	tartrate dehydrogenase			3.55	1.32E-03
COG1018C	Z3828	*hmpA*	nitric oxide dioxygenase	6.26	4.72E-11	7.86	7.17E-16
COG0426C	Z4018	- (*norVs*)	anaerobic nitric oxide reductase flavorubredoxin	10.95	2.77E-21	12.35	9.08E-26
COG1251C	Z4019	*ygbD* (*norW*)	nitric oxide reductase	5.33	5.42E-07	9.85	1.74E-19
COG0716C	Z4106	-	flavodoxin			2.16	1.29E-02
COG1979C	Z4364	*yqhD*	oxidoreductase			1.78	4.26E-02
COG3954C	Z4716	*prkB*	phosphoribulokinase			2.20	1.26E-02
COG1018C	Z5469	*fpr*	ferredoxin-NADP reductase			2.48	4.45E-03
*COG0604CR	Z5649	*qor*	quinone oxidoreductase			2.45	4.98E-03
COG3783C	Z5846	*cybC*	cytochrome b562			1.71	4.93E-02
Carbohydrate transport & metabolism (G)							
COG0153G	Z0927	*galK*	galactokinase			1.98	2.11E-02
COG2133G	Z1063	*yliI*	dehydrogenase			2.83	8.45E-03
COG0366G	Z2475m	*ycjM*	glycosidase			2.87	2.51E-03
*COG0451MG	Z3178	-	enzyme of sugar metabolism			1.79	3.74E-02
COG0246G	Z3431	*yeiQ*	oxidoreductase			1.97	2.55E-02
COG2814G	Z3982	-	transporter			2.35	1.91E-02
COG0057G	Z4266	*epd*	erythrose 4-phosphate dehydrogenase			2.04	1.84E-02
COG3250G	Z4429	*ebgA*	cryptic beta-D-galactosidase subunit alpha			2.20	3.04E-02
*COG1349KG	Z4483	*agaR*	DNA-binding transcriptional regulator AgaR			1.76	4.32E-02

*COG2610GE	Z4804	*gntU*	low affinity gluconate transporter			3.11	4.85E-04
COG3265G	Z4805	*gntK*	gluconate kinase	4.82	4.02E-07	4.72	2.31E-07
COG2211G	Z5085	*yicJ*	transporter			2.40	1.85E-02
COG2814G	Z5255	*yieO*	transporter			2.91	8.61E-04
COG2211G	Z5412	*yihO*	permease			2.26	2.52E-02
COG2814G	Z5523	-	citrate permease			2.11	2.91E-02
*COG0702MG	Z5822	*ytfG*	oxidoreductase			3.34	7.50E-04
COG1172G	Z5841	*yjfF*	ABC transporter permease			2.43	9.02E-03
Amino acid transport & metabolism (E)							
COG0527E	Z0002	*thrA*	bifunctional aspartokinase I/homoserine dehydrogenase I			1.86	3.36E-02
COG1113E	Z0122	*aroP*	aromatic amino acid transporter			2.02	2.11E-02
COG1506E	Z0300	*frsA*	fermentation/respiration switch protein			2.27	1.00E-02
COG1280E	Z0424	*yahN*	cytochrome subunit of dehydrogenase			2.88	1.75E-03
COG2066E	Z0606	*ybaS*	glutaminase			2.16	1.48E-02
COG1113E	Z0607	*ybaT*	amino acid/amine transport protein			2.88	1.05E-03
COG0624E	Z0671	*ylbB*	allantoate amidohydrolase			2.51	8.81E-03
COG0436E	Z0743	*ybdL*	aminotransferase			2.09	2.59E-02
COG1446E	Z1051m	-	L-asparaginase			2.54	8.09E-03
COG0076E	Z2215	*gadB*	glutamate decarboxylase			2.57	2.88E-03
*COG0473CE	Z2843	*yeaU*	tartrate dehydrogenase			3.55	1.32E-03
COG0549E	Z4213	*yqeA*	carbamate kinase			2.07	2.77E-02
COG0509E	Z4241	*gcvH*	glycine cleavage system protein H			1.93	2.56E-02
COG0754E	Z4342	*gsp*	bifunctional glutathionylspermidine amidase/glutathionylspermidine synthetase			2.24	8.98E-03
COG3633E	Z4442	*ygjU*	serine/threonine transporter SstT			1.82	4.32E-02
*COG2610GE	Z4804	*gntU*	low affinity gluconate transporter			3.11	4.85E-04
COG0076E	Z4930	*gadA*	glutamate decarboxylase			2.55	3.18E-03
COG0440E	Z5164	*ilvN*	acetolactate synthase 1 regulatory subunit			2.03	4.45E-02
COG3033E	Z5203	*tnaA*	tryptophanase			3.92	2.12E-05
COG2502E	Z5245	*asnA*	asparagine synthetase AsnA			2.18	1.08E-02
*COG0059EH	Z5285	*ilvC*	ketol-acid reductoisomerase			2.11	1.59E-02
COG0531E	Z5735	*cadB*	lysine/cadaverine antiporter			2.48	5.04E-03
COG0078E	Z5866	*argI*	ornithine carbamoyltransferase subunit I			2.54	5.66E-03
Nucleotide transport & metabolism (F)							
COG0208F	Z3978	*nrdF*	ribonucleotide-diphosphate reductase subunit beta			1.98	3.43E-02
COG1781F	Z5855	*pyrI*	aspartate carbamoyltransferase			2.04	3.62E-02
Coenzyme transport & metabolism (H)							
COG2226H	Z0237	*yafS*	hypothetical protein			1.77	4.14E-02
COG2896H	Z1000	*moaA*	molybdenum cofactor biosynthesis protein A			1.89	2.87E-02
COG0521H	Z1001	*moaB*	molybdopterin biosynthesis, protein B			2.86	9.77E-04
*COG1052CHR	Z2329	*ldhA*	D-lactate dehydrogenase	2.36	3.86E-02	3.84	1.07E-05
*COG1120PH	Z4385	-	ABC transporter ATP-binding protein			2.14	1.31E-02
COG0635H	Z4914	*chuW*	coproporphyrinogen III oxidase			3.35	2.88E-04
*COG0059EH	Z5285	*ilvC*	ketol-acid reductoisomerase			2.11	1.59E-02

COG1763H	Z5388	*mobB*	molybdopterin-guanine dinucleotide biosynthesis protein B			2.72	1.89E-03
Lipid transport & metabolism (I)							
COG1960I	Z0045	*caiA*	crotonobetainyl-CoA dehydrogenase			3.69	3.38E-05
COG1182I	Z2315	*acpD*	azoreductase	2.42	3.36E-02	6.03	2.95E-11
COG1443I	Z4227	-	isopentenyl-diphosphate delta-isomerase			1.74	4.60E-02
Inorganic ion transport & metabolism (P)							
COG0475P	Z0053	*kefC*	glutathione-regulated potassium-efflux system protein KefC			2.02	2.08E-02
COG2217P	Z0604	*copA*	copper exporting ATPase			2.04	1.77E-02
COG2382P	Z0725	*fes*	enterobactin/ferric enterobactin esterase			1.83	3.43E-02
COG0609P	Z0732	*fepD*	iron-enterobactin transporter membrane protein			2.52	3.76E-03
COG1230P	Z0922	*ybgR*	zinc transporter ZitB			2.63	8.59E-03
COG3793P	Z1173	*terB*	phage inhibition, colicin resistance and tellurite resistance protein			2.05	2.28E-02
COG4771P	Z1178	-	bifunctional enterobactin receptor/adhesin protein			2.27	9.45E-03
COG3793P	Z1612	*terB_2*	phage inhibition, colicin resistance and tellurite resistance protein			1.96	2.79E-02
COG4771P	Z1617	-	bifunctional enterobactin receptor/adhesin protein			2.45	5.27E-03
COG4773P	Z1741	*fhuE*	ferric-rhodotorulic acid outer membrane transporter			2.16	2.47E-02
COG4771P	Z1961	*prrA*	TonB dependent outer membrane receptor			2.68	2.65E-03
COG1275P	Z2289	*tehA*	potassium-tellurite ethidium and proflavin transporter			3.51	1.19E-04
COG4256P	Z2734	*ydiE*	hypothetical protein			2.06	1.77E-02
COG3615P	Z2839	*yeaR*	hypothetical protein			2.26	8.45E-03
COG1914P	Z3658	-	manganese transport protein MntH	2.77	8.68E-03	4.19	2.34E-06
COG0607P	Z3967	*ygaP*	hypothetical protein			1.84	4.56E-02
COG0609P	Z4384	-	iron ABC transporter permease			2.20	1.38E-02
*COG1120PH	Z4385	-	ABC transporter ATP-binding protein			2.14	1.31E-02
COG4773P	Z4386	-	iron compound receptor			2.50	3.93E-03
COG0475P	Z4710	*kefB*	glutathione-regulated potassium-efflux system protein KefB			2.51	4.28E-03
COG4558P	Z4913	*chuT*	periplasmic binding protein			4.62	8.03E-07
COG2223P	Z4972	*yhjX*	resistance protein			2.09	1.47E-02
COG3119P	Z5314	*aslA*	arylsulfatase			1.98	4.21E-02
COG1283P	Z5611	*yjbB*	alpha helix protein			2.38	6.29E-03
COG0735P	Z5645	*yjbK*	zinc uptake transcriptional repressor			2.06	2.81E-02
Translation, ribosomal structure & biogenesis (J)							
COG3130J	Z1303	*rmf*	ribosome modulation factor			3.25	2.97E-04
COG1544J	Z3890	*yfiA*	translation inhibitor protein RaiA			3.80	1.28E-05
COG1544J	Z4566	*yhbH*	sigma(54) modulation protein			2.06	1.60E-02
COG1670J	Z4809	*yhhY*	acetyltransferase YhhY			3.04	9.89E-04
COG1490J	Z5426	*yihZ*	D-tyrosyl-tRNA(Tyr) deacylase			1.94	2.62E-02
Transcription (K)							
COG2186K	Z0123	*pdhR*	transcriptional regulator PdhR			1.73	4.45E-02
COG0583K	Z0230	*yafC*	LysR family transcriptional regulator			2.82	1.54E-03

COG3609K	Z0509	-	hypothetical protein			1.83	3.32E-02
COG1309K	Z1016	*ybiH*	DNA-binding transcriptional regulator			3.07	8.86E-04
*COG2747KNU	Z1709	*flgM*	anti-sigma-28 factor FlgM			2.42	4.96E-03
COG1309K	Z1750	*ycfQ*	hypothetical protein			1.77	4.42E-02
*COG1221KT	Z2484	*pspF*	phage shock protein operon transcriptional activator			2.35	6.81E-03
COG0583K	Z2535	*cysB*	transcriptional regulator CysB			2.44	4.83E-03
COG2207K	Z2765	*celD*	DNA-binding transcriptional regulator ChbR			1.95	2.34E-02
COG0583K	Z3177	*yeeY*	LysR family transcriptional regulator			3.81	1.47E-05
COG1476K	Z3663	*yfeD*	hypothetical protein			2.15	1.31E-02
COG1737K	Z3692	*yfeT*	hypothetical protein			2.74	6.87E-03
*COG3604KT	Z4017	*ygaA*	anaerobic nitric oxide reductase transcriptional regulator			2.11	4.03E-02
COG3722K	Z4274	*yggD*	DNA-binding transcriptional regulator			2.34	7.33E-03
COG2207K	Z4363	*yqhC*	AraC family transcriptional regulator			2.18	1.59E-02
COG1695K	Z4424	*yqjI*	hypothetical protein	2.37	4.33E-02	3.63	3.44E-05
COG2002K	Z4481	*sohA*	regulator PrlF			1.91	2.63E-02
*COG1349KG	Z4483	*agaR*	DNA-binding transcriptional regulator AgaR			1.76	4.32E-02
COG0789K	Z4662	*zntR*	zinc-responsive transcriptional regulator			2.87	1.14E-03
COG2207K	Z4929	*yhiX* (*gadX*)	DNA-binding transcriptional regulator GadX			3.94	8.10E-06
COG0583K	Z4934	*yhjC*	LysR family transcriptional regulator			2.11	2.91E-02
COG1609K	Z4994	*xylR*	regulator of xyl operon			1.97	2.49E-02
COG0583K	Z5004	*yiaU*	LysR family transcriptional regulator			1.76	4.21E-02
COG2207K	Z5175	*yidL*	AraC family transcriptional regulator			3.30	2.39E-04
COG1522K	Z5244	*asnC*	DNA-binding transcriptional regulator AsnC			2.25	1.31E-02
COG2186K	Z5258	*yieP*	hypothetical protein			2.20	1.04E-02
COG2390K	Z5619	-	transcriptional regulator of sorbose uptake and utilization genes			3.61	9.22E-05
COG2207K	Z5661	*soxS*	DNA-binding transcriptional regulator SoxS			2.47	4.32E-03
COG0789K	Z5662	*soxR*	redox-sensitive transcriptional activator SoxR			3.04	8.81E-04
COG1959K	Z5785	*yjeB*	transcriptional repressor NsrR			2.26	8.36E-03
COG2186K	Z5922	*uxuR*	DNA-binding transcriptional repressor UxuR			1.90	3.32E-02
Replication, recombination & repair (L)							
COG2963L	L7045	-	hypothetical protein			2.01	1.98E-02
COG3077L	Z0285	*dinJ*	damage-inducible protein J			1.92	2.66E-02
COG1943L	Z0288	*yafM*	hypothetical protein			3.31	7.27E-04
COG2826L	Z1133	-	transposase			2.21	1.84E-02
COG0210L	Z1313	*helD*	DNA helicase IV			1.76	4.34E-02
COG4973L	Z1323	-	integrase for cryptic prophage CP-933M			2.12	1.38E-02
COG2826L	Z1572	-	transposase			2.01	3.29E-02

*COG0494LR	Z4147	*ygdP*	dinucleoside polyphosphate hydrolase			2.03	1.84E-02
COG0582L	Z4313	-	pathogenicity island integrase			1.88	2.87E-02
COG3436L	Z4317	-	hypothetical protein			2.10	1.50E-02
COG0322L	Z4450	*yqjB*	hypothetical protein			2.22	1.28E-02
*COG0758LU	Z4656	*smf*	DNA protecting protein DprA			2.94	7.27E-04
COG0272L	Z5073	*ligB*	NAD-dependent DNA ligase LigB			1.95	3.91E-02
COG1943L	Z5815	-	transposase			2.19	1.27E-02
Cell cycle control, cell division, chromosome partitioning (D)							
COG2161D	Z0293	*yafN*	antitoxin of the YafO-YafN toxin-antitoxin system			2.47	4.49E-03
COG2846D	Z5820	*ytfE*	iron-sulfur cluster repair di-iron protein	7.06	3.00E-13	8.47	1.42E-17
Defense mechanisms (V)							
COG1566V	Z1015	-	hypothetical protein			2.89	1.70E-03
COG3023V	Z1100	-	regulator			2.18	1.80E-02
COG1136V	Z1116	*ybjZ*	macrolide transporter ATP-binding /permease			1.87	3.31E-02
COG1131V	Z4885	*yhiH*	ABC transporter ATP-binding protein, fragment 1			2.85	1.72E-03
COG1566V	Z4886	*yhiI*	hypothetical protein			4.08	2.31E-05
COG1566V	Z5021	*yibH*	hypothetical protein			3.96	1.59E-04
Signal transduction mechanisms (T)							
COG0589T	Z0751	*ybdQ*	hypothetical protein			2.62	2.35E-03
COG2199T	Z2219	-	hypothetical protein			2.36	6.41E-03
COG2199T	Z2421	-	hypothetical protein			2.26	2.77E-02
COG0589T	Z2435	*ydaA*	universal stress protein UspE			2.15	1.24E-02
*COG1221KT	Z2484	*pspF*	phage shock protein operon transcriptional activator			2.35	6.81E-03
COG0589T	Z2948	*yecG*	universal stress protein UspC			4.10	3.16E-06
*COG3604KT	Z4017	*ygaA*	anaerobic nitric oxide reductase transcriptional regulator			2.11	4.03E-02
COG0642T	Z4378	*qseC*	sensor protein QseC			1.89	3.41E-02
COG0589T	Z4895	*uspA*	universal stress protein; broad regulatory function?			1.87	2.87E-02
COG0589T	Z5468	*yiiT*	universal stress protein UspD			2.36	5.95E-03
Cell wall/membrane/envelope biogenesis (M)							
*COG3468MU	Z0469	-	hypothetical protein			1.71	4.72E-02
COG0845M	Z1115	-	macrolide transporter subunit MacA			1.91	3.33E-02
COG1462M	Z1670	*csgG*	curli production assembly/transport component, 2nd curli operon			2.00	4.04E-02
COG1044M	Z2290	-	hypothetical protein			4.41	6.71E-06
COG3203M	Z3057	-	hypothetical protein			2.42	1.77E-02
*COG0451MG	Z3178	-	enzyme of sugar metabolism			1.79	3.74E-02
COG1346M	Z3397	*yohK*	hypothetical protein	2.73	9.83E-03	3.55	5.15E-05
*COG3468MU	Z3449	*yejO*	ABC transporter ATP-binding protein			1.92	2.95E-02
*COG0702MG	Z5822	*ytfG*	oxidoreductase			3.34	7.50E-04
Cell motility (N)							
COG5571N	Z4973	*yhjY*	lipase			2.95	1.72E-03
*COG1459NU	Z0116	*hofC*	type IV pilin biogenesis protein			1.89	3.07E-02
*COG3539NU	Z0146	*yadC*	fimbrial protein			2.00	1.97E-02
*COG3121NU	Z1534	-	chaperone			2.11	2.40E-02
*COG2747KNU	Z1709	*flgM*	anti-sigma-28 factor FlgM			2.42	4.96E-03

*COG1886NU	Z4190	-	surface presentation of antigens protein SpaO			2.18	1.94E-02
*COG3539NU	Z5220	-	fimbrial protein			1.86	3.79E-02
Intracellular trafficking, secretion, & vesicular transport (U)							
*COG1459NU	Z0116	*hofC*	type IV pilin biogenesis protein			1.89	3.07E-02
*COG3539NU	Z0146	*yadC*	fimbrial protein			2.00	1.97E-02
*COG3468MU	Z0469	-	hypothetical protein			1.71	4.72E-02
*COG3121NU	Z1534	-	chaperone			2.11	2.40E-02
*COG2747KNU	Z1709	*flgM*	anti-sigma-28 factor FlgM			2.42	4.96E-03
*COG3468MU	Z3449	*yejO*	ABC transporter ATP-binding protein			1.92	2.95E-02
*COG1886NU	Z4190	-	surface presentation of antigens protein SpaO			2.18	1.94E-02
*COG0758LU	Z4656	*smf*	DNA protecting protein DprA			2.94	7.27E-04
*COG3539NU	Z5220	-	fimbrial protein			1.86	3.79E-02
Posttranslational modification, protein turnover, chaperones (O)							
COG0330O	Z0642	*ybbK*	protease			2.43	5.42E-03
COG0450O	Z0749	*ahpC*	alkyl hydroperoxide reductase			1.70	4.74E-02
COG0695O	Z1076	*grxA*	glutaredoxin			1.76	4.06E-02
COG1180O	Z1246	*pflA*	pyruvate formate lyase-activating enzyme 1			2.11	1.36E-02
COG0484O	Z1418	*cbpA*	curved DNA-binding protein CbpA			2.25	1.02E-02
COG0396O	Z2710	*sufC*	cysteine desulfurase			3.01	1.11E-03
COG0719O	Z2711	*ynhE*	cysteine desulfurase			3.41	1.14E-04
COG0542O	Z3886	*clpB*	protein disaggregation chaperone			2.41	5.12E-03
COG0695O	Z3975	*nrdH*	glutaredoxin-like protein			4.50	5.10E-07
COG0071O	Z5182	*ibpB*	heat shock chaperone IbpB			3.31	2.41E-04
COG0071O	Z5183	*ibpA*	heat shock protein IbpA			3.32	1.36E-04
COG0606O	Z5277	*yifB*	ATP-dependent protease			2.04	3.36E-02
General function prediction only (R)							
COG2249R	Z0052	*yabF*	glutathione-regulated potassium-efflux system ancillary protein KefF			4.36	5.07E-05
COG1073R	Z0347	-	hypothetical protein			2.78	5.31E-03
COG4619R	Z0643	*ybbL*	ABC transporter ATP-binding protein			2.04	1.85E-02
COG0670R	Z1005	*ybhL*	hypothetical protein			2.09	1.51E-02
COG2333R	Z1259	*ycaI*	hypothetical protein			2.22	1.42E-02
COG2819R	Z1341	-	hypothetical protein			2.28	8.59E-03
*COG1052CHR	Z2329	*ldhA*	D-lactate dehydrogenase	2.36	3.86E-02	3.84	1.07E-05
COG3136R	Z2608	*ydgC*	hypothetical protein			1.81	3.54E-02
COG3443R	Z3065	-	hypothetical protein			2.40	5.54E-03
COG2373R	Z3135	-	invasin			2.18	1.41E-02
COG1380R	Z3396	*yohJ*	hypothetical protein	3.02	2.83E-03	3.29	1.64E-04
COG2103R	Z3693	*murQ*	N-acetylmuramic acid 6-phosphate etherase			2.31	1.01E-02
COG0400R	Z3732	*ypfH*	esterase			5.64	6.43E-10
COG2373R	Z3787	-	hypothetical protein			1.89	2.77E-02
COG3445R	Z3862	*yfiD*	autonomous glycyl radical cofactor GrcA			3.96	5.86E-06
COG1611R	Z4112	*ygdH*	hypothetical protein			2.07	1.63E-02
*COG0494LR	Z4147	*ygdP*	dinucleoside polyphosphate hydrolase			2.03	1.84E-02
COG1272R	Z4237	-	oxidoreductase			2.55	3.44E-03
COG1279R	Z4260	*yggA*	arginine exporter protein			3.15	3.59E-04

COG1811R	Z4311	*yqgA*	transporter			2.85	2.52E-03
COG1741R	Z4460	*yhaK*	hypothetical protein	4.82	9.72E-06	8.19	6.44E-15
COG3529R	Z4708	-	hypothetical protein			2.26	1.05E-02
COG2194R	Z4756	*yhgE*	transport			2.13	1.41E-02
COG1741R	Z4807	*yhhW*	hypothetical protein			6.32	8.09E-12
COG0673R	Z4808	*yhhX*	dehydrogenase			2.69	1.93E-03
COG2425R	Z5246	*yieM*	hypothetical protein			2.04	1.98E-02
COG0714R	Z5247	*yieN*	regulatory ATPase RavA			1.78	3.91E-02
*COG0604CR	Z5649	*qor*	quinone oxidoreductase			2.45	4.98E-03
COG1160R	Z5711	*yjdA*	hypothetical protein			2.95	6.44E-04
Function unknown (S)							
COG3112S	Z0129	*yacL*	hypothetical protein			2.36	6.20E-03
COG3021S	Z0232	*yafD*	hypothetical protein			1.82	3.64E-02
COG0393S	Z1099	-	hypothetical protein			2.02	2.01E-02
COG2989S	Z1272	*ycbB*	hypothetical protein			2.02	1.92E-02
COG3120S	Z1306	*ycbG*	hypothetical protein			3.21	2.05E-04
COG2719S	Z1951	*ycgB*	SpoVR family protein			2.01	3.28E-02
COG2841S	Z2292	*ydcH*	hypothetical protein			3.21	2.52E-04
COG3784S	Z2326	*ydbL*	hypothetical protein			2.06	2.03E-02
COG1376S	Z2706	*ynhG*	hypothetical protein			2.11	2.47E-02
COG0316S	Z2712	*sufA*	iron-sulfur cluster assembly scaffold protein			5.08	2.09E-07
COG2926S	Z3168	*yeeX*	hypothetical protein			2.67	1.82E-03
COG4679S	Z3230	-	hypothetical protein			2.25	8.58E-03
COG5606S	Z3231	-	hypothetical protein			1.93	2.39E-02
COG0586S	Z3385	*yohD*	hypothetical protein			2.39	6.65E-03
COG2128S	Z3974	-	hypothetical protein			2.05	4.45E-02
COG0586S	Z4362	*yghB*	hypothetical protein			1.86	3.42E-02
COG3384S	Z4396	*ygiD*	hypothetical protein	3.16	1.85E-03	7.42	6.58E-15
COG2268S	Z4403	-	hypothetical protein			2.40	5.58E-03
COG0586S	Z4449	*yqjA*	hypothetical protein			2.16	1.31E-02
COG2259S	Z4455	*yqjF*	hypothetical protein			6.10	2.33E-10
COG4804S	Z4578	*yhcG*	hypothetical protein			2.17	2.01E-02
COG2922S	Z4655	*smg*	hypothetical protein			3.32	1.37E-04
COG4226S	Z4882	-	hypothetical protein			2.71	1.67E-03
COG3247S	Z4923	*hdeD*	acid-resistance membrane protein			2.06	1.66E-02
COG1295S	Z4935	*yhjD*	hypothetical protein			1.96	4.45E-02
COG4737S	Z5150	-	hypothetical protein			1.79	4.32E-02
COG3978S	Z5280	*ilvM*	acetolactate synthase 2 regulatory subunit			2.01	2.61E-02
COG3692S	Z5287	-	hypothetical protein			2.14	1.32E-02
COG1295S	Z5425	*rbn*	ribonuclease BN			2.47	4.46E-03
COG3152S	Z5466	*yiiR*	hypothetical protein			1.80	3.91E-02
COG3223S	Z5628	*yjbA*	phosphate-starvation-inducible protein PsiE			2.53	7.71E-03
COG0432S	Z5655	*yjbQ*	hypothetical protein			2.06	2.14E-02
COG3592S	Z5728	*yjdI*	hypothetical protein			2.19	1.22E-02
not assigned							
-	L7056	-	replication protein			3.30	1.53E-04
-	L7083	-	hypothetical protein			3.66	9.81E-05
-	Z0001	*thrL*	thr operon leader peptide			2.40	5.31E-03
-	Z0040	-	DNA-binding transcriptional activator CaiF			2.11	2.41E-02
-	Z0078	-	hypothetical protein			2.13	1.35E-02
-	Z0084	*leuL*	leu operon leader peptide			1.99	2.06E-02

-	Z0175	*yaeH*	hypothetical protein			2.36	6.09E-03
-	Z0425	*yahO*	hypothetical protein			2.01	2.06E-02
-	Z0574	*ybaJ*	hypothetical protein			2.98	5.85E-04
-	Z0656	-	hypothetical protein			2.21	2.18E-02
-	Z0846	*ybfA*	hypothetical protein	4.41	1.33E-06	4.58	1.96E-07
-	Z0868	*ybgO*	hypothetical protein			3.04	2.33E-03
-	Z1023	*ybiJ*	hypothetical protein	5.06	4.07E-08	7.00	6.93E-14
-	Z1077	*ybjC*	hypothetical protein			1.77	4.91E-02
-	Z1141	-	hypothetical protein			1.99	2.19E-02
-	Z1196	-	hypothetical protein			2.14	1.32E-02
-	Z1226	-	hypothetical protein			2.39	1.72E-02
-	Z1386	-	hypothetical protein			1.84	4.82E-02
-	Z1500	-	hypothetical protein			1.79	4.47E-02
-	Z1516	-	hypothetical protein			2.47	5.27E-03
-	Z1560	-	hypothetical protein			1.84	3.32E-02
-	Z1580	-	hypothetical protein			1.94	2.59E-02
-	Z1636	-	hypothetical protein			2.05	1.77E-02
-	Z1664	-	hypothetical protein			3.44	1.24E-03
-	Z1697	*bssS*	biofilm formation regulatory protein BssS			3.54	4.52E-05
-	Z1751	*ycfR*	hypothetical protein	3.74	7.15E-05	5.01	1.87E-08
-	Z1940	*ycgK*	hypothetical protein			2.98	1.04E-03
-	Z2121	-	hypothetical protein			2.06	2.15E-02
-	Z2323	-	hypothetical protein			1.79	4.30E-02
-	Z2327	*ynbE*	hypothetical protein			1.86	3.61E-02
-	Z2368	-	hypothetical protein			3.93	7.27E-04
-	Z2753	-	hypothetical protein			2.22	2.19E-02
-	Z2967	-	hypothetical protein			1.90	2.70E-02
-	Z3024	-	hypothetical protein			2.27	1.84E-02
-	Z3043	-	hypothetical protein			2.08	2.62E-02
-	Z3306	-	hypothetical protein			2.29	2.19E-02
-	Z3360	-	hypothetical protein			1.88	2.74E-02
-	Z3642	-	hypothetical protein			4.08	5.71E-06
-	Z3662	*yfeC*	hypothetical protein			1.85	3.07E-02
-	Z3897	-	hypothetical protein			1.99	2.11E-02
-	Z3931	-	hypothetical protein			2.11	1.53E-02
-	Z3970	-	hypothetical protein			2.67	1.91E-03
-	Z4041	*ygbA*	hypothetical protein	5.93	3.54E-09	6.75	6.67E-12
-	Z4148	-	hypothetical protein			3.04	1.30E-03
-	Z4301	*yggM*	alpha helix chain			2.25	1.00E-02
-	Z4325	-	hypothetical protein			3.44	1.59E-04
-	Z4326	-	enterotoxin			2.32	7.32E-03
-	Z4401	*glgS*	glycogen synthesis protein GlgS			2.60	2.51E-03
-	Z4402	-	oxidoreductase			3.40	9.55E-05
-	Z4461	*yhaL*	hypothetical protein			3.46	2.58E-04
-	Z4482	*yhaV*	hypothetical protein			2.21	1.09E-02
-	Z4597	*yhcN*	hypothetical protein	2.80	6.37E-03	3.31	1.30E-04
-	Z4601	*yhcR*	hypothetical protein			3.10	3.71E-03
-	Z4663	*yhdN*	hypothetical protein			2.19	1.19E-02
-	Z4815	*yhhA*	hypothetical protein			3.76	2.16E-05
-	Z4883	-	hypothetical protein			2.24	8.95E-03
-	Z4887	*yhiJ*	hypothetical protein			1.82	4.08E-02
-	Z4894	*yhiO*	universal stress protein UspB			2.89	1.01E-03
-	Z4912	-	hypothetical protein			4.94	5.83E-08
-	Z4952	*yhjS*	protease			2.74	1.44E-03

-	Z4953	*yhjT*	hypothetical protein	2.95	1.77E-03
-	Z5022	*yibI*	hypothetical protein	4.64	1.33E-05
-	Z5070	*dinD*	DNA-damage-inducible protein D	2.04	2.12E-02
-	Z5278	*ilvL*	ilvG operon leader peptide	2.78	1.25E-03
-	Z5292	*rhoL*	rho operon leader peptide	1.73	4.37E-02
-	Z5621	*yjbD*	hypothetical protein	2.05	1.90E-02
-	Z5712	*yjcZ*	hypothetical protein	2.62	2.65E-03
-	Z5808	*yjfY*	hypothetical protein	4.94	2.08E-05
-	Z5890	-	integrase	2.43	5.27E-03
-	Z6074	-	hypothetical protein	1.96	2.28E-02

*Genes assigned to more than one COG class

Table A 10: Down-regulated genes in response to an acidified $NaNO_2$ 10 min shock or 1 h exposure in EHEC EDL933 WT

				10 min		1 h	
COG	EDL933 identifier	Gene name	Product	log_2 FC	p-value (BH-adjusted)	log_2 FC	p-value (BH-adjusted)
Energy production & conversion (C)							
COG0716C	Z0832	*fldA*	flavodoxin FldA			-2.82	1.12E-03
COG4657C	Z2633	-	Na(+)-translocating NADH-quinone reductase subunit E			-3.08	8.69E-04
COG2878C	Z2634	-	electron transport complex protein RnfB			-2.34	8.59E-03
COG4656C	Z2636	-	electron transport complex protein RnfC			-2.67	2.40E-03
COG3038C	Z3067	*yodB*	cytochrome			-1.84	3.84E-02
COG1894C	Z3543	*nuoF*	NADH dehydrogenase I subunit F			-1.95	2.42E-02
COG0649C	Z3545	*nuoC*	bifunctional NADH:ubiquinone oxidoreductase subunit C/D			-1.89	2.95E-02
COG0282C	Z3558	*ackA*	acetate kinase			-1.84	3.31E-02
COG0280C	Z3559	*pta*	phosphate acetyltransferase			-2.32	7.23E-03
COG1143C	Z3842	*yfhL*	hypothetical protein			-3.76	4.74E-04
COG0644C	Z4076	*ygcN*	hypothetical protein			-2.71	1.82E-03
COG1301C	Z4942	*dctA*	C4-dicarboxylate transporter DctA			-2.20	1.14E-02
COG0056C	Z5232	*atpA*	ATP synthase F0F1 subunit alpha			-2.04	1.77E-02
COG0712C	Z5233	*atpH*	ATP synthase F0F1 subunit delta			-2.98	6.27E-04
COG0711C	Z5234	*atpF*	ATP synthase F0F1 subunit B			-3.04	4.74E-04
COG0636C	Z5235	*atpE*	ATP synthase F0F1 subunit C			-2.40	5.17E-03
COG0356C	Z5236	*atpB*	ATP synthase F0F1 subunit A			-2.26	8.49E-03
COG3312C	Z5238	*atpI*	F0F1 ATP synthase subunit I			-2.65	2.05E-03
COG0716C	Z5243	*mioC*	flavodoxin			-2.48	3.98E-03
Carbohydrate transport & metabolism (G)							
COG2211G	Z0536	*ampG*	muropeptide transporter			-2.45	8.95E-03
COG0524G	Z0596	*gsk*	inosine-guanosine kinase			-2.03	2.08E-02
COG2814G	Z0733	*ybdA*	enterobactin exporter EntS			-2.16	2.96E-02
COG4677G	Z0943	*ybhC*	pectinesterase			-2.67	2.30E-03
*COG0451MG	Z1102	-	nucleotide di-P-sugar epimerase or dehydratase			-2.49	1.05E-02
COG2814G	Z1244	*ycaD*	MFS family transporter protein			-1.86	3.36E-02
COG0574G	Z2731	*ppsA*	phosphoenolpyruvate synthase			-2.28	7.81E-03
COG2814G	Z2875	-	transporter			-2.17	2.31E-02
*COG0451MG	Z3206	-	UDP-galactose 4-epimerase			-2.25	8.59E-03
COG4211G	Z3403	*mglC*	beta-methylgalactoside transporter inner membrane protein			-1.87	4.16E-02

COG1129G	Z3404	*mglA*	galactose/methyl galaxtoside transporter ATP-binding protein			-2.35	7.14E-03
COG1879G	Z3405	*mglB*	galactose-binding transport protein; receptor for galactose taxis			-2.51	3.97E-03
COG2814G	Z3441	*bcr*	bicyclomycin/multidrug efflux system protein			-1.96	3.08E-02
COG0406G	Z3510	*ais*	protein induced by aluminum			-3.81	1.47E-05
COG0738G	Z4725	*yhfC*	hypothetical protein			-2.96	9.77E-04
*COG1349KG	Z4781	*glpR*	DNA-binding transcriptional repressor GlpR			-1.98	2.66E-02
COG3839G	Z5633	*malK*	maltose ABC transporter ATP-binding protein			-2.77	1.44E-03
COG0158G	Z5842	*fbp*	fructose-1,6-bisphosphatase			-2.24	8.95E-03
COG0366G	Z5849	*treC*	trehalose-6-phosphate hydrolase			-1.92	2.59E-02
COG1263G	Z5850	*treB*	PTS system trehalose(maltose)-specific transporter subunit IIBC			-2.02	1.86E-02
Amino acid transport & metabolism (E)							
COG1586E	Z0130	*speD*	S-adenosylmethionine decarboxylase			-2.05	1.79E-02
COG0263E	Z0303	*proB*	gamma-glutamyl kinase			-2.19	1.82E-02
COG1113E	Z0500	*proY*	permease			-1.94	3.25E-02
COG0765E	Z0803	*gltK*	glutamate/aspartate transport system permease			-3.42	2.48E-03
COG1126E	Z1031	*glnQ*	glutamine ABC transporter ATP-binding protein			-2.36	8.41E-03
COG0765E	Z1032	*glnP*	glutamine ABC transporter permease			-2.69	2.65E-03
COG0531E	Z1245	-	transport			-1.99	3.28E-02
COG0128E	Z1254	*aroA*	3-phosphoshikimate 1-carboxyvinyltransferase			-2.91	1.40E-03
COG1176E	Z1830	*potB*	spermidine/putrescine ABC transporter			-1.86	4.03E-02
COG3842E	Z1831	*potA*	putrescine/spermidine ABC transporter ATPase			-3.12	4.74E-04
*COG0462FE	Z1978	*prsA*	ribose-phosphate pyrophosphokinase			-4.40	7.72E-07
COG2066E	Z2179	*yneH*	glutaminase	-2.90	1.18E-02		
COG0531E	Z2605	-	arginine/ornithine antiporter			-2.69	2.83E-03
COG3104E	Z2646	*tppB*	tripeptide transporter permease			-2.79	1.22E-03
COG0722E	Z2733	*aroH*	phospho-2-dehydro-3-deoxyheptonate aldolase			-2.91	1.38E-03
*COG0252EJ	Z2801	*ansA*	asparaginase			-2.00	2.56E-02
COG1280E	Z2841	*yeaS*	leucine export protein LeuE			-1.96	2.70E-02
COG1760E	Z2857	*sdaA*	L-serine dehydratase 1			-1.81	4.02E-02
COG0531E	Z3176	*yeeF*	amino acid/amine transport protein			-3.97	5.86E-06
COG0833E	Z3413	*lysP*	lysine transporter			-2.76	1.63E-03
COG0136E	Z3581	*usg*	semialdehyde dehydrogenase			-1.85	3.96E-02
COG0347E	Z3829	*glnB*	nitrogen regulatory protein P-II 1			-2.94	9.77E-04
COG4175E	Z3979	*proV*	glycine betaine transporter ATP-binding subunit			-2.88	2.88E-03
COG0814E	Z4113	*sdaC*	serine transporter			-3.35	1.56E-04
COG1760E	Z4114	*sdaB*	L-serine dehydratase			-2.28	1.06E-02
COG0703E	Z4743	*aroK*	shikimate kinase I			-1.89	2.76E-02
COG0814E	Z4956	*yhjV*	transporter protein			-2.23	1.93E-02
COG0174E	Z5406	*glnA*	glutamine synthetase			-2.55	3.04E-03
COG0531E	Z5764	*yjeM*	transport			-3.25	4.83E-04
COG0560E	Z5989	*serB*	phosphoserine phosphatase			-3.00	4.54E-03

Nucleotide transport & metabolism (F)							
COG0634F	Z0136	*hpt*	hypoxanthine-guanine phosphoribosyltransferase			-1.92	2.73E-02
COG0503F	Z0299	*gpt*	xanthine-guanine phosphoribosyltransferase			-3.98	1.12E-05
COG0503F	Z0586	*apt*	adenine phosphoribosyltransferase	-2.33	4.60E-02	-5.17	1.71E-08
COG0563F	Z0591	*adk*	adenylate kinase			-4.35	7.58E-07
COG0283F	Z1256	*cmk*	cytidylate kinase			-3.26	2.41E-04
COG0167F	Z1294	*pyrD*	dihydroorotate dehydrogenase 2			-3.70	7.20E-05
COG0015F	Z1860	*purB*	adenylosuccinate lyase			-1.78	4.30E-02
*COG0462FE	Z1978	*prsA*	ribose-phosphate pyrophosphokinase			-4.40	7.72E-07
COG1435F	Z2015	*tdk*	thymidine kinase	-2.79	7.83E-03	-4.22	2.47E-06
COG0284F	Z2525	*pyrF*	orotidine 5'-phosphate decarboxylase			-2.72	5.31E-03
COG0572F	Z3234	*udk*	uridine kinase			-2.85	1.11E-03
COG0209F	Z3489	*nrdA*	ribonucleotide-diphosphate reductase subunit alpha			-1.72	4.58E-02
COG1972F	Z3659	*nupC*	permease of transport system for 3 nucleosides			-2.36	6.00E-03
COG2233F	Z3760	*uraA*	uracil transporter			-2.08	2.19E-02
COG0035F	Z3761	*upp*	uracil phosphoribosyltransferase			-1.87	3.11E-02
COG0150F	Z3762	*purM*	phosphoribosylaminoimidazole synthetase			-2.37	1.90E-02
COG0516F	Z3772	*guaB*	inosine 5'-monophosphate dehydrogenase			-1.91	2.88E-02
COG0105F	Z3781	*ndk*	nucleoside diphosphate kinase			-3.66	3.01E-05
COG0127F	Z4299	*yggV*	deoxyribonucleotide triphosphate pyrophosphatase			-2.44	1.28E-02
COG0756F	Z5064	*dut*	deoxyuridine 5'-triphosphate nucleotidohydrolase			-2.66	6.00E-03
COG0104F	Z5784	*purA*	adenylosuccinate synthetase			-2.24	9.45E-03
COG0044F	Z5927	*iadA*	isoaspartyl dipeptidase			-3.56	9.76E-04
Coenzyme transport & metabolism (H)							
COG0262H	Z0055	*folA*	dihydrofolate reductase			-2.88	9.62E-04
COG4143H	Z0077	*tbpA*	thiamine transporter substrate binding subunit			-3.43	1.54E-03
COG0801H	Z0153	*folK*	2-amino-4-hydroxy-6-hydroxymethyldihydropteridine pyrophosphokinase			-2.65	8.95E-03
COG0054H	Z0516	*ribH*	6,7-dimethyl-8-ribityllumazine synthase			-2.71	2.48E-03
COG0301H	Z0526	*yajK*	thiamine biosynthesis protein ThiI			-2.25	9.51E-03
*COG1169HQ	Z0735	*entC*	isochorismate synthase			-2.15	1.81E-02
COG0321H	Z0775	*lipB*	lipoate-protein ligase B			-1.97	2.65E-02
COG2240H	Z2648	*pdxY*	pyridoxamine kinase			-3.07	7.27E-04
COG0307H	Z2688	*ribE*	riboflavin synthase subunit alpha			-1.82	3.39E-02
COG2226H	Z2923	*yecO*	hypothetical protein			-2.95	3.18E-03
COG2227H	Z2924	*yecP*	hypothetical protein			-2.55	4.54E-03
COG1477H	Z3472	*yojL*	thiamine biosynthesis lipoprotein ApbE			-2.73	6.30E-03
COG0163H	Z3573	*ubiX*	3-octaprenyl-4-hydroxybenzoate carboxy-lyase			-2.16	1.80E-02
COG0720H	Z4075	*ygcM*	6-pyruvoyl tetrahydrobiopterin synthase			-3.29	1.91E-04
COG0635H	Z4300	*yggW*	coproporphyrinogen III oxidase			-1.78	4.57E-02
COG0669H	Z5058	*coaD*	phosphopantetheine adenylyltransferase			-2.84	2.88E-03

COG0452H	Z5063	*dfp (coaBC)*	bifunctional phosphopantothenoylcysteine decarboxylase/phosphopantothenate synthase			-2.10	1.69E-02
COG1575H	Z5477	*menA*	1,4-dihydroxy-2-naphthoate octaprenyltransferase			-2.34	1.75E-02
COG1072H	Z5545	*coaA*	pantothenate kinase			-2.22	9.90E-03
Lipid transport & metabolism (I)							
*COG0761IM	Z0034	*ispH*	4-hydroxy-3-methylbut-2-enyl diphosphate reductase			-2.01	3.43E-02
COG0020I	Z0185	*yaeS*	undecaprenyl pyrophosphate synthase			-2.57	2.88E-03
COG0825I	Z0197	*accA*	acetyl-CoA carboxylase carboxyltransferase subunit alpha			-2.15	1.25E-02
*COG1028IQR	Z0738	*entA*	2,3-dihydroxybenzoate-2,3-dehydrogenase			-2.13	2.91E-02
COG0671I	Z1068	*ybjG*	undecaprenyl pyrophosphate phosphatase			-1.94	2.92E-02
COG0764I	Z1304	*fabA*	3-hydroxydecanoyl-ACP dehydratase			-3.83	1.33E-05
COG1835I	Z1681	*mdoC*	glucans biosynthesis protein			-2.00	3.04E-02
COG0416I	Z1729	*plsX*	glycerol-3-phosphate acyltransferase PlsX			-2.93	7.27E-04
COG0332I	Z1730	*fabH*	3-oxoacyl-ACP synthase			-1.77	4.02E-02
COG1607I	Z2031	*yciA*	acyl-CoA thioester hydrolase			-3.32	2.02E-04
COG0623I	Z2512	*fabI*	enoyl-ACP reductase			-3.02	5.34E-04
*COG1028IQR	Z2539	*yciK*	short chain dehydrogenase			-1.79	4.99E-02
COG0671I	Z3433	-	hypothetical protein			-2.61	2.48E-03
COG0777I	Z3578	*accD*	acetyl-CoA carboxylase subunit beta			-2.00	1.97E-02
COG1502I	Z3870	*pssA*	phosphatidylserine synthase			-3.05	4.74E-04
COG0511I	Z4615	*accB*	acetyl-CoA carboxylase biotin carboxyl carrier protein subunit			-3.38	1.14E-04
COG0764I	Z4857	-	hypothetical protein			-2.13	3.28E-02
COG0204I	Z5394	*yihG*	acyltransferase			-2.90	1.20E-03
COG2134I	Z5463	*cdh*	CDP-diacylglycerol pyrophosphatase			-2.81	2.20E-03
Inorganic ion transport & metabolism (P)							
COG1178P	Z0076	*thiP*	thiamine transporter membrane protein			-2.76	1.00E-02
COG0614P	Z0163	*fhuD*	iron-hydroxamate transporter substrate-binding subunit			-2.76	3.41E-03
COG0609P	Z0164	*fhuB*	iron-hydroxamate transporter permease subunit			-2.46	2.11E-02
COG4774P	Z1026	-	catecholate siderophore receptor Fiu			-2.97	8.86E-04
COG0672P	Z1519	-	hypothetical protein			-2.43	5.42E-03
COG2822P	Z1520	*ycdO*	hypothetical protein			-2.19	1.07E-02
COG0659P	Z1977	*ychM*	sulfate transporter YchM			-2.71	2.88E-03
COG2223P	Z2000	*narK*	nitrite extrusion protein	-3.36	1.20E-02		
COG2076P	Z2593	-	multidrug efflux system protein MdtI			-3.02	2.88E-03
COG2076P	Z2594	-	multidrug efflux system protein MdtJ			-2.94	2.88E-03
*COG4615QP	Z3469	*yojI*	multidrug transporter membrane protein/ATP-binding component			-2.80	1.61E-03
COG0529P	Z4058	*cysC*	adenylylsulfate kinase			-3.68	4.32E-04
COG0861P	Z4150	-	transporter			-2.97	1.57E-03

COG0614P	Z4382	-	iron ABC transporter substrate-binding protein	-2.01	4.04E-02
COG0306P	Z4893	*pitA*	low-affinity phosphate transport protein	-2.39	5.91E-03
COG0607P	Z5038	*yibN*	hypothetical protein	-2.60	2.51E-03
COG0226P	Z5219	*pstS*	phosphate ABC transporter substrate-binding protein	-2.26	1.23E-02
COG1965P	Z5323	*cyaY*	frataxin-like protein	-1.76	4.85E-02
Secondary metabolites biosynthesis, transport & catabolism (Q)					
*COG1169HQ	Z0735	*entC*	isochorismate synthase	-2.15	1.81E-02
*COG1028IQR	Z0738	*entA*	2,3-dihydroxybenzoate-2,3-dehydrogenase	-2.13	2.91E-02
*COG1028IQR	Z2539	*yciK*	short chain dehydrogenase	-1.79	4.99E-02
COG1335Q	Z2802	*ydjB*	nicotinamidase/pyrazinamidase	-1.99	3.83E-02
*COG4615QP	Z3469	*yojI*	multidrug transporter membrane protein/ATP-binding component	-2.80	1.61E-03
COG0767Q	Z4557	*yrbE*	hypothetical protein	-1.82	4.14E-02
Translation, ribosomal structure & biogenesis (J)					
COG0268J	Z0027	*rpsT*	30S ribosomal protein S20	-3.71	2.00E-05
COG0617J	Z0154	*pcnB*	poly(A) polymerase	-2.83	1.26E-03
COG0008J	Z0155	*yadB*	glutamyl-Q tRNA(Asp) synthetase	-2.61	7.51E-03
COG0809J	Z0504	*queA*	S-adenosylmethionine--tRNA ribosyltransferase-isomerase	-3.10	5.91E-04
COG0215J	Z0681	*cysS*	cysteinyl-tRNA synthetase	-3.18	2.96E-04
COG0621J	Z0810	*yleA*	(dimethylallyl)adenosine tRNA methylthiotransferase	-1.89	3.04E-02
COG0008J	Z0827	*glnS*	glutaminyl-tRNA synthetase	-2.71	1.75E-03
*COG0513LKJ	Z1017	*rhlE*	ATP-dependent RNA helicase RhlE	-2.02	2.14E-02
COG0621J	Z1061	*rimO*	ribosomal protein S12 methylthiotransferase	-2.04	1.93E-02
COG0361J	Z1228	*infA*	translation initiation factor IF-1	-2.96	6.36E-04
COG0539J	Z1257	*rpsA*	30S ribosomal protein S1	-1.80	3.50E-02
COG0017J	Z1278	*asnC*	asparaginyl-tRNA synthetase	-2.61	2.40E-03
COG1530J	Z1722	*rne*	ribonuclease E	-1.90	2.69E-02
COG0564J	Z1725	*yceC*	23S rRNA pseudouridylate synthase C	-3.11	7.27E-04
COG0482J	Z1862	*mnmA*	tRNA-specific 2-thiouridylase MnmA	-4.08	5.86E-06
COG0012J	Z1974	*ychF*	GTP-dependent nucleic acid-binding protein EngD	-2.66	2.13E-03
COG0193J	Z1975	*pth*	peptidyl-tRNA hydrolase	-3.16	8.86E-04
COG0216J	Z1982	*prfA*	peptide chain release factor 1	-2.86	1.32E-03
*COG0513LKJ	Z2417	*dbpA*	ATP-dependent RNA helicase DbpA	-2.01	2.67E-02
COG1187J	Z2541	*yciL*	23S rRNA pseudouridylate synthase B	-2.51	3.97E-03
COG0162J	Z2650	*tyrS*	tyrosyl-tRNA synthetase	-2.06	1.72E-02
COG0016J	Z2743	*pheS*	phenylalanyl-tRNA synthetase subunit alpha	-2.50	4.78E-03
*COG0252EJ	Z2801	*ansA*	asparaginase	-2.00	2.56E-02
COG0349J	Z2847	*rnd*	ribonuclease D	-2.28	1.17E-02
COG0018J	Z2929	*argS*	arginyl-tRNA synthetase	-3.26	2.02E-04
COG0143J	Z3282	*metG*	methionyl-tRNA synthetase	-1.90	2.70E-02
COG0231J	Z3430	*yeiP*	elongation factor P	-3.93	1.07E-05
COG0008J	Z3665	*gltX*	glutamyl-tRNA synthetase	-1.93	2.55E-02
COG0806J	Z3902	*rimM*	16S rRNA-processing protein RimM	-3.48	6.05E-05

COG0228J	Z3903	*rpsP*	30S ribosomal protein S16			-2.33	6.66E-03
COG1190J	Z4228	*lysS*	lysyl-tRNA synthetase			-2.15	1.26E-02
COG1186J	Z4229	*prfB*	peptide chain release factor 2			-2.94	8.69E-04
COG0828J	Z4418	*rpsU*	30S ribosomal protein S21			-2.35	6.09E-03
*COG0513LKJ	Z4523	*deaD*	ATP-dependent RNA helicase DeaD			-3.13	3.35E-04
COG1534J	Z4542	*yhbY*	RNA-binding protein YhbY			-2.87	8.86E-04
COG0211J	Z4547	*rpmA*	50S ribosomal protein L27			-2.30	7.31E-03
COG0261J	Z4549	*rplU*	50S ribosomal protein L21			-2.17	1.11E-02
COG0102J	Z4589	*rplM*	50S ribosomal protein L13			-2.18	1.08E-02
COG2264J	Z4619	*prmA*	50S ribosomal protein L11 methyltransferase			-1.92	3.04E-02
COG0042J	Z4620	*yhdG*	tRNA-dihydrouridine synthase B			-3.57	4.34E-05
COG0203J	Z4664	*rplQ*	50S ribosomal protein L17			-2.27	8.09E-03
COG0522J	Z4666	*rpsD*	30S ribosomal protein S4			-1.71	4.56E-02
COG0100J	Z4667	*rpsK*	30S ribosomal protein S11			-2.16	1.16E-02
COG0096J	Z4676	*rpsH*	30S ribosomal protein S8			-1.68	4.99E-02
COG0199J	Z4677	*rpsN*	30S ribosomal protein S14			-1.87	2.87E-02
COG0094J	Z4678	*rplE*	50S ribosomal protein L5			-2.14	1.24E-02
COG0198J	Z4679	*rplX*	50S ribosomal protein L24			-1.92	2.48E-02
COG0093J	Z4680	*rplN*	50S ribosomal protein L14			-1.76	4.03E-02
COG0088J	Z4690	*rplD*	50S ribosomal protein L4			-1.98	2.06E-02
COG0087J	Z4691	*rplC*	50S ribosomal protein L3			-2.26	8.36E-03
COG0051J	Z4692	*rpsJ*	30S ribosomal protein S10			-2.32	6.90E-03
COG0048J	Z4700	*rpsL*	30S ribosomal protein S12			-1.78	3.78E-02
COG0752J	Z4984	*glyQ*	glycyl-tRNA synthetase subunit alpha			-1.88	3.20E-02
COG0267J	Z5060	*rpmG*	50S ribosomal protein L33			-1.96	2.19E-02
COG0227J	Z5061	*rpmB*	50S ribosomal protein L28			-1.77	3.86E-02
COG0689J	Z5068	*rph*	ribonuclease PH			-2.47	4.91E-03
COG0230J	Z5194	*rpmH*	50S ribosomal protein L34			-1.98	2.05E-02
COG0594J	Z5195	*rnpA*	ribonuclease P			-1.86	2.91E-02
COG0244J	Z5558	*rplJ*	50S ribosomal protein L10			-2.13	1.29E-02
COG0222J	Z5559	*rplL*	50S ribosomal protein L7/L12			-1.96	2.17E-02
COG1187J	Z5620	*yjbC*	23S rRNA pseudouridine synthase F			-2.28	1.80E-02
COG0231J	Z5752	*efp*	elongation factor P			-2.82	1.01E-03
COG2269J	Z5763	*yjeA*	lysyl-tRNA synthetase			-1.87	3.18E-02
COG2813J	Z5972	*rsmC*	16S ribosomal RNA m2G1207 methyltransferase			-1.79	4.46E-02
COG4108J	Z5976	*prfC*	peptide chain release factor 3			-2.19	1.25E-02
Transcription (K)							
*COG0553KL	Z0067	-	ATP-dependent helicase HepA			-1.71	4.91E-02
COG0781K	Z0518	*nusB*	transcription antitermination protein NusB			-2.43	7.37E-03
COG0782K	Z0754	*rnk*	nucleoside diphosphate kinase regulator			-2.24	9.77E-03
COG1278K	Z0769	*cspE*	cold shock protein CspE	-2.54	1.87E-02	-3.63	2.86E-05
*COG0513LKJ	Z1017	*rhlE*	ATP-dependent RNA helicase RhlE			-2.02	2.14E-02
COG2378K	Z1164	*terW*	hypothetical protein			-2.10	1.80E-02
COG3561K	Z1503	-	hypothetical protein			-1.86	3.96E-02
COG3710K	Z1531	-	hypothetical protein	-2.59	3.86E-02		
COG2378K	Z1603	*terW_2*	hypothetical protein			-2.02	2.26E-02
COG1802K	Z2157	*ydfH*	hypothetical protein	-2.58	2.83E-02		
*COG0513LKJ	Z2417	*dbpA*	ATP-dependent RNA helicase DbpA			-2.01	2.67E-02

COG1609K	Z2461	*ycjW*	LACI-type transcriptional regulator			-2.70	2.88E-03
COG4776K	Z2514	*rnb*	exoribonuclease II			-2.40	5.48E-03
*COG0745TK	Z2609	*rstA*	DNA-binding transcriptional regulator RstA			-2.19	1.25E-02
COG1609K	Z2681	*purR*	DNA-binding transcriptional repressor PurR			-3.64	4.62E-05
COG1609K	Z3407	*galS*	DNA-binding transcriptional regulator GalS	-3.54	1.85E-03		
COG0571K	Z3848	*rnc*	ribonuclease III			-3.11	3.59E-04
COG3710K	Z4167	*yqeI*	sensory transducer	-3.79	2.33E-04	-3.44	1.87E-04
COG0583K	Z4470	*tdcA*	DNA-binding transcriptional activator TdcA	-3.91	6.74E-03		
*COG0513LKJ	Z4523	*deaD*	ATP-dependent RNA helicase DeaD			-3.13	3.35E-04
COG0195K	Z4530	*nusA*	transcription elongation factor NusA			-2.01	2.01E-02
COG5007K	Z4553	*yrbA*	hypothetical protein	-2.73	1.91E-02	-3.39	3.59E-04
COG0202K	Z4665	*rpoA*	DNA-directed RNA polymerase subunit alpha			-2.29	7.35E-03
COG1278K	Z4981	*cspA*	cold-shock protein	-3.62	1.10E-04	-5.42	1.17E-09
COG1309K	Z5065	*slmA*	nucleoid occlusion protein			-2.96	9.62E-04
*COG1200LK	Z5078	*recG*	ATP-dependent DNA helicase RecG			-2.35	8.45E-03
COG1609K	Z5481	*cytR*	DNA-binding transcriptional regulator CytR			-2.01	2.26E-02
COG0085K	Z5560	*rpoB*	DNA-directed RNA polymerase subunit beta			-2.14	1.25E-02
COG1414K	Z5609	*iclR*	IclR family transcriptional regulator			-2.10	2.12E-02
*COG2901KL	Z4621	*fis*	Fis family transcriptional regulator			-2.11	1.36E-02
*COG1349KG	Z4781	*glpR*	DNA-binding transcriptional repressor GlpR			-1.98	2.66E-02
Replication, recombination & repair (L)							
*COG0553KL	Z0067	-	ATP-dependent helicase HepA			-1.71	4.91E-02
COG0164L	Z0195	*rnhB*	ribonuclease HII			-3.08	1.27E-03
COG0420L	Z0496	*sbcD*	exonuclease SbcD			-2.19	2.69E-02
COG1722L	Z0525	*xseB*	exodeoxyribonuclease VII small subunit			-2.45	1.23E-02
COG2812L	Z0587	*dnaX*	DNA polymerase III subunits gamma and tau			-2.37	8.95E-03
*COG0513LKJ	Z1017	*rhlE*	ATP-dependent RNA helicase RhlE			-2.02	2.14E-02
COG0084L	Z1739	*ycfH*	metallodependent hydrolase			-2.17	1.37E-02
COG0863L	Z2060	-	DNA adenine methyltransferase encoded by prophage CP-933O			-2.19	1.94E-02
*COG0513LKJ	Z2417	*dbpA*	ATP-dependent RNA helicase DbpA			-2.01	2.67E-02
COG0550L	Z2536	*topA*	DNA topoisomerase I			-1.96	2.19E-02
COG0648L	Z3416	*nfo*	endonuclease IV			-2.60	6.94E-03
COG0188L	Z3484	*gyrA*	DNA gyrase subunit A			-2.80	1.18E-03
COG0582L	Z3613	*intC*	prophage integrase			-2.24	1.59E-02
COG0249L	Z4043	*mutS*	DNA mismatch repair protein MutS			-1.80	4.89E-02
COG0258L	Z4115	*xni*	exonuclease IX			-2.67	9.51E-03
COG0188L	Z4373	*parC*	DNA topoisomerase IV subunit A			-1.81	3.92E-02
COG0187L	Z4387	*parE*	DNA topoisomerase IV subunit B			-1.72	4.93E-02
*COG0513LKJ	Z4523	*deaD*	ATP-dependent RNA helicase DeaD			-3.13	3.35E-04
*COG2901KL	Z4621	*fis*	Fis family transcriptional regulator			-2.11	1.36E-02
*COG0494LR	Z4751	*nudE*	ADP-ribose diphosphatase NudE	-3.43	3.26E-04		

*COG1200LK	Z5078	*recG*	ATP-dependent DNA helicase RecG	-2.35	8.45E-03
COG2816L	Z5571	*nudC*	NADH pyrophosphatase	-2.64	5.89E-03
COG0305L	Z5650	*dnaB*	replicative DNA helicase	-2.25	9.51E-03
COG0629L	Z5658	*ssb*	single-stranded DNA-binding protein	-2.30	1.05E-02
Cell cycle control, cell division, chromosome partitioning (D)					
COG3095D	Z1270	*mukE*	condesin subunit E	-1.80	4.86E-02
COG0037D	Z2416	*ydaO*	C32 tRNA thiolase	-2.40	6.00E-03
COG1077D	Z4610	*mreB*	rod shape-determining protein MreB	-2.93	8.86E-04
COG4942D	Z5040	*yibP*	hypothetical protein	-2.42	6.37E-03
COG0445D	Z5241	*gidA*	tRNA uridine 5-carboxymethyl-aminomethyl modification protein GidA	-2.28	8.99E-03
Defense mechanisms (V)					
COG1680V	Z0472	*yaiH*	beta-lactam binding protein AmpH	-2.71	2.20E-03
COG1132V	Z1260	*msbA*	lipid transporter ATP-binding protein/permease	-1.91	2.66E-02
COG1136V	Z1758	*lolD*	lipoprotein transporter ATP-binding subunit	-2.94	1.89E-03
COG1566V	Z2659	-	hypothetical protein	-2.11	3.21E-02
COG1566V	Z3986	*emrA*	multidrug resistance secretion protein	-2.09	1.78E-02
COG1403V	Z5894	-	hypothetical protein	-2.18	1.29E-02
Signal transduction mechanisms (T)					
COG2200T	Z1057	-	hypothetical protein	-2.85	7.32E-03
*COG0745TK	Z2609	*rstA*	DNA-binding transcriptional regulator RstA	-2.19	1.25E-02
COG2199T	Z2826	*yeaJ*	hypothetical protein	-2.96	7.27E-04
COG3109T	Z2878m	*proQ*	solute/DNA competence effector	-2.66	2.08E-03
COG3275T	Z3303	*yehU*	2-component sensor protein	-1.95	2.42E-02
COG2204T	Z3830	*yfhA*	2-component transcriptional regulator	-2.43	6.00E-03
COG3851T	Z5158	*uhpB*	sensory histidine kinase UhpB	-2.92	6.09E-03
Cell wall/membrane/envelope biogenesis (M)					
*COG0761IM	Z0034	*ispH*	4-hydroxy-3-methylbut-2-enyl diphosphate reductase	-2.01	3.43E-02
COG1043M	Z0193	*lpxA*	UDP-N-acetylglucosamine acyltransferase	-1.83	3.36E-02
COG0763M	Z0194	*lpxB*	lipid-A-disaccharide synthase	-1.98	2.36E-02
COG1181M	Z0477	*ddl*	D-alanyl-alanine synthetase A	-2.15	1.31E-02
COG3248M	Z0512	*tsx*	nucleoside channel phage T6/colicin K receptor	-2.33	6.90E-03
COG3056M	Z0537	*yajG*	hypothetical protein	-2.44	5.27E-03
COG3765M	Z0728	*fepE*	ferric enterobactin transport protein FepE	-2.44	1.20E-02
COG1686M	Z0777	*dacA*	D-alanyl-D-alanine carboxypeptidase	-1.71	4.72E-02
COG0768M	Z0781	*mrdA*	penicillin-binding protein 2	-1.89	2.77E-02
*COG0451MG	Z1102	-	nucleotide di-P-sugar epimerase or dehydratase	-2.49	1.05E-02
COG1663M	Z1261	*lpxK*	tetraacyldisaccharide 4'-kinase	-2.41	1.39E-02
COG4591M	Z1757	*ycfU*	outer membrane-specific lipoprotein transporter subunit LolC	-3.76	1.14E-04
COG0741M	Z1956	*mltE*	murein transglycosylase E	-2.02	3.33E-02
COG0791M	Z2677	*ydhO*	lipoprotein	-1.97	2.56E-02

COG3713M	Z2822	*yeaF*	hypothetical protein			-4.37	7.72E-07
COG0739M	Z2908	*yebA*	hypothetical protein			-2.50	5.23E-03
COG1686M	Z3171	*dacD*	D-alanyl-D-alanine carboxypeptidase			-2.61	3.41E-03
COG3765M	Z3189	*wzzB*	regulator of length of O-antigen component of lipopolysaccharide chains			-2.59	2.51E-03
COG1004M	Z3190	*ugd*	UDP-glucose 6-dehydrogenase			-1.92	2.62E-02
COG0463M	Z3204	*wbdN*	glycosyl transferase			-2.08	1.51E-02
COG1210M	Z3205	*galF*	UTP-glucose-1-phosphate uridylyltransferase			-1.96	2.21E-02
*COG0451MG	Z3206	-	UDP-galactose 4-epimerase			-2.25	8.59E-03
COG1686M	Z3383	*pbpG*	D-alanyl-D-alanine endopeptidase			-1.95	2.59E-02
COG0791M	Z3434	*spr*	outer membrane lipoprotein	-2.53	1.91E-02	-3.66	2.58E-05
COG0399M	Z3511	-	UDP-4-amino-4-deoxy-L-arabinose--oxoglutarate aminotransferase			-3.08	5.75E-04
COG0463M	Z3512	-	undecaprenyl phosphate 4-deoxy-4-formamido-L-arabinose transferase			-2.95	1.18E-03
COG4623M	Z3838	*yfhD*	transglycosylase			-1.93	3.75E-02
COG2951M	Z4004	*mltB*	murein hydrolase B			-3.83	9.77E-04
COG1792M	Z4609	*mreC*	rod shape-determining protein MreC			-1.81	3.92E-02
COG5009M	Z4750	*mrcA*	peptidoglycan synthetase			-2.06	1.99E-02
COG2834M	Z4860	-	hypothetical protein			-2.09	2.63E-02
COG2885M	Z4977	*yiaD*	outer membrane lipoprotein			-2.44	6.66E-03
COG0859M	Z5047	*rfaF*	ADP-heptose--LPS heptosyltransferase			-2.21	1.25E-02
COG0859M	Z5048	*rfaC*	ADP-heptose--LPS heptosyltransferase			-3.57	8.24E-05
COG3307M	Z5049	*waaL*	LPS biosynthesis rpteon			-4.70	1.10E-07
COG0859M	Z5056	*waaQ*	lipopolysaccharide core biosynthesis protein			-1.70	4.99E-02
COG0449M	Z5227	*glmS*	glucosamine--fructose-6-phosphate aminotransferase			-1.76	4.14E-02
COG1207M	Z5228	*glmU*	bifunctional N-acetylglucosamine-1-phosphate uridyltransferase/glucosamine-1-phosphate acetyltransferase			-2.14	1.31E-02
COG0472M	Z5295	*rfe*	UDP-GlcNAc:undecaprenylphosphate GlcNAc-1-phosphate transferase			-2.05	1.87E-02
COG0381M	Z5297	*wecB*	UDP-N-acetylglucosamine 2-epimerase			-1.82	3.91E-02
COG0677M	Z5298	*wecC*	UDP-N-acetyl-D-mannosamine dehydrogenase			-1.89	3.26E-02
COG2829M	Z5342	*pldA*	phospholipase A			-1.99	2.26E-02
COG2885M	Z5895	-	hypothetical protein			-3.73	3.35E-05
Cell motility (N)							
*COG3539NU	Z1678	-	hypothetical protein			-2.07	1.75E-02
*COG1261NO	Z1710	*flgA*	flagellar basal body P-ring biosynthesis protein FlgA			-1.87	2.87E-02
COG1815N	Z1711	*flgB*	flagellar basal-body rod protein FlgB			-3.47	8.16E-05
COG1558N	Z1712	*flgC*	flagellar basal body rod protein FlgC			-1.91	2.74E-02
COG1843N	Z1713	*flgD*	flagellar basal body rod modification protein			-2.53	3.51E-03

COG1749N	Z1714	*flgE*	flagellar hook protein FlgE			-2.53	3.34E-03
COG4787N	Z1715	*flgF*	flagellar basal body rod protein FlgF			-1.75	4.60E-02
COG4786N	Z1716	*flgG*	flagellar basal body rod protein FlgG			-1.74	4.52E-02
*COG1298NU	Z2932	*flhA*	flagellar biosynthesis protein FlhA			-2.16	1.31E-02
*COG1377NU	Z2934	*flhB*	flagellar biosynthesis protein FlhB			-2.53	4.44E-03
*COG1677NU	Z3027	*fliE*	flagellar hook-basal body protein FliE			-2.84	1.19E-03
*COG1766NU	Z3028	*fliF*	flagellar MS-ring protein			-2.90	8.81E-04
*COG2882NUO	Z3032	*fliJ*	flagellar biosynthesis chaperone			-2.00	2.13E-02
COG1868N	Z3035	*fliM*	flagellar motor switch protein FliM			-2.68	1.89E-03
*COG1886NU	Z3036	*fliN*	flagellar motor switch protein FliN			-2.76	1.61E-03
*COG1338NU	Z3038	*fliP*	flagellar biosynthesis protein FliP			-3.20	5.85E-04
*COG1987NU	Z3039	*fliQ*	flagellar biosynthesis protein FliQ			-4.45	8.10E-06
*COG1684NU	Z3040	*fliR*	flagellar biosynthesis protein FliR			-5.02	5.55E-07
COG5567N	Z4849	-	hypothetical protein	-3.91	3.32E-05	-3.42	9.93E-05
Intracellular trafficking, secretion, & vesicular transport (U)							
COG1826U	Z0772	*tatE*	twin arginine translocase E			-1.77	3.91E-02
COG0811U	Z0905	*tolQ*	colicin uptake protein TolQ			-2.39	6.00E-03
*COG3539NU	Z1678	-	hypothetical protein			-2.07	1.75E-02
*COG1298NU	Z2932	*flhA*	flagellar biosynthesis protein FlhA			-2.16	1.31E-02
*COG1377NU	Z2934	*flhB*	flagellar biosynthesis protein FlhB			-2.53	4.44E-03
*COG1677NU	Z3027	*fliE*	flagellar hook-basal body protein FliE			-2.84	1.19E-03
*COG1766NU	Z3028	*fliF*	flagellar MS-ring protein			-2.90	8.81E-04
*COG2882NUO	Z3032	*fliJ*	flagellar biosynthesis chaperone			-2.00	2.13E-02
*COG1886NU	Z3036	*fliN*	flagellar motor switch protein FliN			-2.76	1.61E-03
*COG1338NU	Z3038	*fliP*	flagellar biosynthesis protein FliP			-3.20	5.85E-04
*COG1987NU	Z3039	*fliQ*	flagellar biosynthesis protein FliQ			-4.45	8.10E-06
*COG1684NU	Z3040	*fliR*	flagellar biosynthesis protein FliR			-5.02	5.55E-07
COG1314U	Z4537	*secG*	preprotein translocase subunit SecG	-4.06	1.20E-05	-3.14	2.96E-04
COG0805U	Z5360	*tatC*	twin-arginine protein translocation system subunit TatC			-1.93	2.73E-02
COG0690U	Z5554	*secE*	preprotein translocase subunit SecE			-2.78	1.72E-03
COG0811U	Z5896	-	hypothetical protein			-5.02	3.01E-08
Posttranslational modification, protein turnover, chaperones (O)							
COG0760O	Z0548	*ybaU*	peptidyl-prolyl cis-trans isomerase			-2.26	8.59E-03
COG0652O	Z0680	*ppiB*	peptidyl-prolyl cis-trans isomerase B			-2.48	3.83E-03
COG0829O	Z1142	*ureD*	urease accessory protein D			-3.13	2.88E-03
COG1067O	Z1305	-	ATP-dependent protease			-3.00	7.32E-04
*COG1261NO	Z1710	*flgA*	flagellar basal body P-ring biosynthesis protein FlgA			-1.87	2.87E-02
COG0826O	Z2284	*ydcP*	collagenase			-1.90	3.36E-02
COG1214O	Z2850	*yeaZ*	hypothetical protein			-3.54	6.36E-04
*COG2882NUO	Z3032	*fliJ*	flagellar biosynthesis chaperone			-2.00	2.13E-02
COG0443O	Z3238	*yegD*	chaperone			-2.05	1.88E-02
COG1225O	Z3739	*bcp*	thioredoxin-dependent thiol peroxidase	-2.35	4.60E-02	-1.99	2.16E-02
COG0545O	Z4705	*fkpA*	FKBP-type peptidylprolyl isomerase			-1.76	4.01E-02
COG0330O	Z5781	*hflK*	FtsH protease regulator HflK			-2.22	1.07E-02
COG0545O	Z5818	*fklB*	peptidyl-prolyl cis-trans isomerase			-2.10	1.44E-02

General function prediction only (R)							
*COG1028IQR	Z0738	*entA*	2,3-dihydroxybenzoate-2,3-dehydrogenase			-2.13	2.91E-02
COG3129R	Z1028	*ybiN*	SAM-dependent methyltransferase			-3.12	4.88E-03
COG0488R	Z1042	*ybiT*	ABC transporter ATP-binding protein			-2.54	3.71E-03
COG0670R	Z1322	*yccA*	hypothetical protein			-1.80	3.91E-02
COG1054R	Z1691	*yceA*	hypothetical protein			-3.45	8.43E-05
COG0728R	Z1707	*mviN*	virulence factor			-1.92	3.91E-02
COG1399R	Z1727	*yceD*	hypothetical protein			-1.76	3.96E-02
COG2915R	Z1861	*ycfC*	hypothetical protein			-2.25	2.39E-02
COG4178R	Z2212	*yddA*	ABC transporter ATP-binding protein			-3.02	2.88E-03
*COG1028IQR	Z2539	*yciK*	short chain dehydrogenase			-1.79	4.99E-02
COG0714R	Z3291	*ppiB*	hypothetical protein			-2.11	2.67E-02
COG3081R	Z3445	*yejK*	nucleoid-associated protein NdpA			-2.93	8.81E-04
COG3083R	Z3447	*yejM*	sulfatase			-2.40	6.33E-03
COG1286R	Z3575	*cvpA*	colicin V production protein			-1.81	4.60E-02
COG0820R	Z3780	*yfgB*	ribosomal RNA large subunit methyltransferase N			-3.37	1.42E-04
COG1159R	Z3847	*era*	GTP-binding protein Era			-1.91	2.77E-02
COG2916R	Z3968	*stpA*	DNA binding protein			-1.98	3.43E-02
COG0701R	Z4510	*yraQ*	hypothetical protein			-2.47	9.52E-03
COG2962R	Z4546	*yhbE*	hypothetical protein			-2.93	8.81E-04
COG2969R	Z4586	*sspB*	ClpXP protease specificity-enhancing factor			-2.05	1.91E-02
*COG0494LR	Z4751	*nudE*	ADP-ribose diphosphatase NudE	-3.43	3.26E-04		
COG0705R	Z4784	*glpG*	intramembrane serine protease GlpG			-2.45	6.89E-03
COG4261R	Z4858	-	hypothetical protein			-1.75	4.70E-02
COG2081R	Z4891	*yhiN*	hypothetical protein			-2.15	2.14E-02
COG0612R	Z4941	*yhjJ*	hypothetical protein			-2.38	7.71E-03
COG2992R	Z4995	*bax*	hypothetical protein			-2.37	6.27E-03
COG2962R	Z5340	*rarD*	hypothetical protein			-1.97	2.81E-02
COG2334R	Z5391	*yihE*	serine/threonine protein kinase			-1.95	2.47E-02
COG0218R	Z5400	*engB*	ribosome biogenesis GTP-binding protein YsxC			-2.32	8.36E-03
COG0456R	Z5974	*rimI*	ribosomal-protein-alanine N-acetyltransferase			-2.37	1.34E-02
COG0488R	Z5993	*yjjK*	ABC transporter ATP-binding protein			-2.27	8.95E-03
Function unknown (S)							
COG3034S	Z0282	*yafK*	hypothetical protein			-2.60	2.88E-03
COG3680S	Z0319	-	hypothetical protein			-2.30	7.35E-03
COG2908S	Z0679	*ybbF*	UDP-2,3-diacylglucosamine hydrolase			-2.88	8.86E-04
COG1576S	Z0782	*ybeA*	rRNA large subunit methyltransferase			-2.41	1.36E-02
COG0799S	Z0783	*ybeB*	hypothetical protein			-3.07	7.27E-04
COG1729S	Z0910	*ybgF*	tol-pal system protein YbgF			-2.46	4.33E-03
COG2431S	Z1108	*ybjE*	surface protein			-3.18	1.63E-03
COG2990S	Z1112	*ybjX*	hypothetical protein			-2.25	9.03E-03
COG1944S	Z1251	*ycaO*	hypothetical protein			-3.10	3.77E-04
COG3304S	Z1312	*yccF*	hypothetical protein			-2.91	2.48E-03
COG2983S	Z1943	*ycgN*	hypothetical protein			-1.87	4.73E-02
COG3781S	Z2185	-	hypothetical protein			-3.03	1.45E-03
COG2606S	Z2827	*yeaK*	hypothetical protein			-2.15	1.48E-02

COG3102S	Z2928	*yecM*	hypothetical protein			-1.84	4.14E-02
COG4886S	Z3026	-	hypothetical protein			-2.11	1.41E-02
COG2949S	Z3399	*sanA*	hypothetical protein			-2.42	7.05E-03
COG3101S	Z3589	-	transporting ATPase			-2.33	8.09E-03
COG2976S	Z3776	-	hypothetical protein			-1.90	2.87E-02
COG3148S	Z3868	*yfiP*	hypothetical protein			-4.28	1.67E-04
COG0779S	Z4531	*yhbC*	hypothetical protein			-3.21	2.58E-04
COG3924S	Z4617	*yhdT*	hypothetical protein			-2.77	8.45E-03
COG1289S	Z4719	*yhfK*	hypothetical protein			-2.03	2.26E-02
COG1285S	Z4920	*yhiD*	Mg(2+) transport ATPase			-1.76	4.15E-02
COG2861S	Z5041	*yibQ*	hypothetical protein			-2.40	6.67E-03
COG5510S	Z5753	*ecnA*	entericidin A			-2.42	1.31E-02
COG3242S	Z5783	*yjeT*	hypothetical protein			-2.92	6.76E-03
COG0700S	Z5928	*yjiG*	hypothetical protein			-3.52	1.67E-03
not assigned							
-	Z0132	*yacC*	hypothetical protein	-3.47	4.12E-03		
-	Z0208	*rcsF*	outer membrane lipoprotein			-2.06	2.06E-02
-	Z0879	-	hypothetical protein			-1.73	4.56E-02
-	Z1062	*bssR*	biofilm formation regulatory protein BssR	-2.54	2.44E-02		
-	Z1080	*ybjN*	sensory transduction regulator			-2.13	1.80E-02
-	Z1155	-	hypothetical protein			-2.28	2.66E-02
-	Z1193	-	hypothetical protein	-5.86	1.10E-04		
-	Z1387	-	hypothetical protein	-3.07	5.09E-03	-2.57	4.80E-03
-	Z1401	*ymcA*	hypothetical protein			-1.97	2.47E-02
-	Z1402	*ymcB*	hypothetical protein			-2.97	1.77E-03
-	Z1403	*ymcC*	regulator			-3.31	5.63E-04
-	Z1594	-	hypothetical protein	-3.97	5.09E-03	-2.22	3.19E-02
-	Z1633	-	hypothetical protein	-4.95	3.26E-04		
-	Z2238	*yddG*	hypothetical protein			-3.69	1.70E-03
-	Z2274	-	hypothetical protein			-2.06	3.00E-02
-	Z2873	-	hypothetical protein	-2.82	2.47E-02		
-	Z2891	*holE*	DNA polymerase III subunit theta			-2.76	4.33E-03
-	Z2931	*flhE*	flagellar protein			-2.08	2.08E-02
-	Z2959	-	hypothetical protein			-5.28	5.33E-08
-	Z3362	-	superinfection exclusion protein B of prophage CP-933V			-1.81	4.82E-02
-	Z3400	-	hypothetical protein			-2.02	4.62E-02
-	Z3519	*pmrD*	polymyxin resistance protein B	-2.81	8.21E-03		
-	Z3583	*flk*	flagella biosynthesis regulator			-2.04	2.19E-02
-	Z3588	-	hypothetical protein	-2.98	3.22E-03	-3.37	1.19E-04
-	Z4057	*ygbE*	hypothetical protein			-2.95	9.92E-04
-	Z4284	*yqgB*	hypothetical protein			-2.98	7.27E-04
-	Z4851	-	hypothetical protein			-2.28	1.27E-02
-	Z5128	-	hypothetical protein			-2.42	1.17E-02
-	Z5187	-	hypothetical protein	-2.37	4.75E-02		
-	Z5750	*yjeJ*	hypothetical protein			-2.02	3.04E-02

*Genes assigned to more than one COG class

Table A 11: Up-regulated genes in 1 h vs 10 min reference cultures of EHEC EDL933 WT

COG	EDL933 identifier	Gene name	Product	log_2 FC	p-value (BH-adjusted)
Energy production & conversion (C)					
COG0247C	Z0384	*ykgE*	dehydrogenase subunit	2.13	4.71E-02
COG3069C	Z0766	*dcuC*	C4-dicarboxylate transporter DcuC	3.54	3.78E-04
COG0243C	Z1240	*dmsA*	anaerobic dimethyl sulfoxide reductase subunit A	4.31	4.95E-06
COG0437C	Z1241	*dmsB*	anaerobic dimethyl sulfoxide reductase subunit B	3.56	5.13E-04
COG1882C	Z1248	*pflB*	formate acetyltransferase 1	3.18	3.78E-04
COG5013C	Z2001	*narG*	nitrate reductase 1 subunit alpha	4.58	3.34E-07
COG1140C	Z2002	*narH*	nitrate reductase 1 subunit beta	3.89	1.87E-05
COG2180C	Z2003	*narJ*	nitrate reductase 1, delta subunit, assembly function	4.63	1.87E-05
COG2181C	Z2004	*narI*	nitrate reductase 1, cytochrome b(NR), gamma subunit	4.55	1.25E-06
COG2864C	Z2234	*fdnI*	formate dehydrogenase-N subunit gamma	3.43	9.41E-04
COG0437C	Z2235	*fdnH*	formate dehydrogenase-N, nitrate-inducible, iron-sulfur beta subunit	5.96	5.49E-08
COG0243C	Z2236	*fdnG*	formate dehydrogenase-N, nitrate-inducible, alpha subunit	6.00	6.25E-10
COG3005C	Z3459	*napC*	cytochrome *c*	2.96	1.58E-03
COG3043C	Z3460	*napB*	citrate reductase cytochrome *c* subunit	5.96	7.49E-08
COG0348C	Z3461	*napH*	quinol dehydrogenase membrane component	6.78	5.39E-08
COG0437C	Z3462	*napG*	quinol dehydrogenase periplasmic component	5.27	1.32E-06
COG0243C	Z3463	*napA*	nitrate reductase catalytic subunit	5.91	2.27E-09
COG1149C	Z3465	*napF*	ferredoxin-type protein	3.88	7.95E-05
COG0578C	Z3499	*glpA*	sn-glycerol-3-phosphate dehydrogenase subunit A	2.30	3.90E-02
COG0247C	Z3501	*glpC*	sn-glycerol-3-phosphate dehydrogenase subunit C	4.09	3.20E-04
COG0437C	Z4350	*hybA*	hydrogenase 2 protein HybA	3.59	9.18E-04
COG1740C	Z4351	-	hydrogenase 2 small subunit	3.68	5.86E-05
*COG0604CR	Z4612	*yhdH*	dehydrogenase	2.48	2.04E-02
COG1251C	Z4726	*nirB*	nitrite reductase (NAD(P)H) subunit	3.47	1.72E-04
COG1142C	Z4998	*yiaI*	hypothetical protein	4.02	2.18E-05
COG3080C	Z5758	*frdD*	fumarate reductase subunit D	2.36	3.26E-02
COG3029C	Z5759	*frdC*	fumarate reductase subunit C	3.39	3.20E-04
COG0479C	Z5760	*frdB*	fumarate reductase iron-sulfur subunit	2.85	2.22E-03
COG1053C	Z5762	*frdA*	fumarate reductase flavoprotein subunit	3.17	4.87E-04
Carbohydrate transport & metabolism (G)					
COG0366G	Z2475m	*ycjM*	glycosidase	2.75	1.11E-02
COG3001G	Z2754	-	hypothetical protein	2.07	4.79E-02
COG2271G	Z2813	-	transporter	2.57	4.13E-02
COG4668G	Z3427	*fruB*	bifunctional PTS system fructose-specific transporter subunit IIA/HPr protein	2.93	2.44E-02
COG2271G	Z3498	*glpT*	sn-glycerol-3-phosphate transporter	2.23	2.39E-02
COG0738G	Z4118	*fucP*	L-fucose transporter	3.62	1.79E-04
COG2814G	Z4582	*nanT*	sialic acid transporter	2.93	7.54E-03
COG3833G	Z5630	*malG*	maltose ABC transporter permease	2.12	3.80E-02
COG1175G	Z5631	*malF*	maltose transporter membrane protein	2.47	9.17E-03
COG3839G	Z5633	*malK*	maltose ABC transporter ATP-binding protein	2.57	5.66E-03
COG4580G	Z5634	*lamB*	maltoporin	2.41	1.07E-02
COG1263G	Z5850	*treB*	PTS system trehalose(maltose)-specific transporter subunit IIBC	2.23	2.21E-02
Amino acid transport & metabolism (E)					
COG1115E	Z0007	*yaaJ*	inner membrane transport protein	2.57	1.23E-02
COG1982E	Z0839	*speF*	ornithine decarboxylase	2.58	2.78E-02
COG2195E	Z1832	*pepT*	peptidase T	2.58	6.88E-03

*COG1063ER	Z2815	-	oxidoreductase	2.77	8.25E-03
*COG0493ER	Z3401	-	oxidoreductase	2.82	6.72E-03
*COG0493ER	Z3724	*yffG*	oxidoreductase Fe-S binding subunit	4.31	8.92E-06
COG0019E	Z4156	*lysA*	diaminopimelate decarboxylase	3.43	3.31E-04
COG1003E	Z4240	*gcvP*	glycine dehydrogenase	2.19	2.62E-02
COG0509E	Z4241	*gcvH*	glycine cleavage system protein H	2.43	1.07E-02
COG0404E	Z4242	*gcvT*	glycine cleavage system aminomethyltransferase T	2.27	2.10E-02
*COG0252EJ	Z4302	*ansB*	L-asparaginase II	6.28	1.16E-10
COG0814E	Z4468	*tdcC*	threonine/serine transporter TdcC	2.68	9.17E-03
COG1171E	Z4469	*tdcB*	threonine dehydratase	3.34	4.87E-04
*COG0329EM	Z4583	*nanA*	N-acetylneuraminate lyase	3.08	1.16E-03
COG0405E	Z4813	*ggt*	gamma-glutamyltranspeptidase	3.29	3.17E-03
COG0747E	Z4868	*nikA*	periplasmic binding protein for nickel	6.19	2.27E-09
*COG0601EP	Z4869	*nikB*	nickel transporter permease NikB	4.43	1.87E-05
*COG1173EP	Z4870	*nikC*	nickel transporter permease NikC	3.59	8.83E-04
*COG0444EP	Z4871	*nikD*	nickel transporter ATP-binding protein NikD	3.35	1.23E-03
*COG1124EP	Z4872	*nikE*	nickel transporter ATP-binding protein NikE	4.95	1.28E-06
COG3340E	Z5612	*pepE*	peptidase E	3.26	4.96E-04
COG1027E	Z5744	*aspA*	aspartate ammonia-lyase	2.27	1.95E-02
Nucleotide transport & metabolism (F)					
COG0026F	Z0677	*purK*	phosphoribosylaminoimidazole carboxylase ATPase subunit	2.18	3.97E-02
COG0034F	Z3574	*purF*	amidophosphoribosyltransferase	2.41	1.12E-02
COG0152F	Z3735	*purC*	phosphoribosylaminoimidazole-succinocarboxamide synthase	2.29	1.95E-02
COG0516F	Z3772	*guaB*	inosine 5'-monophosphate dehydrogenase	2.20	2.54E-02
COG0046F	Z3835	*purL*	phosphoribosylformylglycinamidine synthase	2.72	3.84E-03
COG0461F	Z5066	*pyrE*	orotate phosphoribosyltransferase	2.66	4.42E-03
COG2233F	Z5082	*yicE*	transporter	4.75	3.05E-06
COG0151F	Z5582	*purD*	phosphoribosylamine--glycine ligase	2.64	7.62E-03
COG0138F	Z5583	*purH*	bifunctional phosphoribosylaminoimidazolecarboxamide formyltransferase/IMP cyclohydrolase	2.96	1.54E-03
COG1328F	Z5848	*nrdD*	anaerobic ribonucleoside triphosphate reductase	2.47	9.62E-03
COG1781F	Z5855	*pyrI*	aspartate carbamoyltransferase	3.24	1.16E-03
COG0540F	Z5856	*pyrB*	aspartate carbamoyltransferase	2.94	2.94E-03
COG1328F	Z5982	*yjjI*	hypothetical protein	4.58	7.00E-06
Coenzyme transport & metabolism (H)					
COG0521H	Z1001	*moaB*	molybdopterin biosynthesis, protein B	2.15	3.12E-02
COG0132H	Z2585	*bioD*	dithiobiotin synthetase	3.42	2.32E-04
Inorganic ion transport & metabolism (P)					
COG2116P	Z1250	*focA*	formate transporter	3.30	2.32E-04
COG2223P	Z2000	*narK*	nitrite extrusion protein	4.66	3.17E-07
COG2897P	Z2789	-	thiosulfate sulfurtransferase	3.16	1.10E-03
COG1528P	Z2960	*ftn*	ferritin	2.46	9.62E-03
COG3062P	Z3464	*napD*	assembly protein for periplasmic nitrate reductase	6.91	2.74E-07
*COG2146PR	Z4727	*nirD*	nitrite reductase small subunit	3.98	2.42E-03
*COG0601EP	Z4869	*nikB*	nickel transporter permease NikB	4.43	1.87E-05
*COG1173EP	Z4870	*nikC*	nickel transporter permease NikC	3.59	8.83E-04
*COG0444EP	Z4871	*nikD*	nickel transporter ATP-binding protein NikD	3.35	1.23E-03
*COG1124EP	Z4872	*nikE*	nickel transporter ATP-binding protein NikE	4.95	1.28E-06
COG0376P	Z5497	*katG*	catalase	2.90	1.46E-03
COG3303P	Z5669	*nrfA*	cytochrome *c*552	5.17	3.31E-07

Translation, ribosomal structure & biogenesis (J)					
COG1544J	Z3890	*yfiA*	translation inhibitor protein RaiA	2.21	2.38E-02
*COG0252EJ	Z4302	*ansB*	L-asparaginase II	6.28	1.16E-10
Transcription (K)					
*COG2197TK	Z0463	-	response regulator; hexosephosphate transport	2.34	2.39E-02
*COG0378OK	Z4036	*hypB*	hydrogenase nickel incorporation protein HypB	3.14	5.69E-03
COG0583K	Z4413	*ygiP*	transcriptional activator TtdR	4.09	3.20E-04
COG0583K	Z4470	*tdcA*	DNA-binding transcriptional activator TdcA	4.77	2.47E-07
COG2909K	Z4774	*malT*	transcriptional regulator MalT	2.19	2.71E-02
COG0864K	Z4873	*yhhG*	nickel responsive regulator	2.60	2.46E-02
Signal transduction mechanisms (T)					
*COG2197TK	Z0463	-	response regulator; hexosephosphate transport	2.34	2.39E-02
Cell wall/membrane/envelope biogenesis (M)					
COG3047M	Z2034	*yciD*	outer membrane protein W	3.35	2.86E-04
*COG0329EM	Z4583	*nanA*	N-acetylneuraminate lyase	3.08	1.16E-03
Cell motility (N)					
*COG3188NU	Z3277	*yehB*	hypothetical protein	2.46	2.39E-02
*COG3121NU	Z3278	*yehC*	chaperone protein	4.31	2.32E-04
*COG3539NU	Z3279	*yehD*	fimbrial-like protein	3.65	4.57E-05
Intracellular trafficking, secretion, & vesicular transport (U)					
*COG3188NU	Z3277	*yehB*	hypothetical protein	2.46	2.39E-02
*COG3121NU	Z3278	*yehC*	chaperone protein	4.31	2.32E-04
*COG3539NU	Z3279	*yehD*	fimbrial-like protein	3.65	4.57E-05
Posttranslational modification, protein turnover, chaperones (O)					
COG2332O	Z3454	*ccmE*	cytochrome *c* biogenesis protein CcmE	2.79	1.33E-02
*COG0378OK	Z4036	*hypB*	hydrogenase nickel incorporation protein HypB	3.14	5.69E-03
COG0409O	Z4038	*hypD*	pleiotrophic effects on 3 hydrogenase isozymes	2.90	6.16E-03
COG0826O	Z4519	*yhbU*	collagenase	5.26	2.74E-07
COG0826O	Z4520	*yhbV*	hypothetical protein	4.61	1.93E-06
COG0602O	Z5847	*nrdG*	anaerobic ribonucleotide reductase-activating protein	3.32	6.29E-04
General function prediction only (R)					
COG3180R	Z0867	*abrB*	transporter	2.56	1.14E-02
COG3302R	Z1242	*dmsC*	anaerobic dimethyl sulfoxide reductase subunit C	3.07	4.34E-03
*COG1063ER	Z2815	-	oxidoreductase	2.77	8.25E-03
*COG0493ER	Z3401	-	oxidoreductase	2.82	6.72E-03
*COG0493ER	Z3724	*yffG*	oxidoreductase Fe-S binding subunit	4.31	8.92E-06
COG3445R	Z3862	*yfiD*	autonomous glycyl radical cofactor GrcA	3.58	5.45E-05
COG0375R	Z4035	*hypA*	hydrogenase nickel incorporation protein	3.46	4.15E-04
COG1811R	Z4311	*yqgA*	transporter	2.73	9.84E-03
*COG0604CR	Z4612	*yhdH*	dehydrogenase	2.48	2.04E-02
*COG2146PR	Z4727	*nirD*	nitrite reductase small subunit	3.98	2.42E-03
COG0641R	Z5169	*yidF*	transcriptional regulator	2.33	1.83E-02
COG2985R	Z5181	*yidE*	hypothetical protein	2.30	1.93E-02
COG2252R	Z5663	*yjcD*	hypothetical protein	2.25	2.39E-02
Function unknown (S)					
COG1288S	Z3560	*yfcC*	hypothetical protein	4.22	2.17E-05
COG3691S	Z3606	-	hypothetical protein	3.77	2.11E-05
not assigned					
-	Z0040	-	DNA-binding transcriptional activator CaiF	2.21	4.32E-02
-	Z0828	-	hypothetical protein	2.65	7.54E-03
-	Z1062	*bssR*	biofilm formation regulatory protein BssR	2.71	3.05E-03
-	Z1265	-	hypothetical protein	3.21	1.23E-03
-	Z1355	-	hypothetical protein	2.15	4.69E-02
-	Z1881	-	hypothetical protein	4.70	2.18E-05

-	Z2156	-	hypothetical protein	3.26	8.83E-04
-	Z2366	-	hypothetical protein	4.51	9.41E-05
-	Z2783	*ydjY*	hypothetical protein	2.69	1.99E-02
-	Z2962	*yecH*	hypothetical protein	3.29	3.78E-04
-	Z3533	*yfbM*	hypothetical protein	2.19	3.38E-02
-	Z4401	*glgS*	glycogen synthesis protein GlgS	2.30	1.80E-02
-	Z5170	*yidG*	hypothetical protein	2.49	1.48E-02
-	Z5730	*yjdK*	hypothetical protein	4.55	2.63E-06
-	Z5731	-	hypothetical protein	3.45	5.49E-04
-	Z5796	*yjfO*	biofilm stress and motility protein A	2.35	1.51E-02
-	Z5897	-	hypothetical protein	2.21	2.39E-02

*Genes assigned to more than one COG class

Table A 12: Down-regulated genes in 1 h vs 10 min reference cultures of EHEC EDL933 WT

COG	EDL933 identifier	Gene name	Product	log_2 FC	p-value (BH-adjusted)
Energy production & conversion (C)					
COG1622C	Z0535	*cyoA*	cytochrome o ubiquinol oxidase subunit II	-2.07	3.86E-02
COG0372C	Z0873	*gltA*	type II citrate synthase	-2.03	4.54E-02
COG2009C	Z0875	*sdhC*	succinate dehydrogenase cytochrome b556 large membrane subunit	-2.64	4.42E-03
COG1620C	Z5030	*lldP*	L-lactate permease	-2.45	1.07E-02
Carbohydrate transport & metabolism (G)					
COG4993G	Z0134	*gcd*	glucose dehydrogenase	-2.08	3.99E-02
COG2814G	Z0733	*ybdA*	enterobactin exporter EntS	-4.21	8.44E-04
COG0738G	Z4725	*yhfC*	hypothetical protein	-3.03	1.58E-03
*COG2610GE	Z4770	*gntT*	high-affinity transport of gluconate / gluconate permease	-2.14	4.71E-02
COG2814G	Z5149	*nepI*	ribonucleoside transporter	-3.16	4.38E-03
Amino acid transport & metabolism (E)					
*COG0591ER	Z1515	*putP*	major sodium/proline symporter	-2.25	3.80E-02
*COG0834ET	Z3572	*argT*	lysine-, arginine-, ornithine-binding periplasmic protein	-2.51	2.21E-02
*COG2610GE	Z4770	*gntT*	high-affinity transport of gluconate / gluconate permease	-2.14	4.71E-02
Nucleotide transport & metabolism (F)					
COG0209F	Z3977	*nrdE*	ribonucleotide-diphosphate reductase subunit alpha	-3.02	1.71E-02
Coenzyme transport & metabolism (H)					
*COG1120PH	Z0729	*fepC*	iron-enterobactin transporter ATP-binding protein	-2.95	2.84E-03
*COG1169HQ	Z0735	*entC*	isochorismate synthase	-4.81	6.56E-06
*COG1120PH	Z4385	-	ABC transporter ATP-binding protein	-2.34	2.54E-02
Inorganic ion transport & metabolism (P)					
COG1629P	Z0161	*fhuA*	ferrichrome outer membrane transporter	-2.91	1.38E-03
COG4771P	Z0724	*fepA*	outer membrane receptor FepA	-3.53	1.79E-04
COG2382P	Z0725	*fes*	enterobactin/ferric enterobactin esterase	-5.68	7.48E-07
*COG1120PH	Z0729	*fepC*	iron-enterobactin transporter ATP-binding protein	-2.95	2.84E-03
COG4779P	Z0731	*fepG*	iron-enterobactin transporter permease	-9.63	2.83E-06
COG0609P	Z0732	*fepD*	iron-enterobactin transporter membrane protein	-2.77	9.62E-03
COG4592P	Z0734	*fepB*	iron-enterobactin transporter periplasmic binding protein	-3.20	5.44E-03
COG4774P	Z1026	-	catecholate siderophore receptor Fiu	-4.66	2.38E-06
COG0672P	Z1519	-	hypothetical protein	-3.06	9.41E-04
COG4256P	Z2734	*ydiE*	hypothetical protein	-3.52	4.87E-04
COG4771P	Z3411	*cirA*	colicin I receptor	-5.36	5.49E-08

*COG4615QP	Z3469	*yojI*	multidrug transporter membrane protein/ATP-binding component	-3.06	1.23E-03
*COG1120PH	Z4385	-	ABC transporter ATP-binding protein	-2.34	2.54E-02
COG4773P	Z4386	-	iron compound receptor	-2.37	2.61E-02
COG2193P	Z4695	-	bacterioferritin	-2.10	3.81E-02
COG2906P	Z4696	*yheA*	bacterioferritin-associated ferredoxin	-5.11	8.55E-08
COG2223P	Z4972	*yhjX*	resistance protein	-3.41	2.32E-04
Secondary metabolites biosynthesis, transport & catabolism (Q)					
COG1020Q	Z0727	*entF*	enterobactin synthase subunit F	-2.83	2.84E-03
*COG1169HQ	Z0735	*entC*	isochorismate synthase	-4.81	6.56E-06
COG1021Q	Z0736	*entE*	enterobactin synthase subunit E	-4.29	9.14E-06
COG1535Q	Z0737	*entB*	2,3-dihydro-2,3-dihydroxybenzoate synthetase	-2.59	1.63E-02
*COG4615QP	Z3469	*yojI*	multidrug transporter membrane protein/ATP-binding component	-3.06	1.23E-03
COG2050Q	Z5341	*yigI*	hypothetical protein	-2.85	6.21E-03
Translation, ribosomal structure & biogenesis (J)					
COG0042J	Z4620	*yhdG*	tRNA-dihydrouridine synthase B	-2.24	2.21E-02
COG0594J	Z5195	*rnpA*	ribonuclease P	-2.07	3.88E-02
Transcription (K)					
COG0583K	Z2299	-	LysR family transcriptional regulator	-3.04	1.17E-03
COG0583K	Z3395	-	regulator	-2.47	2.44E-02
*COG2901KL	Z4621	*fis*	Fis family transcriptional regulator	-2.21	2.38E-02
COG1278K	Z4981	*cspA*	cold-shock protein	-3.38	1.57E-04
COG2186K	Z5031	*lldR*	DNA-binding transcriptional repressor LldR	-2.18	3.04E-02
Replication, recombination & repair (L)					
*COG2901KL	Z4621	*fis*	Fis family transcriptional regulator	-2.21	2.38E-02
Signal transduction mechanisms (T)					
*COG0834ET	Z3572	*argT*	lysine-, arginine-, ornithine-binding periplasmic protein	-2.51	2.21E-02
Cell wall/membrane/envelope biogenesis (M)					
COG3765M	Z0728	*fepE*	ferric enterobactin transport protein FepE	-3.20	5.44E-03
COG0787M	Z1953	*dadX*	alanine racemase	-2.75	2.77E-02
COG0810M	Z2030	*tonB*	transporter	-2.25	2.64E-02
Cell motility (N)					
*COG3539NU	Z4971	-	major fimbrial subunit	-2.35	2.61E-02
Intracellular trafficking, secretion, & vesicular transport (U)					
COG0848U	Z4358	*exbD*	biopolymer transport protein ExbD	-3.27	3.78E-04
COG0811U	Z4359	*exbB*	biopolymer transport protein ExbB	-2.78	2.67E-03
*COG3539NU	Z4971	-	major fimbrial subunit	-2.35	2.61E-02
Posttranslational modification, protein turnover, chaperones (O)					
COG0695O	Z3975	*nrdH*	glutaredoxin-like protein	-2.99	1.87E-02
General function prediction only (R)					
*COG0591ER	Z1515	*putP*	major sodium/proline symporter	-2.25	3.80E-02
COG1054R	Z1691	*yceA*	hypothetical protein	-2.75	2.84E-03
COG4178R	Z2212	*yddA*	ABC transporter ATP-binding protein	-5.94	1.90E-05
COG0579R	Z3468	*yojH*	malate:quinone oxidoreductase	-2.96	1.16E-03
COG4114R	Z5968	*fhuF*	ferric hydroximate transport ferric iron reductase	-5.32	5.49E-08
Function unknown (S)					
COG3251S	Z0726	-	hypothetical protein	-2.72	4.55E-02
not assigned					
-	Z0001	*thrL*	thr operon leader peptide	-2.12	4.04E-02
-	Z0879	-	hypothetical protein	-2.78	2.76E-03
-	Z1751	*ycfR*	hypothetical protein	-2.74	7.76E-03
-	Z2274	-	hypothetical protein	-3.51	1.41E-03
-	Z2591	*asr*	acid shock protein	-2.32	2.21E-02

-	Z3344	*stx1A*	shiga-like toxin 1 subunit A encoded within prophage CP-933V	-2.77	2.50E-03
-	Z5659	*yjcB*	hypothetical protein	-3.47	2.84E-03

*Genes assigned to more than one COG class

Acknowledgement

Firstly, I would like to express my sincere thanks to Prof. Dr. Scherer for offering me the opportunity to perform this thesis and to gain most of my scientific experience at his chair, for his confidence in my work and useful advice.

I would like to express my deepest gratitude to Dr. Stefanie Müller-Herbst, who supported me greatly with her extensive knowledge, constructive criticism and kind patience. She always believed in my abilities and ideas and guided me also through the tough times of my research.

I thank Prof. Dr. Ehrmann for acting as second examiner of my thesis and for providing pEGFP for the intracellular pH measurements. Prof. Dr. Liebl is acknowledged for serving as chairman of the Examination Committee.

I greatly appreciate the cooperation with our partners from the Max Rubner-Institut, in particular Dr. Rohtraud Pichner and Dr. Jan Kabisch, for many fruitful discussions and for giving me insight into the art of sausage making.

I would like to thank all my colleagues from the Chair of Microbial Ecology for the friendly and helpful working atmosphere. In particular, I thank the AG Fuchs and AG Neuhaus for sharing the *Salmonella* and EHEC protocols with me, Dr. Richard Landstorfer and Christopher Huptas for their help in performing and analyzing the RNA-seq experiments, and my former labmates from the AG Müller-Herbst and AG Bacillus, especially Dr. Daniela Kaspar and Dr. Andrea Rütschle, for cheerful hours at work and the mutual support and encouragement.

I really appreciate the technical assistance of Daniela Eder and Katharina Sturm, who spent a lot of time pipetting Bioscreen runs and supported me in mutant construction.

A great thanks goes to Jakob Schardt, Lisa Schürch and Ludwig Klermund, who contributed to this thesis in the framework of their practical courses, bachelor or master thesis. Jakob Schardt and Lisa Schürch also helped a lot in the insertion mutant library screening while working as HIWIs.

I am grateful to Dr. Jürgen Behr (TUM Chair of Technical Microbiology) for his time and help with the fluorescence spectrophotometer, Dr. Carsten Kröger (Trinity College Dublin) for providing phage P22 and the associated protocols, and Dr. Svenja Simon (University of Konstanz) for helping with the RNA-seq data analysis.

I would have never finished this thesis without the endless and loving support of family and friends. Most of all, I thank my parents, who were always there for me and had a sympathetic ear and comforting and encouraging words. A big thanks also goes to my parents-in-law, who enthusiastically jumped in as babysitters whenever I needed time for writing.

Last but not least, I heartily thank my husband Walter for his love, patience and support through good and bad times, and my daughter Sophia, for being as lovely as she is and for sharing with me her curiosity in exploring the world.